Durham University

Durham E-Theses

The application of pulsed plasmas towards controlled surface functionalisation

Hynes, Alan

How to cite:

Hynes, Alan (1998) *The application of pulsed plasmas towards controlled surface functionalisation*, Durham theses, Durham University. Available at Durham E-Theses Online: http://etheses.dur.ac.uk/4887/

Use policy

The full-text may be used and/or reproduced, and given to third parties in any format or medium, without prior permission or charge, for personal research or study, educational, or not-for-profit purposes provided that:

- a full bibliographic reference is made to the original source
- a link is made to the metadata record in Durham E-Theses
- the full-text is not changed in any way

The full-text must not be sold in any format or medium without the formal permission of the copyright holders.

Please consult the full Durham E-Theses policy for further details.

Academic Support Office, The Palatine Centre, Durham University, Stockton Road, Durham, DH1 3LE
e-mail: e-theses.admin@durham.ac.uk Tel: +44 0191 334 6107
http://etheses.dur.ac.uk

THE APPLICATION OF PULSED PLASMAS TOWARDS CONTROLLED SURFACE FUNCTIONALISATION

Ph.D. Thesis

by

Alan Hynes

The copyright of this thesis rests with the author. No quotation from it should be published without the written consent of the author and information derived from it should be acknowledged.

University of Durham

Department of Chemistry

1998

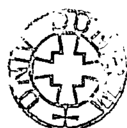

- 2 JUL 1998

For Mam, Paul, Jennifer and Denis

Acknowledgements

On this the most consulted page of any thesis I take great pleasure in expressing my appreciation to the following who made this work possible and my time in Durham so enjoyable.

To all with whom I served time in Lab 98 for the ideas, laughs and laughable ideas over the three years! In particular to Janet and Martin for their support and encouragement during the 'final push'.

To 'magical' George in the electronics workshop for apparently overcoming the laws of physics in maintaining the ES200 and to Gordon and Ray for the wonders of glassblowing and the local history lessons.

To my supervisor Prof. J.P.S. Badyal and the E.C. for providing the opportunity to do the work.

To all the friends I gained over the three years, in particular 'The Celts' for their support and distractions.

To Grad. Soc. A.F.C. for making my Durham years unforgettable. In particular the Execs. for all the work and the Tourists for broadening my knowledge of the game(s), the everlasting friendships and the great memories.

To the cast of 'Nellies' for their friendship and support and for never letting there be a dull moment!

Finally sincere thanks goes to my family and particular Marion, my mother. For all you've done to get me here, thank you.

"The most exciting phrase to hear in science, the one that heralds new discoveries, is not 'Eureka' but ' That's funny ...' "

---Isaac Asimov

DECLARATION

STATEMENT OF COPYRIGHT

The copyright of this thesis rests with the author. No quotation from it should be published without his written consent and information derived from it should be acknowledged.

The work described in this thesis was carried out in the Department of Chemistry at the University of Durham between October 1993 and September 1996. It is original work by the author except where otherwise acknowledged or where specific reference is made to other sources.

Atomic force microscopy analysis (chapter 4) was performed by Prof. J.P.S. Badyal.

Work in this thesis has formed all or part of the following publications:

- *"Plasma polymerisation of trifluoromethyl-substituted perfluorocyclohexane monomers"*, Hynes, A.M.; Shenton, M.J.; Badyal, J.P.S. *Macromolecules*, **1996**, *29,* 18-21.
-
- *"Pulsed plasma polymerisation of perfluorocyclohexane"*, Hynes, A.M.; Shenton, M.J.; Badyal, J.P.S. *Macromolecules*, **1996**, *29 (12)*, 4220-4225.

ABSTRACT

Pulsed plasmas were investigated as a means of controlling the composition of the surfaces generated via plasma polymerisation. A variety of precursors were studied under a range of plasma conditions using both continuous wave and pulsed plasmas. Surface and bulk analytical techniques were used to characterise the deposited plasma polymers whilst deposition rate measurements aided in understanding the effects of altering the various plasma parameters.

Continuous wave plasma polymerisation of saturated cyclic fluorocarbons yielded plasma polymers with high fluorine/carbon ratios. Plasma instability at low powers limits the extent to which continuous wave power can be used to achieve good selectivity in the polymerisation process.

Pulsed plasma polymerisation of perfluoroallylbenzene was studied in detail to investigate the influence of pulsing parameters on the surface composition. Highly aromatic surfaces were obtained through retention of the perfluorophenyl group from the precursor. Deposition rate experiments confirmed polymerisation was taking place in the off-portion of the duty cycle for precursors with a functional group susceptible to radical initiated reactions.

A cyclic siloxane precursor with vinyl substituents was used to generate surface consisting of siloxane rings in an organic matrix. The monomer structure was retained through the reaction of the vinyl groups in the off-portion of the duty cycle. For low duty cycle pulsed plasma polymers the Si:O ratio of the plasma polymers was identical to that of the monomer, indicating successful retention of monomer structure using pulsed plasmas.

Preliminary investigations into the pulsed plasma polymerisation of styrene oxide yielded a range of polymer compositions with varying oxygen contents. The properties of the surfaces varied with oxygen content.

The results indicate that pulsed plasmas can give significant enhancements over continuous wave plasmas in controlling surface composition and properties.

CONTENTS

CHAPTER 1:

INTRODUCTION TO PULSED PLASMAS AND ANALYTICAL TECHNIQUES

1.1 INTRODUCTION 2

1.2 PLASMAS 2

1.2.1 Definition of plasma 3

1.2.2 Classification of plasmas 4

1.2.2.1 Equilibrium Plasmas. 4

1.2.2.2 Non-Equilibrium Plasmas 4

1.2.3 Plasma properties 7

1.2.3.1 Electron energy 7

1.2.3.2 Electron energy distribution function 7

1.2.3.3 Plasma potential 8

1.2.3.4 Plasma sheath 8

1.2.4 General Applications of Plasmas. 9

1.2.4.1 Surface modification 9

1.2.4.2 Etching 9

1.2.4.3 Deposition 10

1.3 PULSED PLASMA POLYMERISATION 10

1.3.1 Plasma Polymerisation 11

1.3.1.1 Origin of the glow discharge 11

1.3.1.2 Advantages of plasma polymerisation 12

1.3.1.3 Plasma polymerisation mechanism 13

1.3.2 Pulsed Plasmas 15

1.3.2.1 Advantages of pulsed plasmas 16

1.3.2.2 Pulsing parameters 17

1.3.2.3 Experimental set-up for pulsed plasmas 17

1.3.2.4 Typical timescales in pulsed plasmas 19
1.3.3 Pulsed plasmas in the literature 24
1.3.4 Aims of current work 27
1.4 CHARACTERISATION TECHNIQUES 27
1.4.1 X-ray Photoelectron Spectroscopy (XPS) 27
1.4.1.1 Introduction 27
1.4.1.2 The photoelectric effect 28
1.4.1.3 Surface sensitivity 29
1.4.1.4 Instrumentation 29
1.4.1.5 Spectral Interpretation 32
1.4.2 Infrared Spectroscopy 37
1.4.3 Atomic Force Microscopy 38
1.5 REFERENCES 40

CHAPTER 2:
PLASMA POLYMERISATION OF TRIFLUOROMETHYL SUBSTITUTED PERFLUOROCYCLOHEXANE MONOMERS

2.1 INTRODUCTION 45
2.2 EXPERIMENTAL 46
2.2.1 Experimental Apparatus and Procedure for Plasma Polymerisation. 47
2.2.2 Flow Rate Calculation 50
2.2.3 Sample Characterisation 50
2.3 RESULTS 51
2.4 DISCUSSION 57
2.5 CONCLUSION 60
2.6 REFERENCES 61

CHAPTER THREE

HIGHLY FLUORINATED SURFACES VIA CONTINUOUS AND PULSED PLASMA POLYMERISATION OF PERFLUOROCYCLOHEXANE AND PERFLUOROCYCLOPENTENE

3.1 INTRODUCTION 64

3.2 EXPERIMENTAL 66

3.3 PERFLOUROCYCLOHEXANE: RESULTS 67

3.3.1 X-ray Photoelectron Spectroscopy 67

3.3.1.1 Continuous Wave Plasma Polymerisation 68

3.3.1.2 Pulsed Plasma Polymerisation 68

3.3.2 Transmission Infrared Spectroscopy. 74

3.4 DISCUSSION 76

3.4.1.1 Pulsed Plasma Polymerisation 78

3.5 PERFLOUROCYCLOPENTENE: RESULTS 81

3.5.1 X-ray Photoelectron Spectroscopy 81

3.5.2 Transmission Infrared Spectroscopy. 86

3.6 PERFLOUROCYCLOPENTENE: DISCUSSION 91

3.7 CONCLUSIONS 96

3.8 REFERENCES 99

CHAPTER FOUR

AN INVESTIGATION OF THE PULSED PLASMA POLYMERISATION OF PERFLUOROALLYLBENZENE

4.1 INTRODUCTION 102

4.1.1 Background 102

4.1.2 Previous approaches towards improving selectivity 102

4.1.3 Factors influencing choice of starting material 103

4.1.4 Summary 105

4.2 EXPERIMENTAL 105

4.3 RESULTS AND DISCUSSION 107

4.3.1 Pulsed polymerisation studies with varying average powers 107

4.3.1.1 X-ray Photoelectron Spectroscopy 107

4.3.1.2 Transmission Infrared Spectroscopy. 113

4.3.1.3 Ultraviolet/visible spectroscopy 116

4.3.1.4 Atomic Force Microscopy 117

4.3.2 Discussion of variable average power results. 120

4.3.3 Effect of average power on reactor profile. 121

4.3.4 Pulsed plasma polymerisation studies using constant average power. 124

4.3.5 Deposition rate studies. 129

4.4 CONCLUSION 136

4.5 REFERENCES 141

CHAPTER FIVE

ORGANOSILOXANE SURFACES VIA PULSED PLASMA POLYMERISATION

5.1 INTRODUCTION 143

5.1.1 Background 143

5.1.2 Poly(siloxanes) 143

5.1.3 Plasma polymerisation of siloxane precursors 145

5.1.4 Applications of polysiloxane plasma polymers 145

5.2 EXPERIMENTAL 149

5.3 RESULTS 149

5.3.1 Infrared Absorption Spectroscopy 149

5.3.2 X-ray Photoelectron Spectroscopy 154

5.3.3 Deposition Rate Studies 159

5.4 DISCUSSION 162

5.4.1 Continuous Wave Plasma Polymerisation 162

5.4.2 Pulsed Plasma Polymerisation 164

5.4.3 Deposition Rate Studies 165

5.5 CONCLUSIONS 167

5.6 REFERENCES 171

CHAPTER SIX

PULSED PLASMA POLYMERISATION OF STYRENE OXIDE

6.1 INTRODUCTION 173

6.1.1 Applications of plasma polymers from aromatic precursors 174

6.2 EXPERIMENTAL 175

6.3 RESULTS 177

6.3.1 Infrared Spectroscopy 177

6.3.1.1 Infrared Absorption Bands of Styrene Oxide 177

6.3.1.2 Infrared spectra of plasma polymers of styrene oxide 179

6.3.2 X-ray photoelectron spectroscopy 182

6.3.3 Physical properties of the plasma polymers 183

6.3.4 Deposition Rate Studies 186

6.4 DISCUSSION 189

6.5 CONCLUSION 193

6.6 REFERENCES 194

CHAPTER SEVEN

CONCLUSIONS 197

CHAPTER ONE

INTRODUCTION TO PULSED PLASMAS AND ANALYTICAL TECHNIQUES

CHAPTER ONE

INTRODUCTION TO PULSED PLASMAS AND ANALYTICAL TECHNIQUES

1.1 INTRODUCTION

Advances in the application and understanding of plasma processes have resulted in plasma technology becoming a key technology for modern life. Plasma processing is currently a multi-billion pound global industry. Intensive research is now being undertaken to gain further insights into the theory and practical application of plasma processing as a manufacturing technique for a large range of applications. This thesis studies the technique of plasma polymerisation as a means of depositing organic coatings. In particular it aims to investigate the extent to which pulsed power can be used to achieve additional control over the stoichiometry of the resultant surfaces.

In this chapter the basic principles of plasma processing are introduced followed by a brief introduction to the analytical techniques used to characterise the plasma polymers deposited in the work.

1.2 PLASMAS

The plasma state is often referred to as the fourth state of matter, Fig. 1-1, and its occurrence is, perhaps surprisingly, quite common. Gas discharges are present in a variety of forms from the natural examples of the solar wind, lightening and the Aurora Borealis (Northern light) or Aurora Australis (Southern light), to man-made fluorescent tubes, neon signs and the new energy efficient light bulbs. In fact up to 99% of the matter in the universe may be in the plasma state. Given the fact that recent theories on the origin of life on earth propose that the first amino acids, the building blocks of living systems, were a result of an electrical discharge in a

"primordial soup" of gaseous hydrocarbons, we may even owe our very existence to plasmas!

Although gas discharges have been examined since the first studies on cathode ray tubes in the latter half of the nineteenth century, it was Langmuir in 1928 who coined the word *plasma* to denote the ionised gases formed in electrical discharges.[1] Today as our understanding of the plasma state grows, plasmas find more and more applications in our everyday lives. The electronics revolution of the past thirty years could not have taken place without the development of plasma processing. The etch and deposition processes enabled by plasma technology are essential for the manufacture of integrated electronic circuits.[2] In 1991 the plasma processing industry had world-wide revenues of US$ 1 billion.

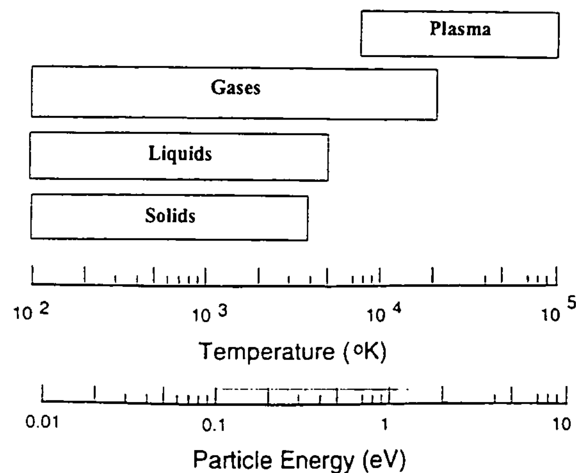

Fig. 1-1: State of matter versus temperature indicating why the plasma state is often referred to as the 'fourth state of matter'.

1.2.1 Definition of plasma

A plasma (or gas discharge) is an ionised gas and is more rigorously defined as a *quasineutral gas of charged and neutral particles which exhibits collective behaviour.*[3,4] The gas remains electrically neutral when the dimensions of the discharge gas volume are significantly greater than the Debye length λ_d, which defines the distance over which a charge imbalance can occur.

$$\lambda_d = \left(\frac{E_0 k T_e}{n_e e^2} \right)^{1/2} \qquad \text{Eq. 1-1}$$

where E_0 = permittivity of free space, k is the Boltzman constant, T_e is the electron temperature, n_e is the electron density and *e* is the charge on the electron. The number of positive and negative species in the plasma remains equal and the plasma is said to be quasi-neutral.

1.2.2 Classification of plasmas

Plasmas can be broadly classified as either equilibrium or non-equilibrium plasmas depending on the relationship between the average electron energy and the energy of the ions and neutral species in the plasma.

1.2.2.1 Equilibrium Plasmas.

These are also referred to as 'hot' plasmas. In an equilibrium plasma the rate of energy transfer from the electrons to the atoms and molecules in the plasma is sufficient to raise these neutral species to the same energies as the electrons. These plasmas are stable to small alterations in plasma conditions as they are in an equilibrium condition and hence thermodynamically stable. Examples of equilibrium plasmas include the stars, arc discharges and plasma torches.[5]

1.2.2.2 Non-Equilibrium Plasmas.

In non-equilibrium plasmas, also known as glow discharges, the temperature of the electrons, T_e, typically in the range 1-30 eV, is not equal to the temperature of the gas molecules or atoms, T_g. In fact the T_e/T_g ratio is usually 10^2 - 10^3 and hence this type of plasma is used where ambient temperatures are required.

For example the average electron energy in a fluorescent light bulb is about 2 eV $\approx$ 15,000 degrees Kelvin,[6] yet the bulb doesn't melt because the electron and neutral

temperatures are unequal. Another consequence of non-equilibrium transport is that in contrast to equilibrium plasmas, non-equilibrium plasmas are not thermodynamically stable to small perturbations in plasma conditions.

Plasmas can be characterised in terms of their average electron temperature and the charge density within the gas. The particular non-equilibrium plasmas used in this work and for the majority of laboratory plasma studies are termed *glow discharges.* Fig. 1-2 shows the electron energy and electron density of glow discharges relative to other plasmas (ref. 4, p. 18).

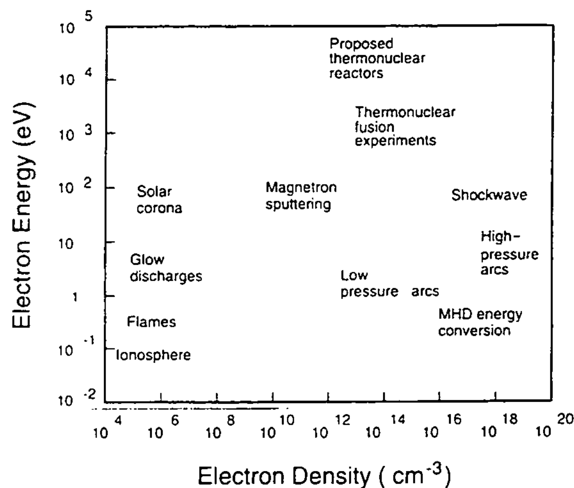

Fig. 1-2: Classification of plasmas according to ionisation density and electron energy.

Glow discharges can be further subdivided depending on the experimental method used to ignite and sustain the discharge.

1.2.2.2.1 Parallel Plate Discharge.

This is a discharge produced due to the application of a voltage between two flat electrodes in a tube filled with a gas at low pressure. The electrons respond to the applied electric field and transfer their energy to the atoms and/or molecules in the tube. These excited molecules relax via radiative emission to produce the characteristic glow of the fluorescent tube and neon sign. Due to the low pressure and mass throughput however the parallel plate discharge has not found major application in the industrial production of chemicals or films.

1.2.2.2.2 Corona Discharge.

At higher pressures the glow discharge becomes highly unstable. One way to avoid this is to alter the geometries of the electrodes e.g. a point and a plane.[16] Using this electrode geometry discharges can be produced at pressures up to 1 atmosphere. The name corona comes from the localised glow at the point electrode. Due to the small active volume around the point, corona discharges also do not find major application in the industrial production of chemicals. They are used for some applications however, for example in copying machines where they are used to produce charged particles and also in the surface modification of some plastics.

1.2.2.2.3 Silent Discharge.

The silent discharge combines the high pressure of the corona discharge with the large excitation volume of the glow discharge to give a discharge which can be used for volume plasma chemistry. It consists of two parallel electrodes one of which is covered with a dielectric layer. As a result of the dielectric, microdischarges occur between the electrodes in most gases. The reduced field at breakdown corresponds to electron energies of 1-10 eV, ideal for the excitation of atomic and molecular species and the breaking of chemical bonds.

1.2.2.2.4 Radio-Frequency Discharges.

These are also known as *electrodeless discharges* as the electrodes are not in direct contact with the species in the plasma. This is a great advantage as contamination of the products from electrode decomposition or sputtering is avoided. The energy is transferred to the gas via inductive or capacitive coupling depending on the electrode geometry employed. In the case of inductively coupled plasmas two types of discharge can exist depending on the applied power and plasma conditions, an electrostatic or E-type discharge and an electromagnetic or H-type discharge.[7] The most common frequency used is the industrial frequency 13.56 MHz. Since the

wavelength of the applied field is large compared to the reactor dimensions relatively homogeneous plasmas can be generated. As long as the collision frequency is higher than the frequency of the applied field the discharge behaves very much like a dc discharge.[8] This implies that non-equilibrium conditions can be expected at low pressures while equilibrium conditions will be expected at higher pressures i.e. 1 atmosphere. Radio frequency plasmas are widely used in laboratories for both optical emission and plasma-chemical studies.

1.2.3 Plasma properties

This section introduces some of the elementary physical characteristics of glow discharges which will be referred to in later chapters.

1.2.3.1 Electron energy

The electrons in the plasma have energies in the range 1-10 eV. One electron volt = 1.6×10^{-19} J. The kinetic theory of gases relates the translational energy to temperature via the equation $\varepsilon = 3/2\ kT$ where ε is the average electron energy, k is the Boltzmann constant and T is temperature in degrees Kelvin.[9] Therefore one electron volt corresponds to

$$\left(\frac{1.602 \times 10^{-19}}{k}\right)\left(\frac{2}{3}\right) = 7739\ \text{K.} \qquad \text{Eq. 1-2}$$

Hence for electrons in the 2-8 eV range this corresponds to temperatures in the range 10^4 - 10^5 K. However as these are non-equilibrium plasmas this energy is not transferred to the atoms or molecules within the gas which remain at or relatively close to ambient temperatures.

1.2.3.2 Electron energy distribution function

The electrons span a range of energies however, governed by the *electron energy distribution function (EEDF)*.[10] The exact nature of the EEDF depends on plasma

conditions but may be either Maxwellian or Druyvesteyn in nature, or a combination of both, Fig. 1-3. As can be seen a certain fraction of the electrons have energies considerably greater than the average electron energy. These are important as it is they that are responsible for the ionisation that occurs in glow discharge plasmas.

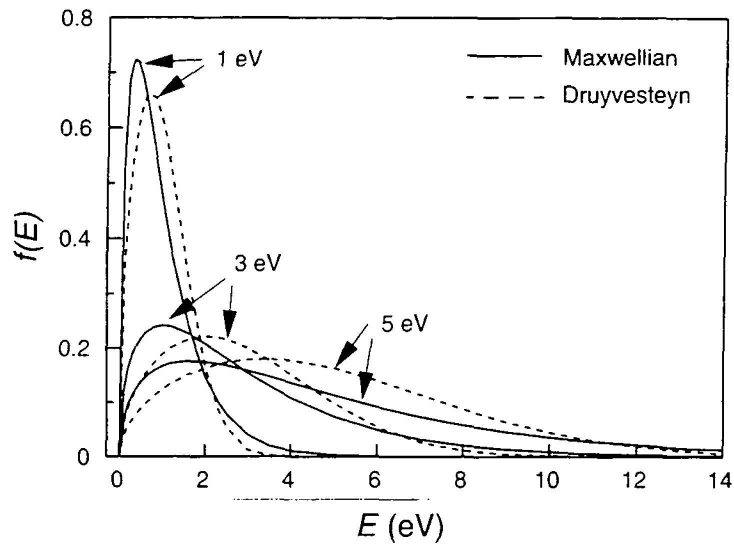

Fig. 1-3: Plot showing electron energy distributions for various average electron energies.

1.2.3.3 Plasma potential

The potential of the plasma is usually several volts more positive than the least negative surface in contact with it.[4,8] This is a direct result of the greater mobility of electrons relative to positive ions. Following the initiation of the electric field the highly mobile electrons rapidly leave the plasma resulting in the build up of a positive potential. Eventually the potential of the plasma gets to a value, the plasma potential, where the flux of electrons and positive ions leaving the system becomes equal and hence the plasma remains electrically *quasi-neutral.*

1.2.3.4 Plasma sheath

The potential difference between the plasma and the surfaces in contact with it, occurs mainly in a narrow region at the edge of the plasma.[3,4] This region, known as the plasma sheath has a negative potential relative to the rest of the plasma and hence a lower electron density. As a result of this lower electron density the plasma sheath

appears dark due to the reduced excitation of gas species. Positive ions are accelerated within the sheath prior to bombarding the substrate surface.

1.2.4 General Applications of Plasmas.

1.2.4.1 Surface modification

Exposing the surface of a solid to a plasma results in observable changes in its physical and chemical properties. Chemical changes can be monitored via analysis techniques such as X-ray photoelectron spectroscopy (XPS), secondary ion mass spectrometry (SIMS), attenuated total reflection FTIR spectroscopy, and atomic force microscopy. Physical properties which are often altered include morphology,[11] wettability,[12,13] adhesion characteristics,[14,15,16] hydrophobicity[17,18] and refractive index.[19,20] Hence treatment of a normally unreactive polymer such as polypropylene with an oxygen plasma for example, results in the incorporation of oxygen containing functional groups such as C=O, OH and C-OOH onto the surface. This results in the polymer having improved wettability and adhesion properties and processes such as painting and printing on the polypropylene can now be carried out with greater ease and efficiency. Cross-linking can also occur, changing the chemical nature of the surface. It has been shown[21] that treatment of polyethylene with an oxygen plasma followed by ageing results in the formation of a polypropylene type structure on the surface.

1.2.4.2 Etching

Surfaces in contact with a plasma can not only be chemically modified but also physically etched[22,23] resulting in the development of microstructures with large depth to width ratios. For example in devices for integrated circuits, trenches in silicon for charge storage can be a mere 0.2 μm wide and 4μm deep. Aspect ratios of this size on structures of these dimensions are not achievable using conventional wet

chemical processes. The basic principle behind plasma etching lies in inducing surface reactions to transform the solid starting material e.g. silicon, into volatile products, e.g. silicon halides, which desorb from the surface into the gas phase.

1.2.4.3 Deposition

In addition to modifying or etching the surfaces of substrates, it is also possible to deposit new materials onto surfaces in contact with the plasma. Plasma polymerisation can deposit polymeric organic coatings from almost any precursor onto substrates placed within the plasma at temperatures at or near ambient. Section 1.3.1 deals with this topic in more detail.

Plasma Enhanced Chemical Vapour Deposition (PECVD) can be used to deposit inorganic coatings. In contrast to thermal CVD where the activation energy for film formation reactions at the surface is supplied thermally, PECVD relies on the low activation energy of the radicals produced in a plasma to generate an inorganic thin film on lower temperature substrates. Along with metallic coatings PECVD is currently extensively used to deposit amorphous silicon hydride, silicon carbide, silicon dioxide, silicon nitride and diamond-like carbon (DLC) films.

1.3 PULSED PLASMA POLYMERISATION

This section aims to outline the basic principles behind the plasma polymerisation technique as a means of depositing thin films. This is followed by a discussion of the advantages and principles of pulsed plasmas along with the timescales of some typical plasma processes. Finally some examples of pulsed plasmas from the literature are presented.

1.3.1 Plasma Polymerisation

One of the major advantages of plasmas in terms of modifying the surfaces of substrates is their ability to form polymeric coatings from precursors which would not under normal circumstances be considered polymerisable. In this way the surface properties of the substrate can be altered whilst the bulk properties remain unchanged. This ability to polymerise normally unreactive monomers arises from the very nature of the non-equilibrium plasma itself. Once initiated the glow discharge contains species with sufficient energy to break chemical bonds and generate reactive precursors from any compound with sufficient vapour pressure.

1.3.1.1 Origin of the glow discharge

Any gas at low pressure contains a small amount of free electrons as a result of natural ionisation processes such as radioactivity, photoionisation or cosmic rays. When an electric field is applied across such a gas electrons respond instantly (ns) reach energies of several electron volts. These energetic electrons then undergo inelastic collisions with gas molecules which are still 'cold' resulting in ionisation and subsequent release of further electrons. The ionisation increases to a certain level at which the loss of ions to the surrounding walls is balanced by their generation within the plasma. At this point the plasma contains high energy electrons, ions and photons all leading to the formation of a wide variety of highly excited and reactive species. These excited species have a lower energy of activation for reaction and can react to form the products of the plasma polymerisation process. Table 1-1 shows the range of energies present within the plasma environment.

Species	Range of energies /eV
Electrons	0-20
Ions	0-2 (gas phase)
Metastables	0-20
UV/visible photons	3-40

Table 1-1: Range of energies associated with a glow discharge. [24]

As a consequence of the range of species within a plasma, e.g. ions, metastables and photons along with the distribution of electron energies, sec. 1.2.3.2, p. 7, a wide variety of reactive species can be generated from a single precursor. In addition to this range of potential reactants i.e. positive and negative ions, radicals and neutrals, there are a variety of potential reaction mechanisms within the plasma, both gas-phase and at the surface of the growing plasma polymers. Consequently plasma polymerised films are usually highly crosslinked films whose composition and structure can be significantly different from that of the original monomer. In order to control the properties of the resultant surfaces it is necessary to control the composition of the plasma polymers.

1.3.1.2 Advantages of plasma polymerisation

Despite the inherent complexity of the plasma polymerisation process and the difficulty in controlling the reaction products, there are several advantages to using plasma technology over conventional chemical processes. It is because of these advantages that the plasma industry has experienced such growth over recent years.

1. It is a simple and dry method to modify the surface properties and composition of substrates. Simple in-house apparatus can be constructed relatively easily. The widespread application of plasma technology has now made plasma processing equipment and/or diagnostic equipment available commercially.
2. A wide range of precursors allows an extensive range of chemical groups to be introduced onto surfaces.

3. Plasma deposition can deposit coatings onto almost any substrate over a wide temperature range.
4. Surface modification and/or deposition can take place uniformly over the surface
5. Bulk properties of the substrate are generally not affected by plasma processing.
6. Film thickness can be easily controlled to a few nanometers, provided the deposition rate is well established and the run-run uniformity of the process is properly characterised.
7. Due to the unique nature of the process films with novel properties can be prepared.
8. Plasma polymerised films are generally pin-hole free and can be highly crosslinked leading to excellent properties as barrier layers.
9. In plasma etching the use of low pressure gases allows sub-micron high aspect ratio structures to be produced in a clean environment. This capability is essential for the modern micro-electronics industry.
10. Plasma technology is an environmentally friendly technique relative to wet chemical processes, due to the relative lack of the need for solvents and liquid waste.

1.3.1.3 Plasma polymerisation mechanism

The overall mechanism for glow discharge polymerisation is extremely complex consisting of both gas phase and surface reactions and being strongly dependent on plasma parameters. A schematic indicating this complexity is shown in Fig. 1-4.

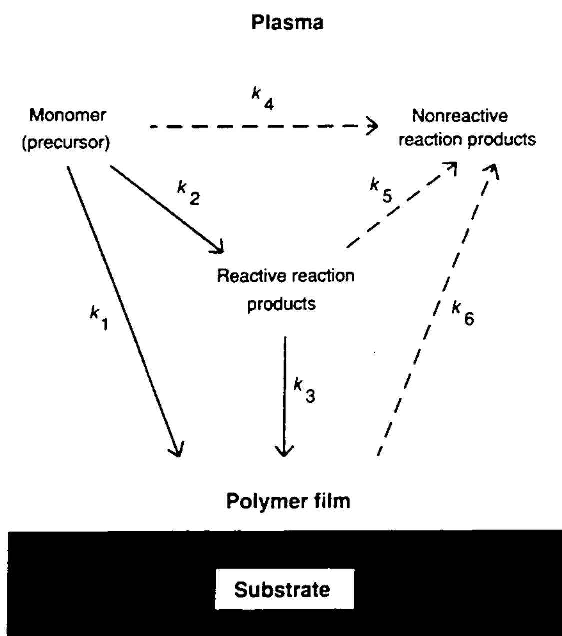

Fig. 1-4: Schematic of reaction pathways and processes occurring during plasma processing. [25]

The overall plasma polymerisation mechanism consists of the three fundamental steps common to most polymerisation mechanisms, i.e. initiation, propagation and termination. The significant difference between plasma polymerisation and conventional polymerisation lies in the inherent complexity of each of the individual steps. Initiation and propagation can occur either through reactions of monomer with previously excited species in the gas phase *or* with radicals at the surface of the polymer. Termination reactions occur with much greater frequency that in conventional polymerisation due to the large number of free-radicals present, however *re-initiation* occurs readily due to irradiation or electron or ion bombardment of the plasma polymer or gas phase species. Previously deposited polymer can react further to yield volatile by-products hence resulting in etching of the plasma polymer and re-incorporation of the products into the gas-phase.

Electron impact can lead to dissociation or desorption of adsorbed molecules or bond breaking within a polymer network. Any surface in contact with the plasma will be subjected to positive ion bombardment due to the presence of the plasma sheath, sec.1.2.3.4. Depending on plasma conditions these ions can have energies anywhere

in the range 10 - 500 eV. The ultraviolet radiation from the plasma has sufficient energy to break chemical bonds and can penetrate to greater depths than any other process.[4,26,27]

The important point to take from Fig. 1-4 is that everything that comes in contact with a plasma can become part of the polymerisation process. Some studies[28] have shown that even the substrate can become part of the plasma polymerisation system. It is precisely because of the enormous number of reactions occurring within the reaction chamber that it is so difficult to determine the exact mechanism of polymerisation in a plasma. The majority of processes occurring within the plasma are highly dependent on not only the type of monomer used but also the operational parameters of the plasma. Hence to gain control over the plasma polymer composition it is necessary to have control or knowledge of a wide variety of plasma parameters.

1.3.2 Pulsed Plasmas

From the discussion so far it is clear that an important aspect of plasma deposition of thin films is the degree of control which can be attained by varying parameters such as pressure, position of the substrate in the reactor, substrate temperature and bias, along with absorbed power and the monomer flow rate which controls the residence time of each molecule in the discharge region. The majority of experiments are conducted under continuous wave conditions whereby the plasma is sustained by continuous supply of power to the system. Even at low powers extensive fragmentation of the monomer molecules occurs resulting in polymeric films formed which often have little structural resemblance to the precursor gas. Hence control of the film properties by choosing appropriate monomers is restricted. An alternative strategy for gaining control over plasma properties and over the properties of the deposited films is by the use of *pulsed power*.

1.3.2.1 Advantages of pulsed plasmas

The nature of pulsed plasmas leads to them having several advantages over continuous wave plasmas including;

1. Reduced heat load on substrates and reactors due to a time averaged reduction of the ion and electron bombardment of the surrounding surfaces. The iona and electron bombardment decay rapidly with the sheath following the start of the off-time. As a result thin films can be produced without damaging a thermally sensitive substrate or any layers which may have been previously deposited.
2. Possibility of production of layered structures by altering the duty cycle of the pulsing the composition of the plasma polymers can be altered during the experiment. Also by syncronising gas pulsing with power pulsing layered structures of completely different compositions can be deposited.
3. Reduced UV emission from the plasma due to the reduction in ion and electron energy results in less crosslinking[29] and loss of structure.
4. Reduced residual free radicals in plasma polymers as a consequence of reduced ion, electron and UV bombrdment in parallel with reaction of surface free radicals with gas phase species in the off-time.[30,46]
5. Control over level of dissociation of parent gas. Extremely high power, short pulses at a low duty cycle allow complete dissociation of precursor gas with minimal heat load on the reactor..
6. The possibility of alternative reaction mechanisms in off-time offers the potential for highly selective reactions hence controlling the composition of the plasma polymer.
7. Elimination of suspended macroscopic particles which sometimes appear in continuous wave reactors, or control over the size and density of particles formed..
8. Possibility for measurement of lifetimes of excited species.

Sec. 1.3.3, p.24 gives examples of where these advantages have been exploited in the literature.

1.3.2.2 Pulsing parameters

In pulsed plasma operation the r.f. power to the system is modulated at a frequency much lower than the usual applied radio frequency. The parameters which can be varied are therefore the plasma on-time, t_{on}, plasma off-time, t_{off} and the amplitude of the pulse in volts which controls the peak power applied to the plasma. These can be represented schematically as shown in Fig. 1-5.

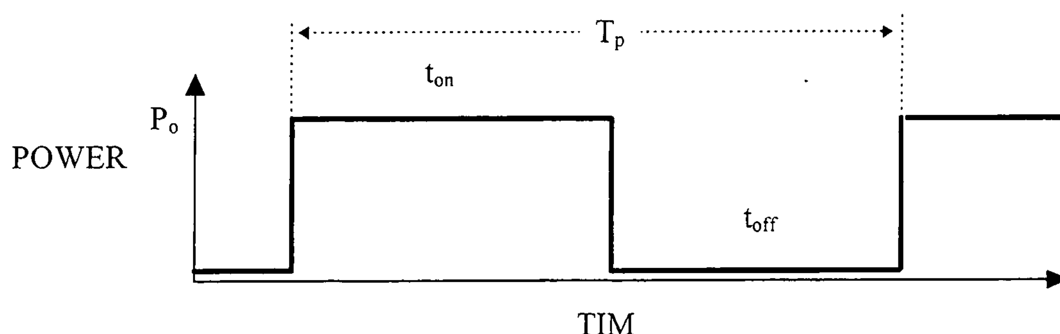

Fig. 1-5: Schematic indicating the relationship between the various pulsing parameters.

T_p is the pulse period and $1/T_p$ is the pulse frequency. The duty cycle is defined as $[t_{on} / (t_{off} + t_{on})] \times 100$ and the average power supplied to the plasma is given by

$$< P >= P_o \times \left(\frac{t_{on}}{t_{on} + t_{off}} \right) \qquad \text{Eq. 1-3}$$

where P_o is the peak r.f. power supplied by the r.f. generator. The average power delivered to the plasma and the frequency of the pulsing are altered by changing the length of the on and off-times.

1.3.2.3 Experimental set-up for pulsed plasmas

Pulsing the r.f. power to the plasma is achieved by driving the r.f. generator with a pulsed analog d.c. voltage from a pulse generator. The various pulsing parameters, frequency, duty cycle etc. can be monitored on an oscilloscope attached to the pulse generator. The oscilloscope can also be used to monitor the response of the plasma to the pulse generator. Fig. 1-6 shows pictures of the oscilloscope screen before and during a typical pulsed plasma polymerisation run.

The appearance of the r.f. is monitored by an antenna inserted into the Faraday cage. Upon plasma ignition the r.f. voltage is detected by the antenna and appears as the central trace on the oscilloscope screen. In this way the response of the r.f. generator to the pulse generator can be monitored. There is a slight delay, $< 10\ \mu s$, after the d.c. signal before r.f. is detected. This is a function of the response time of the r.f. generator, and the ignition of the plasma. Note also that the narrow focused lines on the scope screen from the pulse generator become slightly wider as the oscillating r.f. signal (13.56 MHz) is superimposed on the d.c. signal. This provides a strong indication of the r.f. integrity of the set-up as any r.f. leaks are readily apparent on the d.c. trace.

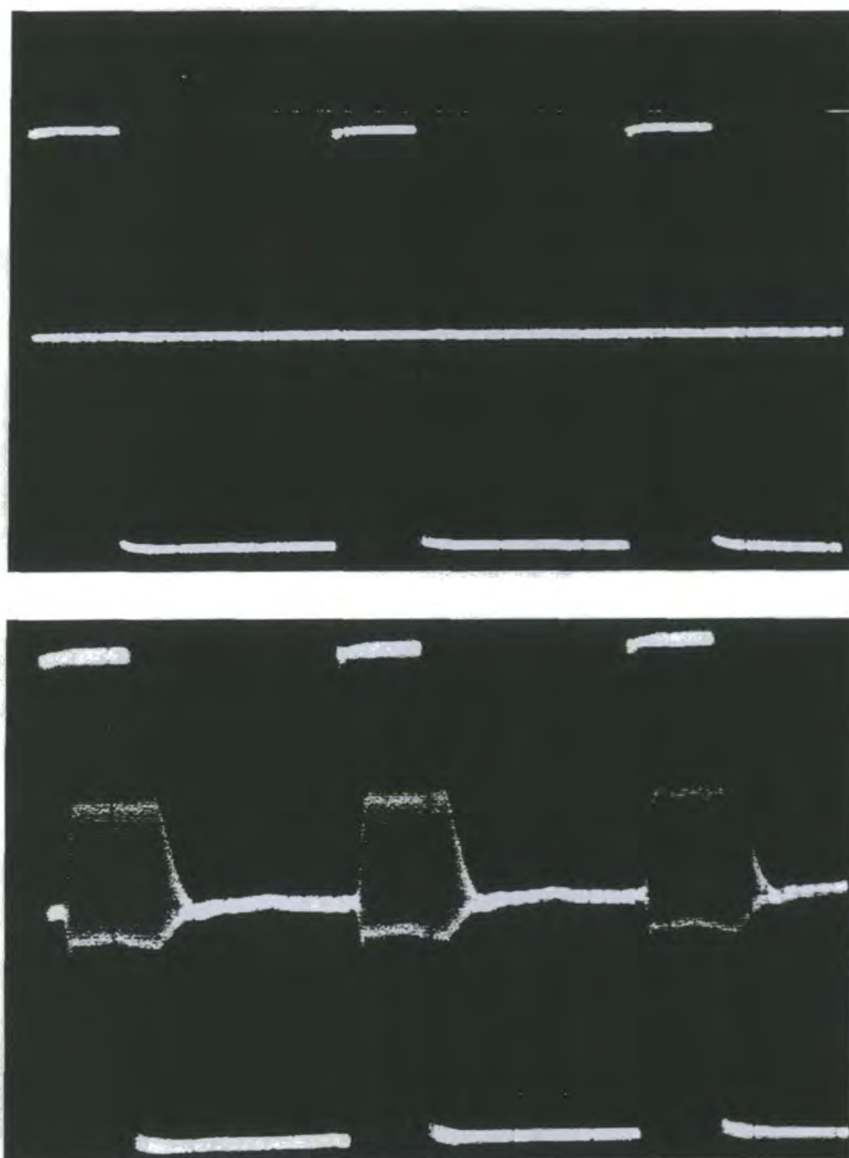

Fig. 1-6: Pictures of oscilloscope screen before (top) and during typical pulsed plasma operation. The upper and lower signals in both figures are the d.c. pulse on and off signals respectively from the pulse generator. The central signal is the voltage reading from the r.f. antenna placed inside the Faraday cage. On-time = 10 μs, off-time = 25 μs.

1.3.2.4 Typical timescales in pulsed plasmas

One of the principle reasons for the use of pulsed plasmas previously was to allow investigation into the timescales of the various processes occurring within glow discharges. By igniting and extinguishing a discharge the rate of decay and formation of various gas-phase species and plasma parameters have been measured. A brief overview of the typical timescales for various processes occurring within a plasma is given below.

1.3.2.4.1 Gas Breakdown.

Before any reactions can take place the plasma must be initiated and hence the first process to be looked at is the breakdown or ionisation of the gas. When a high frequency electric field is applied across a gas, charged particles in the gas are accelerated. Electrons are almost always present in the gas due to ionising cosmic radiation and natural background radiation.[4,31] These electrons will oscillate within the gas provided the walls of the container are sufficiently far apart. Elastic collisions between electrons with sufficient energy and gas molecules will eventually produce excited neutral or ionised atoms resulting in breakdown of the gas.[32] The length of time required before breakdown occurs depends on several factors such as electrode configuration, applied power, ionisation potential of the gas and gas pressure.

Haydon and Plumb[33] studied the electrical breakdown of nitrogen and dry air at pressures in the range ten to hundreds of torr. RF voltages of up to 10 kV with a pulse width of 10 μs were applied across a parallel plate discharge. The length of time needed to produce breakdown i.e. the *formative time* is reduced upon increasing the overvoltage across the gap. With large overvoltages the ionisation growth is rapid and the impedance of the discharge falls rapidly. From DC studies[34] it was found that overvoltages in the range 57 to 75% greater than the voltage needed to sustain the discharge, produce formative times of a fraction of a microsecond in nitrogen. Once the impedance of the discharge is reduced (due to the presence of ions and electrons) the voltage drop across it is reduced and a lower applied voltage is sufficient to sustain the discharge. Haydon found that immediately following the voltage drop there is a large increase in the discharge current and photon output from the discharge. In his model the plasma has attained a steady state after approximately 0.7μs

Boswell[35] studied the plasma breakdown using a pulsed helicon wave plasma. His

plasma conditions involved a 250 W argon plasma at 0.5 mT. The helicon wave pulsed plasma had a magnetic field = 35G and source diameter of 20cm. He found that at breakdown there is initially a high plasma potential associated with high ion energy and low density. Again once breakdown has occurred the density rises rapidly and the voltage decreases with the impedance of the plasma. At the beginning of the pulse the maximum energy of the ions is decreasing and the density is increasing. The potential drops rapidly (50 μs) as the ionisation and loss rates are equalised. The electron density rises rapidly at the start of the pulse to reach a plateaux (100μs). There is an initial high energy spike of electrons which is explained as follows. Initially high energy electrons are produced due to the electric field components along the axis of the reactor. These can cause ionisation and some of them escape to reach the analyser. The loss of these electrons leads to a rapid rise in plasma potential which reduces further loss and results in increased ionisation. It is stated that the plasma potential cannot start to decrease until ions begin to leave the system. The timescale for an ion to be lost radially is of the order of 10 ms. The electron energy distribution changes during the duration of the pulse. The distribution during the occurrence of the spike shows 5% of electrons have energies in excess of 500 eV. As the plasma potential falls the higher energy electrons can escape from the plasma and the average electron energy falls. Also the antenna voltage decreases due to the reduced loading as a results of greater densities in the plasma. This reduces the fields in the plasma so that electrons are not accelerated to such high energies. If the delay between pulses were to be reduced to the decay time of the plasma then the initial spike would be greatly reduced. It should be possible to choose an average electron energy and modify the dissociation by choosing the appropriate repetition rate for the pulsing. Bouchoule and Ranson[36] studied volume and surface processes in a low pressure hydrogen-argon plasma. They found that it took a few microseconds for the electron density to rise and estimated that it took between five and twenty milliseconds to establish chemical equilibrium.

1.3.2.4.2 Effects of pulsing parameters on plasma processes.

Once breakdown has occurred and the discharge is initiated the pulse width and duty cycle determine how much the discharge resembles a continuous wave discharge. If the discharge is sustained for a period of several hundreds of milliseconds or seconds then the plasma behaves much like a continuous wave plasma. Any advantages which could be gained from employing the pulsed technique such as reduced fragmentation or less UV emission will be lost. The only advantage in such a case would be the opportunity for reactions to occur in the off-phase of the cycle which would of course not be possible in the continuous wave mode of operation. It is the off-phase of the cycle and the effects of variation of the off time of the pulse which will now be examined more carefully.

1.3.2.4.3 Plasma Relaxation Mechanisms

Once the power to the discharge has been disconnected the electron density in the gas falls rapidly. The length of time necessary for the electron density to drop depends on the nature of the gas present in the reactor. Overzet[37] *et al* have been studying the effect of pulsing the power on the negative ion flux from radio frequency reactors. The electron energy relaxation times are of the order of a microsecond for the pressures studied.[38,39] The electrons within the gas are completly attached within 5 μs. The decay time constant in CF_4 discharges is of the order of 100 μs, indicating that the attachment processes in the CF_4 discharges are slower than in the helium chlorine discharges and are only slightly faster than the 400 μs seen in Ar discharges Fleddermann *et al*[40] undertook measurements of the electron density and attachment rate coefficient in silane helium discharges and showed that the addition of silane to the gas mixture resulted in a large reduction of the electron density. They concluded that the major loss mechanism was a volumetric loss process most likely dissociative attachment of electrons to a product of the silane dissociation as these fragments would be electronegative.

By comparison the majority of negative ions are swept out of the system on timescales of tens of microseconds. These negative ions would previously have been confined to the central region of the plasma due to the electrostatic sheath surrounding the plasma and would most likely have formed from electron attachment reactions during either the on-time or the off-time of the duty cycle. Havelag and Kono[41] have measured negative ion densities in a radiofrequency plasma of fluorocarbon gases. The results indicate that the negative ion densities are about one order of magnitude greater than the electron densities.

Along with ions there are of course various other excited species in the afterglow of the plasma such as metastable radicals and neutrals. Nieman[42] *et al* studied the formation and decay of metastable fluorine atoms in pulsed fluorocarbon/oxygen discharges using laser induced fluorescence. They suggest that electron impact on CF_4 and ground state fluorine atoms result in the formation of a metastable excited fluorine which has a lifetime of 500 μs. Table 1-2 is a summary of the timescales measured for various plasma processes.

Process	**Timescale**	**Reference**
Gas Breakdown	<1 μs	2
Electron Density Rise	100 μs	3
Steady State	0.7 μs	1
Dissociation of CHF_3	10-100 μs	12
Excited F lifetime	500 μs	11
Chemical Equilibrium	5-20 ms	4
Electron Attachment	5-400 μs	6
Electron energy relaxation times	1-10 μs	6
Radial loss of an ion	10 ms	3
Loss of negative ions	10-100 ms	9

Table 1-2: Timescales of processes occurring in plasmas. Refer to Fig 1-6 and experimental sections of later chapters for a comparision to timescales used in this work.

1.3.3 Pulsed plasmas in the literature

The principle of pulsing the power to the plasma as another means of controlling the plasma properties and composition of the plasma products has been recognised since studies on plasma polymerisation became an important field in their own right. A patent from 1969 seems to be the first reported application of a pulsed glow discharge with advantages over a CW discharge.[43] In it a pulsed styrene vapour discharge resulted in more flexible coatings than the corresponding CW plasma. This same benefit was recently reported for flexible fluorocarbon wire coatings deposited from hexafluoropropylene oxide.[44] Other early studies on the use of pulsed plasmas[45,46] confirmed that different products could be obtained through the use of modulated power. Since these earlier studies the use of pulsed power as a means of controlling the composition the plasma polymers has been largely overlooked. However in the past 3-4 years there has been renewed interest in the area.

Yasuda and Hsu[45,46] studied the effect pulsing power to a glow discharge had on various perfluorocarbon and hydrocarbon monomers by investigating the contact angles and radical densities of the substrates in contact with the plasmas. They found the contact angles changed in response to the compositional changes induced at the surface by depositing plasma polymers using a range of pulsing conditions. They also studied the pressure changes observed upon plasma ignition and deposition rates of plasma polymers from these discharges. The results indicated significant differences between the behaviour of hydrocarbons and perfluorocarbons in plasma polymerisation along with the fact that certain monomers were more sensitive to pulsing that others. Monomers without any functional group susceptible to off-time reaction showed little variation in the products of the plasma polymerisation whether pulsed or continuous wave power was used.

The possibility of off-time reactions allows for novel approaches to be taken to achieve specific surface properties. Off-time reduction of halide containing

organometallic films can reduce or even completely eliminate the halide content at the surface resulting in a metallic film at low substrate temperatures.[47-49] Llewellyn *et al* have used pulsed plasma deposition to deposit aluminium and tin onto room temperature substrates. By using high powered short pulses they were able to completely dissociate the precursor gas allowing high quality metal films to be deposited without the need for high substrate temperatures.

Pulsed plasmas have also been shown to be effective in controlling the density and size distribution of nanosized particles formed in organometallic plasma polymers.[50,51] Varying duty cycle effects the size and distribution of the nanoparticles and the metallic nature of the films. Pulsing also aids in reducing powder formation in silane discharges.[52] It is suggested that negative ions are the precursors to powder formation. Pulsing reduces the build-up of these negative ions by allowing diffusion to the surrounding surfaces in the off-time.[37]

Pulsed plasmas are particularly useful for modifying the surfaces of substrates with non-planar geometries. Treatment of the inside surfaces of catheters to improve their biocompatibility has been carried out using pulsed plasma polymerisation. During the off-time the reactive species can diffuse along the inside of the tube resulting in uniform deposition on all surfaces.[53] Pulsed microwave plasmas have been used for homogeneous deposition of siloxane plasma polymers on three-dimensional substrates.[54]

Timmons *et al*[55-57] studied the effect of a radio frequency pulsed plasma on fluorocarbon monomers. The compositions of the films produced were analysed using X-ray photoelectron spectroscopy and Fourier transform infrared spectroscopy. The studies showed progressive and substantial change in the molecular composition of the plasma deposited films with variations in duty cycle. Significantly it appears that a relatively high level of compositional control is possible, a fact which could be exploited in designing films with specific properties. Further work by the same

author and other workers in recent years has indicated the extent to which pulsed plasmas can be exploited to control plasma polymer composition.[58-61]

Pulsed plasmas have also found application in plasma-etch technology.[62] Samukawa[63] used a time modulated ECR plasma discharge for controlling the polymerisation in SiO_2 etching. 10-100 μs pulse widths were used and good correlation was found between the density ratio of CF_2 radicals and atoms in the CHF_3 plasma and the combination of the pulse duration and intervals. This method provides for control of the polymerisation and achievement of highly selective etching to Si during SiO_2 etching. For highly selective SiO_2 etching it is effective to reduce F-atom generation and to deposit low-fluorine polymer by using a pulsed discharge of 10-20 μs. The authors claim this also leads to an increase in deposition rate due to an increase in the relative number of CF_x radicals absorbed onto the surface at this repetition rate. At a fixed pulse width of 10 μs the F/CF_2 ratio changed with changing pulse interval. This is attributed to the difference in the rates of reactions producing the different species. When the interval time is more than 10 μs the CF_2 radical density decreases and this is considered to be due to the difference in lifetimes between CF_2 radicals and F atoms.

Boswell and Porteus[64] have studied the etching of silicon using SF_6 gas in a pulsed plasma. The advantage of pulsing the plasma is a reduced heat load on the reactor. With a duty cycle of 20% the temperature could be held within a few degrees of ambient. For long pulses the mean etch rate is approximately 20% of the continuous wave etch rate as would be expected. However for decreasing pulse lengths the etch rate is seen to increase until at a pulse duration of 2 ms the etch rate is the same as for the continuous wave experiment. Recently there has been much interest in pulsed plasmas as a means of reducing lateral etching at oxide interfaces in silicon etch processes.[65]

1.3.4 Aims of current work

The aim of this thesis is to explore to what extent pulsed plasmas can be used to control the composition of plasma polymers deposited from a range of monomers in an low pressure glow discharge. By investigating the chemical structure of the resultant surfaces, this thesis will aim to examine the effect of varying pulsing parameters on the plasma polymerisation process and to what extent monomer structure influences the amount of selectivity attainable through the use of pulsed power.

1.4 CHARACTERISATION TECHNIQUES

Plasma polymers have been analysed by a wide variety of techniques since studies in this area began.[57,82,86-89] This work provides examples of the use of X-ray photoelectron spectroscopy, transmission FT-IR spectroscopy, UV-visible spectroscopy, atomic force microscopy and deposition rate studies. Work was also carried out using the synchrotron radiation source at Daresbury using X-ray Absorption Spectroscopy (XAS) to study pulsed plasma polymer composition. This work has been reported elsewhere.[66]

1.4.1 X-ray Photoelectron Spectroscopy (XPS)

1.4.1.1 Introduction.

The establishment of X-ray photoelectron spectroscopy as an important technique for determining not only the elemental, but also the chemical composition of a surface, can be traced back to the work of Kai Siegbahn's group in Uppsala, Sweden in the period 1955-1970.[67] It was Siegbahn, who was awarded a Nobel prize for his work, who first realised that the chemical environment of the atom had a significant effect on the apparent binding energy of the electrons in the sample. He coined the

acronym ESCA, electron spectroscopy for chemical analysis, to allow for this, and for the fact that Auger peaks were also present in an 'XPS' spectrum.[68] X-ray photoelectron spectroscopy is now an extensively used non-destructive technique in the characterisation of surfaces. It has been used to study the surfaces of polymers,[69,70] copolymers[71,72,73] and blends along with monitoring the modification of surfaces via plasma treatment and/or UV irradiation.[21,74,75] For surfaces containing functional groups which are normally indistinguishable via XPS, there are now a wide variety of reagents available for the chemical derivatisation of the surface to allow the individual species to be identified.[76]

1.4.1.2 The photoelectric effect

In its simplest form XPS involves irradiating a sample with photons from the X-ray region of the electromagnetic spectrum and studying the kinetic energies of the photoemitted electrons which escape from the sample as a result of absorption of the X-rays. The photoemission of electrons can be represented schematically as in Fig. 1.11.[77]

The process involves energy transfer from the photon to the atom and momentum is conserved. As the energy of each incident photon is known, if the kinetic energy of the photoelectron is measured, then the binding energy of the electron in the original atom can be calculated. This can be seen from the basic equation of photoelectron spectroscopy

$$KE = h\nu - BE - \phi_s \qquad \text{Eq. 1-4}$$

where KE = kinetic energy of the photoemitted electron, h = Planck's constant, ν = frequency of X-rays, BE = the binding energy of the electron in the atom and ϕ^s is the work function of the spectrometer.

1.4.1.3 Surface sensitivity

As stated earlier XPS is a surface sensitive technique due to the fact that only electrons from a few tens of Angstroms of the surface can escape to be analysed. Fig. 1-8 shows a plot of inelastic scattering mean free paths of electrons as a function of energy. As can be seen, for the energies of interest, 100-1000 eV, the mean free paths vary between 10 and 100 monolayers.[78] Hence the electrons are only originating from the first few atomic layers and the technique is a highly surface sensitive one.

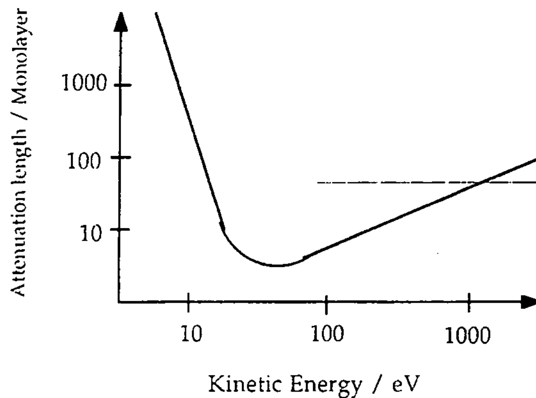

Fig. 1-8: Inelastic mean free paths of electrons in a solid as a function of energy.

1.4.1.4 Instrumentation

A schematic of the essential components of an XPS spectrometer is shown in Fig. 1-9 followed by a brief description of the harware requirements and features of the spectrometer.

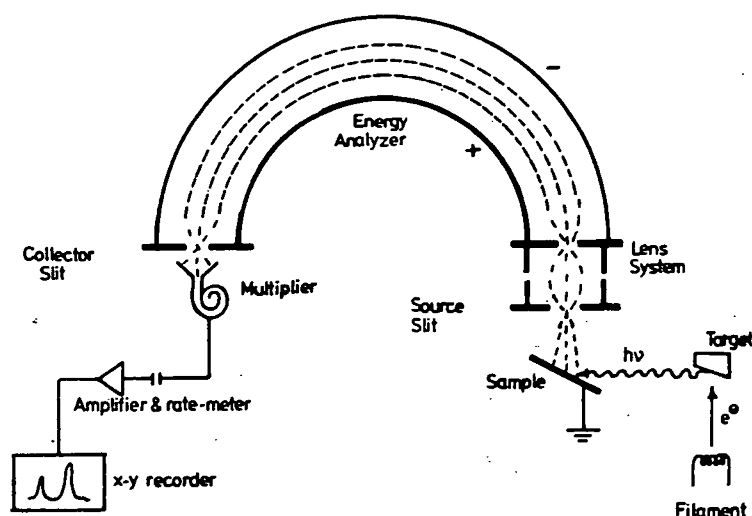

Fig. 1-9: Schematic of an XPS spectrometer.

1.4.1.4.1 Ultra high vacuum requirement.

In XPS as in most other surface characterisation techniques ultra high vacuum, between 10^{-8} and 10^{-10} torr, is required. This is essential to prevent surface contamination of the sample and minimise inelastic collisions of the photoelectrons.

1.4.1.4.2 Photon Sources.

X-rays are generated by bombarding a target with high energy electrons which have sufficient energy to knock out core electrons from atoms of the target. Electrons from higher levels within these atoms then fill the holes in the inner level and release their extra energy in the form of X-rays.

The target needs to have several specific properties. It should be a good conductor of heat as the heat generated by the colliding electrons will need to be dissipated easily. This requires that the target be made of metal. The emission spectrum of the target should consist of a few sharp lines against a low background caused by bremsstrahlung. These sharp lines should have a narrow linewidth and be of sufficiently high energy to excite the electrons of interest in the sample. Aluminium and magnesium are the most common metals used as anodes. The Mg $K\alpha_{1,2}$ line which was used in this work, has a linewidth of 0.7 eV and generates photons of

energy 1253.6 eV.[79] Emission occurs as a result of electron decay from the $2p_{1/2}$ and $2p_{3/2}$ levels to the 1s energy level.[80] The spectrum is dominated by the $\alpha_{1,2}$ emission but the $\alpha_{3,4}$ lines are important also. This doubly ionised transition gives rise to satellite lines in the XPS spectrum of about 8% the intensity of the parent peak and with kinetic energies about 8 eV higher.

The target is separated from the sample by a thin (several microns) aluminium window. This protects the sample from both stray electrons from the X-ray source filament and hydrocarbon contamination which may be boiled off the X-ray target.

1.4.1.4.3 Electron Analyser.

Once the electrons have been emitted from the sample they need to be analysed to determine the range of kinetic energies present. A concentric hemispherical analyser (CHA) as shown schematically in Fig. 1-9 consists of two concentric hemispherical[81] surfaces with a potential difference applied across them. The potential is such that the outer hemisphere is at a negative potential relative to the inner. Electrons enter the analyser at the source slit and for a given ΔV only electrons of a certain kinetic energy will be deflected in the right path to exit the analyser at the collection slit. Here they are collected by a channeltron which amplifies the signal to the data collection software. Varying electrostatic fields act as lenses to allow only electrons of a specific kinetic energy through the analyser.

The resolving power of the analyser is given by $\Delta E/E$ where ΔE is the half-width and E is the kinetic energy of the electrons entering the analyser. The resolving power of the analyser is given by:

$$\frac{\Delta E}{E} = \frac{R}{W} \qquad \text{Eq. 1-5}$$

where R is the mean radius of the hemisphere and W is the combined width of the slits. The easiest way to improve the resolution of the spectrometer is to reduce the kinetic energy of the electrons prior to them entering the analyser. The CHA is

usually operated in one of two retarding modes. In FRR (fixed retardation ratio) mode the electrons are retarded by a constant ratio of their initial kinetic energies. In the second retarding mode the electrons are decelerated to a constant pass energy and hence the analyser is set at a constant absolute resolution. This mode is known as fixed analyser transmission, FAT mode.

1.4.1.5 Spectral Interpretation

The position of the peaks in the XPS spectrum not only depends on the binding energy of the core electron prior to excitation, but also on any collisions or energy transfer processes it undergoes following excitation. An example of a typical widescan XPS spectrum is shown in Fig. 1-10

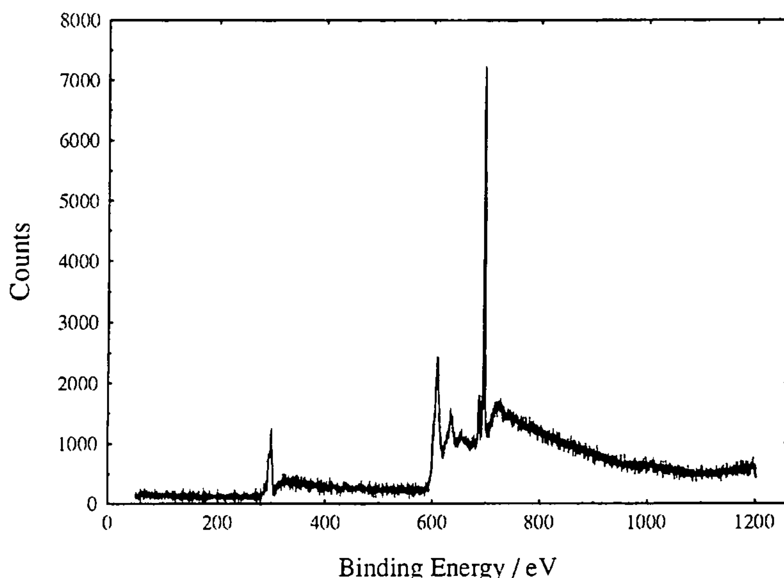

Fig. 1-10: Low resolution XPS spectrum of a plasma polymer deposited from a perfluorocyclohexane discharge.

The characteristic step-like spectrum shows both primary XPS features and secondary Auger features. The step-like appearance of the spectrum is a result of the cumulative effects of the inelastic kinetic energy tails on the lower kinetic energy side of the elastic peaks. As the excited primary electrons pass through the solid, prior to reaching the surface a certain fraction of them undergo inelastic collisions whereby they lose energy. When these electrons enter the analyser they have slightly

less energy than the elastically scattered electrons and result in the formation of the low kinetic energy tail behind the main peak.

When the photoelectron loses energy to another electron resulting in the excitation of that other electron to a higher energy level within the atom, the process is known as *shake-up*. Shake-up peaks are particularly prominent in polymers containing aromatic rings and are often used as an indication of the level of aromaticity of a material.[82] When the photoelectron loses energy to another electron resulting in the emission of that other electron, the process is known as *shake-off*.

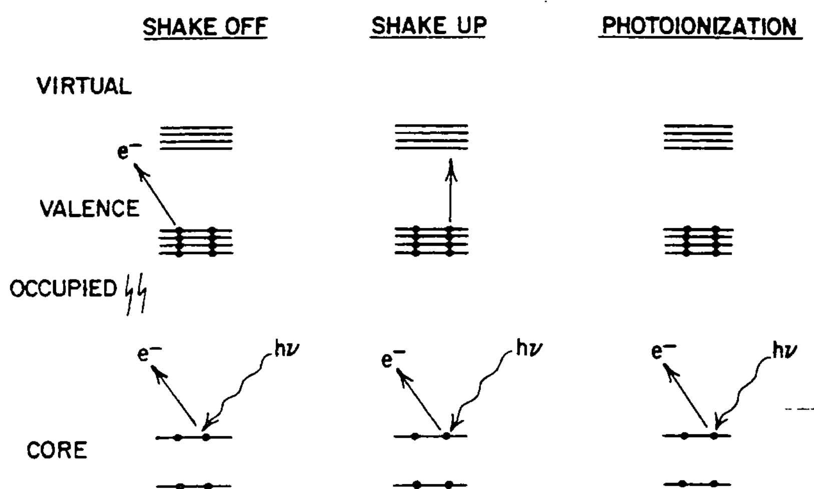

Fig. 1-11: Schematic of shake-up and shake-off energy loss mechanisms.

1.4.1.5.1 Chemical Shift in XPS

Core level spectroscopy can be used not only for determination of the elemental composition of the surface region but also provides information on the oxidation states of the various elements present and the chemical environment surrounding the atoms.[83] The *chemical shift* of a core level is due to the fact that the electron density around a nucleus is dependent on the nature of the atoms bonded to it. The binding energy of an electron is a balance between the potential of the nucleus and the repulsive Coulomb interaction with other electrons. The change in the electron density distribution as a result of bonding causes a shift in binding energy of core level electrons. A highly electronegative element such as fluorine induces a large

change in binding energy due to the large effect it has on the charge density surrounding the target atom.

Fig. 1-12 shows part of the photoelectron spectrum of ethyl chloroformate.[84] The three separate peaks in the C 1s region are due to the different chemical environments surrounding the three carbon atoms, whilst the presence of the chlorine peak indicates the use of XPS for elemental analysis..

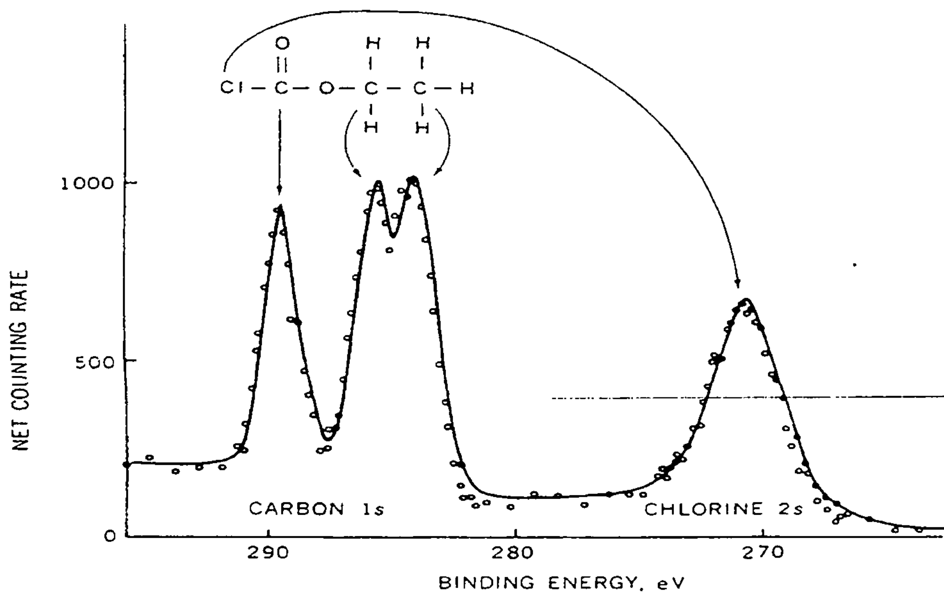

Fig. 1-12: XPS spectrum of ethyl chloroformate.

Fig. 1-13 shows a carbon 1s spectrum of polyvinylidene difluoride (PVDF).[85] The carbon bonded to hydrogen gives a peak at 286.1 eV while the carbon bonded to fluorine gives a peak at 290.6 eV. The increase in binding energy of C-F_x carbons is due to a reduction in the level of electrostatic screening on the carbon core electrons due to the high electronegativity of the fluorine atoms. Fluorine attached to carbon induces a very large chemical shift which is also dependant on the number of fluorine atoms bonded to the carbon. The fluorine effect of fluorine is strong enough such that even carbons not directly attached to fluorine have their core levels shifted. The effect of fluorine makes XPS an ideal method for investigating the composition of fluorine containing plasma polymers.

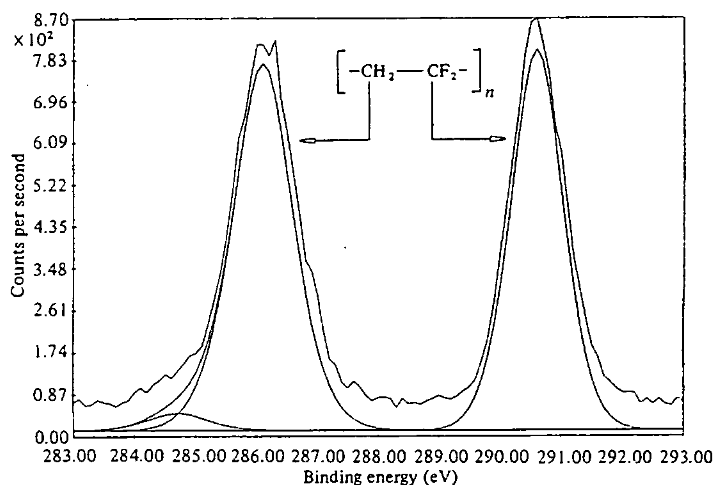

Fig. 1-13: XPS spectrum of PVDF.

1.4.1.5.2 Line Shape Analysis of XPS spectra

Line shape analysis or peak fitting of XPS spectra involves deconvoluting the broad XPS envelope into its individual component peaks of narrower linewidth. Clark *et al* have carried out extensive studies[86-93] on fluorocarbon polymers using XPS techniques, and with the aid of peak fitting software the various C-F functionalities can be distinguished. Peaks were assigned based on binding energy values from the literature. Fig. 1-14 shows the peak fitted high resolution XPS spectrum of plasma polymerised perfluoroallylbenzene.

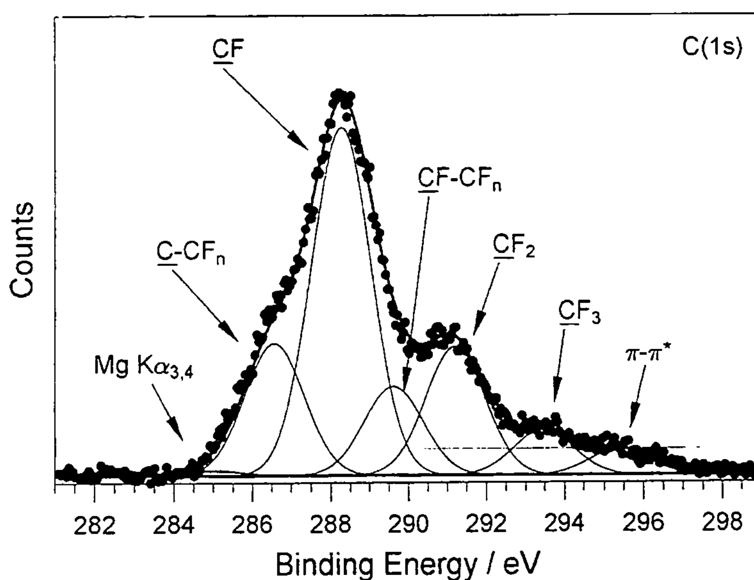

Fig. 1-14: C 1s spectrum of a perfluoroallylbenzene plasma polymer.

The measured linewidth, full width at half maximum (FWHM), for core levels is a combination of the following;

(a) linewidth of the X-ray source,

(b) the contribution to the FWHM due to the spectrometer

(c) the natural width of the core level under investigation

The contributions from (a) and (c) are essentially Lorentzian line shapes while (b) is usually Gaussian in shape. The combination of the various contributions to the overall line width results in a hybrid shape with a Gaussian distribution dominating and a Lorentzian character to the tails. It has been shown that the assumption of a pure Gaussian shape for the observed peaks introduces only a negligible error in peak fitting.[94]

1.4.1.5.3 Depth Profiling using XPS.

As explained earlier the sampling depth in XPS is limited to between 10 and 100 Å due to the inelastic mean free path of electrons in a solid. The probability of an inelastic scattering event occurring is a random process and is described by the exponential decay law.[85]

$$I(x) = I_o \exp(-x / \lambda(E_k, Z)\cos\theta) \qquad \text{Eq. 1-6}$$

or more simply [95]

$$l = \Phi\cos\theta \qquad \text{Eq. 1-7}$$

where l is the escape depth and Φ is the Inelastic Mean Free Path (IMFP) of the photoelectrons. The important point is that photoelectron intensity is related to cos θ where θ is the angle of emission relative to the normal to the surface. For example a sample studied at normal emission would have three times the sampling depth of one studied at an angle of 70° to the surface normal. Hence by varying the angle at which the electrons are collected the sampling depth can be varied. This allows a compositional depth profile of the sample to be obtained. This method of depth profiling is termed *angle resolved X-ray photoelectron spectroscopy (ARXPS).*

Although it is a non-destructive technique, one of the major limitations of this technique is of course that the sampling depth is limited to about 100 Å due to the limitations imposed by the inelastic mean free paths of the electrons.

1.4.2 Infrared Spectroscopy

Transmission infrared spectroscopy can be used to gain information on the bulk composition of the plasma polymers. Absorption of electromagnetic radiation of wavelength λ increases the energy of the molecule by an amount ΔE according to the equation:[96]

$$\Delta E = hc/\lambda \qquad \text{Eq. 1-8}$$

where h = Planck's constant and c = speed of light.

Depending on the wavelength of the incident radiation the absorbed energy may be in the electronic, vibrational or rotational energy levels of the molecule. Radiation from the infrared region of the electromagnetic spectrum leads to increases in the vibrational and rotational energy of the molecule. The vibration induced by the absorption of the electromagnetic radiation must result in a change in the dipole moment of the molecule in order for absorption to be allowed under classical theory. The intensity of absorption is proportional to this change in dipole moment, hence highly polarised bonds e.g. C=O give rise to stronger absorptions than purely covalent bonds e.g. C-C.

Specific functional groups have characteristic absorption frequencies associated with them. By studying a range of infrared frequencies and the positions of the absorptions information on the functional groups present within the plasma polymer can be gained. Infrared spectra of plasma polymers generally consist of fairly broad bands relative to the monomer. This indicates the formation of a large variety of slightly different chemical environments for each functional group within the plasma polymer.[97]

The transmission infrared spectra of the plasma polymers are collected by placing an IR-transparent potassium bromide disk in the plasma during the polymerisation run. XPS analysis shows that plasma polymers deposited in this way have the same surface composition as those deposited onto glass slides. Attenuated Total Reflectance infrared spectroscopy (ATR-IR) which probes the top several microns of the plasma polymer gives identical IR spectra to the transmission experiments. The results indicate the compositional homogeneity with depth of the plasma polymers deposited from both continuous and pulsed plasmas.

1.4.3 Atomic Force Microscopy

Atomic force microscopy (AFM) is used to study the topography of surfaces and was invented in 1986 by Binnig[98] to study the surfaces of non-conducting samples on the atomic scale.[99] A schematic of the AFM experimental set-up is shown in Fig. 1-15. In AFM a sharp tip mounted on a cantilever is brought close enough to the surface of a sample such that it interacts with the atoms at the surface. The atomic force between the tip and the sample is monitored via the deflection of the cantilever. This is measured using an optical system composed of a laser and a split photodiode.[100] Once the deflection of the cantilever is detected a feedback loop moves the sample stage in the z direction to maintain a constant distance between the sample surface and the tip. This movement of the stage is a mirror of the topography of the surface and can be plotted to generate an image of the surface.

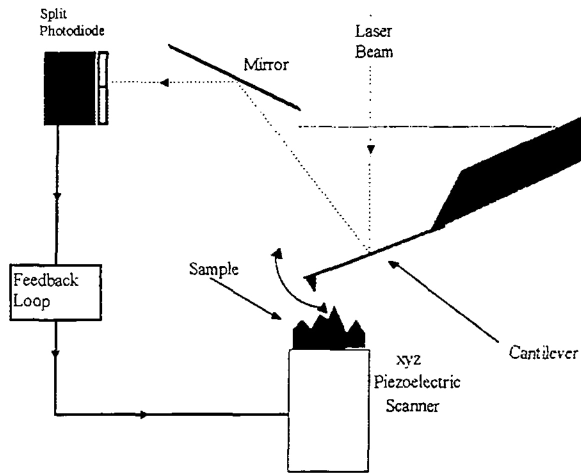

Fig. 1-15: Experimental set-up of atomic force microscope.

The AFM can be operated in various modes in order to measure the surface forces. The two most common operating modes used to determine topography are contact mode and Tapping® mode. In contact mode the sample and tip are in close contact throughout the entire scan. In Tapping® mode[102,101,102] the tip oscillates close to its resonant frequency. The tip is made to strike the surface at the downward apex of each cycle and small changes in the oscillation amplitude can be detected. In this mode the force imparted on the sample is very small, $10^{-10} - 10^{-9}$ N,[103] and since the tip is not dragged along the surface there are virtually no shear forces.

1.5 REFERENCES

(1) Grill, A. *Cold Plasmas in Materials Technology*; IEEE Press: Piscataway: New Jersey, 1994.

(2) Langmuir, I. *Phys. Rev.* **1929**, *33*, 954.

(3) Riley, P.E. *J. Electrochem. Soc.* **1993**, *140(5)*, 1518.

(4) Chen, F.F. *Introduction To Plasma Physics* ; Plenum Press: New York, 1974.

(5) Haaland, P.D., Clarson, S,J. *Trends in Polym. Sci.* **1993**.

(6) Elliasson, B.; Kogelschates, U. *IEEE Trans. on Plasma Science* **1991**, *19*, 6.

(7) Chandrakar, K. *J. Phys. D: Appl. Phys.* **1978**, *11*, 1809.

(8) Hollaghan, J.R.; Bell, A.T.; Eds., *Techniques and Applications of Plasma Chemistry*, Wiley, New York, 1974.

(9) Barrow, *Physical Chemistry 5th ed*, McGraw Hill: London, 1988; p 34.

(10) Rossnagel, S.M. *Thin Film Processes II* Vossen, J.L.; Werner, K. Eds. Academic Press: London, 1991; p. 21.

(11) Sheu, G.S.; Shyu, S.S. *J. Adhes. Sci. & Tech.* **1994**, *8*, 531.

(12) Gerenser, L.J. *J. Adhes. Sci. & Tech.* **1987**, *4*, 303.

(13) Dynes, P.J.; Kaelbe, D.H. *J. Macromol. Sci. Chem.* **1976**, *A10*, 535.

(14) Egitto, F.D.; Matienzo, L.J.; Blackwell,K.J.; Knoll, A.R. *J. Adhes. Sci. & Tech.* **1994**, *8*, 411.

(15) Garbassi, F.; Morra, M. *Surf. Interface Analysis*, **1989**, *17*, 585.

(16) Coburn, J.W. *IEEE Trans.Plasma Sci.* **1991**, *19*, 1048.

(17) Khairallah, Y.; Arefi, F.; Amouroux, J.; Leonard, D.; Bertrard, P. *J. Adhes. Sci. & Tech.* **1994**, *8*, 363.

(18) Hansen, R.H. *J. Polym. Sci.* **1965**, *A3*, 2205.

(19) Tobin, J.A.; Denton, D.D. *Appl. Phys. Letts.* **1992**, *60*, 2595. **60** (21), 2595 (1992).

(20) Berger, J.M.; Ferraton, J.P.; Yous, B.; Donnadieu, A. *Thin Solid Films* **1981**, *86*, 337.

(21) Wells, R.K.; Badyal, J.P.S. Drummond, I.V.V.; Robinson, K.S.; Street, F.J. *J. Chem. Soc. Chem. Comm.* **1991** *(6)*, 549.

(22) Barkanic, J.A.; et al *Solid State Tech.* **1989**, *32(4)*, 109.

(23) Pearton, S.J.; Ren,F. *J. Mater. Sci.- Mat. Electronics.* **1994**, *5(1)*, 1.

(24) Clark, D.T.; Dilks, A.; Shuttleworth,D. *Polymer Surfaces*, Clark,D.T.; Feast, W.J. Eds.; Wiley: New York, 1978; Ch. 9.

(25) Oehrlein, G.S. *Surf. Sci.* **1997**, *386*, 222.

(26) Liston, E.M. *J. Adhesion.* **1989**, *30*, 199.

(27) Clark, D.T.; Dilks, A. *J. Polym. Sci. Chem. Ed.* **1977**, *15*, 2321.

(28) Masuoha, T.; Yasuda, H. *J. Polym. Sci. Polym. Chem. Ed.* **1981**, *19*, 2937.

(29) Lau, K.K.S., Gleason, K.K. *J. Phys. Chem. B* **1997**, *101(35)*, 6839.

(30) Labelle, C.B.; Limb, S.J.; Gleason, K.K. *J. Appl. Phys.* **1997**, *82(4)*, 1784.

(31) Chapman, B. *Glow Discharge Processes*, Wiley: New York, 1980.

(32) M[C]Taggart, F.K. *Plasma Chemistry in Electrical Discharges*; Elsevier Publishing Company: London, 1967.

(33) Haydon, S.C.; Plumb, I.C. *J. Phys. D: Appl. Phys.* **1978**, *11*, 1721.

(34) Chalmers, I.D.; Telford, D.J. *J. Phys. D: Appl. Phys.* **1975**, *8*, 943.

(35) Boswell, R.W.; Perry, A.J.; Vender, D. *J. Vac. Sci. Tech.* **1991**, *B9(2)*, 307.

(36) Bouchoule, A.; Ranson, P. *J. Vac. Sci. Tech.* **1991**, *A9*, 317.

(37) Overzet, L.J. *J. Appl. Phys.* **1992**, *72(12)*, 5579.

(38) Flamm, D.L. *J. Vac. Sci. Tech.* **1986**, *A4*, 729.

(39) Kushner, M.J. *J. Appl.Phys.* **1988**, *63*, 2226.

(40) Fleddermann, C.B.; Bebermann, J.H.; Verdeyen, J.T. *J. Appl. Phys.* **1985**, *58*, 1344.

(41) Haverlag, M.; Kono, A. *J. Appl. Phys.* **1991**, *70*, 3472.

(42) Nieman, G.C.; Colson, S.D. *Appl. Phys. Lett.* **1990**, *56*, 719.

(43) Manuel, E.H. U.S. Patent 3,471,316, 1969: Abstract C.A. 1969, *71*, 114299a.

(44) Limb. S.J.; Gleason, K.K.; Edell, D.J.; Gleason, E.F. *J. Vac. Sci. Tech.* **1997**, *A15(4)*, 1814.

(45) Yasuda, H., Hsu, T. *J. Polym. Sci. Polym. Chem. Ed.* **1977**, *15*, 81.

(46) Yasuda, H., Hsu, T. *J. Polym. Sci. Polym. Chem. Ed.* **1977**, *15*, 2411.

(47) Hiramatsu, K.; Ohnishi, H.; Takahama, T.; Yamanishi, K. *J. Vac. Sci. Tech.* **1996**, *A14(3)*, 1037.

(48) Llewellan, I.P.; Rimmer, N. *Thin Solid Films* **1990**, *191*, 135.

(49) Llewellan, I.P.; Scarsbrook, G. *J. Vac. Sci. Tech.* **1989**, *A7*, 1099.

(50) Chen, Xl; Rajeshwar, K.; Timmons, R.B.; Chen, J.J.; Chyan, O.M.R. *Chem. Mater.* **1996**, *8(5)*, 1067.

(51) Buss, R.J.; Babu, S.V. *J. Vac. Sci. Tech.* **1996**, *A14(2)*, 577.

(52) Courteille, C.; Dorier, J.L.; Hollenstein, C.; Sansonnens, L.; Howling, A.A. *Plasma Sources Sci. & Tech.* **1996**, *5*, 210

(53) Jansen, F.; Krommenhoek, S. *Thin Solid Films* **1994**, *252(1)*, 32.

(54) Soll, C.; Theirlich, D.; Ningel, K.P.; Engemann, J. *Le Vide Science And Technique And Applications* **1997**, *284,* 154.

(55) Timmons, R.B., Savage, C.R., Lin, J.W. *Chem. Mater* **1991**, *3*, 575.

(56) Rinsch, C.L.; Chen, X.; Panchalingam, V.; Savage, C.R.; Wang, Y.H.; Eberhart, R.C.; Timmons, R.B. *Abs. Pap. ACS*, **1995**, *200(2)* 141.

(57) Savage, C.R.; Timmons, R.B.; Lin, J.W. in *Structure-Property Relations in Polymers* Eds. Urban M.W.; Craver, C.D. Advances in Chemistry Series, Vol 236, A.C.S., 1993.

(58) Beyer, D.; Knoll, W.; Ringsdorf, H.; Wang, J.H.; Timmons, R.B. Sluka, P. *J. Biomedical. Mater. Res.*, **1997**, *36*, 181.

(59) Ryan, M.E.; Hynes, A.M.; Badyal, J.P.S. *Chem. Mater.* **1996**, *8*, 37.

(60) Mackie, N.M.; Dalleska, N.F.; Castner, D.G.; Fisher, E.R. *Chem. Mater.* **1997**, *9(1)*, 349.

(61) Mackie, N.M.; Fisher, E.R. *Polymer Preprints*, **1997**, *38(1)*, 1059.

(62) Boswell, R.W.; Henry, D. *Appl. Phys. Lett.* **1985**, *47*, 1095.

(63) Samukawa, S. *Jpn. J. Appl. Phys.* **1993**, *32(12B)*, 6080.

(64) Boswell, R.W., Porteus, R.K. *J.Appl.Phys.* **1987**, *62*, 3123.

(65) Meyyappan, M. *Jap. J. Appl. Phys: Part 1* **1997**, *36(7B)*, 4820.

(66) Ryan. M.E.; Hynes. A.M.; Wheale. S.H.; Badyal. J.P.S.; Hardacre, C.; Ormerod, R.M.; Chem. Mater. **1996**, *8*, 916.

(67) Siegbahn, K.; Nordling,C.; Fahlman, A.; Nordberg, R.; Hamrin, K.; Hedman, J.; Johansson, G.; Berkmsrk, T.; Karlsson, S.E.; Ligren, I.; Lindberg, B. *ESCA, Atomic, Molecular And Solid State Structure Studied By Means Of Electron Spectroscopy,* Almquist And Wiksells: Uppsala; 1967

(68) Wertheim, G.K. *J. Franklin Institute* **1974**, *298*, 289.

(69) *Handbook of X-ray and Ultraviolet Photoelectron Spectroscopy*, Driggs, D. Ed., Heydon: London, 1977.

(70) Clark, D.T. *Characterisation of Metal and Polymer Surfaces* Lee, L.H. Ed., Academic Press: London, 1977.

(71) Thomas, H.R.; O'Malley, J.J. *Macromolecules*, **1979**, *12*, 323.

(72) Clark, D.T., Peeling, J., O'Malley, J.M., *J. Polym. Sci. Polym. Chem. Ed.*, **1976**, *14*, 543.

(73) Alliver, K., et al, *J. Polym. Sci. Polym. Chem. Ed.*, **1990**, *28*, 173.

(74) Shard, A.G.; Munro, H.S.; Badyal, J.P.S. *Polym. Comm.* **1991**, *32*, 152.

(75) Badyal, J.P.S., Chambers, R.D., Chvatal, Z., *J. Chem. Soc. Faraday Trans.* **1991**, *87*, 991.

(76) Redley, C.N., Everhart, D.S., *Applied Electron Spectroscopy for Chemical Analysis;* Windewi, H., Ho, F. Eds.; Wiley-Interscience: New York, 1982.

(77) Ohring, M., *The Materials Science of Thin Films,* Academic Press, 1992, p 278.

(78) Briggs, D., Seah, M.P. Eds.; *Practical Surface Analysis 2nd ed. Vol.1;* Wiley: London, 1990; p. 207.

(79) Sabbatini, L., Zambini, P.G. *Surface Characterisation of Advanced Polymer;* VCH 1993.

(80) Woodruff, D.P., Delchar, T.A. (eds), *Modern Techniques of Surface Science;* Cambridge University Press: Cambridge, 1986; p. 98.

(81) Ref. No. 78, p76.

(82) Clark, D.T., Dilks, A. *J. Polym. Sci. Polym. Chem. Ed.* **1976**, *14*, 533.

(83) Ref. 9, p. 582.

(84) Walls, J.M. *Methods of Surface Analysis;* Cambridge University Press: Cambridge, 1989; p. 136.

(85) Clark, D.T.; Shuttleworth, D. *J. Polym. Sci., Polym. Chem. Ed.* **1980,** *18,* 407.

(86) Clark, D.T.; Shuttleworth, D. *J. Polym. Sci. Polym. Chem. Ed.* **1979,** *17,* 1317.

(87) Clark, D.T.; Shuttleworth, D. *J. Polym. Sci. Polym. Chem. Ed.* **1982,** *20,* 1717.

(88) Clark, D.T.; Shuttleworth, D. *J. Polym. Sci., Polym. Chem. Ed.* **1980,** *18,* 27.

(89) Clark, D.T.; Abrahman, M.Z. *J. Polym. Sci., Polym. Chem. Ed.* **1981,** *19,* 2129.

(90) Clark, D.T.; Abrahman, M.Z. *J. Polym. Sci., Polym. Chem. Ed.* **1981,** *19,* 2689.

(91) Clark, D.T.; Abrahman, M.Z. *J. Polym. Sci., Polym. Chem. Ed.* **1982,** *20,* 691.

(92) Clark, D.T.; Abu-Shbak, M.M. *J. Polym. Sci., Polym. Chem. Ed.* **1983,** *21,* 2907.

(93) Siegbahn, K.; Nordling, C.; Johansson,G.; *ESCA Applied To Free Molecules,* North-Holland Pub. Co.: Amsterdam, 1969

(94) Garbassi, F., Morra, M., Occhiello, E., *Polymer Surfaces;* Wiley: London, 1994.

(95) Atkins, P.W. *Physical Chemistry 4th ed.*; Oxford Uni.: Oxford, 1990.

(96) Shard, A.G. Ph. D. Thesis, University Of Durham, 1992.

(97) Binnig, G.; Quate, C. F.; Gerber, Ch. *Phys. Rev. Lett.* **1986**, *56*, 930.

(98) Reneker, D.H. In *New Characterisation Techniques For Thin Polymer Films;* Tong, H-M.; Nguyen, L.T. Eds.; Wiley: New York, 1990; Chapter 12.

(99) Hues, S.; Colton, R.; Meyer, E.; Guntherodt, H. J. *MRS Bulletin;* January 1993, 41.

(100) Elings, V.; Gurley, J. U.S. Patent 5 266 801, 1993.

(101) Zhong. Q.; Inniss, D.; Kjoller, K.; Elings, V. B. *Surf. Sci. Lett.* **1993**, *290*, 688.

(102) Nanoscope III Operating Manual; Digital Instruments Inc: California.

CHAPTER TWO

PLASMA POLYMERISATION OF TRIFLUOROMETHYL SUBSTITUTED PERFLUOROCYCLOHEXANE MONOMERS

CHAPTER TWO

PLASMA POLYMERISATION OF TRIFLUOROMETHYL SUBSTITUTED PERFLUOROCYCLOHEXANE MONOMERS

2.1 INTRODUCTION

Plasma polymerisation can be used to deposit organic coatings at ambient temperatures from a wide range of precursors onto almost any surface. Polymerisation occurs via activation and reaction of the precursor molecules.[1] Ions, radicals and excited molecules polymerise in the gas phase and react with the growing polymeric film.[2] Plasma polymerisation is recognised as being a clean, dry technique, which generates little waste compared to conventional wet chemical methods. However it does have some limitations, in that the stoichiometry and physical characteristics of the plasma polymer product are strongly influenced by process parameters (e.g. gas composition and flow rate,[3,4] substrate temperature,[5] the position of the substrate relative to the glow discharge,[6] type of substrate,[3,7] discharge power,[7] reactor size[8] etc.). Conventional polymer synthesis tends to produce structures containing repeat units which bear a strong resemblance to the monomer species, whereas the plasma polymer network can be extremely complex.

Low temperature glow discharge polymerisation of perfluorocarbons can yield low surface energy films[16] which find application as hydrophobic,[9,10] protective,[11-14] and biocompatible coatings.[15-17] Fluorinated plasma polymers are also used as dielectrics,[18,19] optical layers,[20] and as permselective membranes.[21] Fluorinated gases are widely used for the etching of silicon wafers hence the study of the mechanism of plasma polymerisation of these compounds is of interest to the semi-conductor industry.[2]

In this chapter the plasma polymerisation of a range of substituted cyclic fluorocarbons is evaluated as a means of generating highly fluorinated surfaces. Cyclic fluorocarbons are reported to undergo plasma polymerisation much more readily than their acyclic counterparts.[22] The monomers investigated are perfluorocyclohexane (PFCH), perfluoromethylcyclohexane (MCH), perfluoro-1,2-dimethyl- cyclohexane (12DM), perfluoro-1,3-dimethylcyclohexane (13DM) and perfluoro-1,3,5-trimethylcyclohexane (TMCH), Fig. 2-1. All of these molecules have equivalent fluorine to carbon ratios (F/C=2).

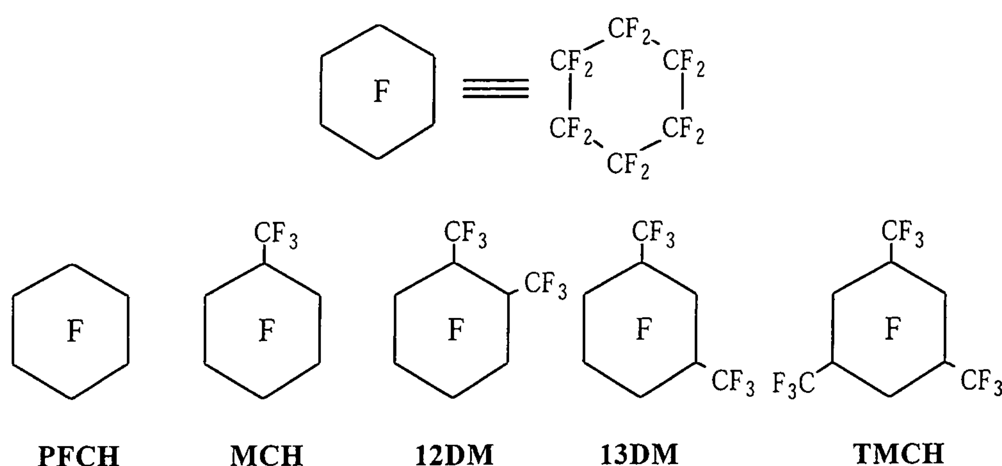

Fig. 2-1: Structures of monomers used in this study.

The resultant plasma polymers are expected to be highly fluorinated and their stoichiometry including the relative abundance of different CF_n ($n = 0\text{-}3$) functionalities will be studied using X-ray photoelectron spectroscopy. This technique is particularly suited to the study of fluorinated surfaces due the highly electronegative nature of fluorine, see sec. 1.4.1.5. This electronegativity allows for the identification and quantification of the various functional groups present at the surface of the sample. Using XPS it should be possible to determine to what extent, if any, the subtle differences between the precursors are retained in the final plasma polymers.

2.2 EXPERIMENTAL

2.2.1 Experimental Apparatus and Procedure for Plasma Polymerisation.

Monomers were purchased from Fluorochem Ltd. and further purified via freeze-thaw cycles. These freeze-pump-thaw cycles ensured complete degassing of the monomer prior to its introduction to the reactor. The purification method is based on the principle that by reducing the vapour pressure of all gases above a liquid the solubility of gases within the liquid decreases,[23] resulting in extraction of any dissolved gases into the vapour from which they can be pumped away. Plasma polymerisation experiments were carried out in an electrodeless cylindrical glass reactor (internal diameter = 5 cm, volume = 490 cm^3) enclosed in a Faraday cage,[24] Fig. 2-2, p. 50. The reactor was fitted with an Edwards needle valve on the gas inlet and pressure measurement was taken from the output voltage of an Edwards ATC-E thermocouple gauge. The reactor was continuously pumped by a 33 dm^3 hr^{-1} Edwards E2M2 mechanical rotary pump via a liquid nitrogen cold trap yielding a base pressure of 2×10^{-3} torr and a leak rate of better than 2.3×10^{-12} kg s^{-1} (calculated assuming ideal gas behaviour,[25] sec. 2.2.2). This ensured that at an operating pressure of 0.2 torr, over 99% of the reactor contents were fluorocarbon monomer.

An ENI ACG-3 r.f. power generator with maximum power output switchable between 30 and 300 Watts with an operating frequency of 13.56 MHz., was inductively coupled to the gas via an LC matching circuit and a copper coil. The copper coil of diameter 0.5 cm consisted of 10-turns wound externally around the reaction chamber spanning 8-16 cm from the gas inlet. Forward and reflected power measurements along with SWR readings (SWR = standing wave ratio = total power generated/power transmitted to the plasma) were taken on an RS SWR/power meter. Following ignition of the plasma the r.f. circuit was balanced by matching the impedance of the load to that of the r.f.

generator i.e. 50 Ohms. This was achieved by adjusting the inductance and capacitance of the LC circuit to reduce the SWR and reflected power readings to a minimum.

In a typical reaction run the reaction vessel was scrubbed with detergent prior to each experiment, rinsed with water and isopropyl alcohol (IPA), oven-dried, then cleaned with a 50 W air plasma at a pressure of 0.2 torr for 30 mins. The reactor was subsequently vented to atmosphere and a glass slide (approx. area 13 mm x 5 mm) was positioned in the centre of the copper coils. The glass slide had previously been ultrasonically washed in detergent and rinsed with deionised water and analar IPA. The reactor was then re-evacuated and the base pressure and leak rate checked to ensure satisfactory vacuum conditions. If the determined leak rate was acceptable (typically better than 1.6×10^{-12} kg s^{-1} calculated assuming ideal gas behaviour),[26] the reactor was purged with monomer for 2 mins prior to igniting the glow discharge. Plasma polymerisation was carried out for 10 mins after which the r.f. power to the plasma was terminated. Upon termination, the reaction zone was purged with monomer for a further 2 mins, the reactor vented to atmosphere and the sample removed.

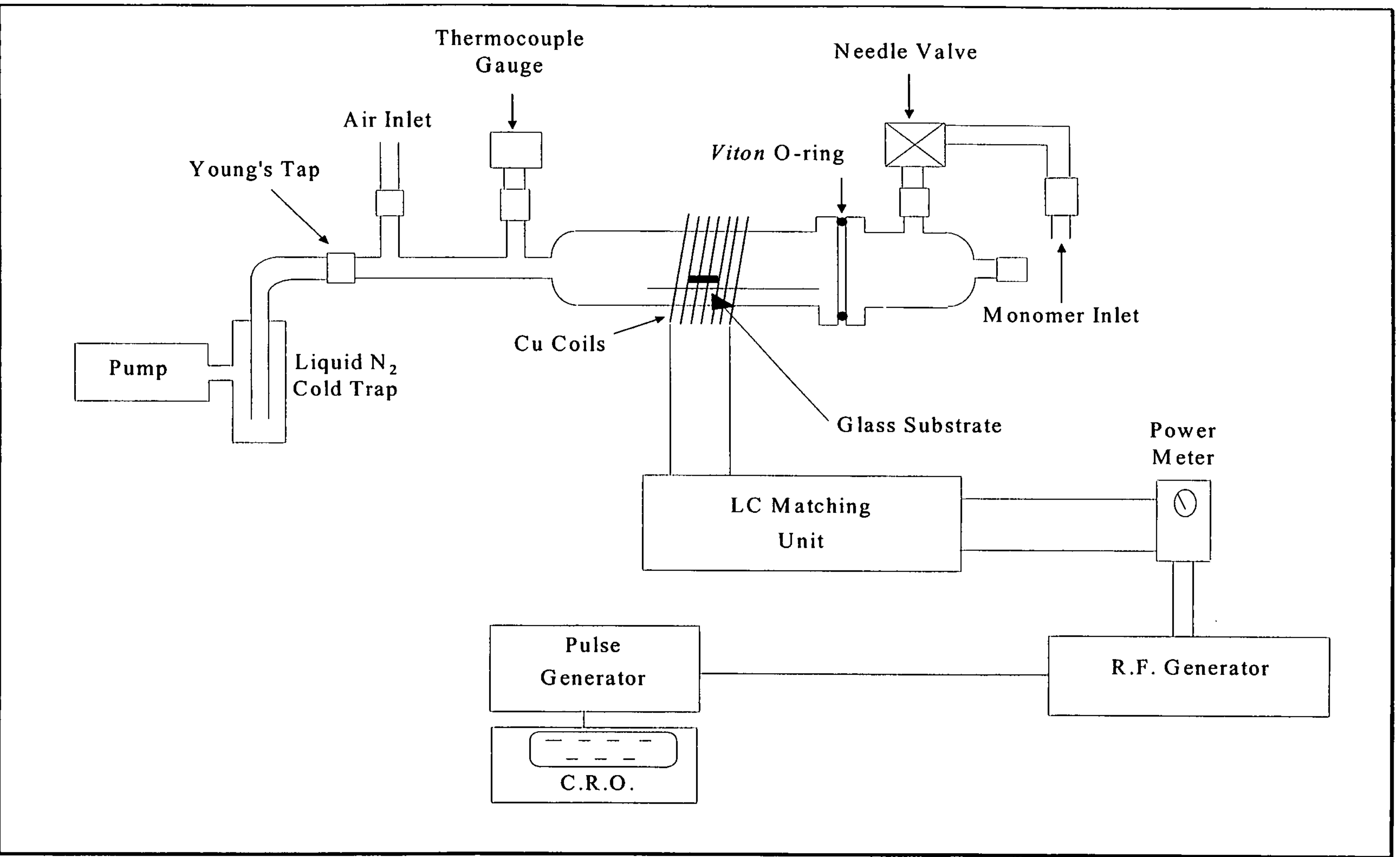

Fig. 2-2: Schematic representation of the plasma rig.

2.2.2 Flow Rate Calculation

At the pressures used in these studies ideal behaviour can be assigned to the gases such that their behaviour is governed by the equation:[25,27]

$$PV = nRT \qquad \text{Eq. 2-1}$$

where P = pressure, V = volume, R = universal gas constant and T = temperature in degrees Kelvin.

Volumetric flow rate F_v defined in Eq. 2-2 can be calculated by measuring the rise in pressure for a given flow (or leak) between times t = 0 and t = t:

$$F_V = \frac{dn}{dt} = \frac{V}{RT} x \int_{t=0}^{t=t} \frac{dP}{dt} \qquad \text{Eq. 2-2}$$

If $\int_{t=0}^{t=t} \frac{dP}{dt}$ is approximated as $\frac{\Delta P}{\Delta t}$ then:

$$F_V \approx \frac{V}{RT} x \frac{\Delta P}{\Delta t} \qquad \text{Eq. 2-3}$$

At STP the volume of one mole of gas is 22414 cm^3 and with V in cm^3, R = 82.06 atm cm^3 K^{-1} mol^{-1}, T in Kelvin, P in atm and t in seconds:[28]

$$F_V \approx \frac{V}{RT} x \frac{\Delta P}{\Delta t} x 22414 \quad cm^3\ s^{-1} \qquad \text{Eq. 2-4}$$

For mass flow rates, F_m, which are referred to in later chapters;

$$F_m \approx \frac{MV}{RT} x \frac{\Delta P}{\Delta t} \quad kg\ s^{-1} \qquad \text{Eq. 2-5}$$

where M = relative molecular mass of the monomer.

2.2.3 Sample Characterisation

2.2.3.1 X-ray Photoelectron Spectroscopy

A Kratos ES200 X-ray photoelectron spectrometer with an unmonochromated X-ray source (Mg $K\alpha_{1,2}$ = 1253.6 eV) was used for chemical characterisation of the deposited fluorocarbon films. The glass slides were mounted on a stainless steel probe tip using Scotch adhesive tape and the probe was wiped with analar IPA prior to insertion in the

spectrometer, typical base pressure < 2 x 10^{-6} torr. Emitted core level electrons were collected at 30° take-off angle from the substrate normal with a concentric hemispherical analyser (CHA) operating in fixed retardation ratio mode (FRR = 22:1). The spectrometer was calibrated with respect to the gold $4f_{7/2}$ peak at 83.8 eV, (FWHM = 1.2 eV).[29] Instrumentally determined sensitivity factors for unit stoichiometry were taken as C(1s): F(1s): O(1s): N(1s): Si(2p)=1.00: 0.53: 0.55: 0.74 : 1.05. The absence of any Si(2p) XPS feature following plasma polymerisation was taken as being indicative of complete coverage of the glass substrate. XPS spectra were collected and analysed on an interfaced IBM PC computer.

2.3 RESULTS

A Marquardt minimisation computer program which assumed a Gaussian peak shape with a fixed relative full width at half maximum (FWHM) was used to fit the C(1s) envelope for each plasma polymer with five different carbon functionalities[30]: $\underline{C}$-CF_n (286.6 eV), $\underline{C}F$ (287.8 eV), $\underline{C}F$-CF_n (289.3 eV), $\underline{C}F_2$ (291.2 eV), and $\underline{C}F_3$ (293.3 eV). The $\underline{C}F_3$ and $\underline{C}F_2$ components could be assigned unambiguously and so the dominant $\underline{C}F_2$ feature at 291.2 eV was used as a reference offset. Mg $K\alpha_{3,4}$ satellite peaks with different FWHM were also taken into account.[30] Fig. 2-3, p. 53 shows a typical C(1s) peak fit for a 5 W PFCH plasma polymer. The relative concentration of each carbon functionality was calculated by dividing the corresponding peak area by the total C(1s) area. The elemental F/C ratio for each film was calculated from the F(1s) and C(1s) peak areas taking into account the appropriate sensitivity factors.

Experiments were carried out employing discharge powers in the 1.5 - 40 W range, Fig. 2-4 - Fig 2-7, pp.54-56. The composition of plasma polymers produced using powers greater than 7 W varied little with changes in discharge power and the degree of substitution of the perfluorocyclohexane precursor molecule, with a F/C ratio of 1.5 ± 0.03 together with 17 ± 0.5% $\underline{C}$-CF_n, 31 ± 0.4% $\underline{C}F$(total), 30 ± 0.5% $\underline{C}F_2$, and 22 ± 0.5% $\underline{C}F_3$. At glow discharge powers lower than 7 W, a strong variation in the relative

concentration of CF_n functionalities was found which depended upon the power used and the structure of the fluorocarbon monomer. In the case of PFCH the contribution of the $\underline{C}$-CF_n peak to the overall C(1s) envelope drops from 19 ± 0.7% at 7 W to 13 ± 0.7% at 1.5 W, which coincides with an increase in the $\underline{C}F_2$ content from 30 ± 0.5% to 40 ± 0.5% respectively, Fig. 2-6. In comparison, for TMCH the $\underline{C}$-CF_n content drops from 19 ± 0.7% at 7 W to 12 ± 0.7% at 1.5 W, and the $\underline{C}F_2$ rises slightly from 29 ± 0.5% at 7 W to 33 ± 0.5% at 1.5W, Fig. 2-7. The $\underline{C}F_3$ contribution for PFCH remains approximately constant at 22 ± 0.5% irrespective of power, whereas for TMCH it rises from 23 ± 0.5% at 7W to 28 ± 0.5% at 1.5 W. The chemical compositions of plasma polymers formed from monosubstituted MCH and disubstituted 12DM and 13DM at low powers fall in-between the values reported for the unsubstituted (PFCH) and trisubstituted (TMCH) plasma polymers. It is of interest to note that the structural isomers perfluoro-1,2-dimethylcyclohexane (12DM), perfluoro-1,3-dimethylcyclohexane (13DM) yield identical plasma polymers at any given power. For all of the substituted perfluorocyclohexane precursors, the F/C ratios found in the plasma polymer deposits decrease with increasing electrical discharge power.

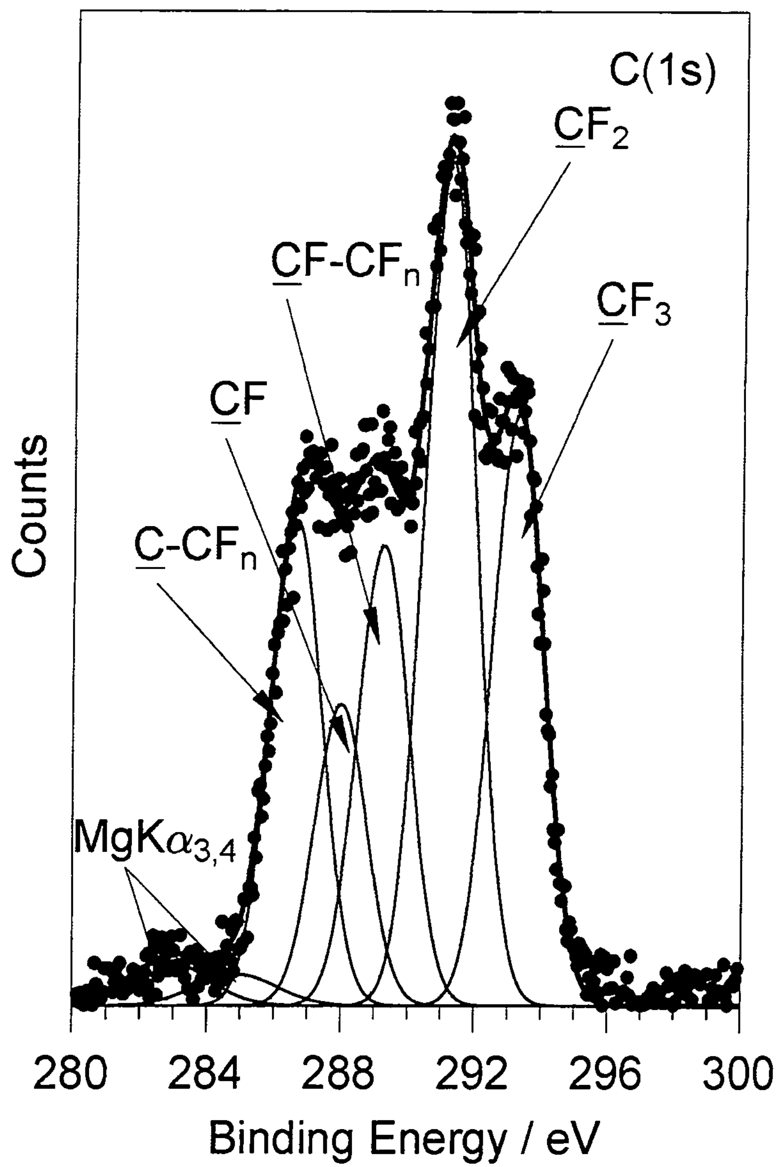

Fig. 2-3: C(1s) peak fit for a 5 W perfluorocyclohexane plasma polymer.

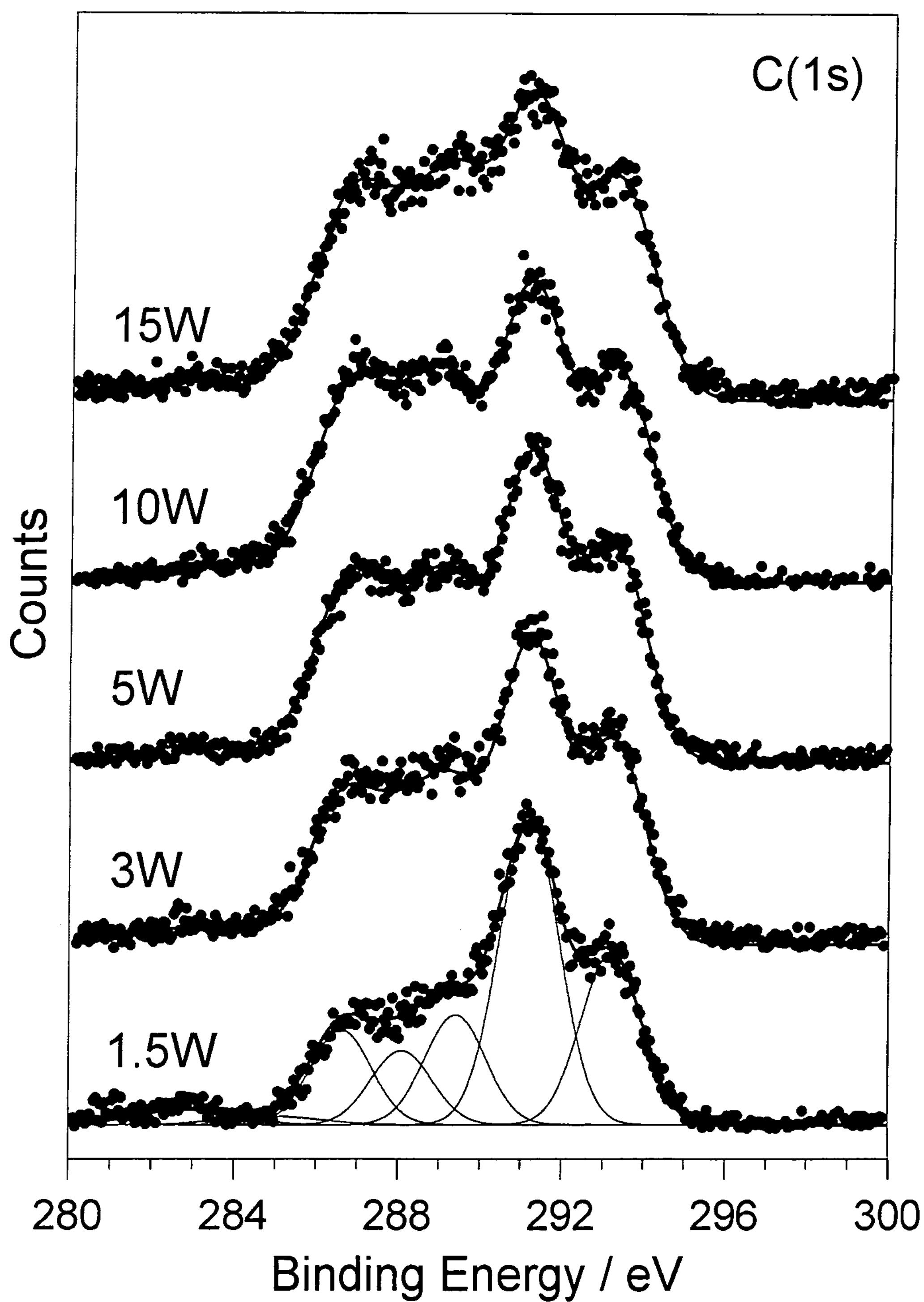

Fig. 2-4: C(1s) XPS spectra of PFCH plasma polymers deposited as a function of discharge energy.

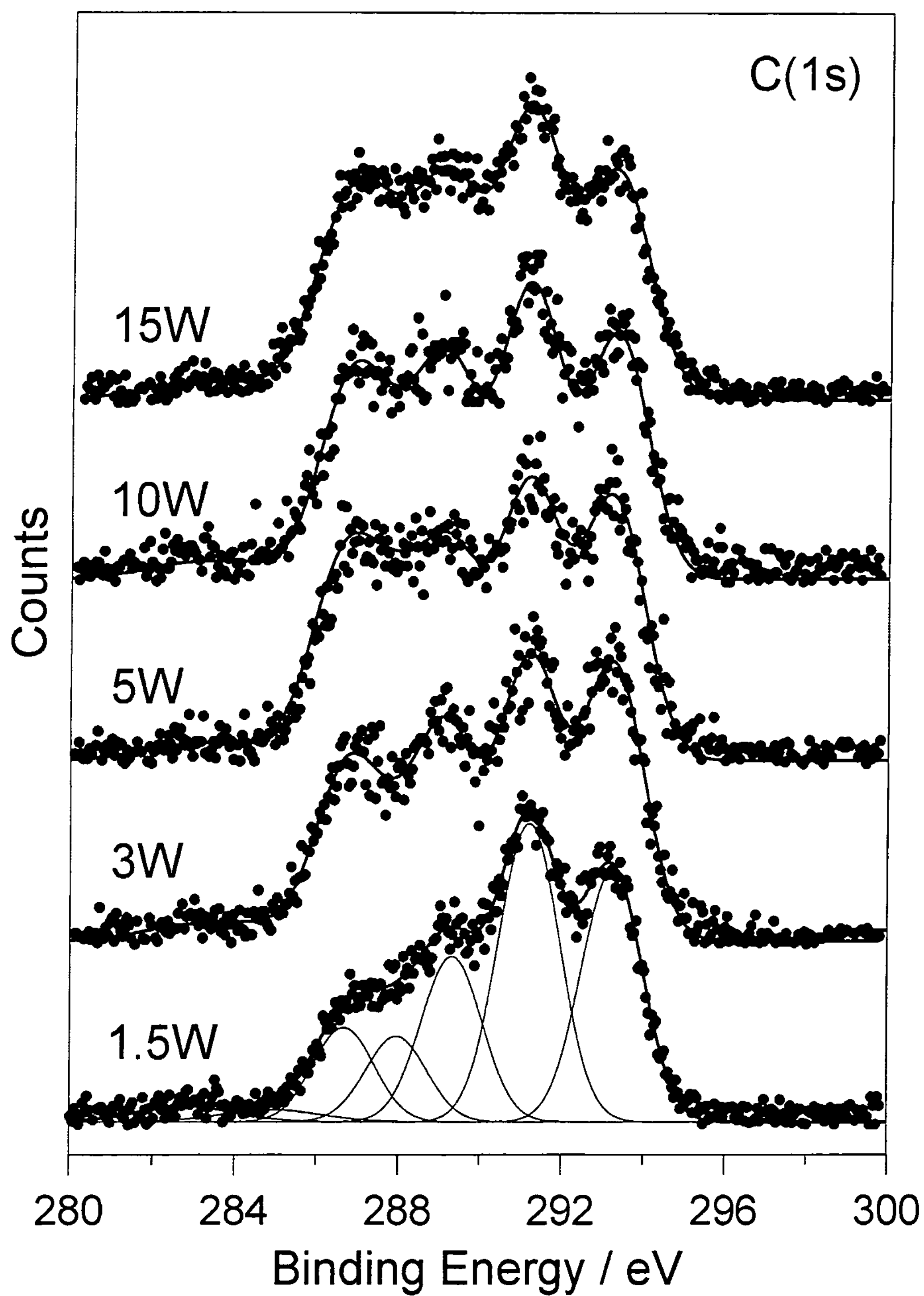

Fig. 2-5: C(1s) XPS spectra of TMCH plasma polymers deposited as a function of discharge energy.

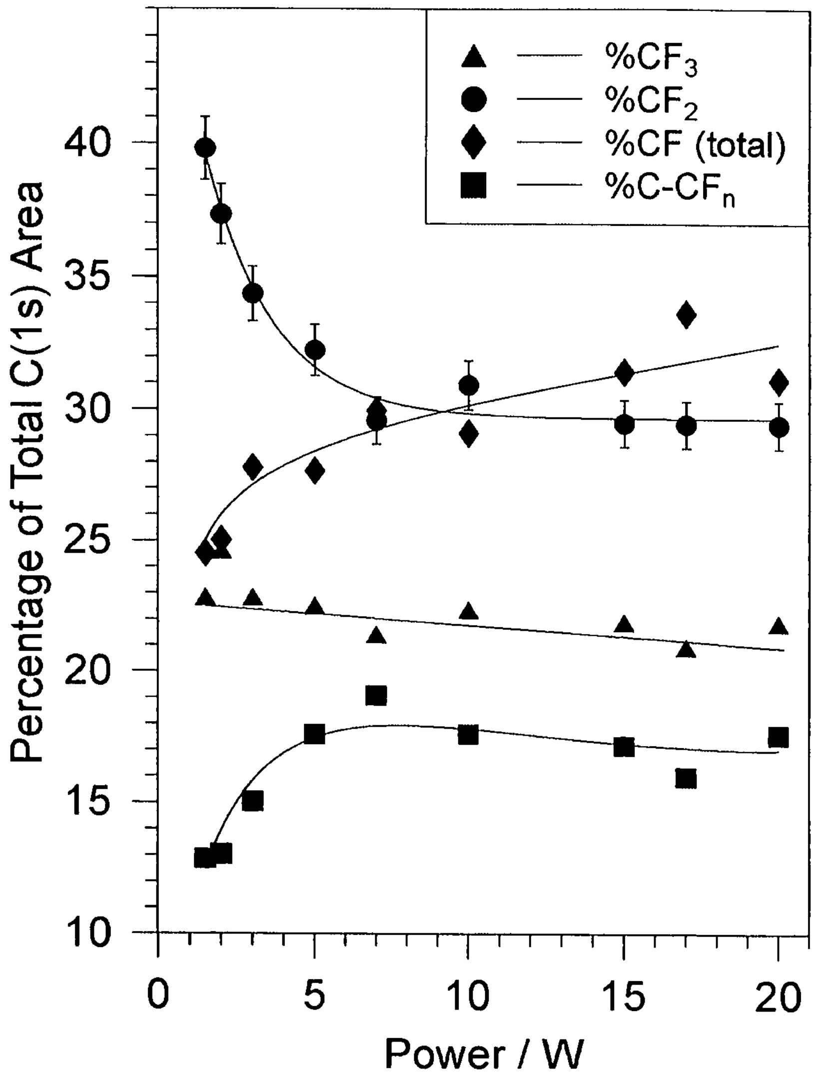

Fig. 2-6: Variation in the relative CF_n concentrations as a function of discharge energy for PFCH plasma polymers.

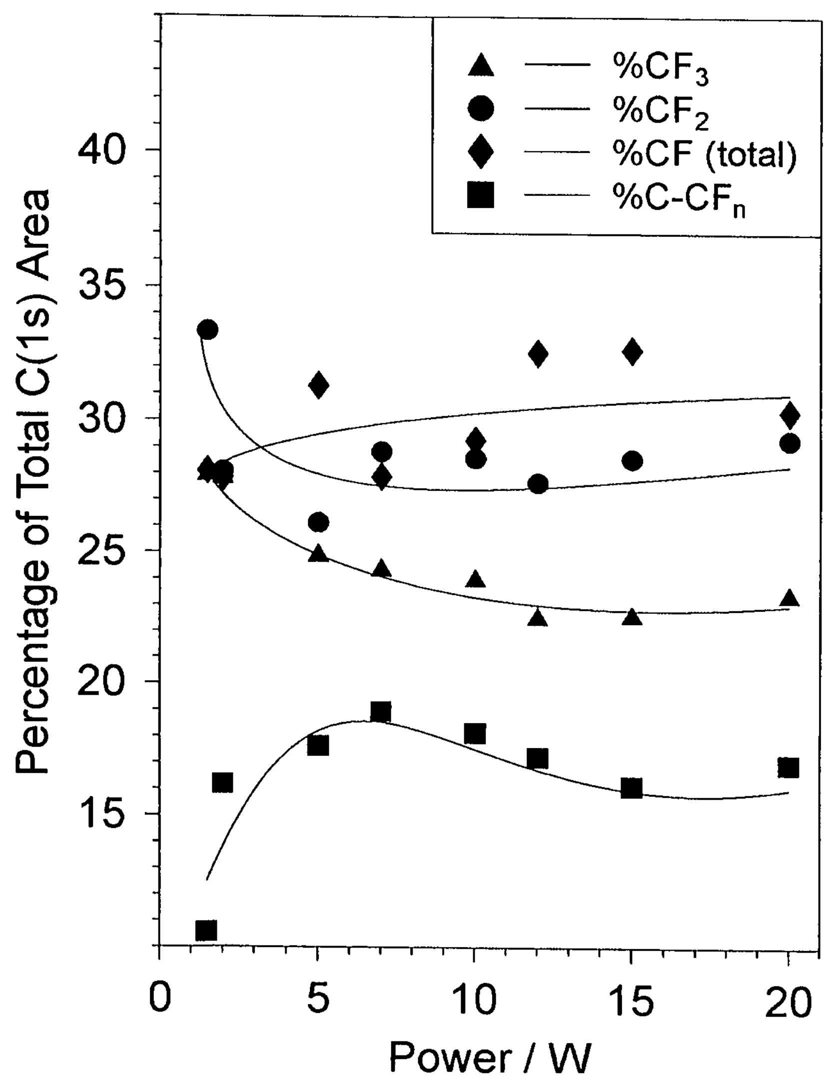

Fig. 2-7: Variation in the relative CF_n concentrations as a function of discharge energy for TMCH plasma polymers.

2.4 DISCUSSION

Plasma polymerisation of cyclic fluorocarbons is an effective way of producing polymeric layers at a high deposition rate and with a high F/C ratio.[31] The effect of altering the discharge power upon the composition of plasma polymers depends not only on the geometry of the reactor, the position of the substrate and the powers used, but also to varying degrees on the structural nature of the precursors.[3,32-36] In the present plasma polymerisation study, where the only difference between the monomers is the number of trifluoromethyl groups on the perfluorocyclohexane ring (ranging from 0 to 3), the relative abundance of CF_n functional groups is dependent upon the discharge power used. At discharge powers greater than approximately 7 W, the chemical composition becomes independent of monomer structure and power. This may be attributed to extensive fragmentation of the precursor molecules to yield effectively the same chemical species in the plasma phase since all of the fluorocarbon monomer structures under investigation possess the same F/C elemental ratio. However, at powers below 7 W, the structure of the deposited polymer is influenced by discharge power and also the chemical structure of the perfluoromonomer. For very low discharge powers the amount of CF_2/CF_3 in the plasma polymer reflects the amount of CF_2/CF_3 in the precursor molecule, Fig. 2-8 and Fig. 2-9. The observed increase in CF_2 and CF_3 content is accompanied by a reduction in crosslinking. This can be attributed to less fragmentation of precursor molecules in the gas phase and within the growing film.

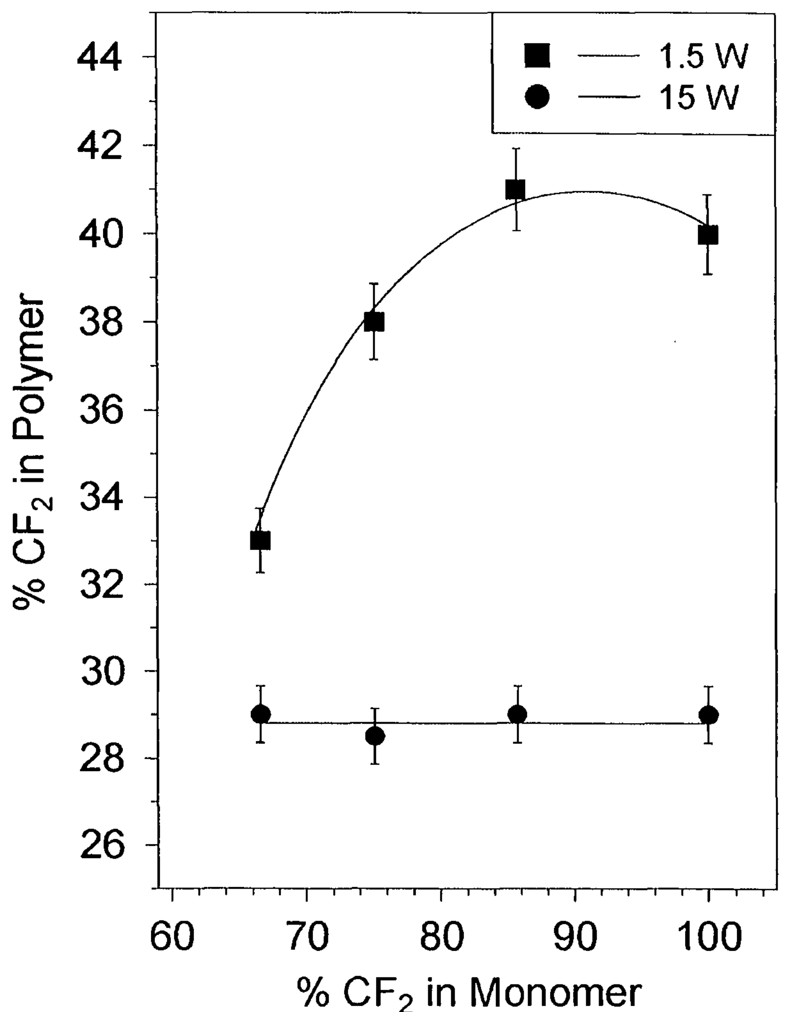

Fig. 2-8: Variation in the relative CF_n concentrations as a function of discharge energy for PFCH plasma polymers.

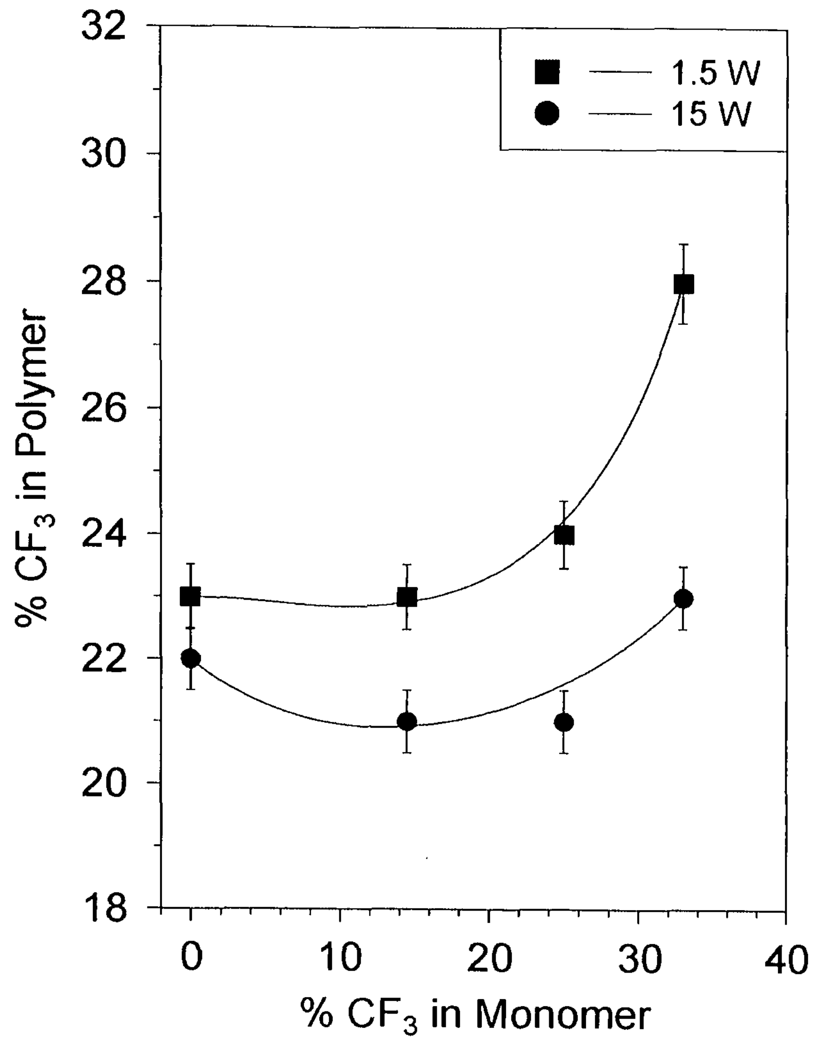

Fig. 2-9: Variation in the relative CF_n concentrations as a function of discharge energy for TMCH plasma polymers.

The average electron energy in low pressure glow discharges is typically only a few electron volts.[2] This is well below the energy needed for the dissociative ionisation of a fluorocarbon ~ 13 eV.[3] Since electrons within a plasma have a range of energies, it will only be electrons from the high energy tail of the distribution which will possess sufficient energy to cause dissociative ionisation. A decrease in the discharge power will cause a drop in the electron population of the high energy tail, leading to a greater number of non-fragmented precursor molecules impinging onto the growing plasma polymer surface. Increased incorporation of these non-fragmented molecules in the plasma polymer would result in the composition of the final plasma polymer bearing more of a resemblance to the starting material. Such a drop in electron energies at lower powers will also reduce the plasma potential (the substrate is at a floating potential) which will produce less ion and electron bombardment of the growing polymeric film and hence less crosslinking.[37] A drop in the number of excited species present within the plasma at lower powers will also cause an attenuation in the VUV irradiation of the growing polymer. VUV irradiation of polymers is known to cause C-C bond scission which can lead to crosslinking.[38]

2.5 CONCLUSION

Plasma polymerisation of perfluorocyclohexane (PFCH), perfluoromethylcyclohexane (MCH), perfluoro-1,2-dimethylcyclohexane (12DM), perfluoro-1,3-dimethylcyclohexane (13DM) and perfluoro-1,3,5-trimethyl- cyclohexane (TMCH) results in highly fluorinated surfaces. XPS analysis shows the relative abundance of the various CF_n (n = 0-3) functionalities found in the respective plasma polymers is shown to be strongly influenced by the electrical discharge power and the structural nature of the fluorocarbon precursor. At electrical discharge powers above 7 W, the chemical nature of the plasma polymer becomes independent of power level and monomer structure. At powers below 7W, the structural differences between the various precursor molecules are reflected in the composition of the final plasma polymers. At low powers crosslinking of the resultant plasma polymer is reduced, however due to the minimum power input required to sustain the discharge there exists a restriction on the extent to which continuous wave power can be used to control the composition of the plasma polymers.

2.6 REFERENCES

(1) Yasuda, H. *Plasma Polymerisation*; Academic Press: Orlando, 1985.

(2) Grill, A. *Cold Plasmas in Materials Technology*; IEEE Press: Piscataway, New Jersey, 1994.

(3) Clark, D.T.; Shuttleworth, D. *J. Polym. Sci. Polym. Chem. Ed.* **1980,** *18*, 27.

(4) d'Agostino, R.; Cramarossa, F.; Illuzzi, F. *J. Appl. Phys.* **1987,** *61*, 2754.

(5) Ratner, B.D.; Lopez, G.P. *J. Polym. Sci. Polym. Chem. Ed.* **1992,** *30*, 2415.

(6) Shard, A.G.; Munro, H.S.; Badyal, J.P.S. *Polym. Chem.* **1991,** *32*, 152.

(7) d'Agostino, R.D.; Favia, P.; Fracassi, F. *J. Polym. Sci. Polym. Chem. Ed.* **1990,** *28*, 3387.

(8) Kim, H.Y.; Yasuda, H.K. *J. Vac. Sci. & Tech.* **1997,** *A15(4)*, 1837.

(9) Kohoma, M.; Okazaki, S.; Uchama, H. *Patent No. JP 06 41755*, Feb. 1994.

(10) Iriyama, Y.; Yasuda, T.; Cho, D.L.; Yasuda, H. *J. Appl. Polym. Sci.* **1990,** *39*, 249.

(11) O'Kane, D.F.; Rice, D.W. *J. Macromol. Sci. Chem.* **1976,** *A10*, 567.

(12) Sato, K.; Omae, S.; Kojima, K.; Hashimoto, T.; Koinuma, H. *Jap. J. Appl. Phys.* **1988,** *27*, L2088.

(13) Sugimoto, I.; Miyake, S.J. *J. Appl. Phys.* **70**, 2618 (1991).

(14) O'Kane, D.F.; Rice, D.W. *J. Macromol. Sci.* **A10**, 567 (1976).

(15) Clarotti, G.; Schue, F.; Sledz, J.; Geckeler, K.E.; Göpel, W.; Orsetti, A. *J. Memb. Sci.* **1991,** *61*, 289.

(16) Clarotti, G.; Aoumar, A.A.B.; Schué, F.; Sledz, J.; Geckeler, K.E.; Flösch, D.; Orsetti, A. *Makromol. Chem.* **1991,** *192*, 2581.

(17) Schue, F.; Clarotti, G.; Benaoumar, A.A.; Sledz, J.; Mas, A.; Geckeler, K.E.; Gopel, W.; Orsetti, A. *J. Macromol. Sci.: Pure & Appl. Chem.* **1994,** *A31*, 1161.

(18) Pratt, I.H.; Lawson, T.C. *Thin Solid Films,* **10**, 151, 1972.

(19) Takeishi, S.; Kudo, H.; Shinohara, R.; Hoshino, M.; Fukayama, S.; Yamaguchi, J.; Yamada, M. *J. Electrochem. Soc.* **1997,** *144(5)*, 1797.

(20) Martinu, L.; Miyake, S. *Vacuum,* **36**, 477 (1986).

(21) Inaki, N.; Tasaka, S.; Murata, T. *J. Appl. Polym. Sci.* **38**, 1869 (1989).

(22) Yasuda, H.; Hsu, T.S. *J. Polym. Sci. Polym. Chem. Ed.* **1977,** *15*, 2411.

(23) Barrow, G.M. *Physical Chemistry 5th ed.* McGraw-Hill: London, 1988; p. 272.

(24) Shard, A.G.; Munro, H.S.; Badyal, J.P.S. *Polym. Chem.* **1991,** *32*, 152.

(25) Ehrlich, C.D.; Basford, J.A. *J. Vac. Sci. Tech.* **1992,** *A10*, 1.

(26) Ehrlich, C.D.; Basford, J.A. *J. Vac. Sci. Tech.* **1992,** *A10*, 1.

(27) Atkins, P.W. *Physical Chemistry 5th Ed.* Oxford University Press: Oxford, 1994, P29.

(28) Ryan, M.E. Ph. D. Thesis, University of Durham, 1995.

(29) Wagner, C.D.; Riggs, W.M.; Davis, L.E.; Moulder, J.F.; Muilenberg, G.E. *Handbook of X-Ray Photoelectron Spectroscopy*; Perkin-Elmer Corporation, 1978.

(30) Wells, R.K.; Ryan, M.E.; Badyal, J.P.S. *J. Phys. Chem.* **1993,** *97*, 12879.

(31) Clark, D.T.; Shuttleworth, D. *J. Polym. Sci. Polym. Chem. Ed.* **1980,** *18,* 27.

(32) Clark, D.T.; Shuttleworth, D. *J. Polym. Sci. Polym. Chem. Ed.* **1980,** *18,* 407.

(33) Clark, D.T.; Abrahman, M.Z. *J. Polym. Sci. Polym. Chem. Ed.* **1981,** *19,* 2129.

(34) Clark, D.T.; Abrahman, M.Z. *J. Polym. Sci. Polym. Chem. Ed.* **1981,** *19,* 2689.

(35) Clark, D.T.; Abrahman, M.Z. *J. Polym. Sci. Polym. Chem. Ed.* **1982,** *20*, 691.

(36) Clark, D.T.; Abu-Shbak, M.M. *J. Polym. Sci. Polym. Chem. Ed.* **1983,** *21,* 2907.

(37) O'Keefe, M.J.; Rigsbee, J.M. *J. Appl. Polym. Sci.* **1994,** *53,* 1631.

(38) Hudis, M.; Prescot, L.E. *Polym. Lett.* **1972,** *10*, 179.

CHAPTER THREE

HIGHLY FLUORINATED SURFACES VIA CONTINUOUS AND PULSED PLASMA POLYMERISATION OF PERFLUOROCYCLOHEXANE AND PERFLUOROCYCLOPENTENE

CHAPTER THREE

HIGHLY FLUORINATED SURFACES VIA CONTINUOUS AND PULSED PLASMA POLYMERISATION OF PERFLUOROCYCLOHEXANE AND PERFLUOROCYCLOPENTENE

3.1 INTRODUCTION

Plasma polymerisation of cyclic fluorocarbons has been shown in chapter two to lead to the formation of highly fluorinated plasma polymers. This results in the generation of surfaces with very low surface energy[1] which find application as hydrophobic,[2,3] protective,[4,5] and biocompatible coatings.[1,6] It was found that the exact composition of these polymers was dependent on the discharge power used and the chemical structure of the precursor, despite the fact that the chemical differences between the starting compounds were very slight. All compounds were fully saturated cyclic compounds, the differences between them being the number and/or position of the trifluoromethyl substituent groups on the perfluorocyclohexane ring. At powers greater than 7 W plasma polymers deposited from all five precursors had identical stoichiometries. However at powers below 7 W the chemical differences in the precursors began to be reflected in the XPS spectra of the plasma polymers. Whereas at 15 W discharge power the plasma polymers from all precursors had ~ 29% CF_2 content, at 1.5 W the percentage CF_2 in the plasma polymers varied from ~ 33% for the trimethyl substituted compound to greater than 40% for the unsubstituted perfluorocyclohexane. Clearly at low power densities there is the potential for the chemistry of the precursor to be exploited as a means of tailoring the composition and hence properties of the final plasma polymer.

In this chapter the influence of precursor chemistry on the composition of plasma polymers will be further investigated. Plasma polymers from perfluorocyclohexane and perfluorocyclopentene will be compared to determine if it is possible to use a plasma to generate surfaces whose compositions reflect those of their precursors. Perfluorocyclohexane contains exclusively CF_2 linkages and therefore is a potential candidate for the synthesis of a PTFE-like plasma polymer. Since the precursor contains only CF_2 groups the appearance of other functionalities and the disappearance of CF_2 groups from the plasma polymer can be used as a measure of the extent of dissociation of the precursor during the plasma polymerisation process. Perfluorocyclopentene is also a cyclic fluorocarbon but significantly has a double bond within the ring structure. The effect of this unsaturation on the plasma polymerisation process and the structure of the final plasma polymers will be investigated.

The results of chapter two indicate however that even at very low power densities sufficient fragmentation of the precursor occurs to yield surfaces with significantly different compositions from the starting material. The control which can be achieved by reducing the power to the gas is limited by the need to input sufficient energy to sustain the ionisation processes within the plasma. During the work carried out for chapter two it was found that for the gas flows and pressures of this work the plasma became unstable at continuous wave powers below ~1.5 W. As an alternative method of gaining control over plasma properties and over the properties of the deposited film the power to the plasma was pulsed.

In pulsed plasmas the power to the system is modulated at a frequency much lower than that of the applied radio frequency. As discussed in chapter one, sec. 1.3.2, pulsing the r.f. power to the plasma has several inherent advantages over continuous wave plasma polymerisation.[7,8] Excessive heating of reactor walls and substrate is avoided because there is reduced ion bombardment of the surfaces in contact with the plasma.[7] Also any decay of short-lived excited species during the off-portion of the duty cycle can help to attenuate both the VUV emission and the variety of species contributing to the overall plasma polymer structure. In addition, conventional polymerisation reactions can occur

during the off-time. The extent to which pulsing can be used to enhance desired chemical reaction pathways within an electrical discharge is not yet fully established.

This chapter will therefore consider the effect of both chemical composition and pulsed power on the plasma polymerisation processes for perfluorocyclohexane and perfluorocyclopentene, with the ultimate aim of gaining control over the chemical structure of the surface of the substrates exposed to the plasma.

3.2 EXPERIMENTAL

Plasma polymerisation experiments were carried out in an electrodeless cylindrical glass reactor (internal diameter = 5 cm, volume = 490 cm^3) enclosed in a Faraday cage. This was continuously pumped by a 33 $dm^3\ hr^{-1}$ Edwards E2M2 mechanical rotary pump via a liquid nitrogen cold trap yielding a base pressure of 2.66×10^{-3} mbar and a leak rate of better than 1.6×10^{-12} kg s^{-1} (calculated assuming ideal gas behaviour,[9]). A 13.56 MHz. r.f. generator was inductively coupled to the gas via an LC matching circuit and a copper coil (0.5 cm diameter, 10-turns) wound externally around the reaction chamber spanning 8-16 cm from the gas inlet. The substrate was positioned in the centre of the copper coils. For the experiments employing pulsed power, a signal generator was attached to the r.f. generator and a cathode ray oscilloscope was used to monitor the pulse duration, interval and amplitude, see chapter 1, sec 1.3.2. The pulse rise and fall time was 100 ns. The peak power (P_p) delivered to the copper coil could be varied between 20-180 W, whilst on-times (t_{on}) and off-times (t_{off}) varied between 20 - 1900 μs and 5 - 1000 μs respectively. The average power <P> delivered during pulsing was calculated using the following expression:

$$\langle P \rangle = P_p \times \left(\frac{t_{on}}{t_{on} + t_{off}} \right) \qquad \text{Eq. 3-1}$$

Prior to each experiment, the reactor was pumped down to base pressure and the monomer vapour was introduced into the reaction chamber at a pressure of 0.2 torr via a fine needle valve at a flow rate of 7.1×10^{-8} kg s^{-1} for perfluorocyclopentene and

1.6×10^{-7} kg s^{-1} for perfluorocyclohexane. The reactor was purged with monomer for 2 mins prior to igniting the glow discharge. Plasma polymerisation was carried out for 10 mins. Upon termination, the reaction zone was purged with monomer for a further 2 mins, and finally vented to air.

A Kratos ES200 X-ray photoelectron spectrometer equipped with an non-monochromatic X-ray source (Mg $K\alpha_{1,2}$ = 1253.6 eV) was used for chemical characterisation of the deposited fluorocarbon films. Emitted core level electrons were collected at 30^{0} take-off angle from the substrate normal with a concentric hemispherical analyser (CHA) operating in fixed retardation ratio mode (FRR = 22:1). The spectrometer was calibrated with respect to the gold $4f_{7/2}$ peak at 83.8 eV, (FWHM = 1.2 eV).[10] Instrumentally determined sensitivity factors for unit stoichiometry were taken as C(1s): F(1s): O(1s): N(1s): Si(2p)= 1.00 : 0.53 : 0.55 : 0.74 : 1.05. The absence of any silicon XPS features following plasma polymerisation was indicative of complete coverage of the glass substrate.

An FTIR Mattson Polaris instrument was used for transmission infrared analysis of plasma polymers deposited onto potassium bromide disks. Typically 100 scans were acquired at a resolution of 4 cm^{-1}.

3.3 PERFLUOROCYCLOHEXANE: RESULTS

3.3.1 X-ray Photoelectron Spectroscopy.

For each plasma polymer, the C(1s) XPS envelope was fitted using a Marquardt minimisation computer program which assumed a Gaussian peak shape with a fixed relative full width at half maximum (FWHM).[11] The C(1s) XPS spectra were fitted using 5 different carbon functionalities: C-CF_n (286.6 eV), CF (287.8 eV), CF-CF_n (289.3 eV), CF_2 (291.2 eV), and CF_3 (293.3 eV). The CF_3 and CF_2 peaks could be assigned unambiguously, and therefore the dominant CF_2 peak was taken as a reference offset at 291.2 eV. As the X-ray source was unmonochromated, Mg $K\alpha_{3,4}$ satellite peaks with

different FWHM were also taken into consideration.[11] The Mg $K\alpha_{1,2}$ C(1s) FWHM were found to vary between 1.9 eV and 2.2 eV. The relative concentration of each carbon functionality was obtained by dividing the corresponding peak area by the total C(1s) envelope area. The elemental F/C ratio for each film was calculated from the F(1s) and C(1s) peak areas taking into account the appropriate XPS sensitivity factors.

3.3.1.1 Continuous Wave Plasma Polymerisation

The change in appearance of the C(1s) XPS spectra with increasing continuous wave power is shown in Fig. 3-1, p. 70. At higher powers, the deposited plasma polymer films exhibit very little variation in composition. At lower powers however the relative concentration of CF_2 functionality increases with decreasing power whilst the number of crosslinked ($C-CF_n$) carbon centres drops, Fig. 3-2. This suggests that the CF_2 content of the films could rise even further if the power can be reduced. Below 1.5 W the continuous wave plasma becomes unstable at the operating pressure of 0.2 torr.

3.3.1.2 Pulsed Plasma Polymerisation

From equation 3-1, p. 66, the average power delivered to the plasma $\langle P \rangle$, is a function of three variables viz. off-time (t_{off}), on-time (t_{on}) and peak power (P_p). The effect of altering each of these variables upon the composition of the deposited film was studied.

Fig. 3-3 shows the C(1s) XPS spectra of plasma polymer films obtained where the off-time was varied (with a fixed peak power of 20 W and on-time of 20 μs). The CF_2 component increases relative to the crosslinked ($C-CF_n$) peak with rising off-times (i.e. decreasing average power). This trend was also observed for shorter on-times (with a fixed peak power of 20 W and off-time of 250 μs), and lower peak powers (with a fixed on-time of 20 μs and off-time of 250 μs), Fig. 3-6 and Fig. 3-8 respectively. These results are consistent with the continuous wave experiments, where decreasing average power was found to yield a higher CF_2 content and a lower level of crosslinked carbon, whilst the CF_3 contribution remains steady. Fig. 3-9 compares the CF_2 content of the

deposited plasma polymer films for all the experiments. It can be concluded that for the same average power, a pulsed glow discharge produces a film with higher CF_2 content than that obtained with a continuous wave plasma at average powers below 7 W.

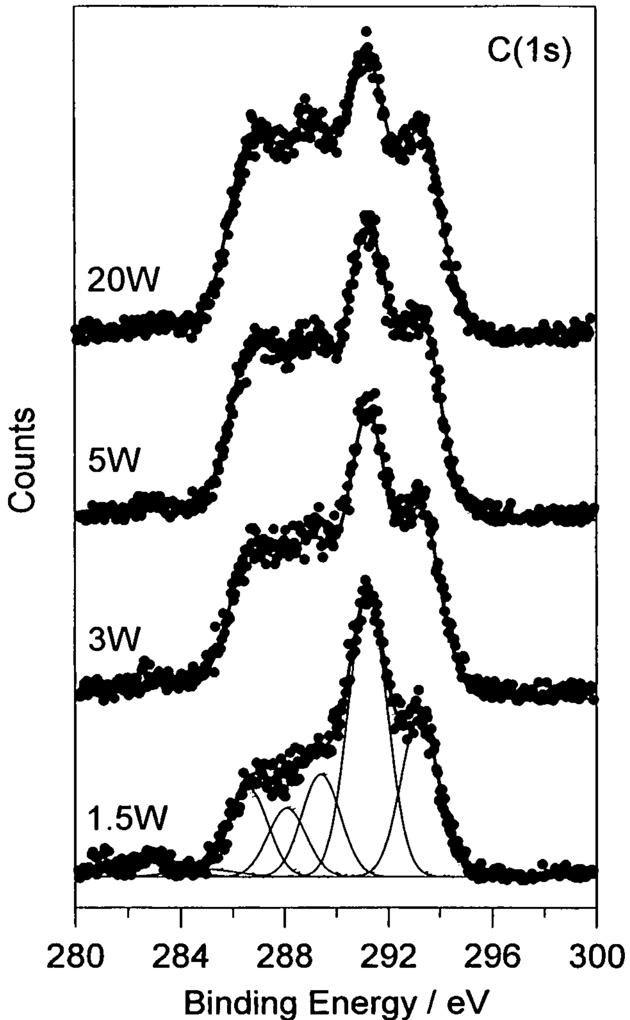

Fig. 3-1: C(1s) XPS spectra of perfluorocyclohexane plasma polymers as a function of discharge power.

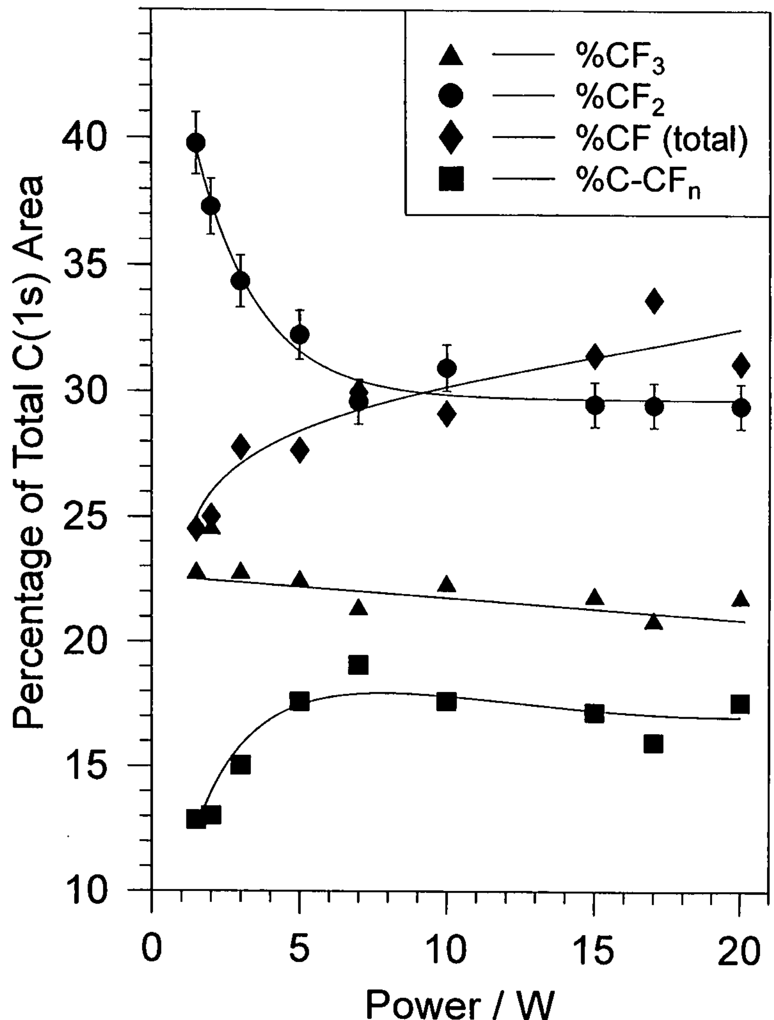

Fig. 3-2: Percentage of total C(1s) areas for each carbon functionality in plasma polymers from perfluorocyclohexane as a function of discharge power.

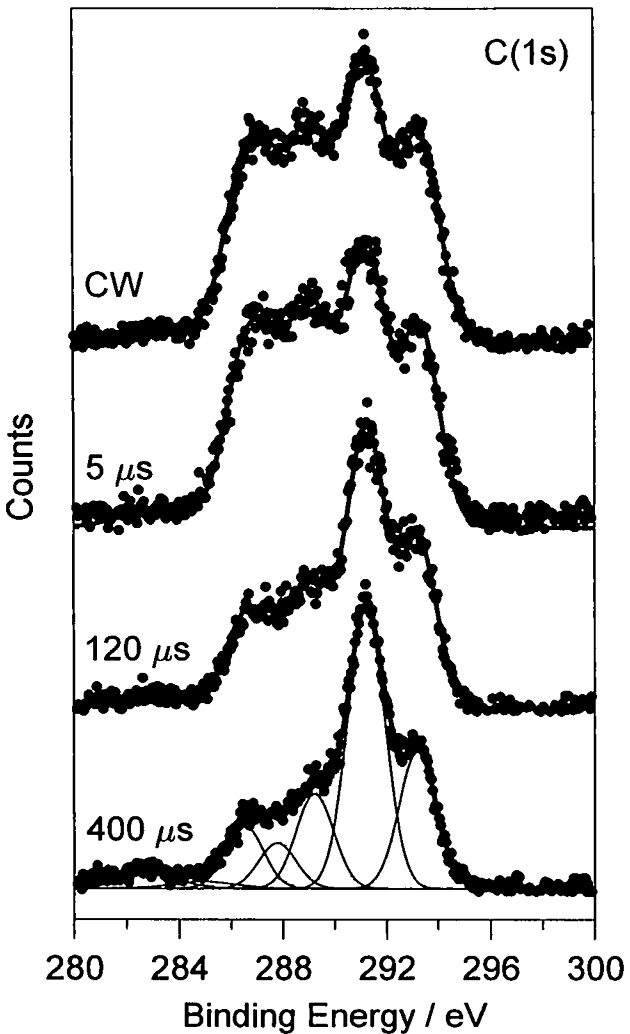

Fig. 3-3: C(1s) XPS spectra of perfluorocyclohexane plasma polymers shown as a function of off-time; peak power = 20 W, on-time = 20 μs.

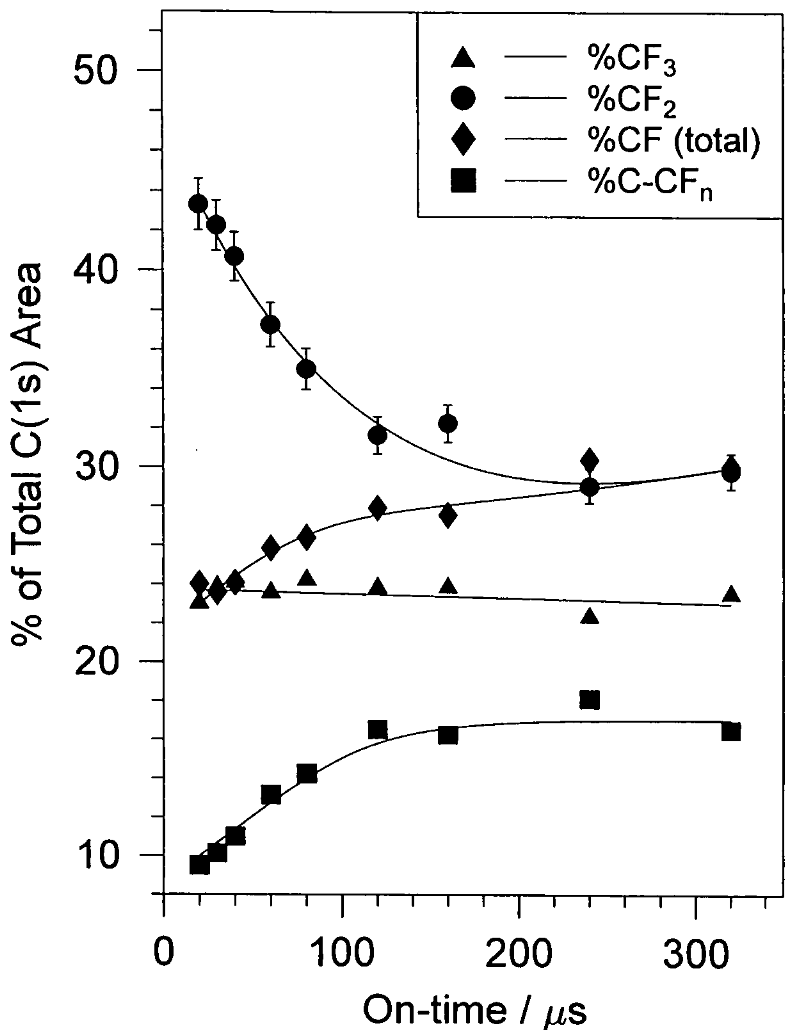

Fig. 3-4: Percentage of total C(1s) areas for each carbon functionality as a function of off-time; peak power = 20 W, on-time = 20 μs.

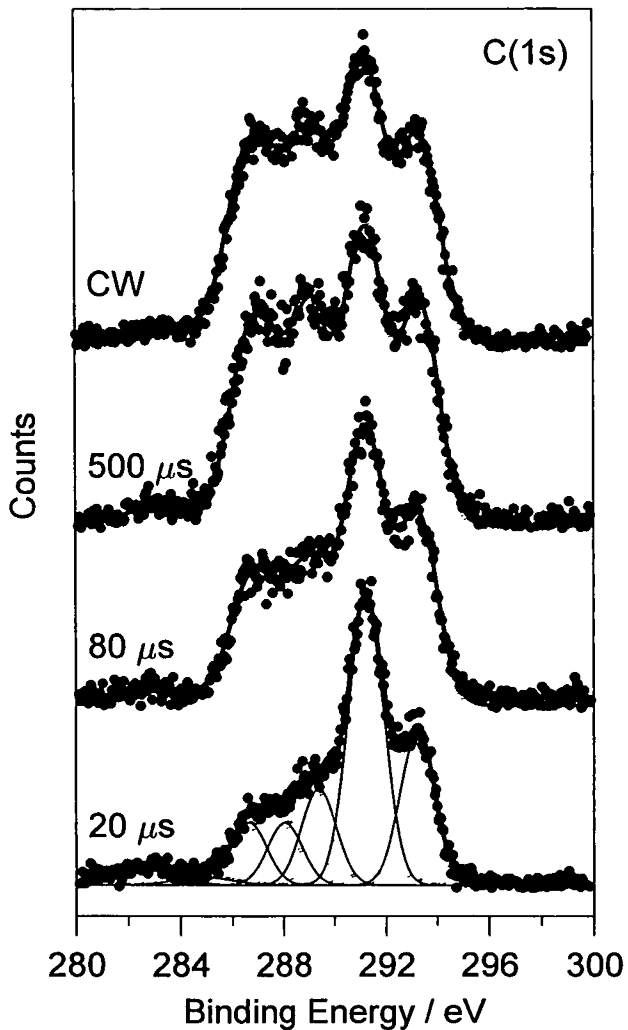

Fig. 3-5: C(1s) XPS spectra of perfluorocyclohexane plasma polymers shown as a function of on-time; peak power = 20 W, off-time = 250 μs.

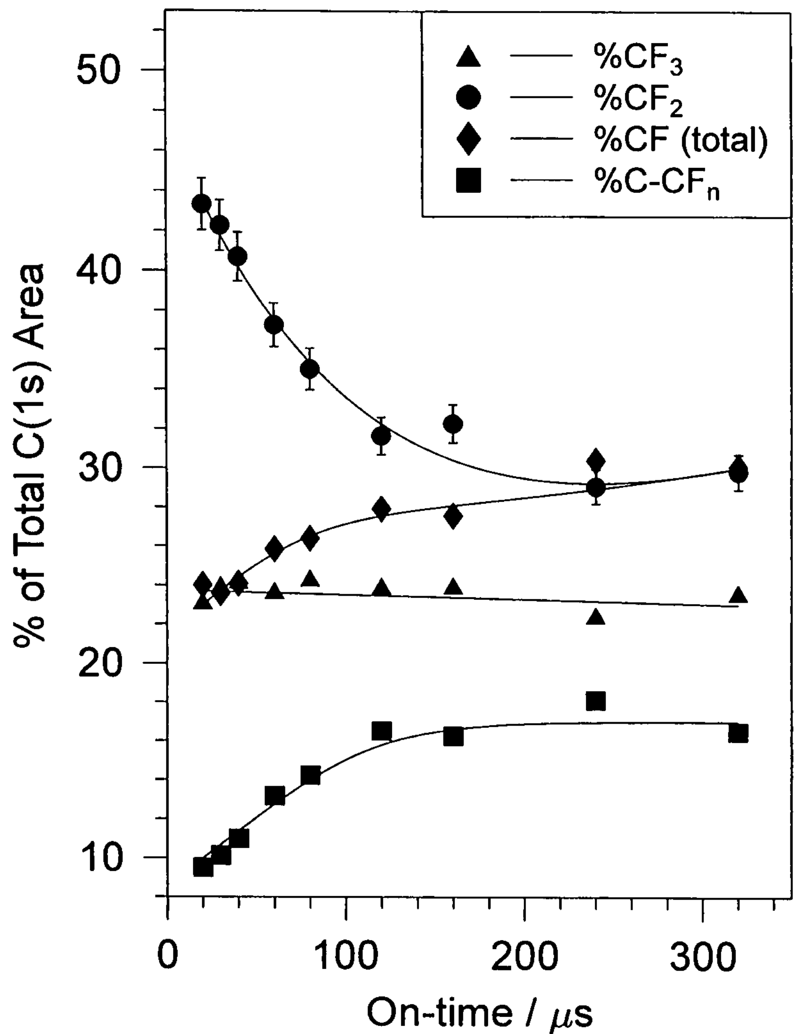

Fig. 3-6: Percentage of total C(1s) areas for each carbon functionality as a function of on-time; peak power = 20 W, off-time = 250 μs.

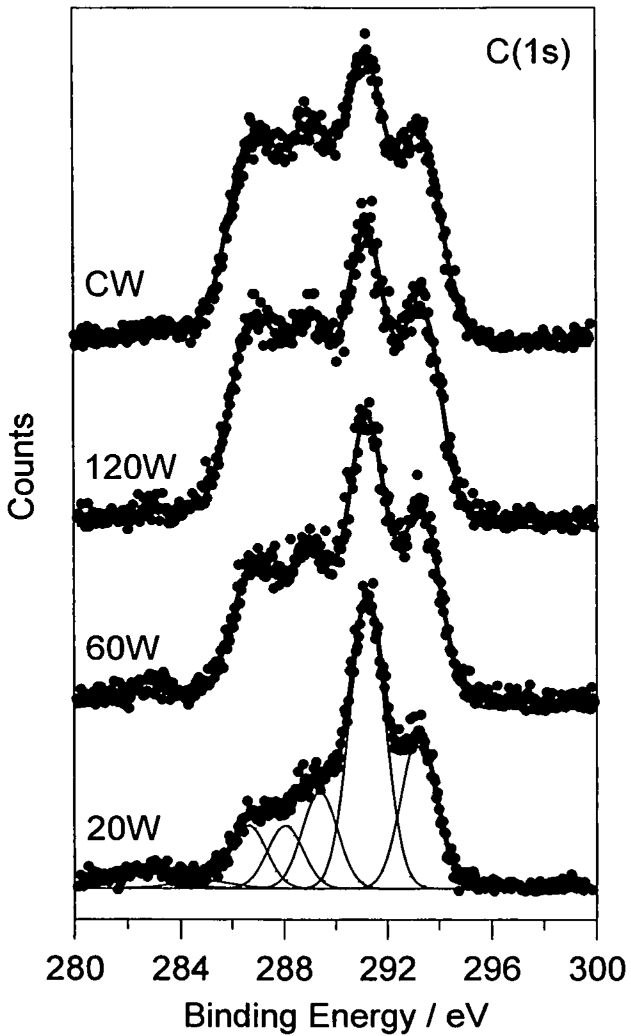

Fig. 3-7: C(1s) XPS spectra of perfluorocyclohexane plasma polymers shown as a function of peak power; on-time = 20 μs, off-time = 250 μs.

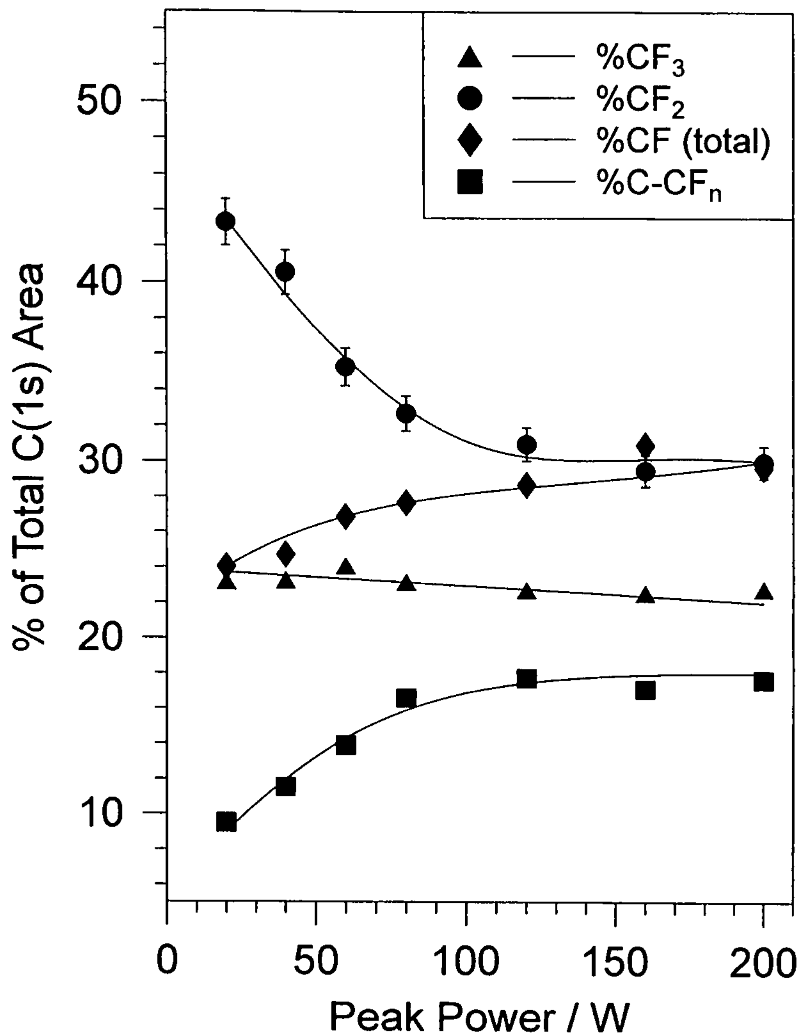

Fig. 3-8: Percentage of total C(1s) areas for each carbon functionality as a function of peak power; on-time = 20 μs, off-time = 250 μs.

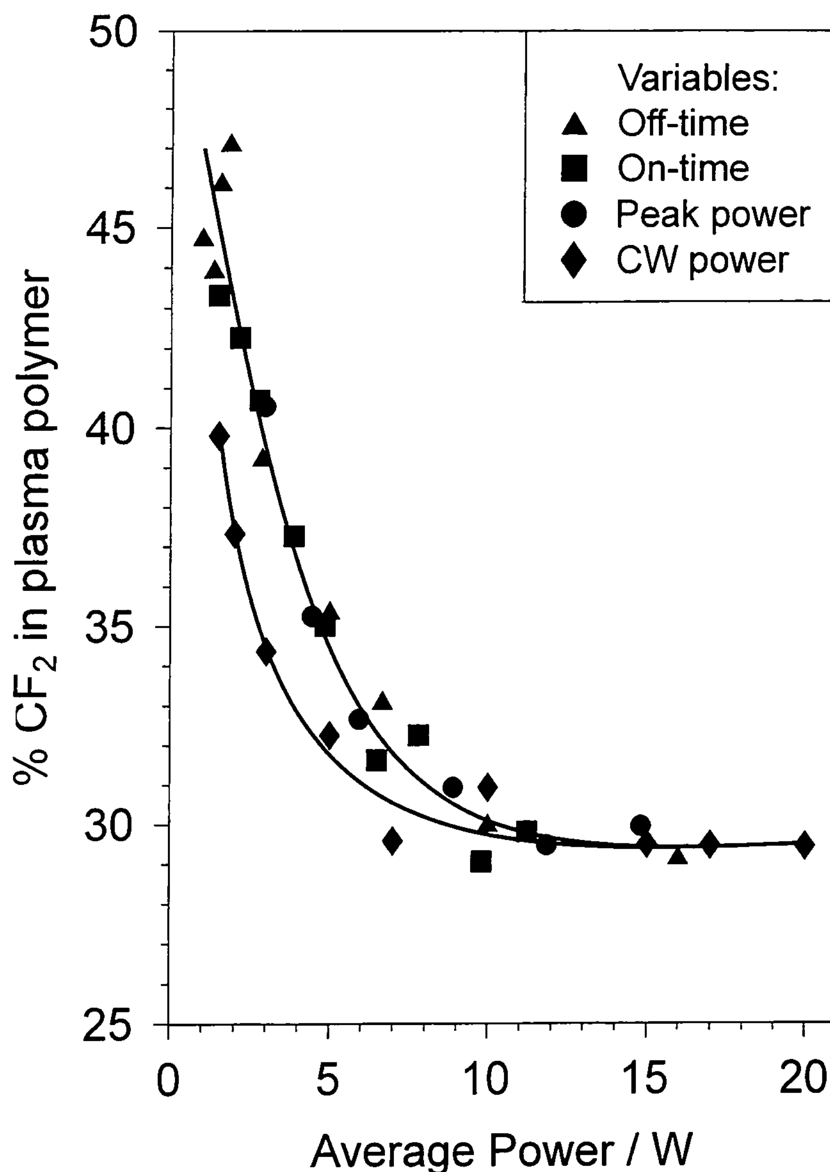

Fig. 0-9: Variation in CF_2 content of plasma polymers, deposited from pulsed and continuous wave perfluorocyclohexane discharges, as a function of average power.

Transmission Infrared Spectroscopy.

Transmission infrared measurements give information on the bulk composition of the plasma polymer. For fluorocarbons the information that can be gained from the infrared spectra of the plasma polymers is limited. This is due to the very intense C-F absorption at ~ 1100 cm^{-1} and the strong coupling between vibrational modes in this region. Due to both these factors exact assignment of the absorptions seen is not attempted. Fig. 3-10 shows a comparison of the transmission IR spectra of two plasma polymers gathered using potassium bromide disks. Despite there being an order of

magnitude difference in the discharge power used to deposit the two plasma polymers the infrared spectra are almost identical.

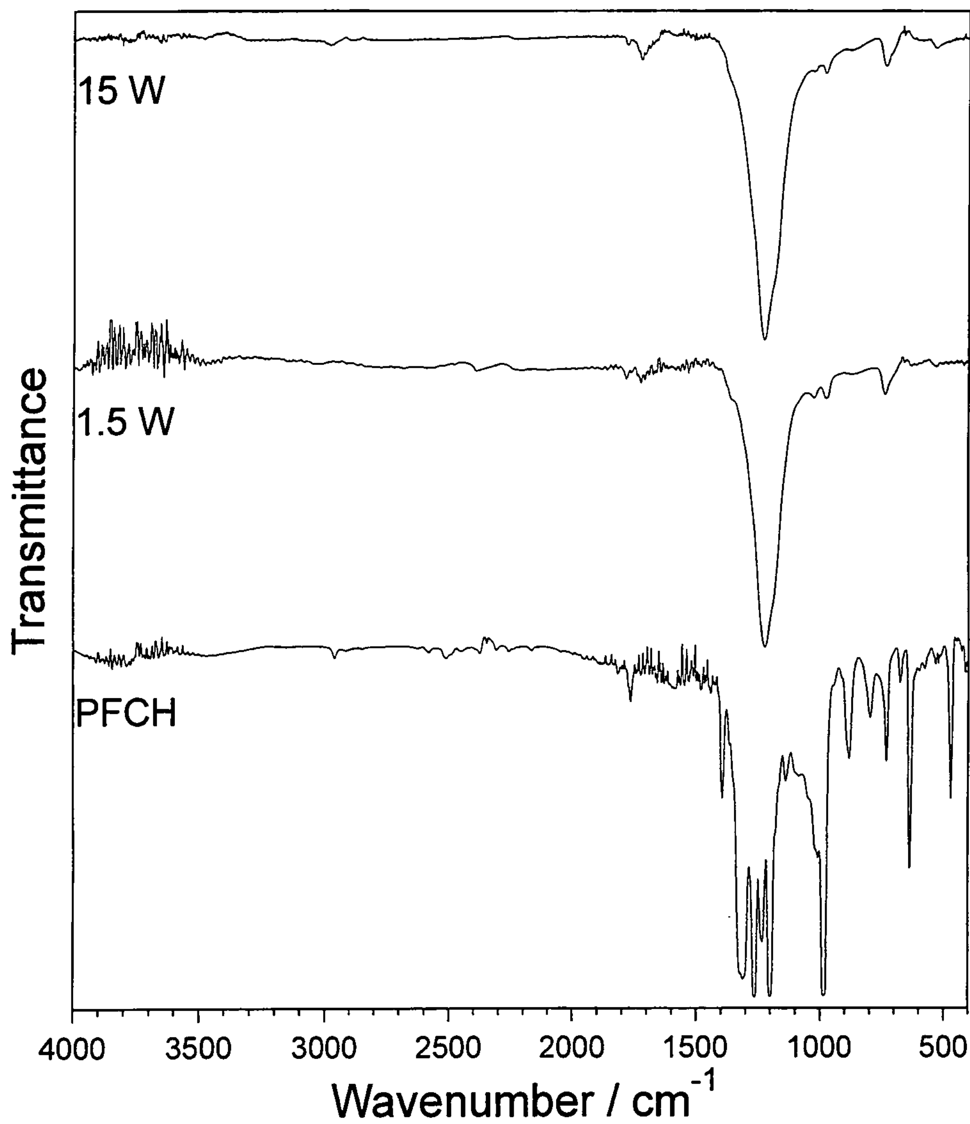

Fig. 3-10: Comparison of the transmission infrared spectra of plasma polymers deposited onto potassium bromide disks from 15 W and 1.5 W perfluorocyclohexane plasmas.

3.4 PERFLUOROCYCLOHEXANE: DISCUSSION

CF_3 and CF_2 functionalities account for up to 65% of the total C(1s) envelope in the continuous wave plasma polymerisation of perfluorocyclohexane, which is consistent with previous studies in the 1-100 W power range.[12] The amount of crosslinking in the plasma polymer has previously been shown to be dependent upon the W/FM parameter,[36] (where W = discharge wattage, F = flow rate in moles/minute and M = molecular mass of the gas). In the present study, both F and M are constants and therefore the degree of crosslinking ($\underline{C}$-CF_n) can be directly correlated to the input power, Fig. 3-1.

A variety of reactions can potentially occur during plasma polymerisation. These can be subdivided into collision induced reactions (e.g. electron impact dissociation, polymerisation in the gas phase, and ion bombardment at the gas-substrate interface) and radiation induced reactions (e.g. unimolecular excitation and dissociation, along with radiative degradation of the growing polymer network). The effect of power level on each of these types of reaction is addressed below.

The input power influences the average electron energy $\langle \varepsilon \rangle$, the population of the high energy tail of the electron energy distribution, and the density of excited species present in the plasma.[13] Any reactions which involve electrons from the high energy tail of the electron energy distribution will be affected by the drop in the number of high energy electrons with decreasing input power.[14] One such reaction is the ionisation of perfluorocyclohexane which has an activation energy of approximately 13 eV.[12] A smaller fraction of perfluorocyclohexane molecules will be expected to undergo dissociation via electron-collision ionisation at lower input powers, resulting in more non-fragmented perfluorocyclohexane molecules impinging upon the substrate. Such a rise in perfluorocyclohexane flux incident upon the surface will lead to a greater CF_2 content in the resultant plasma polymer layer.

The type and relative abundance of CF_n radicals contained in the glow discharge can also influence the composition of the plasma polymer deposit.[15,16] The difluorocarbene radical CF_2, is relatively stable with respect to other types of CF_n radical. It has been shown to be a major constituent and an important precursor to polymer formation in fluorocarbon plasmas.[17,18] Depletion of CF_2 species from fluorocarbon plasmas can occur via electron-collision processes to liberate a fluorine atom as follows;[19]

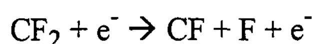

$$CF_2 + e^- \rightarrow CF + F + e^-$$

This reaction has an electron energy threshold of 6.1 eV. Since 6.1 eV is greater than the average electron energy within the plasma (typically about 2 eV), one would also expect a drop in the number of CF_2 species lost through this particular process with a corresponding increase in the CF_2 content of the plasma polymer layer.

It is of interest to note that the CF_3 content of the deposited perfluorocyclohexane plasma polymer films remains fairly constant with respect to CW power level. CF_3 species can be produced in the gas phase both through unimolecular rearrangements, as evidenced by mass spectrometry[20] and through ion-molecule collisions.[21] On the surface, ion bombardment of the fluorocarbon polymer also results in generation of CF_3 functionalities.[28] CF_3 can be removed from the plasma through reactions of the following type:

$$CF_3 + e^- \rightarrow CF_2 + e^- + F$$

Electron-collision dissociation of CF_3 yields CF_2 and fluorine, which requires electrons of 2.2 eV energy . Since this is fairly close in magnitude to the average electron energy within the glow region (typically about 2 eV), then the number of electrons at these energies will be relatively unperturbed by variations in the power supplied to the plasma. Even at low powers there should be an ample supply of 2.2 eV electrons for this reaction to occur.[22]

Another consequence of the drop in high energy electrons at lower powers, is a decrease in the number and energy of electrons able to transverse the plasma sheath, thereby

leading to a reduction in the ion and electron bombardment of the growing film, hence causing less crosslinking at lower continuous wave powers. Excited species within plasmas emit photons with energies between 3 and 40 eV.[22] Such UV radiation from a hydrogen discharge has been shown to cause surface crosslinking in polyethylene.[23] A reduction in power will attenuate the amount of VUV radiation contained in the plasma which in turn will produce less crosslinking in the polymeric product.

In some plasma deposition processes high substrate temperatures are required to encourage surface reactions and achieve good quality films.[24] A lower substrate temperature gives rise to greater adsorption of non-fragmented precursor molecules onto the substrate.[25,26] A drop in the substrate temperature at lower powers should reduce the number of reactions occurring at the surface especially positive enthalpy change reactions, such as bond breaking.

3.4.1.1 Pulsed Plasma Polymerisation

For average powers below 7 W, pulsing of the perfluorocyclohexane glow discharge produces a plasma polymer with a greater CF_2 content and less crosslinked ($C\text{-}CF_n$) carbon than that found for corresponding continuous wave experiments. One possible explanation for the drop in crosslinking during pulsing could be the lower substrate temperature, since a significant advantage of pulsing the fluorocarbon glow discharge is that extensive heating of the reactor walls and substrate can be avoided.[27] The plasma sheath voltage decays rapidly leading to a time-averaged reduction in the number and energy of positive ions bombarding the surface and hence the substrate will experience less heating. Previous XPS studies have shown that ion bombardment of plasma polymerised fluorocarbon films results in a rise in crosslinked carbon centres at the expense of CF_3 and CF_2 functionalities.[28] Therefore less ion bombardment of the growing plasma polymer film will lead to a smaller amount of crosslinking. Also it has been reported that VUV emission from pulsed discharges is lower than from CW discharges,[29] which should further reduce the activation of the substrate, again resulting

in less crosslinking in the final polymer film. The cumulative effect of lower substrate temperature along with reduced ion bombardment and VUV irradiation during pulsed plasma polymerisation will be expected to produce a narrower distribution of electronic environments for a particular type of C(1s) functionality. Indeed this is found to be the case, since the widths (FWHM's) of the component peaks in the C(1s) XPS profiles fall with decreasing peak power, Fig. 3-11.

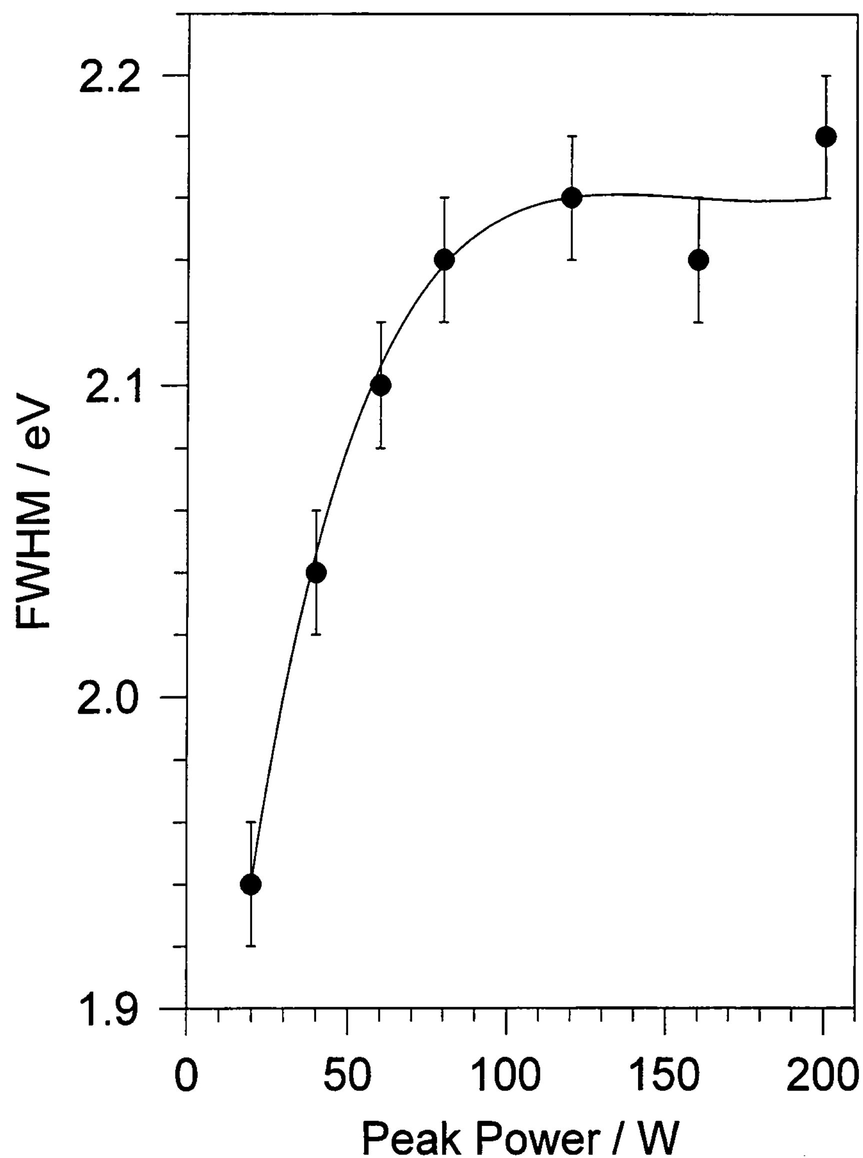

Fig. 3-11: Variation in FWHM of C(1s) component peaks versus peak power (on-time = 20 μs, off-time = 250 μs) from plasma polymers of perfluorocyclohexane.

3.5 PERFLUOROCYCLOPENTENE: RESULTS

3.5.1 X-ray Photoelectron Spectroscopy

At low powers the composition of the plasma polymer is particularly sensitive to the continuous wave power input, Fig. 3-12, Fig. 3-13. On increasing glow discharge power from 1 to 5 W the amount of CF_2 incorporation falls sharply, from 35% to 26%, whilst the other functionalities all rise by between 2% and 3%. Beyond 5 W film composition shows a much lower dependence on discharge power yielding polymers composed of approximately 22 ± 1.2% C-CF_n, 31 ± 1.7% CF, 27 ± 0.9% CF_2 and 19 ± 0.9% CF_3. The F/C ratios of all the polymers deposited from continuous wave discharges are 1.30 ± 0.07, irrespective of discharge power used, compared to a value of 1.6 for the precursor molecule; this corresponds to a 19% loss in fluorine content.

The results from XPS analysis of polymers deposited from pulsed plasmas are also shown below, Fig. 3-14 - Fig. 3-17. When the power to the plasma is pulsed the average power delivered to the glow discharge is a function of three variables, namely off-time, on-time and peak power. All functionalities show the same trends with average power irrespective of which variable is altered; for example the amount of CF_2 incorporation into the plasma polymer rises at the expense of CF_3 with increasing off-time and decreasing on-time and peak power. This is clearly shown when the percentage CF_3 and CF_2 in the plasma polymers are plotted against average power, Fig. 3-18. Evidently decreasing the average power has the same effect of increasing the CF_2 and decreasing the CF_3 content of the polymers regardless of whether it is continuous wave power, off-time, on-time or peak power which is varied. It appears that on average pulsed plasma polymers have a slightly higher CF_2 and lower CF_3 content than continuous wave plasma polymers deposited at the same average power, i.e. pulsing slightly enhances the retention of monomer stoichiometry and reduces rearrangements relative to continuous wave plasma polymerisation. As with the continuous wave experiments the F/C ratio of

all the polymers deposited from pulsed plasmas is constant; the value being only slightly lower at approximately 1.28 ± 0.05.

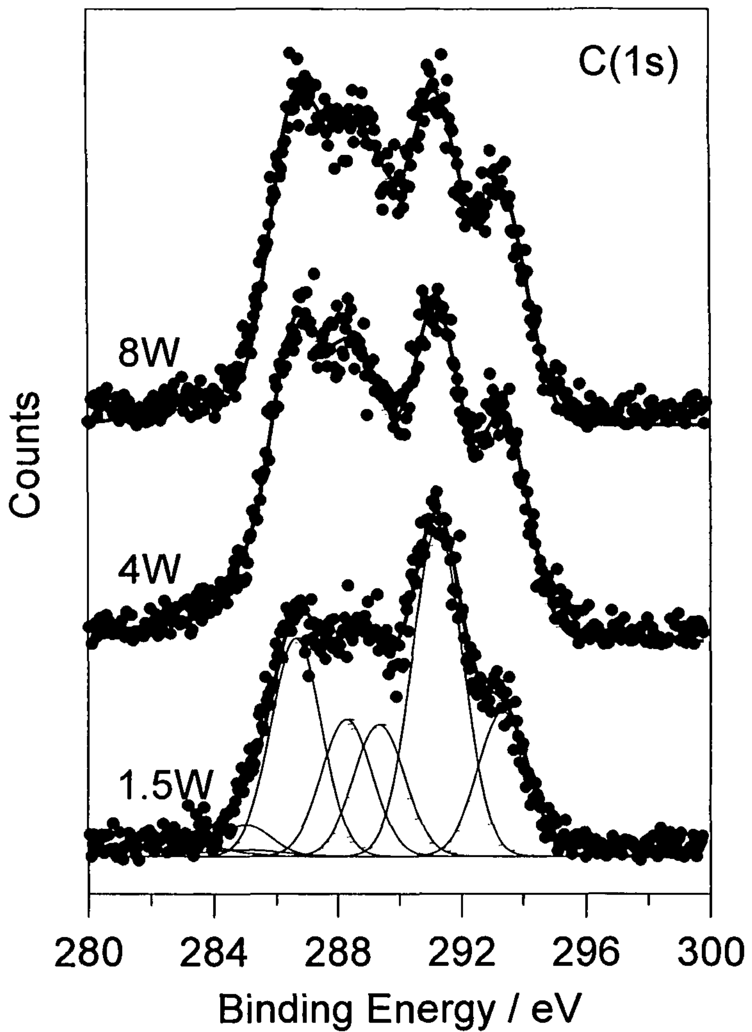

Fig. 3-12: C(1s) XPS spectra of perfluorocyclopentene plasma polymers as a function of continuous wave power.

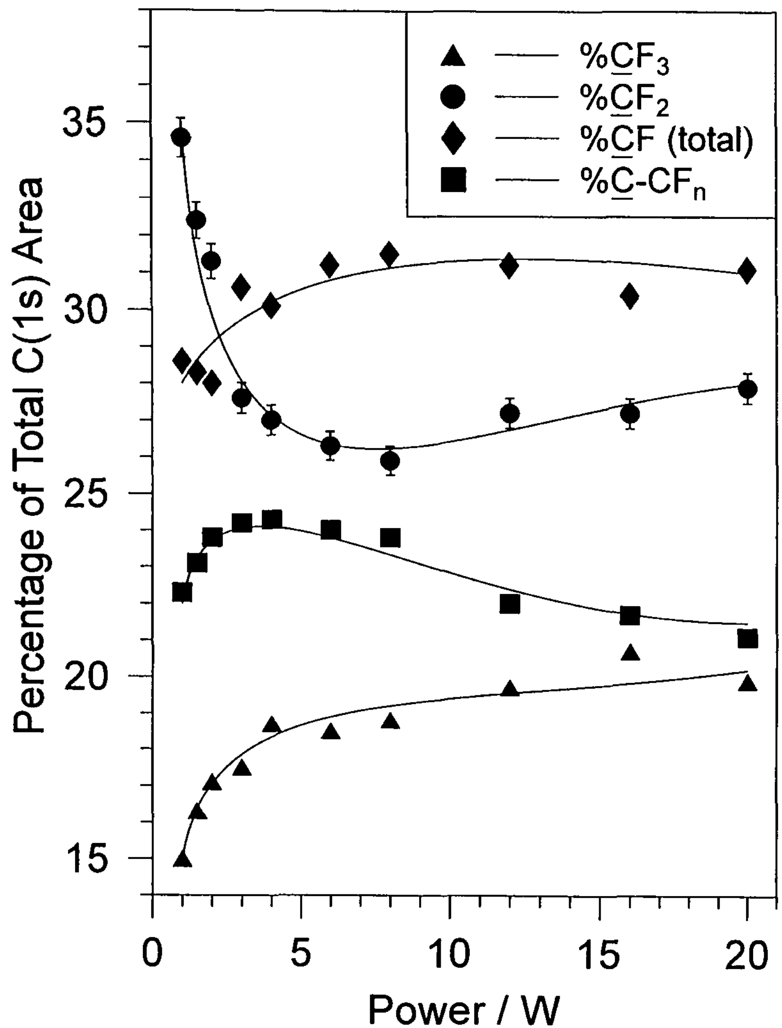

Fig. 3-13: Percentage of total C(1s) areas for each carbon functionality as a function of continuous wave discharge power.

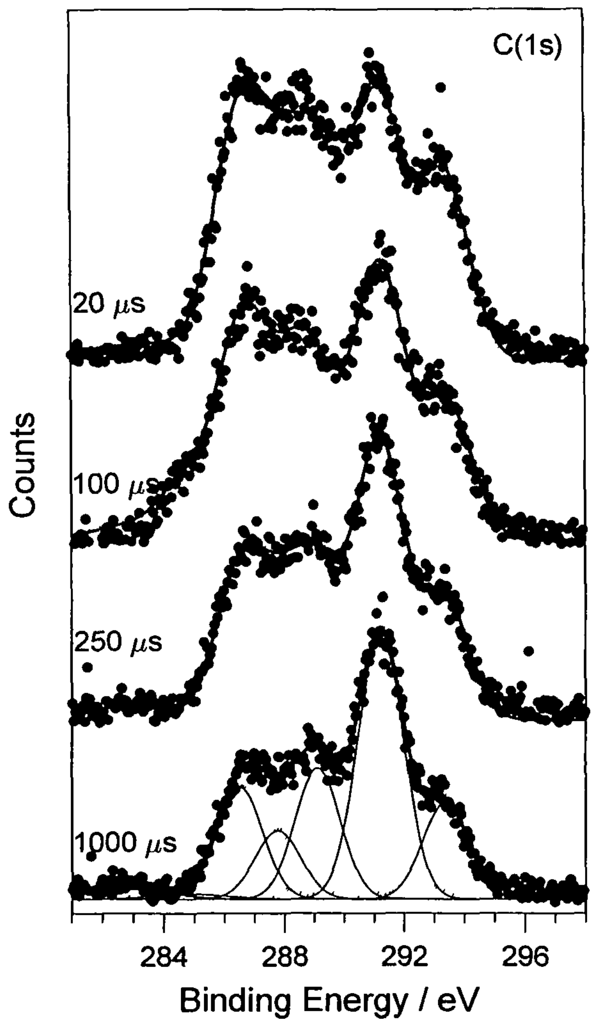

Fig. 3-14: C(1s) XPS spectra of perfluorocyclopentene plasma polymers shown as a function of off-time; peak power = 20 W, on-time = 20 μs.

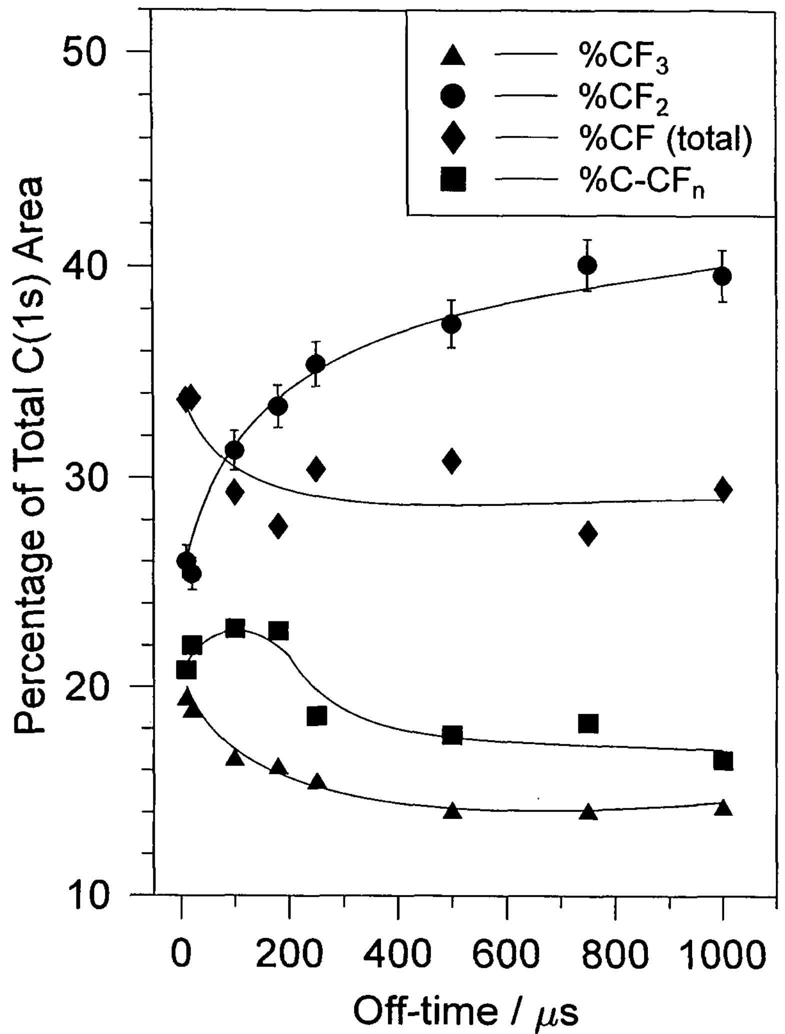

Fig. 3-15: Percentage of total C(1s) areas for each carbon functionality as a function of off-time; peak power = 20 W, on-time = 20 μs.

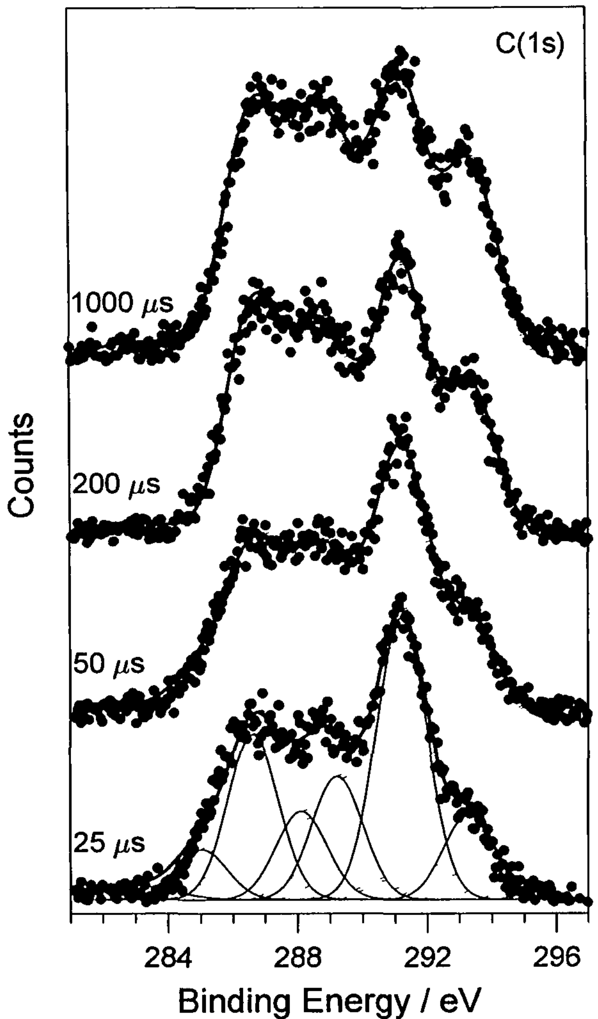

Fig. 3-16: **C(1s) XPS spectra of perfluorocyclopentene plasma polymers shown as a function of on-time; peak power = 20 W, off-time = 250 μs.**

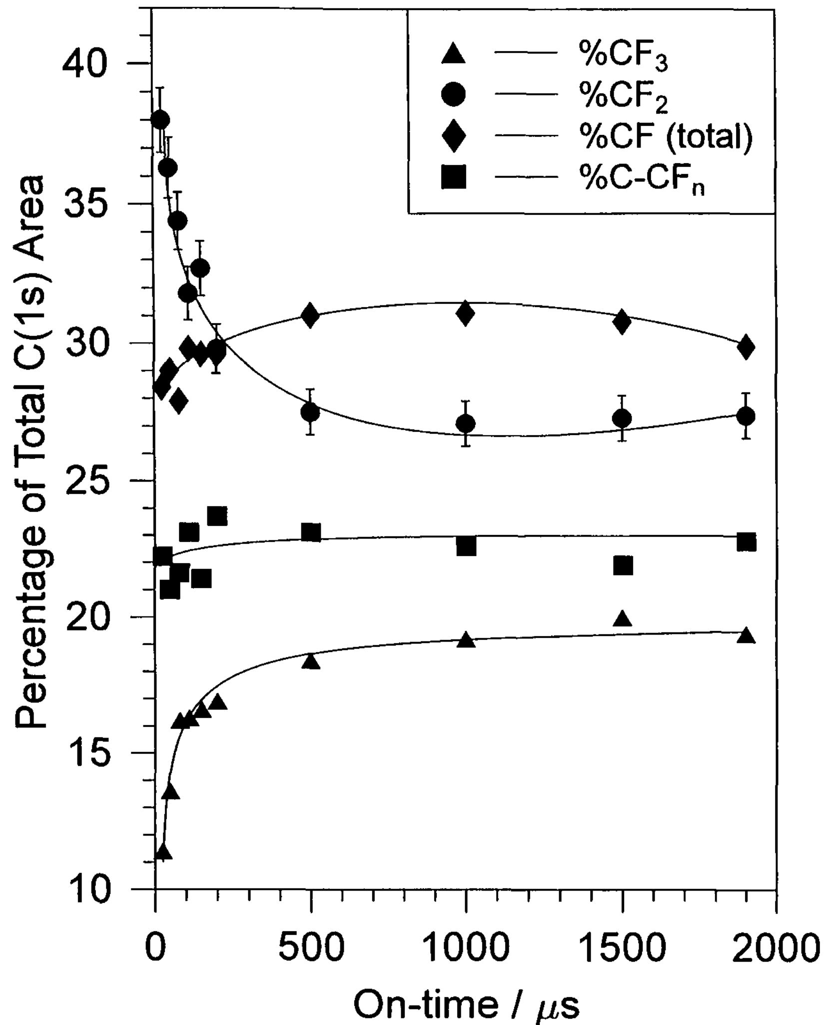

Fig. 3-17: **Percentage of total C(1s) areas for each carbon functionality as a function of on-time; peak power = 20 W, off-time = 250 μs.**

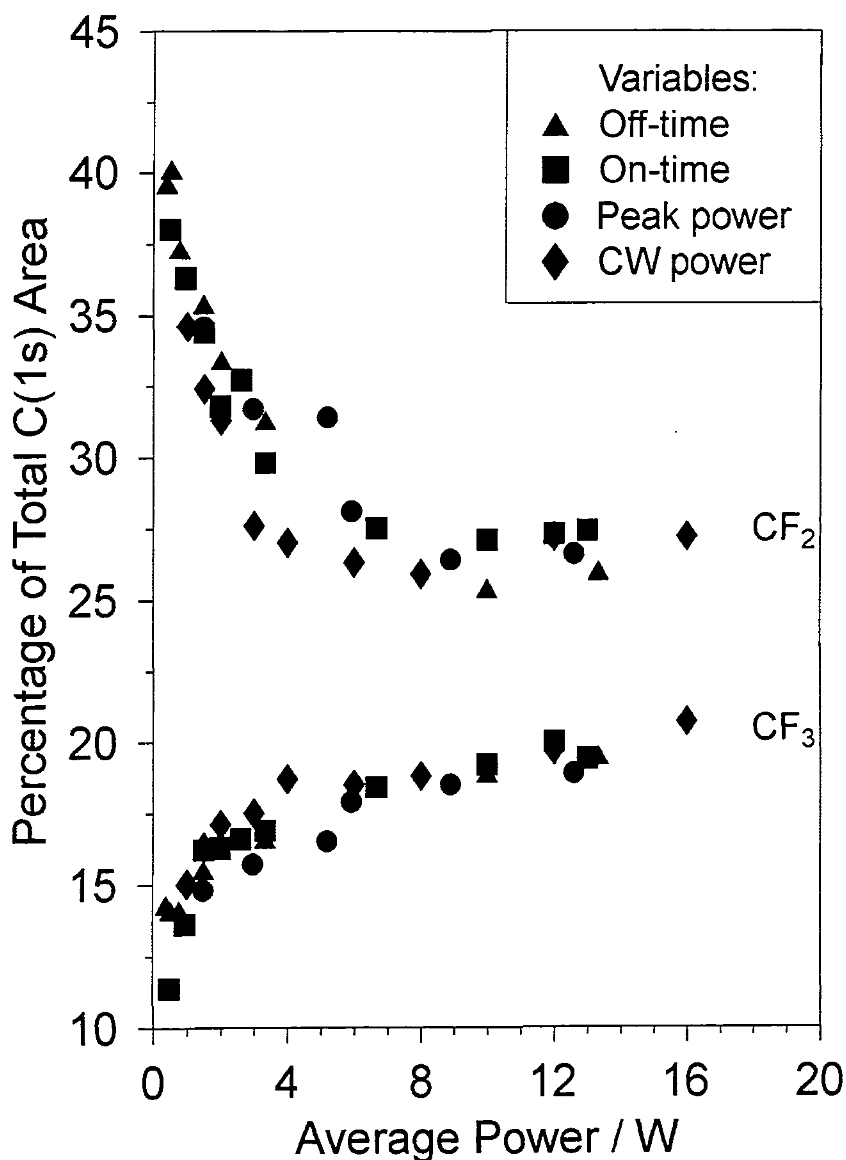

Fig. 3-18: Comparison of the percentage CF_2 and CF_3 in plasma polymers of PFCP as a function of average power delivered to the plasma.

3.5.2 Transmission Infrared Spectroscopy.

The IR spectrum of PFCP vapour, Fig. 3-19, shows well resolved and intense absorption peaks at 1769(m), 1396(s), 1327(m), 1299(m), 1219(m), 1178(vs), 1011(vs), 986(vs) and 601(m) cm^{-1}. The peak at 1769 cm^{-1} is assigned to the C=C stretch in perfluorocyclopentene[30,31] while the peaks below 1400 cm^{-1} are characteristic of all fluorocarbons due to C-F stretching vibrations.[32-34] Coupling between C-C and C-F stretching vibrations in this region means it is not possible to assign these peaks to particular vibrational modes.[30]

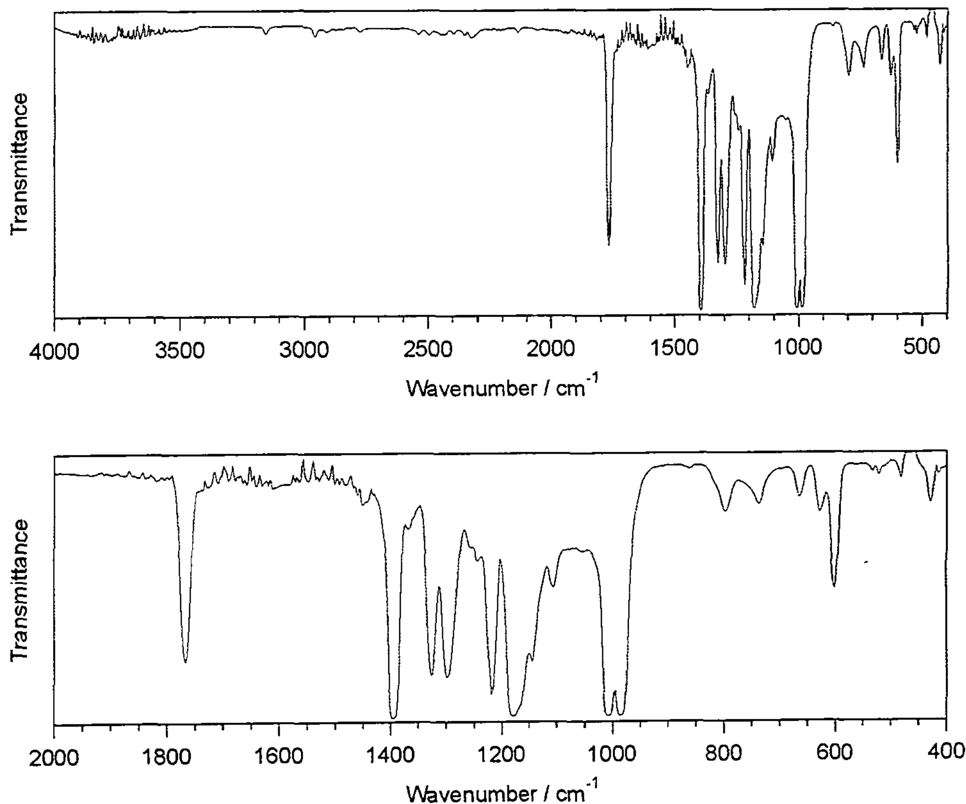

Fig. 3-19: Transmission infrared spectrum of perfluorocyclopentene vapour.

In contrast with the well resolved peaks seen in the PFCP spectrum the transmission infrared spectra of the plasma polymers deposited from both continuous wave, Fig. 3-20 and pulsed plasmas, Fig. 3-21 and Fig. 3-22, on potassium bromide disks consist principally of a strong broad absorption band about 1100 cm^{-1} due to C-F stretching vibrations. On the whole changing the continuous wave power and the average power in the case of pulsed plasmas does not alter the IR spectra greatly. However at low powers the spectra of the plasma polymers do begin to show features in common with the monomer, namely smaller peaks appearing more resolved at 1392, 1338, 1026 and 974 cm^{-1}.

Varying the off-times from 250 μs to 20 μs, hence average powers from 1.5 to 10 W causes the peak at 1174 cm^{-1} to be reduced relative to the 1215 cm^{-1} absorption. Also the peaks at 974 cm^{-1} and 1026 cm^{-1} are more clearly resolved at longer off-times. The same trends are in evidence when the on-time is the variable employed to control the power to the plasma. In this case on-times varied between 160 μs and 1000 μs resulted in average powers between 2.7 and 10 W. Fig. 3-22 shows little difference between polymers deposited at 160 μs or 640 μs on-time. However the infrared spectrum of the polymer from the 1000 μs on-time experiment shows a reduction in the peaks at 974 cm^{-1}, 1026 cm^{-1}, 1174 cm^{-1}, and 1714 cm^{-1}.

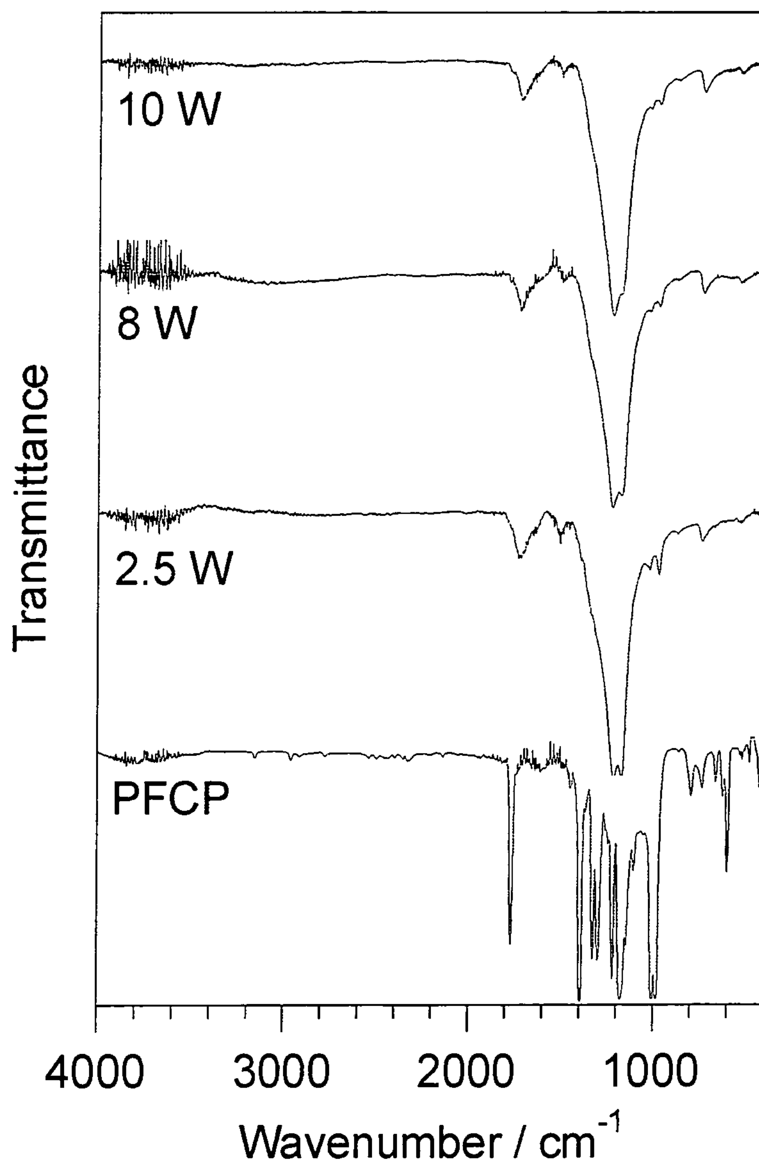

Fig. 3-20: Infrared transmission spectra of plasma polymers deposited from continuous wave perfluorocyclopentene plasmas as a function of discharge power.

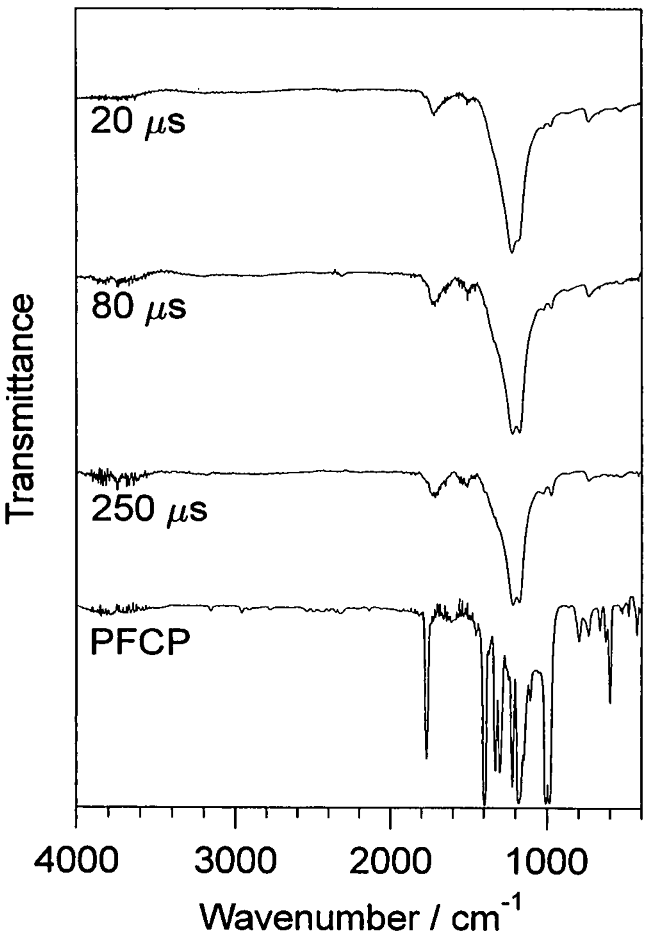

Fig. 3-21: Infrared transmission spectra of plasma polymers deposited from pulsed perfluorocyclopentene plasmas as a function of off-time; peak power = 20 W, on-time = 20 μs.

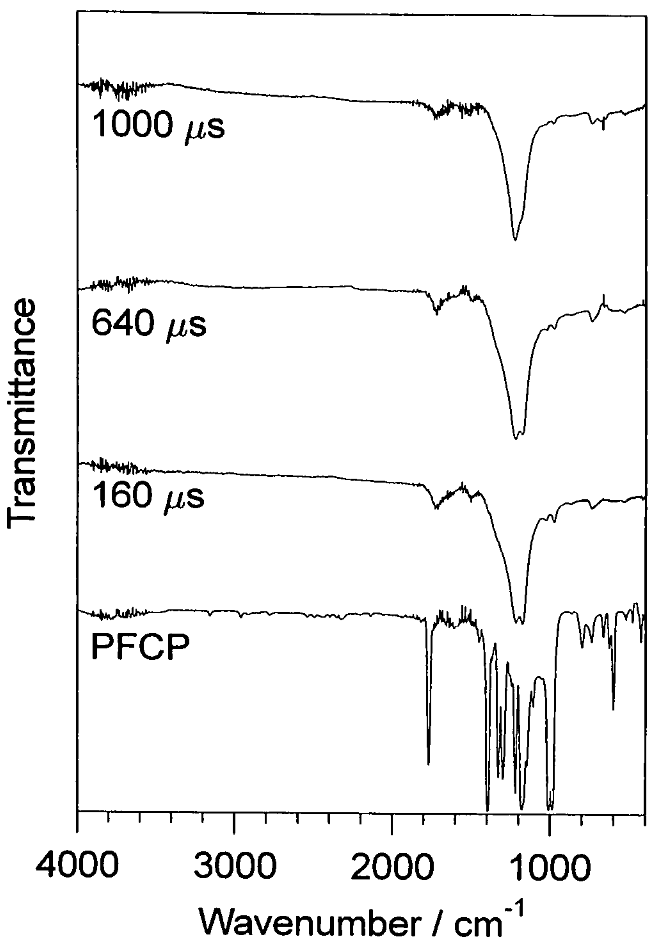

Fig. 3-22: Infrared transmission spectra of plasma polymers deposited from pulsed perfluorocyclopentene plasmas as a function of on-time; peak power = 20 W, off-time = 1000 μs.

3.6 PERFLOUROCYCLOPENTENE: DISCUSSION

The continuous wave plasma polymerisation of perfluorocyclopentene has previously been studied by Eaves[35] who compared the plasma polymers with those obtained from cathodic electropolymerisation. In an inductively coupled reactor at a pressure of 0.1 torr and a power range 5 - 40 W he found the deposited polymer had a F/C ratio of 1.4 and the composition of 21% $\underline{C}$-CF_n, 30% $\underline{C}F$, 30% $\underline{C}F_2$ and 18% $\underline{C}F_3$.

As stated earlier the power input to plasmas can be quoted in terms of the W/FM parameter,[36] (where W = discharge wattage, F = flow rate in moles/minute and M = molecular mass of the gas). In this work the flow rate used was 3.33×10^{-7} moles s^{-1} while Eaves quotes a flow rate of 1.67×10^{-7} moles s^{-1}. Eaves reported no significant variation in polymer composition at power inputs greater than 5 W, which corresponds to an energy input of 142 J kg^{-1}. This agrees with the findings of these investigations where 10 W plasma power corresponds to the same energy input per molecule. No large changes in the composition of the plasma polymers deposited are seen above 10 W continuous wave power in this system. Also the compositions of the polymers in this high power range are in good agreement. Considering the difficulties in comparing results from two different plasma polymerisation systems, the results are remarkably similar.

	$\underline{C}$-CF_n	$\underline{C}F$	$\underline{C}F_2$	$\underline{C}F_3$
Eaves	20%	30%	30%	18%
This work	21%	31%	28%	20%

A variety of reactions can potentially occur during plasma polymerisation. These can be subdivided into collision induced reactions (e.g. electron impact dissociation, polymerisation in the gas phase, and ion bombardment at the gas-substrate interface) and radiation induced reactions (e.g. unimolecular excitation and dissociation, along with radiative degradation of the growing polymer network). The effect of power level on each of these types of reactions has already been considered , however the most

notable points can be summarised as follows; reduced power to the gas results in lower average electron energy and a reduction in the population of the high energy tail of the electron distribution,[37] a reduction in the number of excited species in the plasma and hence a reduction in the ultraviolet and vacuum-ultraviolet emission,[36] and finally a reduction in the number and energy of positive ions bombarding the sample due to a reduction in the plasma potential.

With a reduction in the energy within the gas it is expected that the precursor molecule will dissociate less and that the dissociation process will be dependent to a greater extent on the relative bond strengths and thermodynamics within the perfluorocyclopentene molecules. Hence, at low powers, the structure of the precursor would be expected to have a greater effect on the composition of the final plasma polymer. The structure of perfluorocyclopentene is represented below, Fig. 3-23. As can be seen the monomer consists of three sp^3 carbons and two sp^2 carbons with two and one fluorine atoms attached respectively.

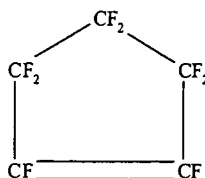

Fig. 3-23: Molecular formula for perfluorocyclopentene; *cyclo*-C_5F_8.

The presence of unsaturation in a perfluorocarbon system is known to activate the system making it more likely that C-F bond scission resulting in formation of a fluorine atom will occur compared to a saturated fluorocarbon system.[38] For example exhaustive defluorination occurs in the dimerisation of perfluorocycloalkenes either through fluorine loss resulting in formation of an allyl radical, or via nucleophilic attack on the double bond.[39] The fact that the F/C ratio of plasma polymers deposited from perfluorocyclopentene discharges remains constant at approximately 19% less than that of the monomer despite changing discharge power is of interest. It suggests that at low powers the chemical structure of perfluorocyclopentene, in particular the presence of

the double bond, causes defluorination of the precursor to become a key step in at least one of the reaction pathways leading to plasma polymer deposition.

This reduction in F/C ratio within the plasma is to be expected based on the results of Fenzlaff and Illenberger[40] who carried out electron beam studies of the unimolecular decomposition of perfluorocompounds in the gas phase. Their results indicate that at thermal or near thermal electron energies attachment of electrons to cyclic fluorocarbons in the gas phase generates metastable parent radical anions, Fig. 3-24. These have lifetimes with respect to autodetachment on the μs-ms timescale at the pressures used in the study.

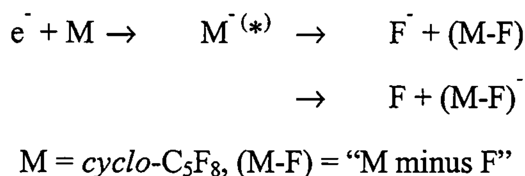

Fig. 3-24: Schematic of defluorination of perfluorocyclopentene under electron bombardment (from reference 40).

At electron energies higher than thermal however, autodissociation results in the production of either F^- and (M-F) or F and $(M\text{-}F)^-$ ion pairs depending on the value of the electron energy. In the case of perfluorocyclopentene at ~2 eV electron energies, the dominant autodissociation mechanism yields a fluoride anion and a defluorinated (M-F) radical. In a plasma these radicals will diffuse to the surface of the polymer and be incorporated either intact or following fragmentation, into the plasma polymer resulting in a lowering of the F/C ratio relative to the starting compound. Since the average electron energy of the discharge is approximately 2 eV,[37] it is to be expected that this reaction pathway would be a significant one within the overall plasma polymerisation process.

A significant loss in CF_2 content of the plasma polymers occurs on increasing from 1 W to 5 W discharge power. This is consistent with increased loss of fluorine from the allyl carbon. However the F/C ratio does not show a corresponding decrease as would be expected, which implies that the fluorine lost must be re-incorporated into the polymer.

This is supported by the presence of CF_3 groups at the surface of the plasma polymer which is evidence of destruction of the ring via C-C bond scission, and subsequent fluorination of CF_2 containing fragments, thus allowing fluorine re-incorporation into the plasma polymer to occur. Not surprisingly the CF_3 content rises with power in this low power region as increasing power will result in a greater number of fluorine atoms available to fluorinate the growing plasma polymer. The increase in CF_3 content does not match the fall in CF_2 content since loss of CF_2 carbons while liberating fluorine atoms, also eliminates potential sites for CF_3 formation.

All plasma polymers in this low power region also contain over 20% crosslinked carbon i.e. C-CF_n. Along with the expected crosslinking processes associated with plasma polymerisation as a result of the energetic nature of the conditions, additional crosslinking could also originate from nucleophilic attack on the olefinic carbons with loss of fluorine, not surprising given the activity of perfluoro-substituted double bonds to such reactions.[38]

At discharge powers above ~7 W, CF_3 and CF_2 content increases in the plasma polymers while CF content levels off and the crosslinked carbon decreases slightly. At first glance this is unexpected as it is to be expected that increasing the power to the plasma will increase the fragmentation of the precursor and hence increase the proportion of crosslinked carbon in the final plasma polymer. Previous studies have indeed shown,[28] that increasing plasma power increases the amount of crosslinking in the resultant polymer. However when the structure of the precursor is accounted for the results are at least plausible.

At low powers, 1-5 W, plasma polymerisation would be expected to yield a polymer with a large degree of retention of monomer structure and stoichiometry. Greater power in the plasma will result in generation of more free fluorine atoms and destruction of the ring systems. The dangling bonds produced will be capped by the fluorine radicals hence reducing the number of non-fluorinated carbons in the plasma polymer. Since

olefinic carbons, C-CF_n and CF, are the most reactive sites these should be preferentially destroyed. Hence one would expect a larger drop in C-CF_n than in CF (since fluorination of C-CF_n produces CF) along with moderate rises in CF_2 and CF_3 content, just as is seen in Fig. 3-13.

The strongest direct evidence for this reaction of the double bond in the perfluorocyclopentene molecule during plasma polymerisation comes from a comparison of the IR spectra of the monomer and the spectra of the plasma polymers. The absence of a strong absorption band at 1768 cm^{-1}, due to C=C stretching vibration,[41] in the plasma polymers indicates that loss of the double bond occurs readily during the plasma polymerisation process.

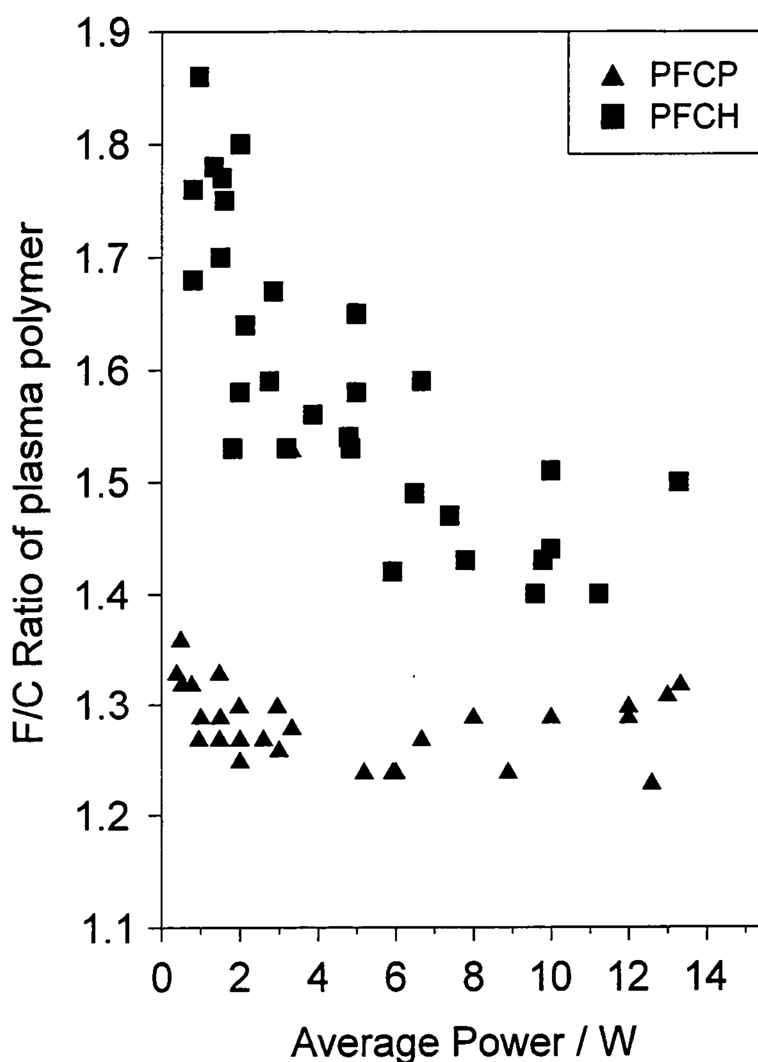

Fig. 3-25: Graph of F/C ratios of plasma polymers as a function of average from pulsed and continuous wave plasmas of perfluorocyclohexane and perfluorocyclopentene.

3.7 CONCLUSIONS

The plasma polymerisation of perfluorocyclohexane was used to generate highly fluorinated surfaces with F/C ratios as high as 1.8. Initially it was found that low discharge powers produced films with the highest fluorine content. In an attempt to further increase the fluorine content of the films, pulsed plasmas were employed. In a pulsed plasma the r.f. power to the discharge was modulated by using the signal from a d.c. pulse generator to control the r.f. generator. It was hoped that the pulsed plasmas would allow greater retention of the stoichiometry of the precursor in the plasma polymer. XPS analysis of the plasma polymers showed that for identical average powers, polymers deposited from a pulsed plasma had a greater F/C ratio than those deposited from continuous wave plasmas. The pulsed plasma polymers also had greater CF_2 content and a lower degree of crosslinking i.e. greater retention of monomer structure.

Perfluorocyclopentene was also used as a precursor to highly fluorinated, low surface energy polymeric coatings. Plasma polymers deposited from perfluorocyclopentene plasmas had a lower F/C ratio (~1.3) and lower CF_3 and CF_2 content than perfluorocyclohexane polymers. This was to be expected given the stoichiometry of the starting material. However the presence of the unsaturation in the ring system of the perfluorocyclopentene molecule was expected to result in a different plasma chemistry to perfluorocyclohexane. This is indeed what was found as the variations observed in plasma polymer composition as a function of discharge power and pulsing parameters were distinctly different for the two precursors.

The difference between the stoichiometries of the plasma polymers from perfluorocyclohexane and perfluorocyclopentene and the changes in the relative contributions of each carbon functionality to the overall polymer stoichiometry with varying plasma conditions are a result of the difference in the structures between the two precursors. These differences in the plasma polymers also give an insight into the

pathways leading to the production of the final polymer from the plasma. The most significant points taken from a comparison of the two sets of results are;

1. In the case of perfluorocyclohexane the F/C ratio depends on the input power whereas for perfluorocyclopentene the F/C ratio of the plasma polymer is independent of discharge power, Fig. 3-25, p. 95.
2. For perfluorocyclohexane the percentage CF_3 in the plasma polymer is independent of power whereas the crosslinked carbon ($C\text{-}CF_n$) content is a function of discharge power. For perfluorocyclopentene the opposite is true with the crosslinked carbon content approximately constant while the CF_3 content increases with discharge power.
3. The amount of crosslinked carbon present in the plasma polymers is much greater for those polymers deposited from perfluorocyclopentene than in those from perfluorocyclohexane.

The differences observed in the plasma polymers are due to the monomers breaking down in fundamentally different manners within the plasma due to their respective chemical structures, in particular the presence of a double bond in the perfluorocyclopentene molecule. A critical step in the plasma polymerisation process for perfluorocyclopentene is removal of one of the fluorine atoms adjacent to the double bond resulting in a carbon with no fluorine attached, ready to be incorporated into the growing plasma polymer. This reaction would allow for the observed high concentration of crosslinked carbon and the constant value of the F/C ratio irrespective of power in the plasma polymers from perfluorocyclopentene. The argument is the same as the one used for explaining why the CF_3 content of the plasma polymers from perfluorocyclohexane plasmas remains high irrespective of power. The necessary reactions are constantly taking place and are not affected by changes in the plasma conditions.

In the case of perfluorocyclohexane the defluorination process was power dependent whereas in the case of perfluorocyclopentene one of the principle means of

defluorination is via the initial and favoured loss of fluorine from beside a double bond. The stoichiometry of the final plasma polymer is a result of the balance between the various fluorinating and defluorinating reactions occurring within the glow discharge. The fact that the F/C ratio remains constant within the power range studied indicates that within this power regime the fluorination/defluorination equilibrium is unaffected by discharge parameters.

3.8 REFERENCES

(1) Clarotti, G.; Schue, F.; Sledz, J.; Geckeler, K.E.; Göpel, W.; Orsetti, A. *J. Memb. Sci.* **1991,** *61*, 289.

(2) Kohoma, M.; Okazaki, S.; Uchama, H. Patent No. JP 06 41755, Feb. 1994.

(3) Iriyama, Y.; Yasuda, T.; Cho, D.L.; Yasuda, H. *J. Appl. Polym. Sci.* **1990**, *39*, 249.

(4) O'Kane, D.F.; Rice, D.W. *J. Macromol. Sci., Chem.* **1976,** *A10*, 567.

(5) Sato, K.; Omae, S.; Kojima, K.; Hashimoto, T.; Koinuma, H. *Jap. J. Appl. Phys.* **1988**, *27*, L2088.

(6) Clarotti, G.; Aoumar, A.A.B.; Schué, F.; Sledz, J.; Geckeler, K.E.; Flösch, D.; Orsetti, A. *Makromol. Chem.* **1991**, *192*, 2581.

(7) Llewellyn, I.; Rimmer, N. *Thin Solid Films*, **1990**, *191*, 135.

(8) Savage, C.R.; Timmons, R.B.; Lin, J.W. *Chem. Mater.* **1991**, *3*, 575.

(9) Ehrlich, C.D.; Basford, J.A. *J. Vac. Sci. Tech.* **1992,** *A10*, 1.

(10) Wagner, C.D.; Riggs, W.M.; Davis, L.E.; Moulder, J.F.; Muilenber, G.E. *Handbook of X-Ray Photoelectron Spectroscopy*; Perkin-Elmer Corporation, 1978.

(11) Wells, R.K.; Ryan, M.E.; Badyal, J.P.S. *J. Phys. Chem.* **1993,** *97*, 12879.

(12) Clark, D.T.; Shuttleworth, D. *J. Polym. Sci., Polym. Chem. Ed.* **1980,** *18*, 27.

(13) McTaggart, F.K. *Plasma Chemistry in Electrical Discharges*; Elsevier Publishing Company: London, 1967.

(14) Grill, A. *Cold Plasmas in Materials Technology*; IEEE Press: Piscataway, New Jersey, 1994.

(15) Takahashi, K.; Hari, M.; Kishimoto, S.; Goto, T. *Jpn. J. Appl. Phys.* **1994,** *33*, 4181.

(16) d'Agostino, R.D.; Cramarossa, F.; Fracassi, F.; Desimoni, E.; Sabbatini, L.; Zambonin, P.G.; Caporiccio, G. *Thin Solid Films*, **1986,** *143*, 163.

(17) d'Agostino, R.D.; Favia, P.; Fracassi, F. J. *Polym. Sci., Polym. Chem. Ed.* **1990,** *28*, 3387.

(18) Millard, M.M.; Kay, E. *J. Electrochem. Soc.*, **1982**, 160.

(19) Bretagne, J.; Epaillard, F.; Ricard, A. *J. Polym. Sci., Polym. Chem. Ed.* **1992,** *30*, 323.

(20) Budzikiewiz, H.; Djerassi, C.; Williams, D.H. *Mass Spectrometry of Organic Compounds*, Holden-Day Inc.: San Francisco, 1967.

(21) Lias, S.G. in *Fluorine-containing Free Radicals*, Root, J.W., Ed.; A.C.S. Symposium Series, A.C.S.: Washington, D.C., 1978.

(22) Clark, D.T.; Dilks, A.; Shuttleworth, D. in *Polymer Surfaces*; Clark, D.T.; Feast, W.J., Ed; Wiley & Sons: Bath, 1978.

(23) Hudis, M.; Prescot, L.E. *Polym. Lett*, **1972**, *10*, 179.

(24) Sherman, A. *Chemical Vapor Deposition for Microelectronics*; Noyes Publications: Park Ridge, New Jersey,1990.

(25) Ratner, B.D.; Lopez, G.P. *J. Polym. Sci. Polym. Chem. Ed.* **1992,** *30*, 2415.

(26) Ratner, B.D.; Lopez, G.P. *Langmuir*, **1991,** *7*, 766.

(27) Scarsbrook, G.; Llewellyn, I.P.; Ojha, S.M.; Heinecke, R.A. *Vacuum*, **1988**, 627.

(28) O'Keefe, M.J.; Rigsbee, J.M. *J. Appl. Polym. Sci.* **1994,** *53*, 1631.

(29) Yasuda, H.; Hsu, T. *J. Polym. Sci., Polym. Chem. Ed.* **1977,** *15*, 81.

(30) Brown, J.K.; Morgan, K.J. in *Advances in Fluorine Chem.*; Stacey, M.; Tatlow, J.C.; Sharpe, A.G., Ed.; Butterworths: London, 1965, p 253.

(31) Colthup, N.B.; Daly, L.H.; Wiberlry, S.E. Eds., *Introduction To Infrared And Raman Spectroscopy 3rd Ed.*, Academic Press: San Diego, 1990, p. 380.

(32) Bellamy, L.J. *The Infrared Spectra of Complex Molecules, Vol. 1, 3rd ed.;* Chapman & Hall: London, 1975, p. 369.

(33) Diaz, K.F.; Hernandez, R. *J. Polym. Sci., Polym. Chem. Ed.* **1984,** *22*, 1123.

(34) Hudlicky, M. *Chemistry Of Organic Fluorine Compounds, 2nd Ed.;* Ellis Horwood: London, 1976, p. 576.

(35) Eaves, J.G. Ph. D. Thesis, University of Durham, 1986.

(36) Yasuda, H. *Plasma Polymerization*; Academic Press: Orlando, 1985.

(37) McTaggart, F.K. *Plasma Chemistry in Electrical Discharges*; Elsevier Publishing Company: London, 1967.

(38) Chambers, R.D. *Fluorine in Organic Chemistry*, Wiley: New York, 1973.

(39) Briscoe, M.W.; Chambers, R.D.; Silvester, M.J.; Drakesmith, F.G. *Tet. Lett.*, **1988**, *29 (11)*, 1295.

(40) Fenzlaff, M.; Illenberger, E. *Chem. Phys.*, **1989**, *136*, 443.

(41) Silverstein, R.M.; Bassler, G.C.; Morrill, T.C. *Spectrometric Identification of Organic Compounds*, Wiley & Sons: New York, 1991.

CHAPTER FOUR

AN INVESTIGATION OF THE PULSED PLASMA POLYMERISATION OF PERFLUOROALLYLBENZENE

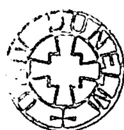

CHAPTER FOUR

AN INVESTIGATION OF THE PULSED PLASMA POLYMERISATION OF PERFLUOROALLYLBENZENE

4.1 INTRODUCTION

4.1.1 Background

The very nature of the plasma polymerisation process lends itself to extensive molecular rearrangements in the route leading to the formation of the deposited film and/or the gaseous by-products. High energy electrons, ultraviolet photons, positive ions accelerated across the plasma sheath and excited neutrals and ions in metastable excited states all possess sufficient energy to dissociate the precursor into many fragments which may bear little or no resemblance to the molecular structure of the precursor.[1,2,3] All this suggests that any attempts to maintain the molecular structure in a plasma polymer face inherent difficulties. In spite or maybe even because of this the quest for retention of precursor structure in plasma polymers is one which has been actively pursued by a number of researchers.[4-12] The ultimate aim of retention of monomer structure is not purely academic as ultimately control over the composition of the surfaces produced leads to control over their properties.

4.1.2 Previous approaches towards improving selectivity

The approaches taken to achieve structural retention in the final plasma polymer can be subdivided into two broad categories. The first involves controlling the physical characteristics of the reaction system such as reactor design,[4] power,[5] pressure,[6] flow rate,[7,8] excitation frequency,[9,10] substrate temperature[11] and bias[12] etc. The second approach is to try to control the chemistry occurring within the reactor by a judicious choice of precursor structure,[13] carrier gas,[14] reactant mixtures[15] and even substrate

composition.[16,17] Ultimately of course most investigations involve finding the optimum balance between physical and chemical parameters to yield the desired products.

In order to control the physical properties of the plasma polymer, and hence the surface which it produces, it is essential that control be gained over its chemical composition. The results of chapter three suggest that pulsing the power to the plasma may be an effective way of enhancing the importance of the chemistry of the precursor in determining the structure of the final plasma polymer. In an effort to examine this prospect more closely it was decided to carry out a more detailed investigation of pulsed plasma polymerisation using another perfluorocarbon precursor, perfluoroallylbenzene (A), C_9F_{10}.

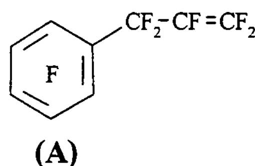

(A)

Fig. 4-1: Structural formula of perfluoroallylbenzene.

4.1.3 Factors influencing choice of starting material

Aromatic vapours have been studied previously[18-24] as precursors for plasma polymerisation with the resultant plasma polymers investigated for applications as protective and impermeable coatings,[25-28] thin film capacitors,[29,30] dielectric layers,[31] reverse osmosis membranes,[32] semiconductive thin films,[33] electroluminescent thin films[34] and permselective membranes.[35]

For this study perfluoroallylbenzene was chosen as a precursor for a variety of reasons. Firstly this is believed to be the first study carried out into the plasma polymerisation of perfluoroallylbenzene, as no other studies of continuous nor pulsed plasma polymerisation of the precursor have been found in the literature. Secondly the structure and properties of perfluoroallylbenzene are ideally suited to allow a detailed study of pulsed plasma polymerisation. The molecule consists of two important functionalities namely the aromatic fluorinated phenyl group and the perfluorinated allyl

substituent. These two functional groups can be expected to behave completely differently under plasma conditions.

As mentioned in chapter three the presence of fluorine in an olefinic carbon bond has the effect of activating the bond relative to its hydrocarbon analogue.[36] As a result of this it is to be expected that not only will the allyl group in perfluoroallylbenzene be easily activated during the on-time of the pulsing cycle, but it will also be highly susceptible to polymerisation reactions in the off-time. Along with the reactivity induced by the fluorine substitution the fact that the perfluoroallyl group is itself a substituent on a phenyl ring will further enhance its reactivity. In gas phase reactions of phenyl based compounds reactions occur preferentially on the side chains while the phenyl ring remains intact. For example methyl radicals react with toluene vapour with a hundred-fold preference for the side chain rather than the ring positions.[37]

In contrast to the fluorinated allyl substituent the perfluorinated phenyl group would be expected to be relatively stable. Studies on the plasma polymerisation of benzene and other aromatic starting materials have yielded films with compositions varying from highly unsaturated with evidence of aromaticity,[38,39] to films with no evidence for retention of the aromatic functionality.[40] The plasma polymerisation of perfluorobenzene has been studied previously as a means of depositing both organic[41,42] and inorganic/metal containing films.[43,44] It has been shown in previous studies on the plasma polymerisation of perfluorobenzene that under certain conditions it is possible to get reasonable retention of the phenyl group in the plasma polymer.[45,46]

Due to the strong and characteristic absorptions of the phenyl group the presence or absence of this functional group from the plasma polymers should be easily determined from its infrared spectrum. The unsaturated allyl group also gives rise to strong infrared active absorptions outside of the 1000-1100 cm^{-1} range. Hence in combination with the obvious opportunity for XPS analysis due to the high fluorine content of the monomer, it

should be possible to obtain a reasonable amount of information on the structure of the plasma polymers.

4.1.4 Summary

The aim of the work in this chapter will be to combine the unique advantages of pulsed plasmas, in terms of their physical characteristics, with the unique chemistry of perfluoroallylbenzene to deposit a plasma polymer which is highly aromatic in character. It is hoped that by having a sacrificial functional group in the form of the perfluorinated allyl substituent, for initiation in the on-time and reaction in the off-time, it will be possible to exploit the chemical properties of the precursor in combination with the physical properties of a pulsed plasma to achieve retention of the perfluorophenyl group in the final plasma polymer.

In addition the effects of pulsing the power to the discharge will be examined in more detail, by examining reactor profiles, the effect of average power and the plasma polymer deposition rate as a function of pulsing parameters.

4.2 EXPERIMENTAL

The experimental apparatus and procedure for continuous wave and pulsed experiments was as described in chapter three. The monomer, perfluoroallylbenzene, was purchased from Aldrich and placed in a pyrex monomer tube. The PFAB liquid was then degassed via five freeze-thaw cycles. The clean reactor was pumped to base pressure and the monomer vapour was introduced to a pressure of 0.2 torr at a flow rate of approximately 1.45×10^{-7} kg s^{-1}. The electrical discharge was ignited and sustained for 10 minutes after which the r.f. was switched off. Continuous wave powers between 1.5 and 8 Watts were employed with pulsing times, t_{on} and t_{off}, varied over the range 10 μs to 6 ms with a peak power between 8 and 200 W. Prior to removing the sample from the

reactor the system was purged with TVS for a further two minutes and finally vented to atmosphere. The samples were then removed and characterised.

The C(1s), O(1s), F(1s) and Si(2p) high resolution XPS spectra were acquired for all plasma polymers. XPS was also used to determine if complete coverage of the substrate surface was occurring. Glass substrates were used for the XPS samples and the absence of a peak in the Si(2p) region of the XPS spectrum was indicative of complete coverage of the substrate. Instrumentally determined sensitivity factors for unit stoichiometry were taken as C(1s) : O(1s) : F(1s) : Si(2p) equal to 1:00 : 0.62 : 0.53 : 1.08.

Transmission infrared spectra were acquired on a Mattson Polaris spectrometer. The monomer spectrum was acquired as a thin film between two potassium bromide disks whilst the plasma polymers were deposited on the surface of a single disk. Typically 100 scans at a resolution of 4 cm^{-1} were collected.

An atomic force microscope (Digital Instruments Nanoscope III) was used to investigate the topography of the substrate surface following plasma polymerisation. The AFM images were acquired in Tapping© mode[47]. The data is presented unfiltered. The technique employs a stiff silicon cantilever oscillating at a large amplitude near its resonant frequency (several hundred kHz), with the position of the cantilever detected by an optical beam system. The advantages of the Tapping© mode of operation include low contact forces and no shear forces during scanning. The large oscillations overcome the capillary attraction of the surface whilst the high oscillation frequency allows the probe tip to strike the surface many times before moving to the next lateral position.

Deposition rate measurements were taken by monitoring the change in mass of a quartz crystal sensor in the plasma with time. A Kronos Digital Film Thickness Monitor[48] records the change in the resonant frequency of a quartz crystal as a function of time. The resonant frequency of the crystal is proportional to its mass. The deposition monitor displays the change in mass as a thickness reading. Successful isolation of the

crystal and electronics from the plasma r.f. allows in-situ monitoring of the plasma polymer deposition.

4.3 RESULTS AND DISCUSSION

4.3.1 Pulsed polymerisation studies with varying average powers.

4.3.1.1 X-ray Photoelectron Spectroscopy

A Marquardt minimisation computer program which assumed a Gaussian peak shape with a fixed relative full width at half maximum (FWHM) was used to fit the carbon (1s) envelope for each plasma polymer with different carbon functionalities: $\underline{C}$-CF_n (286.6 eV); $\underline{C}F$ (288.4 eV); $\underline{C}F$-CF_n (289.4 eV); $\underline{C}F_2$ (291.2 eV); $\underline{C}F_3$ (293.3 eV).[45] There is also a small component with a different FWHM at very high binding energy which is too high in energy to be associated with a direct photoionisation peak, Fig. 4-2. This corresponds to a π-π* shake-up satellite due to unsaturation in the plasma polymer[49,50,5152] and directly associated with the dominant component centred at 288.4 eV corresponding to =C-F aromatic features.[46] The assigned value of ~295 eV is based on previous studies of plasma polymers of perfluorobenzene.[45,53,54] The CF_3 and CF_2 peaks could be assigned unambiguously so the CF_2 peak was taken as a reference offset at 291.2 eV. Mg $K\alpha_{3,4}$ satellite peaks with different FWHM were also taken into consideration.[55] C(1s) FWHM's were found to vary between 2.0 eV and 2.6 eV. The relative concentration of each carbon functionality was obtained by dividing the corresponding peak area by the total C(1s) envelope area including the π-π* shake-up peak. 688.3 eV was the centre of the F(1s) peak which had a FWHM between 2.7 and 2.9 eV. Taking into account the appropriate XPS sensitivity factors, the F/C ratio for each film was calculated from the F(1s) and C(1s) peak areas. Oxygen incorporation into the polymer was always less than 1.5%.

The change in appearance of the overall C(1s) photoelectron spectra with increasing discharge power is shown in Fig. 4-3. At low powers the highest component is centred around 288.4 eV, corresponding to carbons bonded to one fluorine. At higher powers the C(1s) spectra show greater intensity at higher binding energies indicating an increase in the proportion of highly fluorinated carbons in the plasma polymer with increasing discharge power.

These changes in polymer composition with plasma power can be seen when the percentages of the various component peaks in the overall C(1s) XPS spectra are plotted as a function of continuous wave power, Fig. 4-4. As the discharge power is decreased the amount of CF increases from approximately 36% at 16 W to just over 50% at 1.5 W. This is accompanied by a decrease in the relative contributions of CF_3 and CF_2 functionalities to the overall plasma polymer structure. The amount of carbon not bonded to fluorine ($\underline{C}$-CF_n) initially rises to ~23% then falls to a value of ~16% in the higher power polymers.

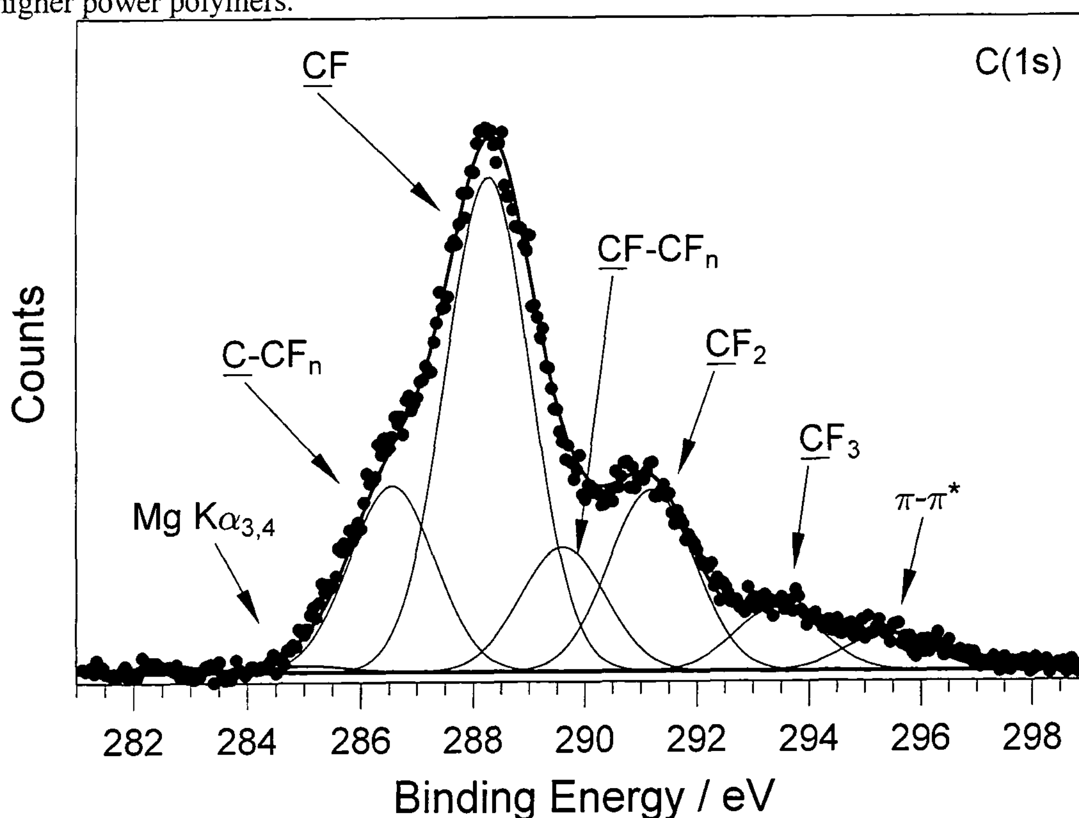

Fig. 4-2: Peak-fitted high resolution C(1s) spectrum of a plasma polymer deposited onto a glass substrate from a pulsed PFAB discharge. Pulsing conditions: on-time 10 μs, off-time 6000 μs, peak power 70 W.

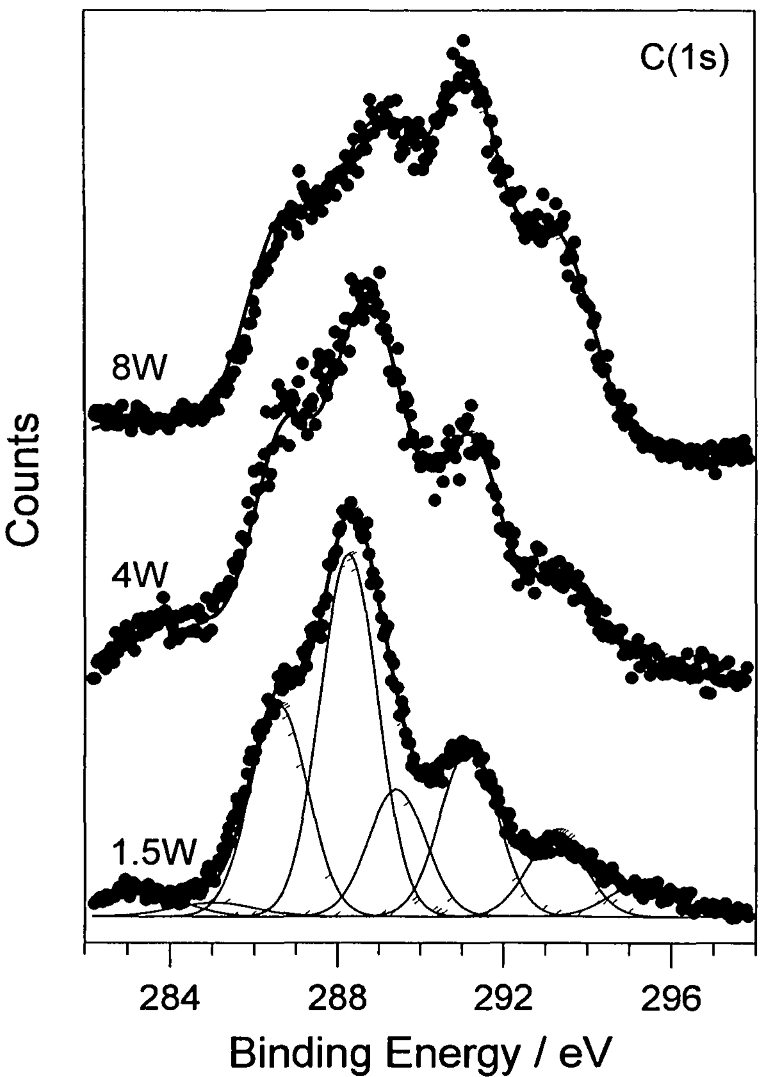

Fig. 4-3: C(1s) XPS spectra of plasma polymers deposited as a function of continuous wave power.

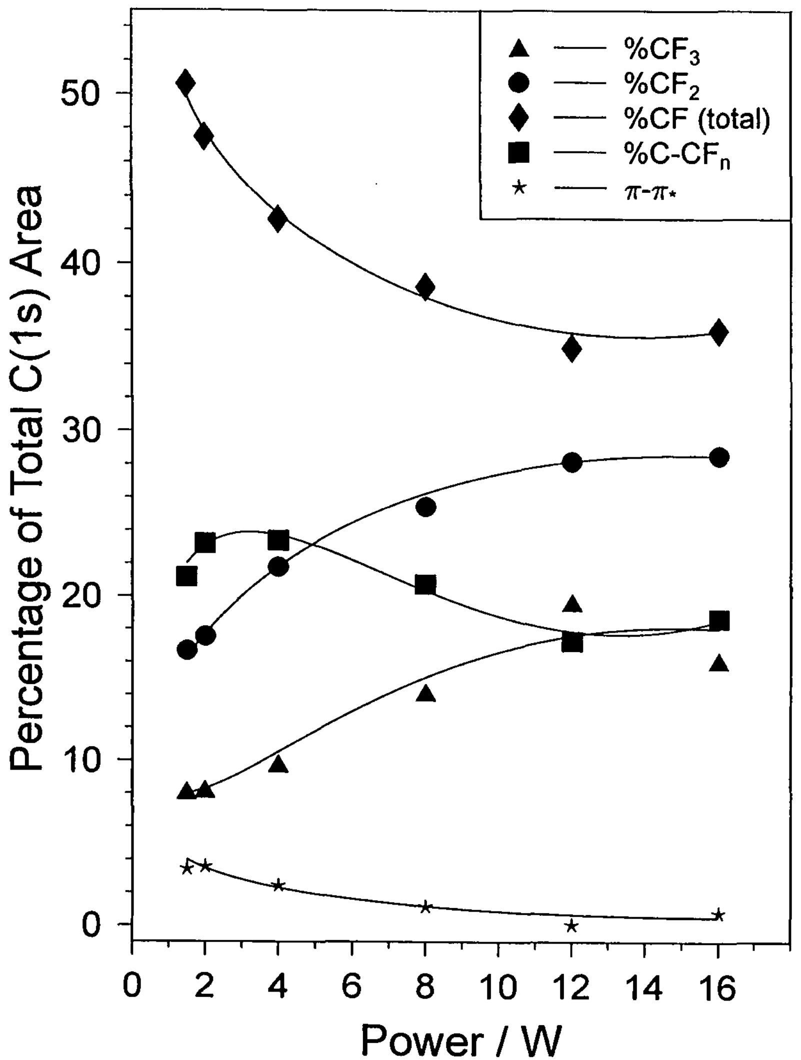

Fig. 4-4: Percentage of total C(1s) areas for each carbon functionality as a function of continuous wave discharge power.

The plasma power can also be adjusted by varying the duty cycle parameters using a pulsed plasma. Changing the off-times with on-time constant at 10 μs and peak power constant at 70 W resulted in changes in the XPS spectra, Fig. 4-5 and polymer composition, Fig. 4-6. For longer off-times the composition of the plasma polymer closely resembles that of the precursor with a high percentage of CF (55%) and a F/C ratio of 0.97 compared to 66% CF and 0.90 for the monomer PFAB. It is of interest to note that 55% of the CF content of the monomer arises from the aromatic ring. As the off-time is decreased, especially below 1000 μs, the amounts of the other functionalities particularly CF_3 and CF_2 increase at the expense of CF.

Comparable results are seen in the on-time experiments on PFAB. The effect of altering the pulse on-time on the XPS spectra and plasma polymer composition is shown in Fig. 4-7 and Fig. 4-8, p. 112. For experiments in which the on-time was changed the off-time was 6000 μs with a peak power of 70 W. This range of duty cycles allowed average powers of between 0.37 and 16 W to be delivered to the plasma. Increasing the on-time from 10 to 2500 μs leads to a reduction in the percentage of CF (from 57 to 31%) and an increase in the amounts of CF_2 and CF_3 in the plasma polymer. The F/C ratio increases with both decreasing off-time and increasing on-time from values close to that of the monomer i.e. 0.9 at low average powers to approximately 1.5 at high average powers, Fig. 4-9, p. 113.

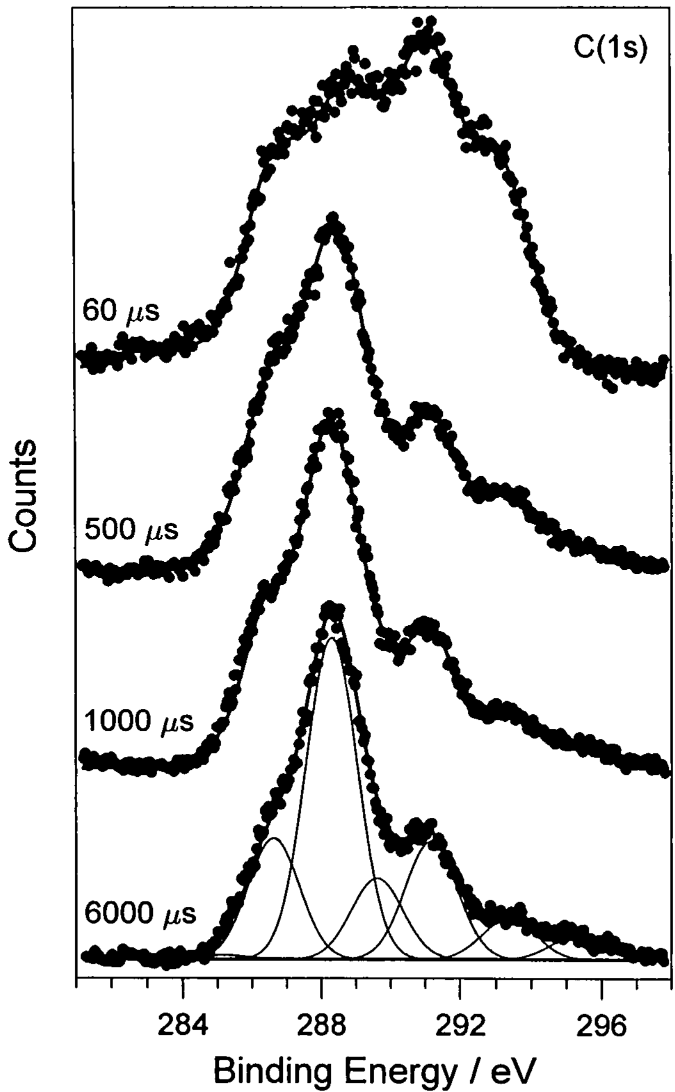

Fig. 4-5: C(1s) XPS spectra of plasma polymers deposited from pulsed plasmas as a function of off-time; on-time = 10 μs, peak power = 70 W.

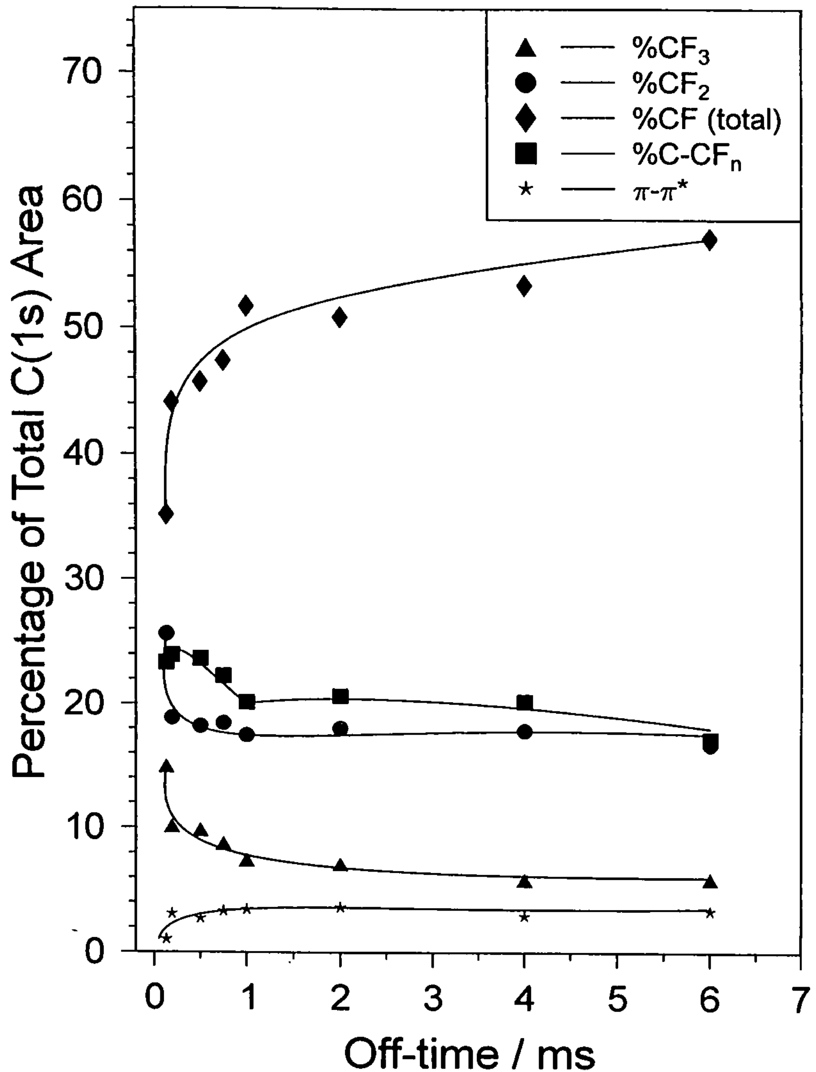

Fig. 4-6: Percentages of total C(1s) areas for each carbon functionality as a function of off-time; on-time = 10 μs, peak power = 70 W.

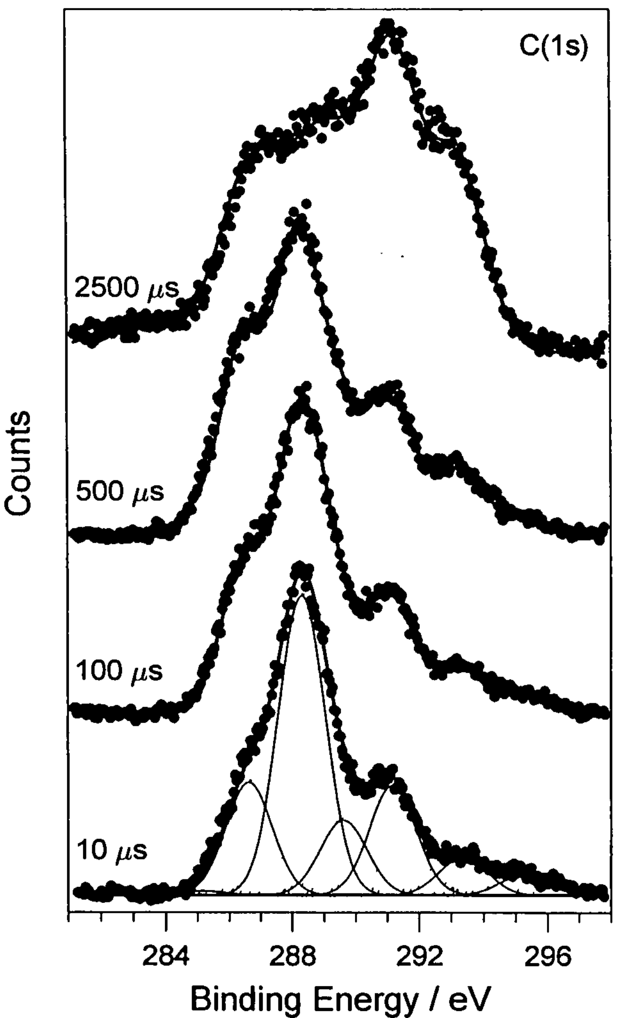

Fig. 4-7: C(1s) XPS spectra of plasma polymers deposited from pulsed plasmas as a function of on-time; off-time = 6000 μs, peak power = 70 W.

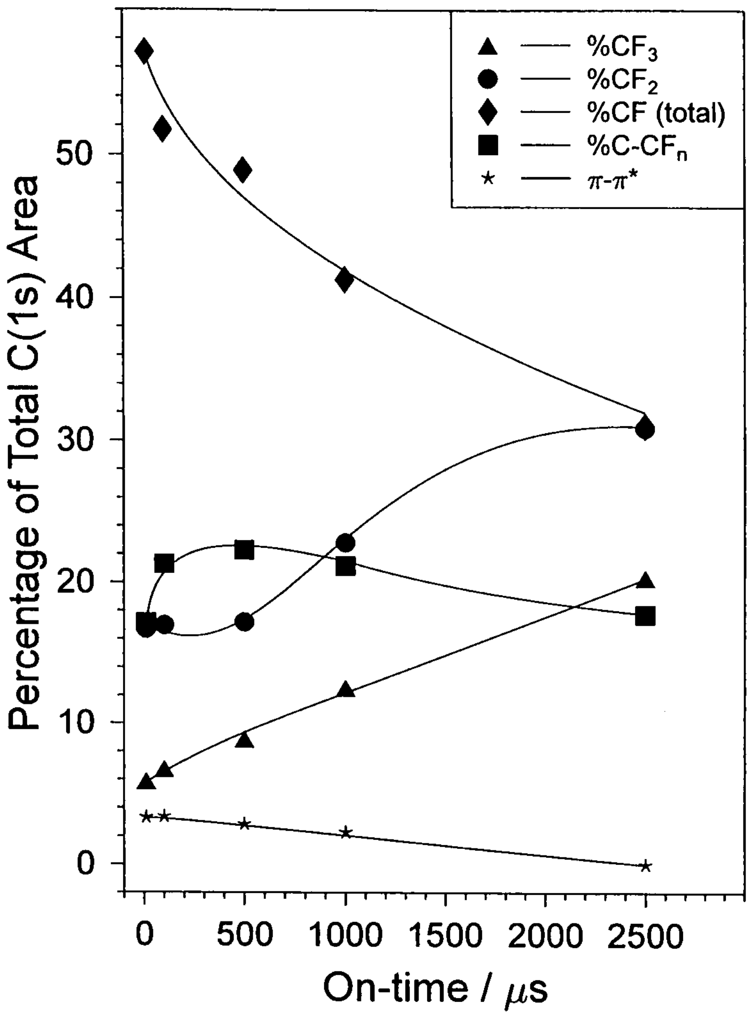

Fig. 4-8: Percentages of total C(1s) areas for each carbon functionality as a function of on-time; off-time = 6000 μs, peak power = 70 W.

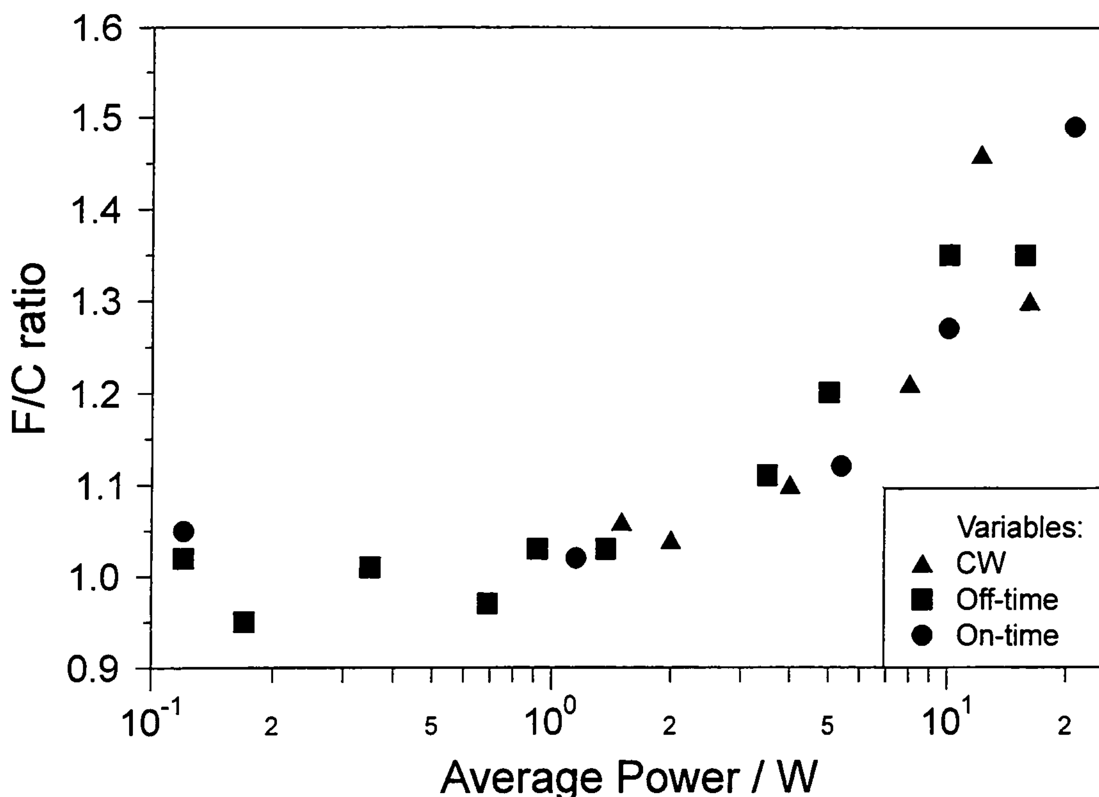

Fig. 4-9: Plot of F/C ratios versus average power for plasma polymers deposited from PFAB discharges with varying continuous wave power, on-time and off-time.

4.3.1.2 Transmission Infrared Spectroscopy.

The infrared spectra of perfluoroallylbenzene and all plasma polymers show no absorption peaks above 2000 cm^{-1}, typical of the spectra of all perfluoro-compounds.[56] The infrared absorption spectrum of PFAB liquid, taken as a thin film between two KBr disks, shows absorption bands at 1788(s), 1655(m), 1530(s), 1510(s), 1427(w), 1356(s), 1335(s), 1295(s), 1175(s), 1082(m), 1001(s), 966(s), 812(s), 737(w) and 685(w) cm^{-1}. The spectra of the plasma polymers from CW and pulsed plasmas are shown in Fig. 4-10, Fig. 4-11 and Fig. 4-12. Of most significance is the behaviour of the single peaks at 1788 cm^{-1} and 1655 cm^{-1} and the doublet at 1530/1510 cm^{-1}. The absorption at 1788 cm^{-1} can be assigned to C=C stretch of the double bond in the allyl substituent[57-60] with the second singlet and doublet assigned to $C\text{-}C_{(aromatic)}$ stretch of the fully fluorinated phenyl group.[61] The doublet and singlet in the 1340-1300 cm^{-1} region of the spectrum of the monomer have also been assigned to the $CF{=}CF_2$ group.[58]

Upon increasing discharge power these peaks disappear from the spectra of the plasma polymers indicating loss of the both the allyl and aromatic functionalities at high plasma powers. However at lower average powers i.e. low CW powers, long off-times or short on-times, the aromatic nature of the monomer is mirrored in the plasma polymers as indicated by the increase in intensity of the $C\text{-}C_{(aromatic)}$ stretch peaks. The peak at 1788 cm^{-1} never shows itself to be present to an extent comparable to that seen in the precursor which suggests that reaction of the C=C double bond on the allyl group is important in the deposition process. Peaks in the region 1400 cm^{-1} to 1000 cm^{-1} are difficult to assign unambiguously but are characteristic of all fluoro-compounds due to C-F stretching vibrations.[36] The peak at 1350 cm^{-1} has previously been assigned to the unsaturated carbon-carbon vibration in the allyl group.[58] All plasma polymers show a broad peak in the 1700 cm^{-1} region. This could be due to C=C or C=O functionalities. However, given the fact that XPS shows the films to contain very little oxygen, with an O/C ratio ≤ 0.03, it is most likely due to the presence of C=C double bonds.

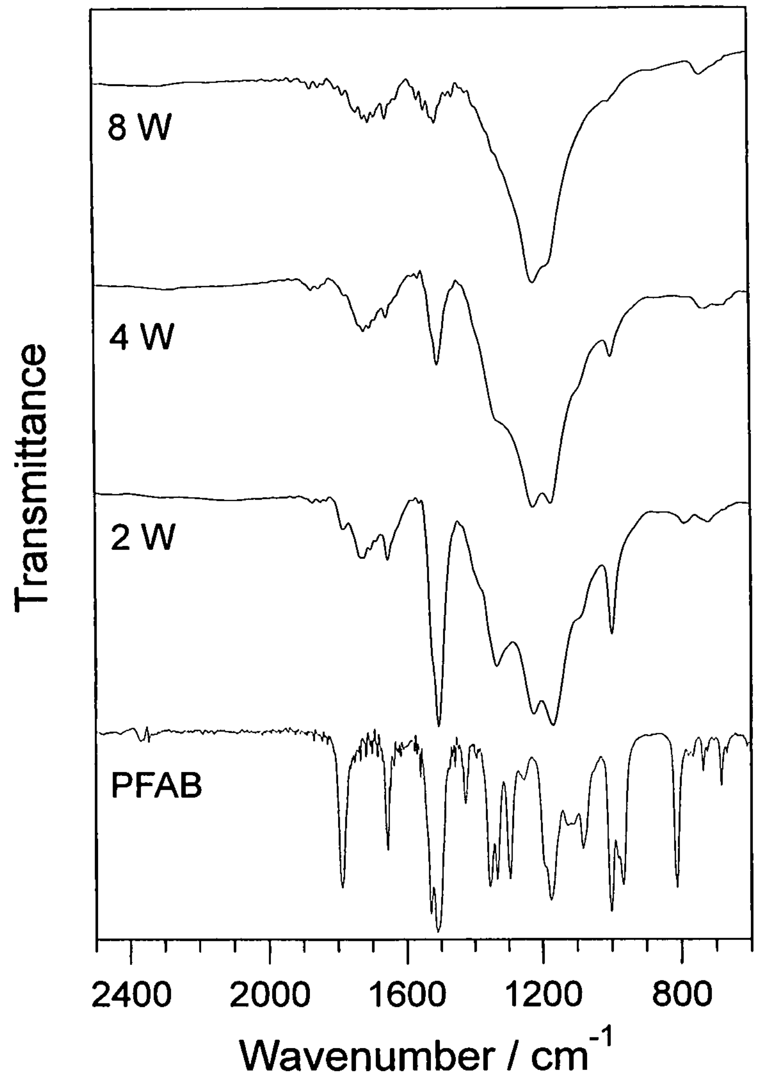

Fig. 4-10: Transmission FT-IR spectra of plasma polymers deposited from CW plasmas as a function of discharge power.

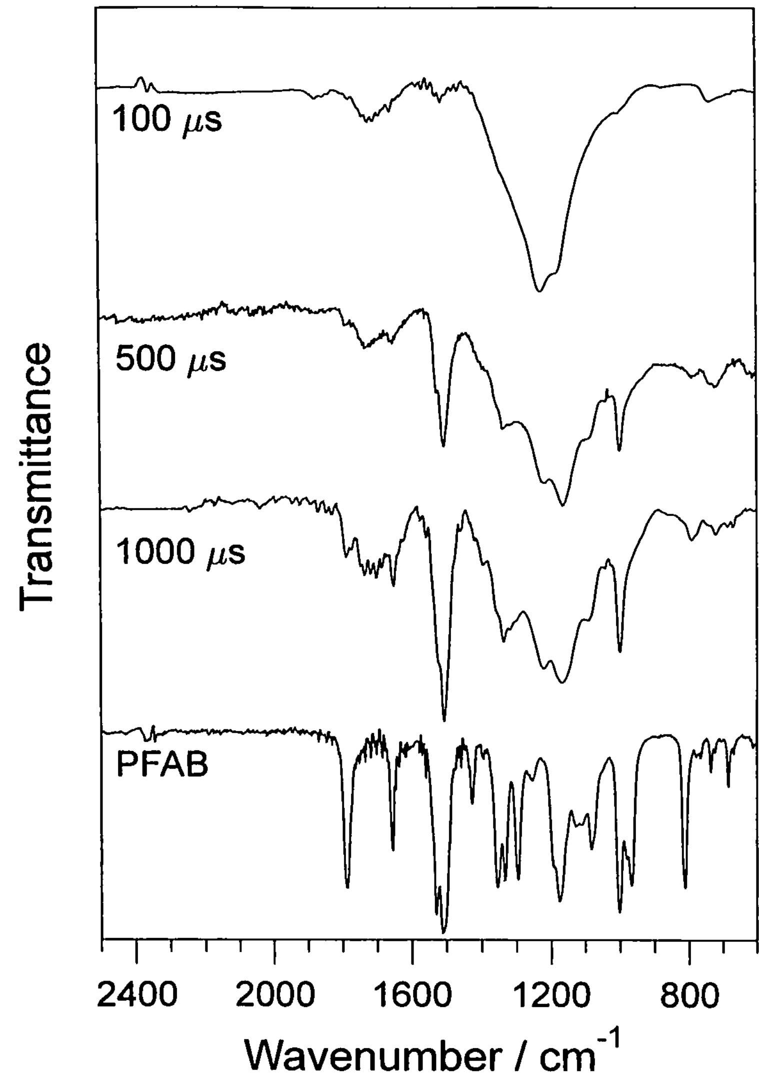

Fig. 4-11: Transmission FT-IR spectra of plasma polymers deposited from pulsed plasmas as a function of off-time; on-time = 10 μs, peak power = 70 W.

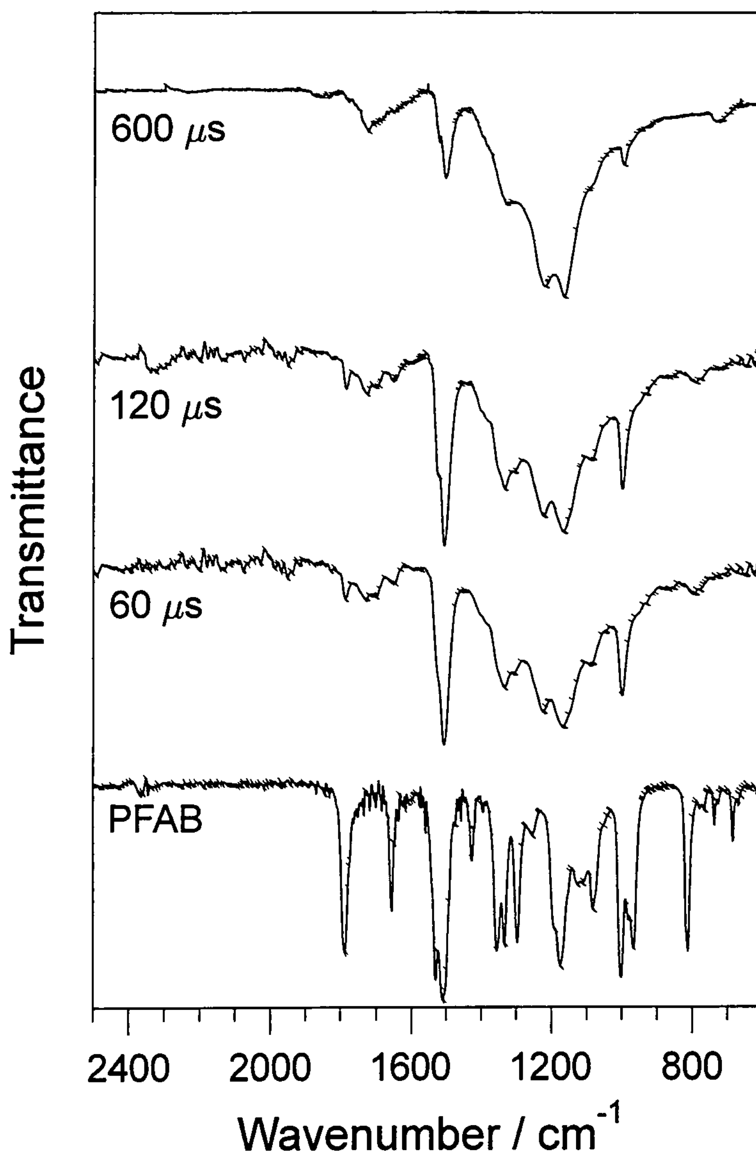

Fig. 4-12: Transmission FT-IR spectra of plasma polymers deposited from pulsed plasmas as a function of on-time; off-time = 6000 μs, peak power = 70 W.

4.3.1.3 Ultraviolet/visible spectroscopy.

The UV/visible spectra of plasma polymers deposited onto quartz substrates were recorded for three different on-times, 60, 120 and 600 μs, Fig. 4-13. All three plasma polymers show intense absorption below 300 nm consistent with a large degree of unsaturation within the polymers. For shorter on-times the spectra become slightly more structured with the 60 μs spectrum showing two clear absorption features at 220 and 270 nm. Phenyl containing molecules show intense absorption in this region and in conjunction with the IR spectrum for this duty cycle, Fig. 4-12, p. 116, the results

confirm that shorter on-times lead to a more ordered and aromatic plasma polymer.

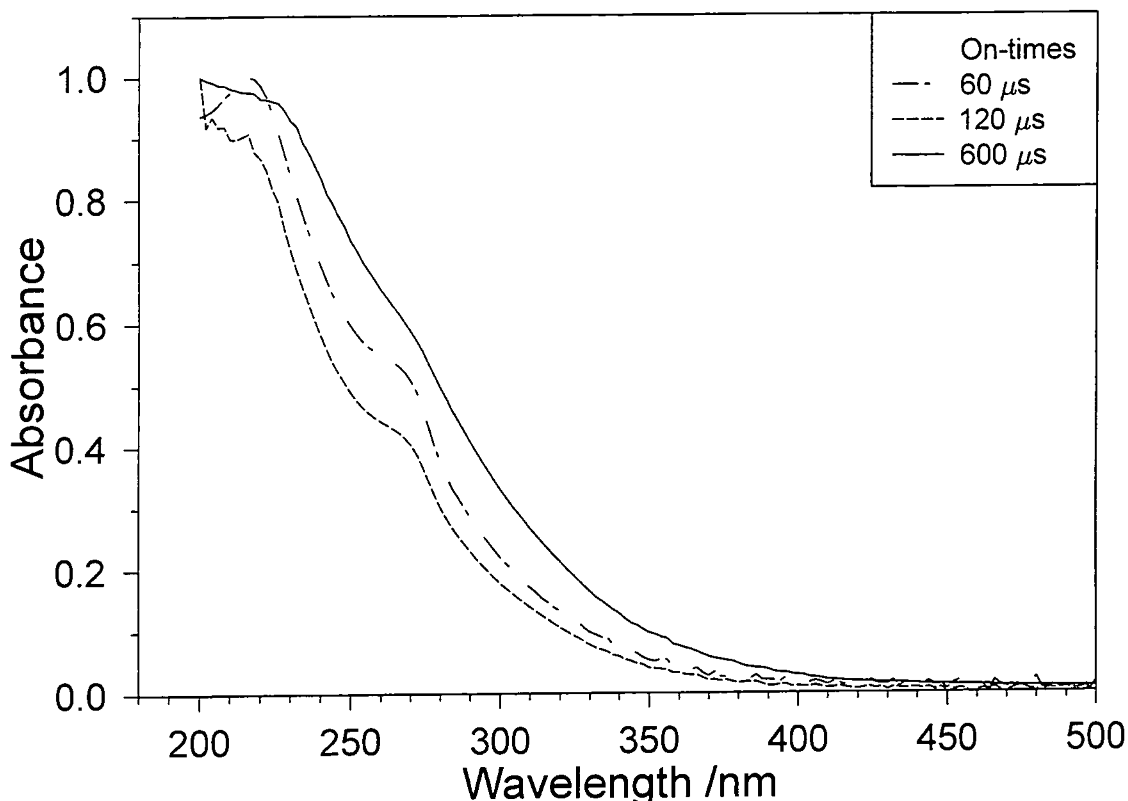

Fig. 4-13: UV/Visible absorption spectra of plasma polymers deposited onto quartz slides for different on-times; off-time = 6000 μs, peak power = 70 W.

4.3.1.4 Atomic Force Microscopy

The surface of the plasma polymer was examined following plasma deposition using atomic force microscopy. Fig. 4-14 shows an AFM image of a plasma polymer deposited from a pulsed plasma with the following conditions; on-time 20 μs, off-time 4000 μs, peak power = 70 W. Upon initial examination the surface appears featureless and flat as has been reported previously for plasma polymerised fluorocarbon films.[62] Following repeated scanning with the AFM tip however the surface of the film undergoes rearrangement.

Vinogradov and co-workers have reported the patterning of thin, 2-10 nm, plasma polymerised organic films by an atomic force microscope.[63] They attribute the patterning process to several factors including mechanical and Coulomb forces, heat

effects, material transfer and electric charge deposition depending on the conditions. The exact reason for the rearrangement of these pulsed plasma polymers is unclear at present and needs further study.

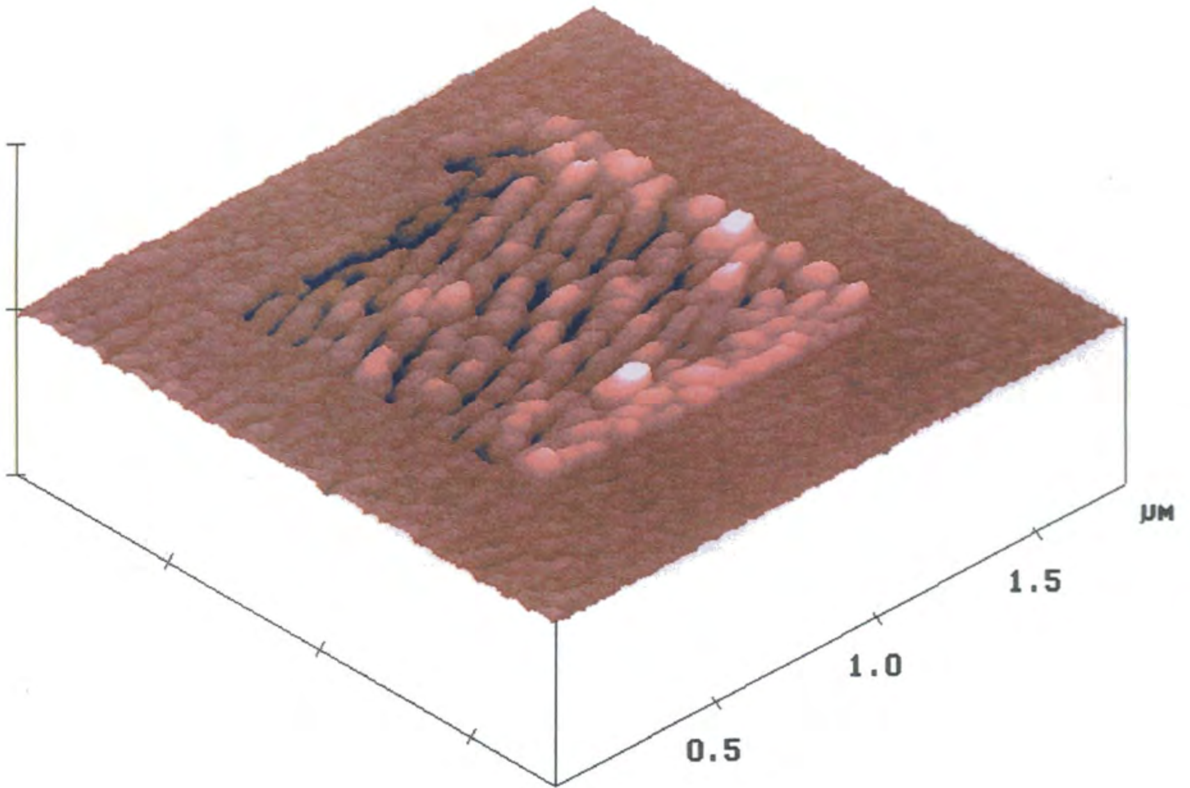

Fig. 4-14: Atomic Force Micrograph of a plasma polymer deposited from a low duty cycle PFAB plasma showing the effect of repeated scanning on the topography of the surface.

4.3.2 Discussion of variable average power results.

The results of the XPS, infrared and UV-visible absorption studies clearly indicate that highly aromatic surfaces can be obtained with pulsed plasmas. By lowering the duty cycle, either by increasing off-time or decreasing on-time, retention of the phenyl ring in the plasma polymer can be enhanced. This can be due to two different effects depending on whether the variable altered is on-time or off-time. If the on-time is reduced there will be less fragmentation and hence rearrangement of the precursor molecules in the gas phase prior to them undergoing conventional radical-induced polymerisation in the off-time.[64] A reduction in on-time also reduces ion bombardment of the growing polymer which is known to induce cross-linking and rearrangement at the surface.[17] On the other hand if the off-time is increased then there is a greater chance for incorporation of non-fragmented perfluoroallylbenzene molecules into the plasma polymer before they become exposed to further excitation and dissociation in the next pulse cycle.[65] Hence it appears that by manipulating the timescales of the duty cycle it is possible to control the aromaticity of the deposited plasma polymer.

When analysed in greater detail however it becomes apparent that there may be another possible explanation for the increase in polymer aromaticity with reduction in duty cycle, which bears no relation to the magnitude of the timescales involved in the pulse cycle. It is possible that the changes in polymer composition may be purely a result of the effect of the *average power* being delivered to the plasma. From Eq. 4-1 it can be seen that altering on or off-time will change the average power delivered to the plasma;

$$\langle P \rangle = P_p \times \left(\frac{t_{on}}{t_{on} + t_{off}} \right) \qquad \text{Eq. 4-1}$$

where $\langle P \rangle$ is average power and P_p is peak power.

Hence any study carried out by varying pulsing parameters will be affected by the associated change in average power supplied to the plasma. In terms of these investigations it has been noted that continuous wave studies indicate that increasing

average power results in a less aromatic plasma polymer in the coil region. This is caused by two contributing factors;

1. Increased power leads to a more energetic plasma resulting in greater fragmentation and dissociation of the precursor.

2. Changing the average power alters the distribution of deposition along the length of the reactor, i.e. the *reactor profile.*

The effect of average power on the reactor profile of this particular experimental configuration was investigated by comparing two reactor profiles, one from a low power plasma, 2 W, and one from a high power plasma, 16 W.

4.3.3 Effect of average power on reactor profile.

Previous studies[66,67] have indicated that substrate position within the reactor can have a pronounced effect on the structure of the plasma polymer and during the continuous wave experiments it was noticed that deposition was not occurring uniformly along the reactor length at higher powers. For the reactor profile experiments substrates were placed in three different positions, namely 4 cm *upstream* from the centre of the coils, in the *centre* of the coils and 4 cm *downstream*. Fig. 4-16 shows that the XPS spectra for the plasma polymers deposited at the different positions are all quite similar. The upstream XPS spectrum does show greater resolution however with a FWHM for the component peaks of 1.84 eV compared with 2.4 eV for the coils and downstream spectra.

The FT-IR transmission spectra, Fig. 4-17, are more informative than the XPS spectra. The IR spectra show that for a 2 W plasma, the peaks associated with the precursor, in particular at 1500, 1350 and 990 cm^{-1}, diminish as the substrate is moved further along the length of the reactor from the gas inlet.

In the case of the 16 W plasma the IR spectra of the deposits are the same regardless of substrate position, Fig. 4-18. Extensive molecular rearrangement and dissociation

results in none of the plasma polymers showing any evidence of a phenyl group with the main feature of the spectra being the strong absorption at 1200 cm^{-1} due to C-F stretch.

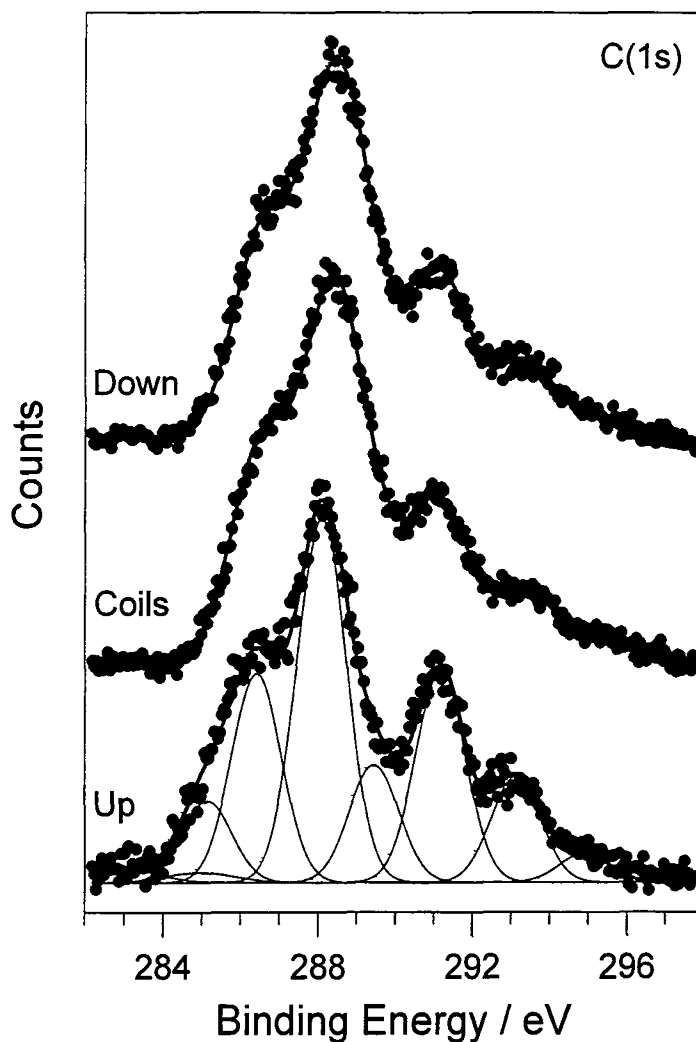

Fig. 4-16: C(1s) XPS spectra of plasma polymers deposited from a 2 W CW plasma with varying reactor positions; 4 cm upstream, in the centre of the coils and 4 cm downstream.

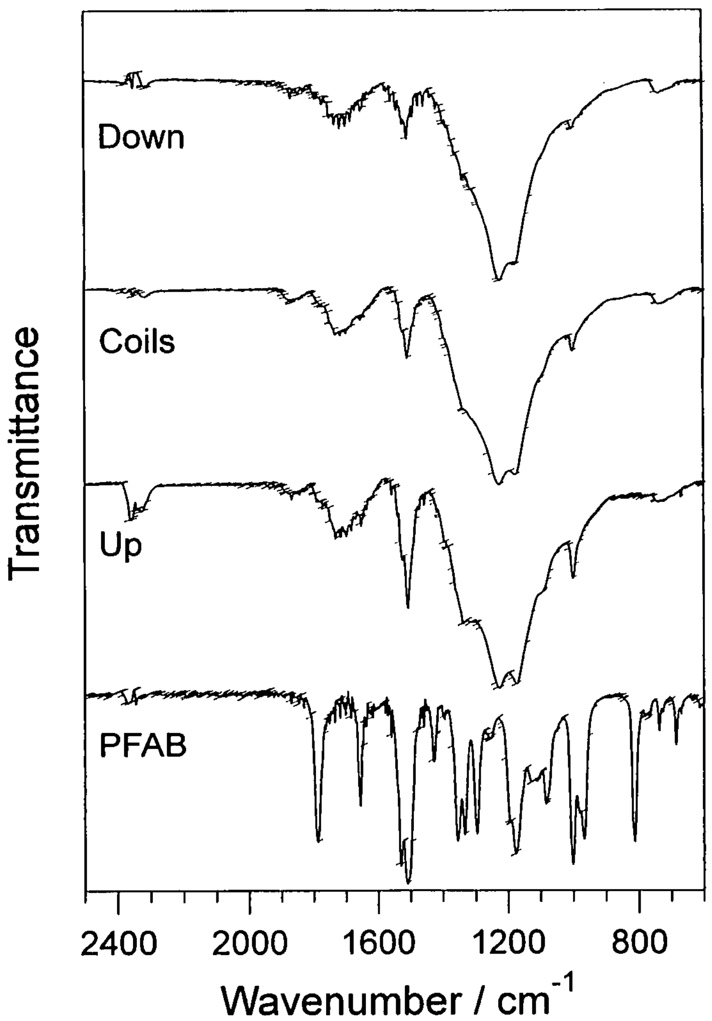

Fig. 4-17: Transmission IR spectra of plasma polymers deposited from a 2 W CW plasma with varying reactor positions.

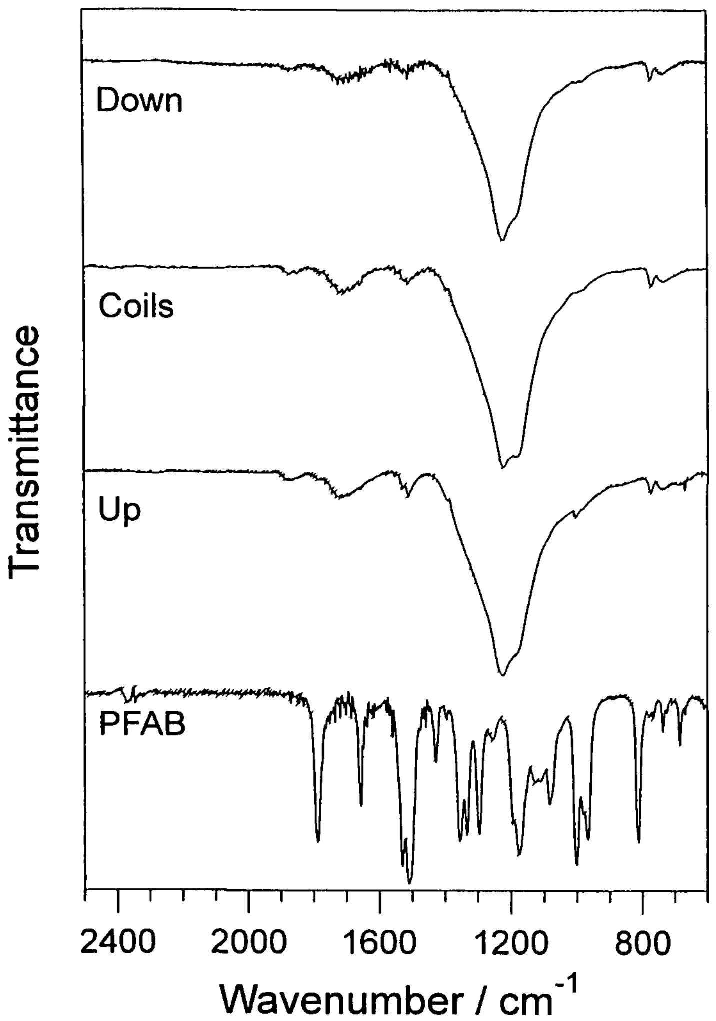

Fig. 4-18: Transmission IR spectra of plasma polymers deposited from a 16 W CW plasma with varying reactor positions.

The results clearly show that on going from 2 to 16 W continuous wave power the loss in aromaticity of the plasma polymers in the coil region can be attributed both to a more energetic environment at the gas/surface interface and to the effects of the difference in reactor profile between the two regimes.

Therefore it is reasonable to assume from these results that the changes in polymer composition seen during the pulsing experiments are not entirely due to the previously discussed factors relating to pulsing timescales, but are also a consequence of the effect increasing average power has on the composition of plasma polymers deposited in the coil region. It is important to determine therefore how much of a factor the average power actually is during the pulsing experiments and if the control over polymer composition obtainable by pulsing the power is attributable in anyway towards the change in pulsing parameters, or is merely an average power effect.

4.3.4 Pulsed plasma polymerisation studies using constant average power.

One of the reasons for the increasing F/C ratios and CF_2 and CF_3 contents in the plasma polymers with increasing average powers is that the deposits in the coil region derive their composition from several different processes. The first is direct activation and polymerisation of the PFAB precursor and incorporation of the stoichiometry and properties of the PFAB into the plasma polymer. Another source of raw material for the growing polymer arises from ablation of polymer deposited upstream from the coil region and subsequent re-deposition onto the substrate within the coils. The former produces an aromatic polymer with F/C ratio less than one; the latter a more highly fluorinated, non-aromatic polymer. The results from the reactor profile experiments show that at low average powers more PFAB is incorporated into the polymer due to more unreacted PFAB reaching the coil region and less ablation of the plasma polymer deposited upstream from the coils.

In order to remove the effect of average power and study more closely the effect of on and off-time on the deposition process, a series of experiments were carried out in which the average power to the plasma was kept constant by varying the peak power of the r.f. while simultaneously altering the on or off-time. The parameters were chosen to produce an average power of 4 W. The conditions used are given in Table 4-1:

Experiment No.	*On-time (μs)*	*Off-time (μs)*	*Peak Power (W)*
1	10	10	8
2	10	90	40
3	10	360	150
4	12	600	200
5	43	600	60
6	150	600	20

Table 4-1: Pulsing parameters for experiments where average power was kept constant at 4 W.

Experiment No.	*% $C\text{-}CF_n$*	*% CF*	*% $CF\text{-}CF_n$*	*% CF(total)*	*% CF_2*	*% CF_3*	*% $\pi\text{-}\pi^*$*
1	22.49	31.18	15.85	47.03	17.14	10.47	2.24
2	22.41	34.19	14.84	49.03	17.24	8.48	2.83
3	23.36	34.22	13.20	47.42	17.61	8.54	3.07
4	19.92	41.56	12.57	54.13	17.21	5.60	3.14
5	22.73	38.41	11.07	49.48	16.92	8.08	2.79
6	23.36	34.22	13.20	47.42	17.61	8.54	3.07

Table 4-2: XPS results from experiments using constant average power of 4 W by varying on-times, off-times and peak powers.

Only plasma polymers deposited in the coil region were investigated. The contributions of the various carbon environments to the overall C(1s) area are shown in Table 4-2. Transmission FT-IR spectra were also gathered for experiments 1 to 3 i.e. the experiments in which the off-time was altered and the peak power adjusted to maintain constant average power. The XPS data for these runs (and run 4) show an increase in the percentage CF and $\pi\text{-}\pi^*$ peaks along with a decrease in the percentage CF_3, indicating increased retention of the precursor stoichiometry and reduced rearrangement respectively with increasing off-time. Fig. 4-19 shows the increase in intensity of the

infrared peaks associated with the phenyl ring with increasing off-time despite the fact that the peak power also increases. Since the average power is constant for these experiments it is reasonable to assume that the increase in retention of the precursor structure is a result of the reduction in duty cycle with increasing off-time. As the off-time increases the species which undergo initiation in the on-time, via UV irradiation, ion or electron bombardment etc. have more time to polymerise either in the gas phase or at the gas/substrate interface. This greater delay time before the next initiation sequence allows for a greater retention of the initial structure of the perfluoroallylbenzene in the plasma polymer. The increase in fragmentation during the on-time due to increasing peak powers at lower duty cycles, obviously is less important than the length of the off-time.

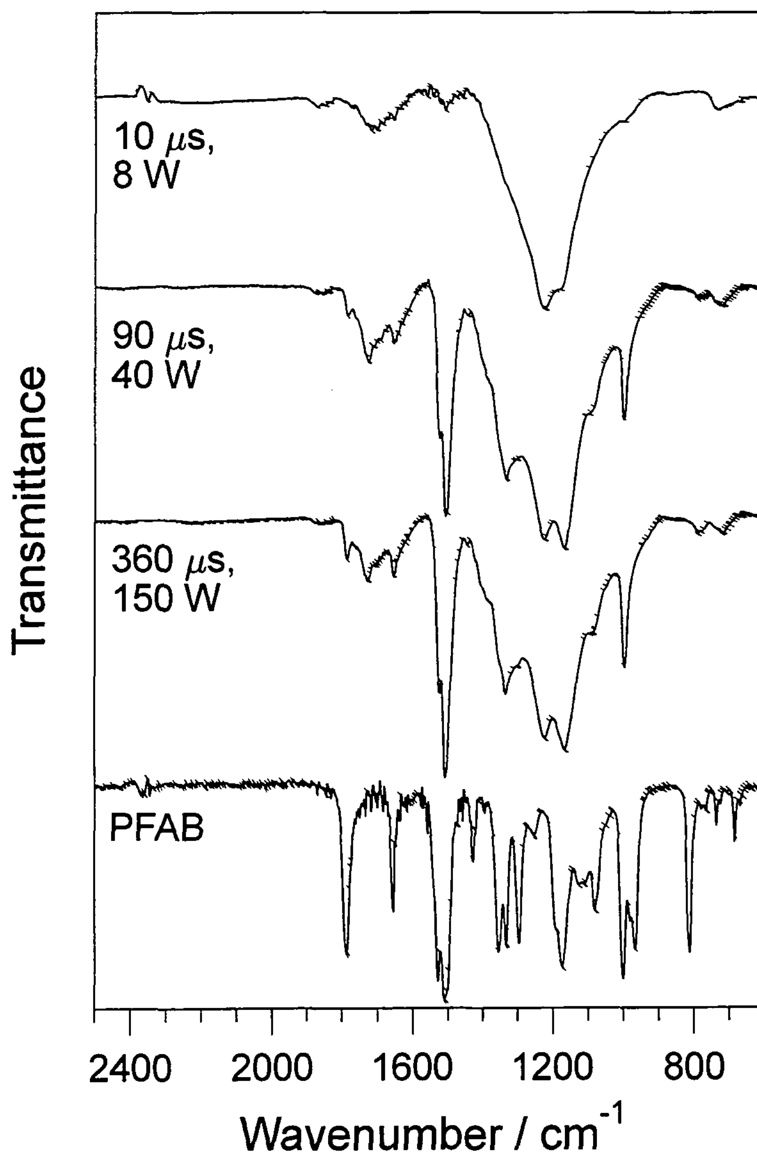

Fig. 4-19: IR Spectra from pulsed plasmas with varying off-times and peak powers to give a fixed average power of 4 W. On-time = 10 μs.

Varying both on and off-times, but keeping duty cycle constant along with peak power allowed another series of experiments with constant average power to be carried out. This allows us to maintain a constant on-time/off-time ratio i.e. initiation/propagation ratio and study the effect of changing the timescales of the pulsing through several orders of magnitude without the variation in peak power. The pulsing ranged in frequency from 1 kHz to 25 Hz and the results are presented in Table 4-3 and Fig. 4-20, p.129.

Pulsing Parameters	% $C\text{-}CF_n$	% CF	% $CF\text{-}CF_n$	% CF_2	% CF_3	% $\pi\text{-}\pi^*$
10/1000	19.96	39.57	11.71	17.30	7.32	3.37
50/5000	20.92	42.84	9.63	16.53	6.38	3.70
100/10000	20.92	39.99	14.12	15.87	6.09	3.01
200/20000	21.49	42.48	10.42	16.48	6.34	2.78
400/40000	22.71	41.44	11.27	15.27	6.25	3.06

Table 4-3: XPS results from experiments using constant average power of 4 W with varying pulse frequency.

The data from this set of experiments show that is no major changes in the composition of the plasma polymers through the range of pulse frequencies studied. Any changes in XPS values are within experimental error however IR spectra of the plasma polymers deposited in these experiments show that upon going through the series 10/1000 μs (10 μs on, 1000 μs off), 50/5000 μs, 100/10000 μs the retention of the phenyl group in the plasma polymers is increased. Increasing the timescales further through 200/20000 μs and 400/40000 μs does not increase retention. In fact the polymers deposited in the latter two cases are less aromatic than the polymer deposited from the 100/10000 μs plasma.

These results suggest there is an optimum time regime for retention of monomer structure using a pulsed plasma. At timescales less than this optimum, the discharge is off for an insufficient length of time for incorporation of the maximum amount of non-fragmented precursor into the plasma polymer. At timescales above the optimum the longer on-times result not only in initiation but also in excessive and undesirable fragmentation of the precursor before the off-period. Additional work is required to investigate this phenomenon further.

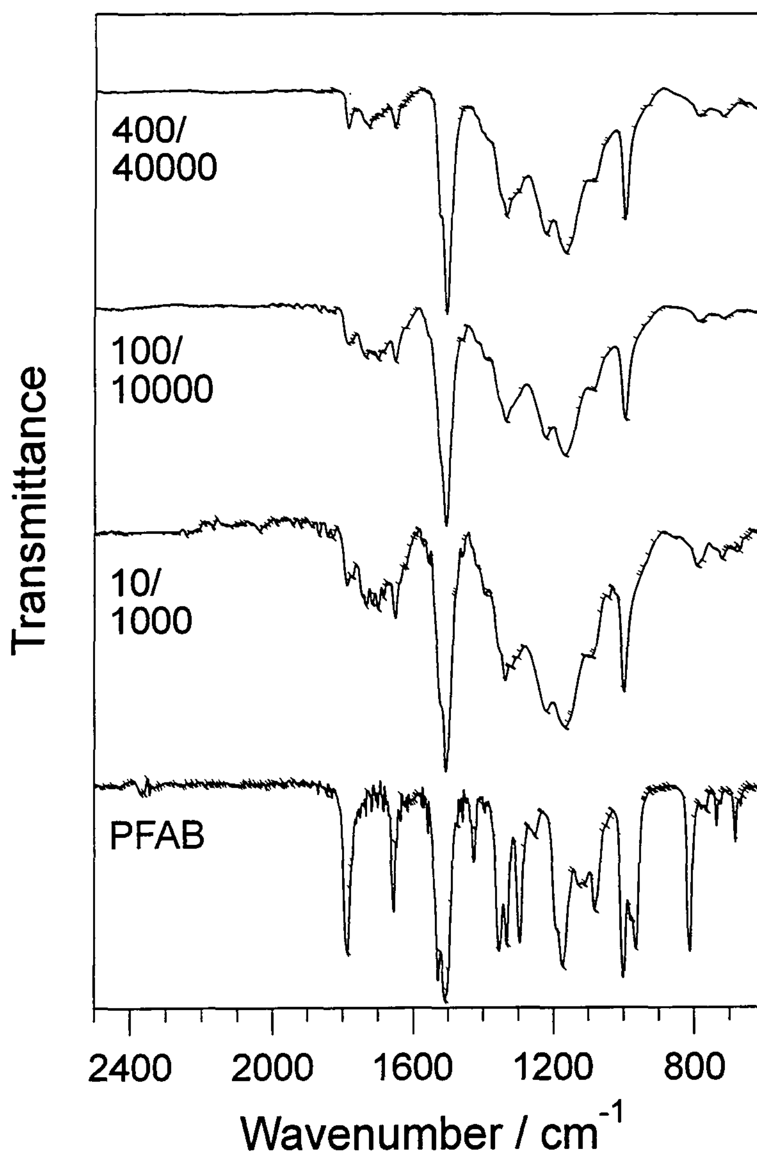

Fig. 4-20: IR Spectra from pulsed plasmas with varying pulse frequency but fixed average power of 0.7 W. Peak Power = 70 W.

4.3.5 Deposition rate studies

In an attempt to gain a greater understanding of the effect of pulsing the power to the plasma studies of the polymer deposition rate from perfluoroallylbenzene plasmas were carried out. Both perfluorocyclohexane and perfluorocyclopentene plasmas were also investigated and the results are presented here rather than in chapter three for the sake of comparison.

In these experiments a gold coated quartz crystal with a surface area of 1 cm^2 is placed in the centre of the plasma. The resonant frequency of the crystal is related to the mass

of the crystal and when the plasma polymer is deposited onto the crystal its mass obviously changes. This change in mass is measured via the change in the resonant frequency of the crystal and displayed as a thickness reading on the deposition monitor. By monitoring the thickness of film deposited over time the deposition rate of the plasma polymer can be calculated.

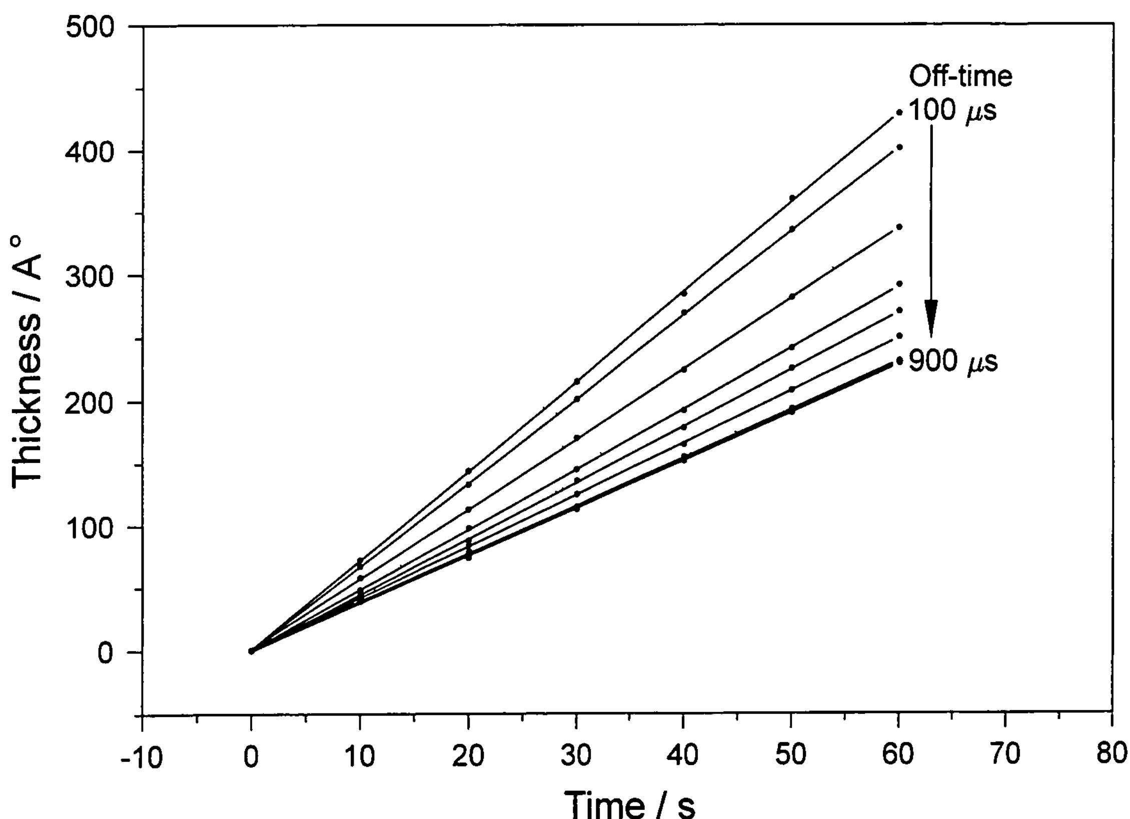

Fig. 4-21: Plot of thickness versus time for plasma polymers deposited from perfluoroallylbenzene pulsed plasmas as a function of off-time, on-time = 20 μs, peak power = 70 W.

Fig. 4-21 shows the effect of increasing off-time on the film thickness per second for plasma polymers from perfluoroallylbenzene pulsed discharges. As expected increasing the off-time reduces the deposition rate due to the reduced power input to the plasma. The same effect is seen for pulsed plasmas of perfluorocyclohexane and perfluorocyclopentene, i.e. reducing the duty cycle of the pulsing reduces the overall deposition rate, Fig. 4-22, p. 132. The reason the same trends are seen for all three monomers is because the effect of changing the average power to the plasmas by altering the duty cycle overshadows any differences between the three precursors due to

their different chemistries. In order to reduce the effect of duty cycle on the deposition rate results it is necessary to consider the *deposition rate per Joule.*[64,69] This gives us an indication of the amount of polymer formed at the surface of the crystal per unit of energy supplied to the discharge.[68] The deposition efficiency in Angstroms/Joule is calculated as follows;

$$\text{Deposition Efficiency } (\text{Å} / \text{J}) = \frac{\text{Dep. Rate } (\text{Å} / \text{s})}{\text{Average Power } (\text{J} / \text{s})} \qquad \text{Eq. 4-2}$$

In contrast to Fig. 4-22 which shows all three precursors showing the same behaviour with increasing off-time, Fig. 4-23 shows that when we consider the deposition rate per Joule the three monomers show significantly different behaviour with a reduction in duty cycle. In the case of perfluorocyclohexane the deposition rate per Joule remains essentially constant regardless of the off-time chosen. For perfluorocyclopentene the deposition rate increases up to an off-time of ~ 300 μs and then remains constant. For perfluoroallylbenzene the deposition rate per Joule increases as the off-time is increased. The changes seen in the deposition rates per Joule must be attributable to polymerisation processes occurring in the off-portion of the duty cycle.[64,69,70]

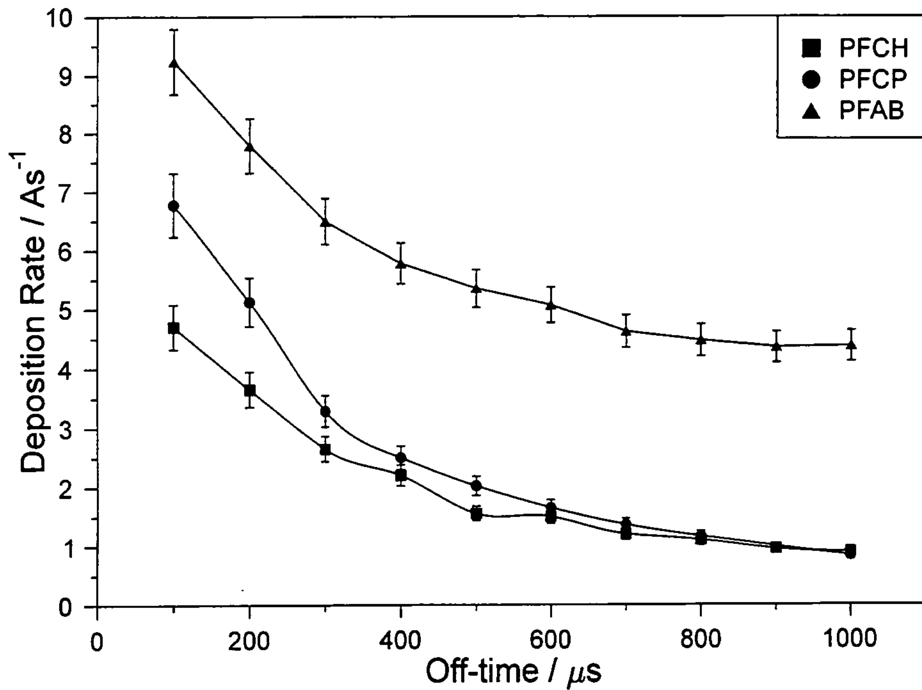

Fig. 4-22: Comparison of the effect of duty cycle on the deposition rate of plasma polymers from pulsed discharges of perfluorocyclohexane, perfluorocyclopentene and perfluoroallylbenzene; on-time = 20 μs, peak power = 70 W.

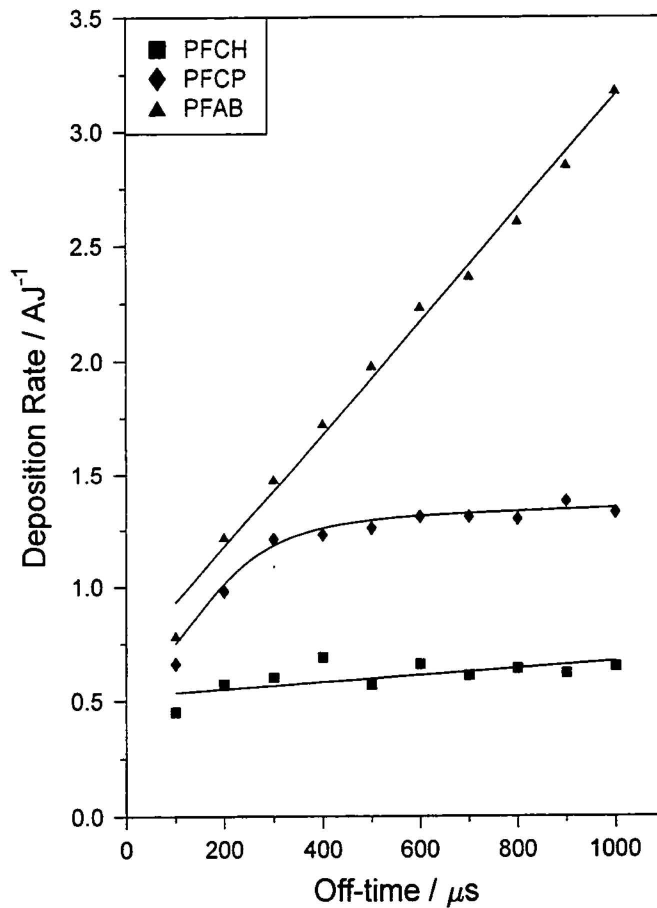

Fig. 4-23: Comparison of deposition rates *per Joule* of plasma polymers from perfluorocyclohexane, perfluorocyclopentene and perfluoroallylbenzene discharges as a function of off-time, on-time = 20 μs, peak power = 70 W.

In the case of perfluoroallylbenzene the increasing deposition rate per Joule with decreasing duty cycle can be explained by deposition occurring during the off-portion of the duty cycle. This being the case then for the same amount of energy input per on-time the amount of polymer deposited over the total duty cycle will be greatest for the longest off-time. The fact that the deposition rate per Joule continues to rise even for off-times as long as 1000 μs suggests perfluoroallylbenzene is susceptible to continued polymerisation in the off-time. The situation is slightly different for perfluorocyclopentene where the deposition rate per Joule initially rises and then levels off with increasing off-time. This suggests that for the first ~ 300 μs of the off-time, deposition processes continue but for off-times greater than this there is no longer any significant polymerisation taking place, i.e. an off-time of 1000 μs will give you the same amount of deposition per Joule as an off-time of 400 μs. In the case of perfluorocyclohexane the deposition rate results indicate there is no significant deposition occurring in the off-portion of the duty cycle as the deposition rate per Joule remains approximately constant regardless of off-time.

It is clear from the above results that the length of the off-time can be important in determining the deposition efficiency of a pulsed plasma depending on the chemistry of the precursor. In the case of perfluoroallylbenzene there is obviously deposition occurring during the off-portion of the duty cycle. It is of interest to determine how long this off-stage polymerisation occurs and also what effect the length of the on-time has on the off-time polymerisation. Further studies which investigated a wider range of duty cycles were therefore carried out on pulsed plasmas of perfluoroallylbenzene. The results are presented in Fig. 4-24.

As can seen the effect of increasing off-time on the deposition efficiency of the pulsed plasmas depends on the on-time. For each on-time there are three different regions of behaviour of the deposition efficiency. The first region is where the deposition efficiency increases with increasing off-time which can be attributed to the off-stage polymerisation compensating for the reduction in average power as a result of the

decreasing duty cycle. In the third region the deposition efficiency drops with increasing off-time. This may be due to there being insufficient energy to effectively initiate the plasma polymerisation due to the very low levels of average power and long off-times. The second level lies between the first and third and corresponds to the duty cycle range where the deposition efficiency remains constant.

The maximum deposition efficiency attainable is also dependent on the on-time. While 10 μs gives a slightly higher maximum deposition rate in Å/J than 20 μs on-time the maximum efficiency is achieved when a 50 μs on-time with greater than 3000 μs off-time. This is most probably due to continued polymerisation in the off-time of the active species/sites generated during the 50 μs on-time.

The results therefore indicate that with a pulsed plasma of perfluoroallylbenzene there is an optimum range of duty cycles where maximum deposition efficiency can be achieved by finding the optimum balance between the on-time (initiation) and off-time (propagation) reactions.

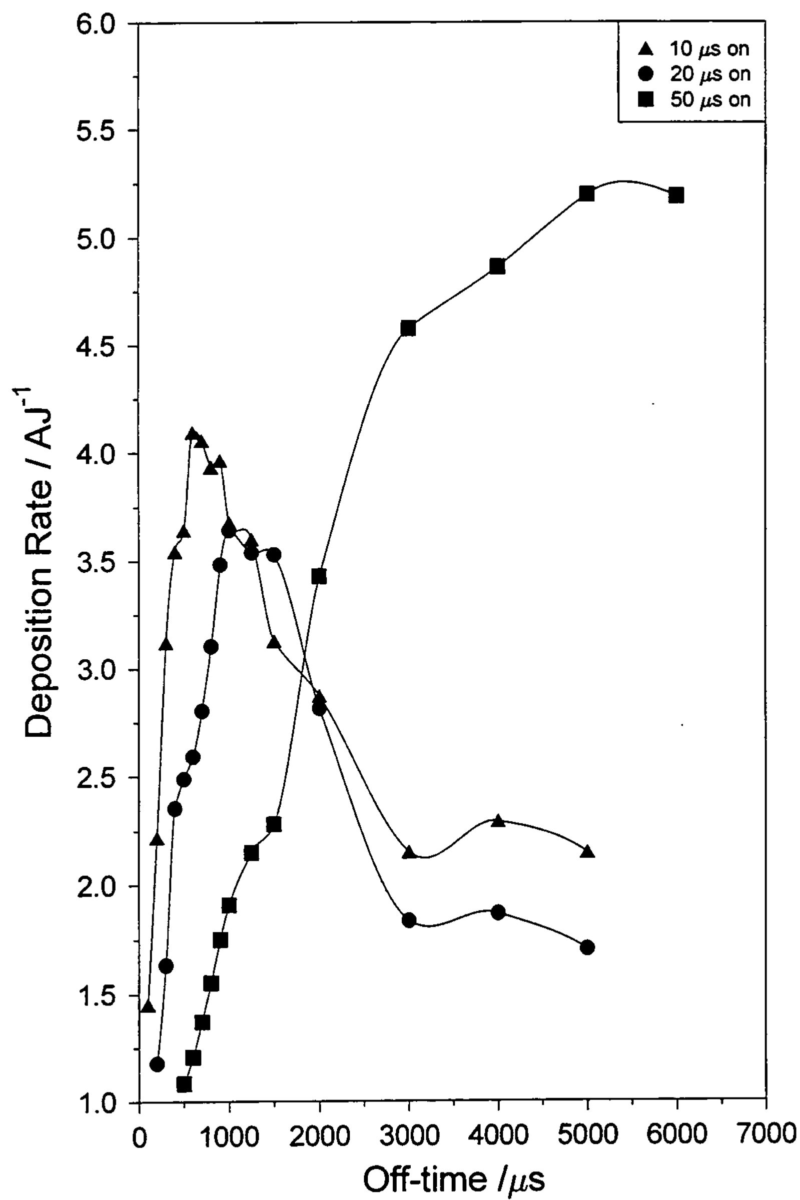

Fig. 4-24: Deposition rate per Joule as a function of off-time for plasma polymers from pulsed plasmas of perfluoroallylbenzene with varying on-times.

4.4 CONCLUSION

A detailed investigation into the pulsed plasma polymerisation of perfluoroallylbenzene has been undertaken resulting in the generation of fluorinated surfaces of a highly aromatic nature. Preliminary continuous wave studies indicated significant differences between plasma polymers deposited at low and high discharge powers. Low powered plasma polymers show an XPS profile centred around $\underline{C}$-F i.e. carbon bonded to one fluorine. High power plasma polymers contain a high fluorine content with the XPS profile shifted to higher binding energies. The conclusion that lower power plasmas retain more of the aromatic nature of the perfluoroallylbenzene precursor is confirmed by the infrared results. Absorptions associated with the precursor are much stronger in the spectra of low power plasma polymers and in some cases are completely missing in the spectra of the polymers deposited from higher power plasmas.

Pulsed plasma polymerisation studies were carried out to study the effect of changing the duty cycle of the pulsing on the composition of the plasma polymer. Increasing the off-time and decreasing the on-time both resulted in an increase in aromaticity of the plasma polymer as indicated by XPS, infrared and ultraviolet/visible spectroscopy. The dramatic reduction in intensity of the infrared absorption at 1788 cm^{-1} in all the plasma polymers indicates that the unsaturated allyl functionality is highly susceptible to plasma reaction and is the most likely site for both initiation and free-radical polymerisation leading to phenyl group incorporation in the final plasma polymer.

Examination of the surface using atomic force microscopy revealed all plasma polymers were smmoth and pin-hole free. However after repeated scanning the surface of low duty cycle pulsed plasma polymers was modified. Further work need to be carried out toinvestigate this phenomenon further.

Reactor profile experiments confirmed the effect average power has not only on the composition of the plasma polymers deposited in the coil region, but also on the

distribution of stoichiometries throughout the reactor. It was discovered that for high plasma powers most of the perfluoroallylbenzene precursor was being deposited upstream from the coil region. This resulted in the principle reactants for plasma deposition in the coil region being non-aromatic, highly fluorinated by-products arising from the ablation of the previously deposited plasma polymer or from dissociation of perfluoroallylbenzene in the gas phase.

It was decided to investigate how significant the variation in average power during the pulsing experiments was in determining the stoichiometry of the plasma polymers. This was established by carrying out a series of experiments where the pulsing parameters were varied in combination to maintain the same average power in each experiment. The results clearly demonstrate that control over the surface composition, in this case the aromatic nature of the plasma polymer, can be achieved by manipulation of the timescale of the pulsing.

Hence the improvement in monomer retention seen in the varying average power experiments with increasing off-time and decreasing on-time is due not only to a reduction in average power delivered to the plasma, but also to the influence of pulsing parameters on the plasma polymerisation process.

The frequency of the pulsing was found to have a slight impact on determining the extent of selectivity of the plasma polymerisation process. By keeping the duty cycle and peak power constant and altering the frequency of the pulsing an optimum frequency range for retention of monomer structure was found. Within this range excessive fragmentation in the on-time is avoided but sufficient time is allowed in the off-time for conventional polymerisation reactions to retain the aromatic nature of the precursor in the surface.

Deposition rate experiments were carried out to further explore the function of the on and off-time reactions in the overall pulsed plasma polymerisation process. As expected monitoring deposition rate in Angstroms/second merely indicated that with decreasing

duty cycle the deposition rate decreased. If deposition efficiency, Angstroms/Joule, was monitored however the effects of the different precursor chemistries and the effects of varying duty cycles and frequencies became more clear. The studies indicate that perfluorocyclohexane is not very susceptible to off-time reactions with the length of the off-time having very little effect on the deposition efficiency. In the case of perfluoroallylbenzene on the other hand the length of the off-time is critical in determining the deposition efficiency of the pulsed plasma. This is attributed to the susceptibility of perfluoroallylbenzene to reactions in the off portion of the duty cycle.

4.5 REFERENCES

(1) McTaggart, F.K. *Plasma Chemistry in Electrical Discharges*; Elsevier Publishing Company: London, 1967.

(2) Chan,C.-M.; Ko, T.-M.; Hiraoka, H. *Surface Science Reports* **1996**, *24*, 1.

(3) Burton, M.; Funabashi, K. *Advances In Chemistry Series* **1969**, *80*, 140.

(4) Yasuda, H.; Hirotsu, T. *J. Polym. Sci. Polym. Chem. Ed.* **1978**, *16*, 313.

(5) Yasuda, H.; Hirotsu, T. *J. Polym. Sci. Polym. Chem. Ed.* **1978**, *16*, 2587.

(6) Donohoe, K.G.; Wydeven, T. *J. Appl. Polym. Sci. 1979, 23*, 2591.

(7) Yasuda, H.; Hirotsu, T. *J. Appl. Polym. Sci. 1977, 21*, 3167.

(8) Yasuda, H.; Hirotsu, T. *J. Appl. Polym. Sci. 1977, 21*, 3139.

(9) Morita, S; Bell. A.T.; Shen, M. *J. Polym. Sci. Polym. Chem. Ed.* **1979,** *17,* 2775.

(10) Harafuji, K.; Yamano, A.; Kubota, M. *Jap. J. Appl. Phys. Part 1* **1994,** *33(4b)*, 2212.

(11) Ohkubo, J.; Inagaki, N. *J. Appl. Polym. Sci. 1990, 41*, 349.

(12) d'Agostino, R.; Martinu, L.; Pische, V. *Plasma Chemistry & Plasma Processing* **1991,** *11(1)*, 1.

(13) Hay, P.M. *Advan. Chem. Ser.* **1969,** *80*, 350.

(14) Yasuda, H.; Lamaze, C.E. *J. Appl. Polym. Sci.* **1971,** *15*, 2277.

(15) Skelly, J.M.; Morosoff, N.C.; Stannett, V.T.; Crumbliss, A.L. *Chem. Mater.* **1994,** *6(2),* 227.

(16) Carbajal, B.G.; Slay, B.G. JR 1967, U.S. Patent 3,318,790; *C.A.* **1967**, *67*, 22975g.

(17) O'Keefe, M.J.; Rigsbee, J.M. *J. Appl. Polym. Sci.* **1994,** *53,* 1631.

(18) Bhat, N.V.; Joshi, N.V. *Plasma Chemistry & Plasma Processing*, **1994,** *14(2)*, 151.

(19) Boluk, M.Y.; Akovali, G. *Polym. Eng. & Sci.* **1981,** *21(11)*, 664.

(20) Diaz, K.F.; Hernandez, R. *J. Polym. Sci. Polym. Chem. Ed.* **1984,** *22, 1123.*

(21) Clark, D.T.; Abrahman, M.Z. *J. Polym. Sci. Polym. Chem. Ed.* **1981,** *19,* 2129.

(22) Clark, D.T.; Abrahman, M.Z. *J. Polym. Sci. Polym. Chem. Ed.* **1981,** *19,* 2689.

(23) Clark, D.T.; Abrahman, M.Z. *J. Polym. Sci. Polym. Chem. Ed.* **1982,** *20*, 691.

(24) O'Connor, P.J.; Ellaboudy, A.S.; Tou, J.C. *J. Appl. Polym.Sci.* **1996,** *60(4)*, 637.

(25) Redmond, J.P.; Pitas, A.F. NASA Contract Rep. NASA-Cr-94310,1968.

(26) Brick, R.M.; Knox, J.R. *Modern Packaging* **1965,** *123.*

(27) Williams, T.; Hayes, M.W. *Nature* **1966,** *209*, 769.

(28) Williams, T.; Edwards, J.H. *Trans. Inst. Metal Finishing* **1966,** *44*, 119.

(29) Connell, R.A.; Gregor, L.V. *J. Electrochem. Soc.* **1965,** *112*, 1198.

(30) Carbajal, B.G. *Trans. Met. Soc. AIME* **1966,** *236*, 365.

(31) Kanazono, T.; Takamura, M.; Kojima, K. *Mem. Inst. Sci. Ind. Res. (Osaka Univ.)* **1967**, *24*, 65.

(32) Yasuda, H., Final Report to Office of Saline Water, U.S. Dept. of the Interior, Contract No. 14-30-2658, Research Triangle Park, N.C., 1972.

(33) Tanaka, K.; Nishio, S.; Matsuura, Y.; Yamabe, T. *Synthetic Metals*, **1993**, *55(2-3)*, 896

(34) Sun, R.G.; Peng, J.B.; Kobayashi, T.; Ma, Y.G.; Zhang, H.F.; Liu, S.Y. *Jap. J. Appl. Phys. Part 2* **1996**, *35(11b)*, L1506-L1508.

(35) Stancell, A.F.; Spencer, A.T. *J. Appl. Polym. Sci.* **1972**, *16*, 1505.

(36) Chambers, R.D. *Fluorine in Organic Chemistry*; Wiley & Sons: London, 1973.

(37) Berezin, I.V.; Kazankaya, N.F.; Martinek, K.; *Zh. Obshch. Khim.* ***1960***, *30*, 4093; *C.A.* **55**, 27153b.

(38) Jesch, K.; Bloor., J.E.; Kronick, P.L. *J. Polym. Sci.* **1966**, *4*, 1487.

(39) Kronick, P.L.; Jesch, K.; Bloor., J.E. *J. Polym. Sci. A1* **1969**, *7*, 767.

(40) Vastola, F.J.; Wightman, J.P., *J. Appl. Chem.* **1964**, *14*, 69.

(41) Haraguchi, T.; Ide, S.; Kajiyama, T. *Abs. Paps. Amer. Chem. Soc.* **1987**, *197(Apr)*, 181.

(42) Inagaki, N.; Kobayashi, N.; Matsushima, M. *J. Membrane Sci.* **1988**, *38(1)*, 85.

(43) Munro, H.S.; Till, C. *J. Polym. Sci. Part A-Polym. Chem.* **1984**, *22(12)*, 3933.

(44) Munro, H.S.; Till, C. *Thin Solid Films*. **1985**, *131(3-4)*, 255.

(45) Clark, D.T.; Shuttleworth, D. *J. Polym. Sci. Polym. Chem. Ed.* **1980**, *18*, 27.

(46) Abrahman, M.Z. Ph.D. Thesis, University of Durham, 1981.

(47) Zhong, Q.; Inniss, D.; Kjoller, K.; Elings, V.B.; *Surface Science* **1993**, *290*, L688

(48) QM-300 Series Film Thickness Monitor, Operation and Service Manual, Kronos Inc.: California, 1971.

(49) Chambers, R.D.; Clark, D.T.; Kilcast, D.; Partington, S. *J. Polym. Sci. Polym. Chem. Ed.* **1974**, *12*, 1647.

(50) Clark, D.T.; Dilks, A.; Thomas, H.R.; Adams, D.B. *J. Electron. Spec. Relat. Phenom.* **1976**, *8*, 51.

(51) Clark, D.T.; Dilks, A. *J. Polym. Sci. Polym. Chem. Ed.* **1976**, *14*, 533.

(52) Clark, D.T.; Dilks, A. *J. Polym. Sci. Polym. Chem. Ed.* **1977**, *15*, 15.

(53) Clark, D.T.; Shuttleworth, D. *J. Polym. Sci. Polym. Chem. Ed.* **1981**, *19*, 2129.

(54) Brennan, W.J. Ph.D. Thesis, University of Durham, 1984.

(55) Wagner, C.D.; Riggs, W.M.; Davis, L.E.; Moulder, J.F.; Muilenberg, G.E. *Handbook of X-Ray Photoelectron Spectroscopy*; Perkin-Elmer Corporation, 1978.

(56) Bellamy, L.J., *Infrared Spectra of Complex Molecules, Vol. 1*; Chapman & Hall: New York, 1975.

(57) Colthup, N.B.; Daly, L.H.; Wiberley, S.E. eds. *Introduction to Infrared and Raman Spectroscopy*, 3rd ed., Academic Press: London, 1990.

(58) Smith, D.C.; Nielson, J.R.; Berryman, L.H.; Classen, H.H.; Hudson, R.L.; *Nav. Res. Lab. Rep.* **1949**, *3567*.

(59) Torkington, P.; Thompson, H.W. *Trans. Faraday. Soc.* **1945**, *41*, 236.

(60) Haszeldine, R.N. *Nature* **1951**, *168*, 1028.

(61) Silverstein, R. M.; Bassler, G. C.; Morrill, T. C. *Spectrometric Identification of Organic Compounds* ; Wiley: New York, 1981.

(62) Knapp, H.F.; Wiegrabe, W.; Heim, M.; Eschrich, R.; Guckenberger, R. *Biophysical Journal* **1995**, *69(2)*, 708.

(63) Vinogradov, G.K.; Gorwadkar, S.; Senda, K.; Morita, S. *Jap. J. Appl. Phys. Part 1* **1994**, *33(11)*, 6410.

(64) Mackie, N.M.; Dalleska,N.F.; Castner, D.G.; Fisher, E.R. *Chem. Mater.* **1997**, *9(1)*, 349.

(65) Labelle, C.B.; Limb, S.J.; Gleason, K. *J. Appl. Phys.* **1997**, *82(4)*, 1784.

(66) Shard, A.G.; Munro, H.S.; Badyal, J.P.S. *Polym. Comm.* **1991**, *32*, 152.

(67) Ratner, B.D.; Castner, D.G.; Lewis, K.B.; Fischer, D.A.; Gland, J.L. *Langmuir* **1993**, *9*, 537.

(68) Panchalingam, V.; Chen, X.; Savage, C.R.; Timmons, R.B.; Eberhart, R.C. *J. Appl. Polym. Sci.: Appl. Polym. Symp.* **1994**, *54, 123.*

(69) Chen, X.; Rajeshwar, K.; Timmons, R.B.; Chen, J-J.; Chyan, O.M.R. *Chem. Mater.* **1996**, *8*, 1067.

(70) Savage, C.R.; Timmons, R.B.; Lin, J.W. in *Structure-Property Relations in Polymers* Ed. Urban M.W.; Craver, C.D. Advances in Chemistry Series, 236: A.C.S. Washington D.C. 1993.

CHAPTER FIVE

ORGANOSILOXANE SURFACES VIA PULSED PLASMA POLYMERISATION

CHAPTER FIVE

ORGANOSILOXANE SURFACES VIA PULSED PLASMA POLYMERISATION

5.1 INTRODUCTION

5.1.1 Background

In recent years there has been much interest in the development of inorganic polymers.[1] These materials generally consist of an inorganic backbone to which is attached organic or organometallic side groups.[2,3,4] The principle behind the design of these macromolecular compounds is that the traditional advantages of inorganic compounds such as heat and radiation resistance, electrical conductivity and electro-optic properties can be combined with the characteristic advantages of organic polymers, for example ease of fabrication, corrosion resistance, flexibility and strength.[1,4] In an inorganic polymer the backbone provides the inorganic character while the side groups can be designed to control properties such as solubility and liquid crystallinity along with surface-related properties such as hydrophobicity, adhesion or biocompatibility.

5.1.2 Poly(siloxanes)

One of the oldest and most widely exploited of the inorganic polymers are the poly(organosiloxanes) (silicones) **(1)**. These consist of a Si-O-Si backbone with side groups attached to the silicon atoms, as represented below.

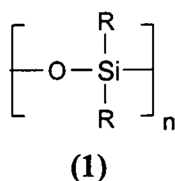

(1)

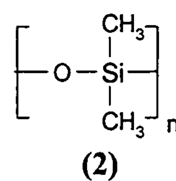

(2)

The chains of alternating silicon and oxygen atoms are among the most flexible units known, which results in the polysiloxanes having some of the lowest glass transition

temperatures (T_g) of all polymers, for example poly(dimethylsiloxane)**(2)** has a T_g = -130°C. The high flexibility of polysiloxane polymers can be attributed to three principle factors;

(i) there is an inherently low barrier to rotation of the Si-O bonds

(ii) the Si-O-Si bond angle is able to widen under moderate tension and

(iii) the side groups are located on every second atom on the backbone compared to all backbone atoms having substituents as is generally the case for conventional organic polymers.

This spacing of the side groups combined with the flexibility of the Si-O-Si bond angle serves to reduce the amount of intramolecular interactions which would otherwise restrict the flexibility of the overall polymer.

Polysiloxanes have a high resistance to both thermo-oxidative and hydrolytic cleavage of their skeletal units.[5] The oxidative stability is at first surprising given the fact that silicon has a high tendency to combine with oxygen. However in the case of polysiloxanes the silicon atoms in the inorganic backbone are already bonded to two oxygen atoms hence there is no driving force for oxidative cleavage of the Si-O-Si bonds. Unlike the linear silicates which are extremely sensitive to hydrolytic cleavage, the silicon-oxygen bonds in the polysiloxanes are stable in aqueous media. This resistance to hydrolysis reflects the protective function of the hydrophobic organic side groups on each Si atom.

Polysiloxanes have been widely exploited for their optical properties.[2,4] The polysiloxane backbone has a broad window of optical transparency. Poly(dimethylsiloxane) is transparent to all wavelengths from 250 nm to the near infrared. In applications where stability to ultraviolet light is important, for example space applications or applications requiring exposure to intense sunlight, this optical transparency of the polysiloxane backbone is important. In experiments where radiation-induced reactions of the side groups are desired the stability of the silicon-oxygen bonds allows the substituents to be manipulated without affecting the overall

polymer backbone. In terms of their use in biomedical and medical applications the polysiloxanes have the further advantage of being resistant to chain cleavage upon exposure to X-rays or γ-radiation. In contrast to the C-C units in their organic counterparts, inorganic backbones such as Si-O-Si are resistant to free-radical cleavage processes.

5.1.3 Plasma polymerisation of siloxane precursors

The interest and exploitation of organosilicon compounds to produce conventional organosilicon polymers and elastomers means they are now extremely important materials both for their industrial applications and their use for fundamental studies in macromolecular science. Such interest in conventional polymers has naturally induced corresponding interest in plasma polymers derived from organosilicon precursors. In fact there has been a very special interest in the organosilicones since the earliest days of plasma polymerisation studies. This may be due to a number of reasons including;[4]

1. There are many organosilicon compounds which are sufficiently volatile at ambient temperatures to be easily and successfully used in standard plasma-chemical procedures.
2. The materials are relatively inexpensive, are commercially available and easy to handle having much lower flammability than organometallics for example.
3. In comparison to fluoropolymers for example, siloxanes are available with a huge variety of sidegroups which therefore offers a wide variety of potential functional groups for grafting onto substrate surfaces.
4. The natural affinity between pure crystalline silicon and organosilicon plasma polymers has meant keen interest in the study of organosilicon plasma polymers for applications in the semi-conductor industry.

5.1.4 Applications of polysiloxane plasma polymers

This wide interest in the plasma chemistry of organosilicones has led to the exploitation of their plasma polymers in a wide variety of applications. Plasma polymers of

organosilicon compounds have been studied as adhesion promoters for various metals[6] including steel,[7,8] and platinum,[9,10] along with non-metallic substrates such as Kevlar,[11] and glass.[10] They have also been deposited for use as dielectrics in capacitors for semi-conductor applications and sensor devices.[12-15] The broad range of transparancies and radiation stability of the siloxane backbone has been exploited in applications such as optical coatings either with variable refractive index[16-18] or as transparent coatings with anti-reflective or scratch resistant properties.[19,20] Plasma polymerized films from mixtures of organosilicons and nitrogen showed absorption in the ultraviolet and were used as UV filters.[21]

A widespread use of plasma polymer films of organosilicones is as barrier coatings for corrosion prevention.[8,22,23] Their usefulness in this application is a result of their extremely low permeability towards water vapour.[24,25] In fact protective overcoats of plasma polymerized hexamethyldisiloxane on evaporated aluminium in automotive headlight reflectors are one of the largest single applications of plasma polymer films. In 1987 Bosch GmbH annually coated over 10 million of its reflectors in order to prevent corrosion of the aluminium.[26] Along with their resistance to water vapour they also have the advantage of being transparent which makes them ideal for use as barrier coatings on plastic food packaging.[27]

Organosilicon plasma polymers are also used in biomedical applications.[28-34] Critical surface tensions of 20-30 mJ m^{-2} are recommended for surfaces with good biocompatibility.[35] Siloxane polymers have a critical surface tension of approximately 22 mJ m^{-2} and are non-toxic. When untreated polypropylene and polypropylene coated with the plasma polymer of hexamethylcyclotrisiloxane were analysed following exposure to blood, the plasma-polymer-treated-polypropylene was found to have fewer adhering blood cells and to have induced fewer morphological changes in the cells than the untreated polypropylene.[36] Plasma polymers deposited from octamethylcyclotetrasiloxane discharges were used as biocompatible coatings for membranes in blood oxygenators.[37]

Plasma polymers of cyclic siloxanes have been studied along with other silicon - containing precursors for their use as permselective membranes for the separation of various gas mixtures into their individual components.[38] Oxygen over nitrogen[39,40] and hydrogen over carbon dioxide[41] are among the mixtures tested. For the enrichment of oxygen from nitrogen/oxygen mixtures e.g. air, plasma polymerized octamethylcyclotetrasiloxane was found to provide the best combination of permeability ratio and O_2 permeation rate.[42] A membrane of the plasma polymer of hexamethylcyclotrisiloxane on a cellulose acetate substrate was used to study the separation of a binary liquid mixture (alcohol/water).[43]

The effects of siloxane chain length on the separation characteristics of pervaporation membranes prepared by plasma polymerisation has recently been studied[44] and it was found that the cyclic siloxane with the longest chain length gave the best performance in terms of high selectivity and high permeation rate. The separation characteristics of the membrane were related to the hydrophobicity of the surface in contact with the ethanol/water solution. The higher permeation rate for monomers with longer siloxane chain lengths was attributed to greater flexibility within the plasma polymer. Recent work details the use of a plasma polymer coating from octamethylcyclotetrasiloxane discharges being used as a membrane with selective gas sorption characteristics to be used in detecting inhalating anaesthetics.[45]

The flexibility of siloxane chains has already been mentioned as leading to lower glass transition temperatures. Lower T_g's are known to enhance ionic conductivity[46] and these two properties have been exploited to produce an ionically conductive thin film from the plasma polymerisation of octamethylcyclotetrasiloxane with organic and ionic co-monomers and dopants.[47]

The choice of the starting material for this study of pulsed plasma polymerisation was influenced by several factors. This is the first study of the plasma polymerisation of tetramethyl-tetravinyl-cyclotetrasiloxane (TVS) **(3)**. The chemical structure of the

precursor is such that it contains an inorganic silicon-oxygen skeleton combined with organic methyl and, more importantly, vinyl substituents. The inorganic siloxane rings will contribute the properties previously discussed in relation to siloxane compounds. The vinyl groups should provide sites to allow polymerisation to proceed both during the on-time and through conventional radical-induced polymerisation in the off-time. Polymerisation through the vinyl groups would be expected to result in a highly crosslinked structure with good chemical stability.

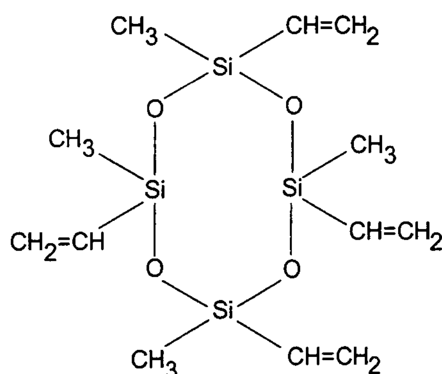

Fig. 5-1: Molecular formula of $C_{12}H_{24}Si_4O_4$, tetramethyl-tetravinyl-cyclotetrasiloxane (TVS).

The work reported in chapters three and four has shown it is possible to enhance retention of precursor structure in the final plasma polymer through the use of pulsed plasmas. In particular the studies of pulsed plasmas of perfluoroallylbenzene demonstrated the presence of a functional group susceptible to free-radical polymerisation enhances the effectiveness of pulsed plasmas as a means of tailoring the surface composition. The aim of the work reported in this chapter is to determine if it is possible to exploit the characteristics of pulsed plasma polymerisation in conjunction with the chemical characteristics of TVS to such an extent as to retain the siloxane rings of the monomer in the final plasma polymer. The objective being to produce a surface consisting of siloxane rings enclosed in a cross-linked organic matrix.

5.2 EXPERIMENTAL

The experimental apparatus and procedure for continuous wave and pulsed experiments was as described in sec 3.2. The monomer, TVS, was purchased from Aldrich and transferred to the monomer tube under an inert atmosphere. The TVS liquid was then degassed via five freeze-thaw cycles. The clean reactor was pumped to base pressure and the monomer vapour was introduced to a pressure of 0.1 torr at a flow rate of approximately 8.4×10^{-8} kg s^{-1}. The electrical discharge was ignited and sustained for 10 minutes after which the r.f. was switched off. Continuous wave powers between 1.5 and 8 Watts were employed with pulsing times t_{on} and t_{off} varied over the range 10 μs to 6 ms with a peak power of 70 W. Prior to removing the sample from the reactor the system was purged with TVS for a further two minutes and finally vented to atmosphere. The samples were then removed and characterised.

The C(1s), O(1s) and Si(2p) high resolution XPS spectra were acquired for all plasma polymers. XPS was also used to determine if complete coverage of the substrate surface was occurring. Nylon films were used as substrates and the N(1s) spectrum of the surface following plasma deposition was recorded. The absence of a peak in this region of the XPS spectrum was indicative of complete coverage of the substrate. Instumentally determined sensitivity factors for unit stoichiometry were taken as C(1s) : O(1s) : N(1s) : Si(2p) equal to 1:00 : 0.62 : 0.46: 1.08.

5.3 RESULTS

5.3.1 Infrared Absorption Spectroscopy

The infrared spectrum of the monomer, TVS is shown in Fig. 5-2 with assignments for the absorption peaks presented in Table 5-1.[44,48-51] The major absorption peaks in all the spectra appear at approximately 1050 cm^{-1} due to Si-O-Si stretch vibrations of the siloxane ring system. Compared to the analogous C-O stretching vibrations seen on carbon compounds these Si-O vibrations are approximately five times more intense.[52]

The C-H stretch vibrations at ca. 3000 cm^{-1} are very weak compared to hydrocarbons however this is a recognised fact in the infrared spectra of organosilicon compounds.[51, 52]

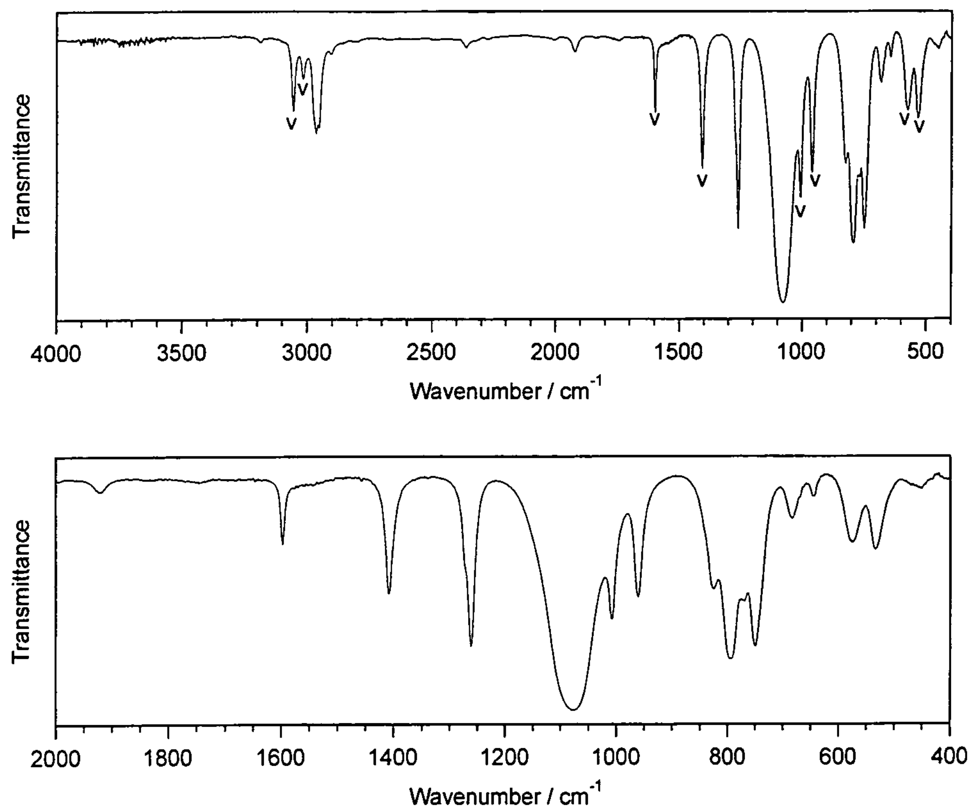

Fig. 5-2: Transmission infrared spectrum of tetramethyl-tetravinyl-cyclotetrasiloxane (TVS) on a KBr disk. Peaks associated with the vinyl groups are labelled V.

σ (cm^{-1})	*Mode*	*Comment*
3055	$\nu^a(=CH_2)$, $\nu^s(=CH_2)$	in vinyl groups
2965	$\nu^a(CH_3)$, $\nu^s(CH_3)$	in Si-Me
1597	ν (C=C)	in vinyl groups
1406	$\delta(=CH_2)$	in vinyl groups
1262	$\delta^s(CH_3)$	in Si-Me
1076	ν^a (Si-O-Si)	
1008	τ (C=C)	in vinyl groups
961	$\omega(=CH_2)$	in vinyl groups
793	$\rho(CH_3)$, ν (SiC)	in Si-Me
575	ν Si-(CH=CH_2)	

Table 5-1: Assignments for IR absorption bands in FT-IR spectrum of TVS; ν, δ, ρ, ω, τ denote stretching, bending, rocking, wagging and twisting modes respectively, a and s asymmetric and symmetric vibrations.

The effect of altering continuous wave power on the infrared spectra of the plasma polymers deposited from TVS discharges is shown in Fig. 5-3. On increasing discharge power the position of the Si-O-Si peak moves to slightly lower wavenumbers relative to the monomer. Even at a power input as low as 1.5 W, the lowest power at which it was possible to maintain a plasma at the pressures used, this peak at ~ 1070 cm^{-1} has broadened and lost its fine structure relative to the parent compound. The shape and position of this peak alters further with increasing discharge power. Whereas at 1.5 W the Si-O-Si vibrations yield a peak resembling an unresolved doublet with a more intense component at higher wavenumbers, for a discharge power of 2 W or greater the doublet is no longer distinguishable and the more intense absorption is toward the lower wavenumber side of the peak. The peak at ~1262 cm^{-1} and the doublet at ~793/750 cm^{-1} attributed to silicon bonded to methyl groups[49,51] decrease in intensity relative to the Si-O-Si peak with increasing power. The doublet has also broadened and the two component peaks can no longer be resolved. It is also noted that the ratio of the intensity of the peak at 1262 cm^{-1} to the peak at 800 cm^{-1} decreases with increasing power.

The most notable difference between the spectrum of the monomer and that of the continuous wave plasma polymers is the disappearance of the absorptions associated with the vinyl functionalities from the polymer spectra. The peaks at 3055 cm^{-1}, 1597 cm^{-1}, 1406 cm^{-1}, 1008 cm^{-1} and 961 cm^{-1} are all absent from the continuous wave plasma polymers.

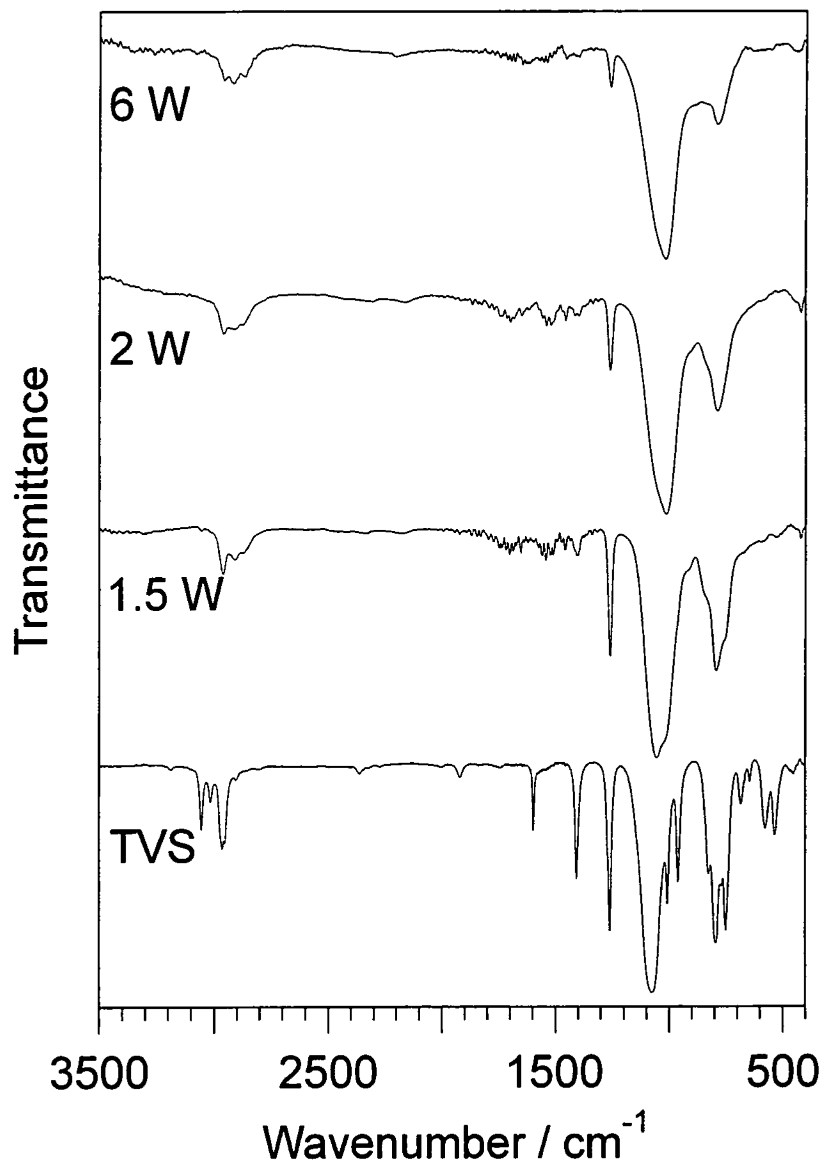

Fig. 5-3: Transmission FT-IR spectra of plasma polymers deposited from continuous wave TVS plasmas as a function of discharge power.

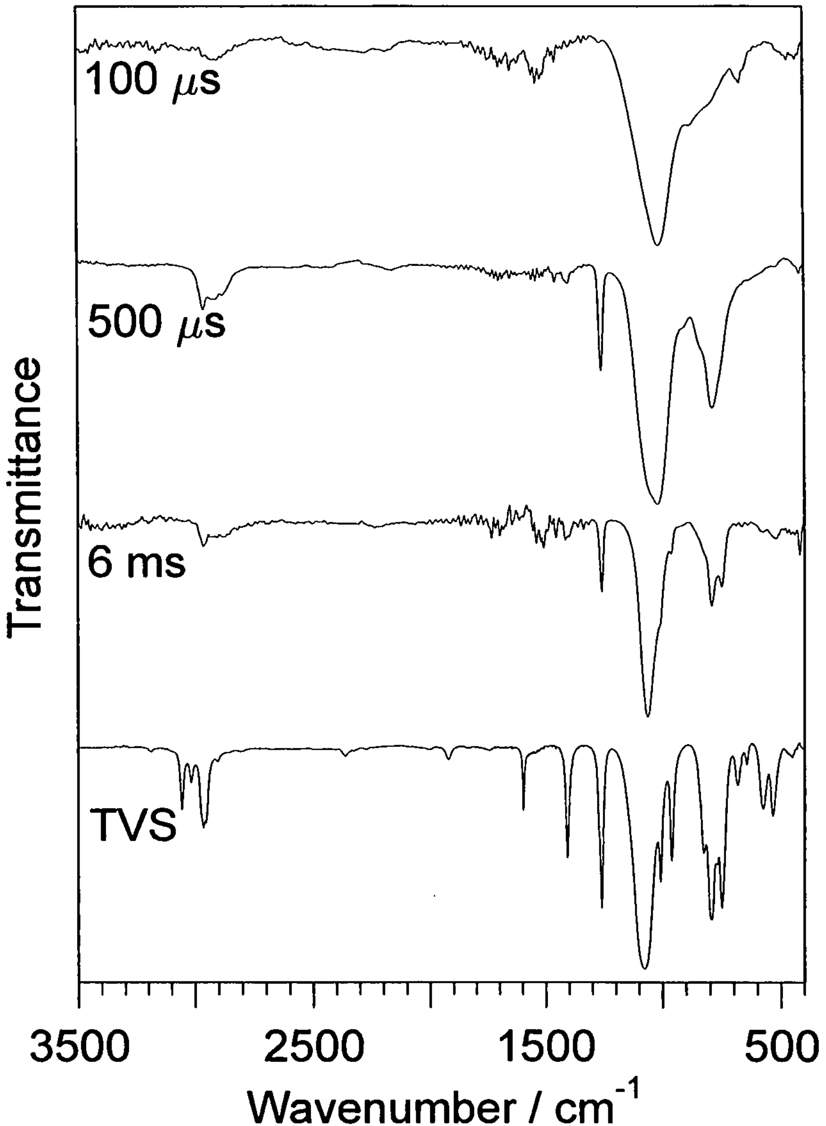

Fig. 5-4: Transmission FT-IR spectra of plasma polymers deposited from pulsed TVS discharges as a function of off-time; on-time = 10 μs, peak power = 70 W.

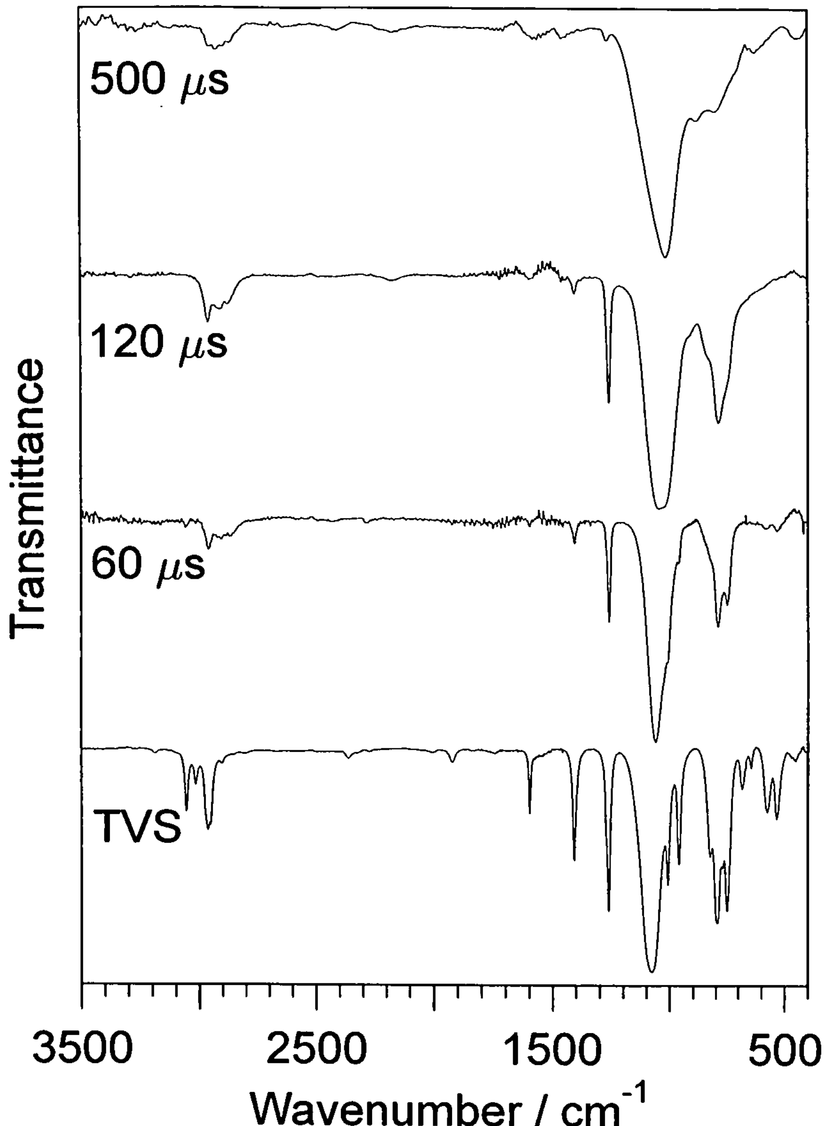

Fig. 5-5: Transmission FT-IR spectra of plasma polymers deposited from pulsed TVS discharges as a function of on-time; off-time = 6 ms, peak power = 70 W.

The infrared transmission spectra of plasma polymers deposited from pulsed TVS discharges are compared in Fig. 5-4 and Fig. 5-5. As was the case with the continuous wave experiments, increasing average power results in a broadening and general loss in resolution of the Si-O-Si peak at ~1080 cm^{-1} . It is of interest to note however that in contrast to the case of the low power continuous wave experiments, for pulsed plasmas with long off-times or short on-times, i.e. low duty cycles, the Si-O-Si peak does retain some of the fine structure evident in the precursor. The width and resolution of the absorptions in this region of the spectra are much smaller for low duty cycle pulsed plasma polymers than for the lowest power CW polymers. Also the position of the Si-O-Si peak is closer to its position in the monomer (1080 cm^{-1}) in the spectra of pulsed plasma polymers compared to the continuous wave plasma polymers. Unlike the plasma polymers form the continuous wave discharges which indicate complete lack of the original vinyl groups from the plasma polymers, the low duty cycle pulsed plasmas yielded polymers which show slight absorptions at wavenumbers associated with the vinyl groups.

5.3.2 X-ray Photoelectron Spectroscopy.

The chemical structure of the starting material and hence the resultant plasma polymers means X-ray photoelectron spectroscopy is not as powerful an analytical tool for the analysis of these surfaces as was the case for the perfluorocarbon surfaces generated in earlier work. The precursor in this case consists of four elements viz. carbon, oxygen, silicon and hydrogen, compared to just fluorine and carbon in the previous studies. Hydrogen is not detectable directly by core level XPS due to it having only a single electron[53] and the lack of a strongly electronegative atom such as fluorine means there is insignificant chemical shift on the C(1s) peak to give identifiable changes in the overall profile of the spectrum with varying plasma parameters. In fact as can be seen in Fig. 5-6, p. 157, there is little change in the profile of the XPS spectra with changing plasma parameters for continuous wave, off-time or on-time experiments in any of the carbon, oxygen or silicon spectra recorded.

Due to silicon and oxygen having approximately the same effect in terms of their induced shift in C(1s) binding energy, peak fitting the overall C(1s) profile has not been attempted. Despite these difficulties the technique does give some information on the composition of the surfaces generated by the plasma polymerisation of TVS by allowing determination of the ratio of carbon:oxygen:silicon at the surface of each plasma polymer taking into account the appropriate XPS sensitivity factors.[54]

The elemental percentages and ratios of the plasma polymers deposited from continuous wave and pulsed plasmas are given in Table 5-2 to Table 5-4 with the changes in elemental composition with plasma parameters shown in Fig. 5-7, Fig. 5-8 and Fig. 5-9, p. 158.

Power (W)	% Carbon	% Oxygen	% Silicon	C:O	C:Si	Si:O
1.5	53.4	23.6	22.9	2.26	2.33	0.97
2	55.1	23.5	21.3	2.34	2.59	0.91
4	56.7	22.0	20.2	2.58	2.81	0.92
6	57.8	23.7	18.5	2.44	3.12	0.78
Error	± 2.24%	±3.8%	2.2%	± 3.02%	±2.22%	±3.0%

Table 5-2: Percentages of each element (hydrogen excluded) in plasma polymers deposited from continuous wave TVS discharges with varying discharge powers.

Off-time (μs)	% Carbon	% Oxygen	% Silicon	C:O	C:Si	Si:O
100	52.6	24.5	22.3	2.26	2.33	0.97
500	53.1	24.0	22.8	2.34	2.59	0.91
1000	52.6	25.0	23.7	2.58	2.81	0.92
3500	52.9	23.6	23.5	2.44	3.12	0.78
6000	54.2	23.0	22.8	2.36	2.38	0.99
Error	± 2.%	±3.8%	2.2%	± 3.02%	±2.22%	±3.0%

Table 5-3: Percentages of each element (hydrogen excluded) in plasma polymers deposited from pulsed TVS discharges with varying off-times: on-time = 10 μs, peak power = 70 W.

On-time (μs)	% Carbon	% Oxygen	% Silicon	C:O	C:Si	Si:O
10	54.2	23.0	22.8	2.36	2.38	0.99
60	52.7	23.9	23.3	2.21	2.26	0.97
120	52.4	24.8	22.8	2.11	2.30	0.92
250	52.5	25.6	21.7	2.05	2.42	0.85
500	59.5	21.7	18.8	2.74	3.16	0.87

Table 5-4: Percentages of each element (hydrogen excluded) in plasma polymers deposited from pulsed TVS discharges with varying on-times: off-time = 6000 μs, peak power = 70 W.

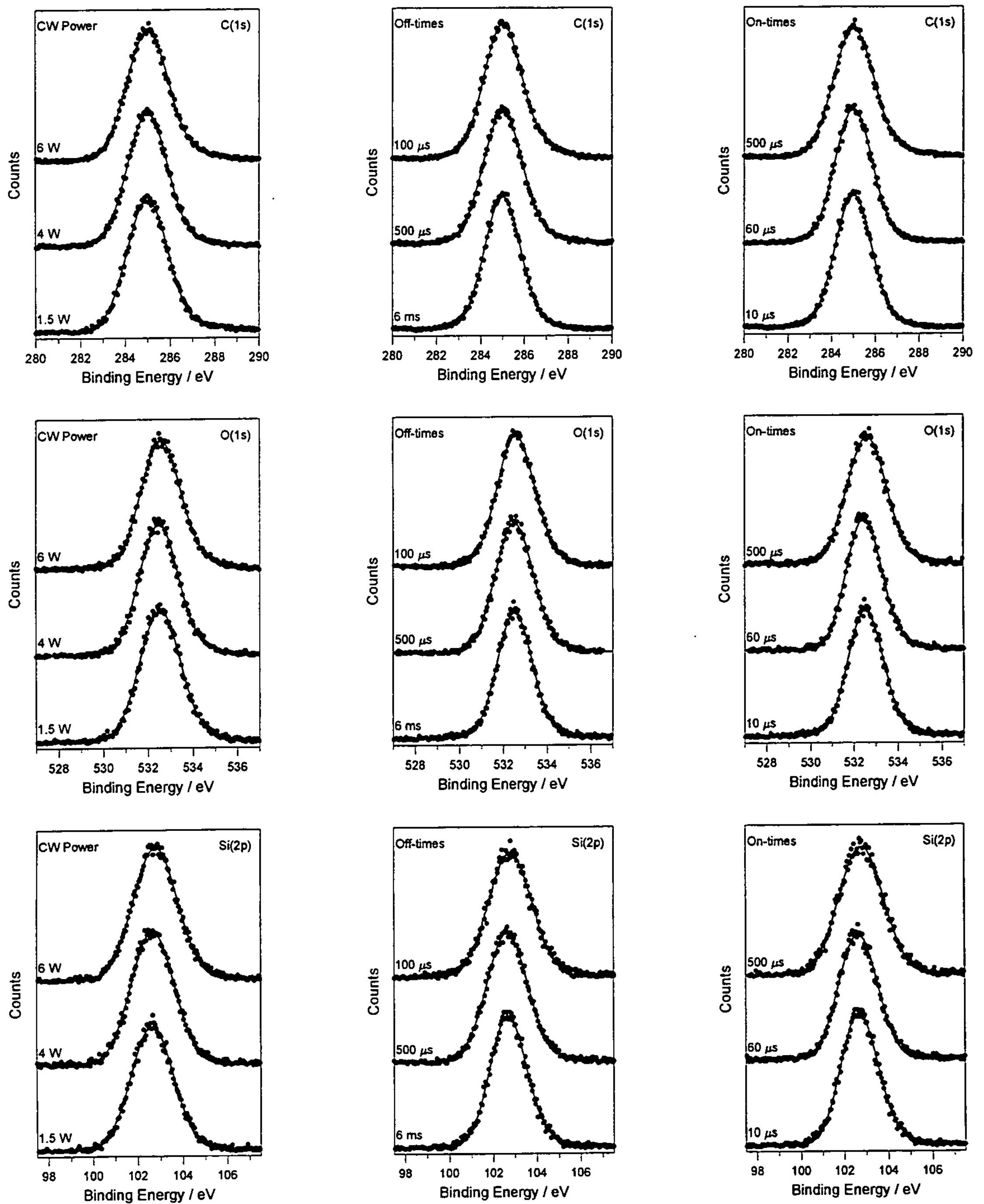

Fig. 5-6: C(1s), O(1s) and Si(2p) high resolution XPS spectra of plasma polymers deposited from continuous wave and pulsed plasmas of tetravinyltetrasiloxane.

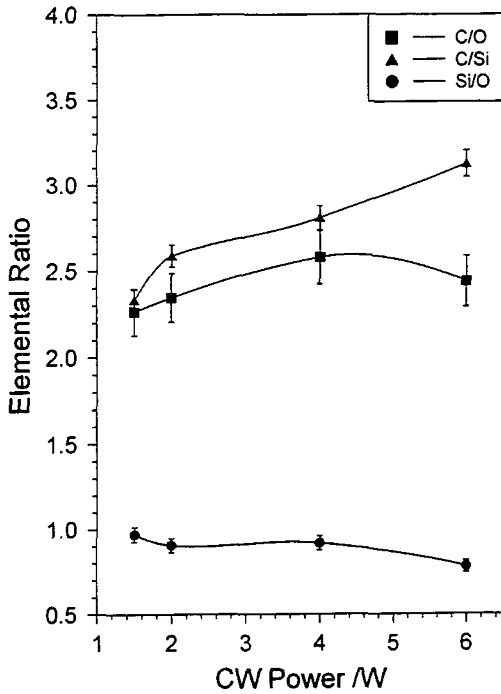

Fig. 5-7: Plot of elemental ratios versus continuous wave power for plasma polymers deposited from TVS discharges onto nylon substrates.

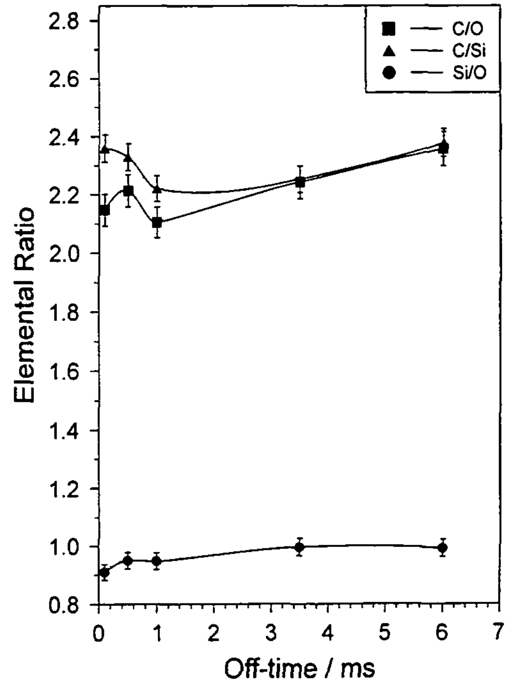

Fig. 5-8: Plot of elemental ratios versus off-time for plasma polymers deposited from pulsed plasmas of TVS onto nylon substrates; on-time = 10 μs, peak power = 70 W.

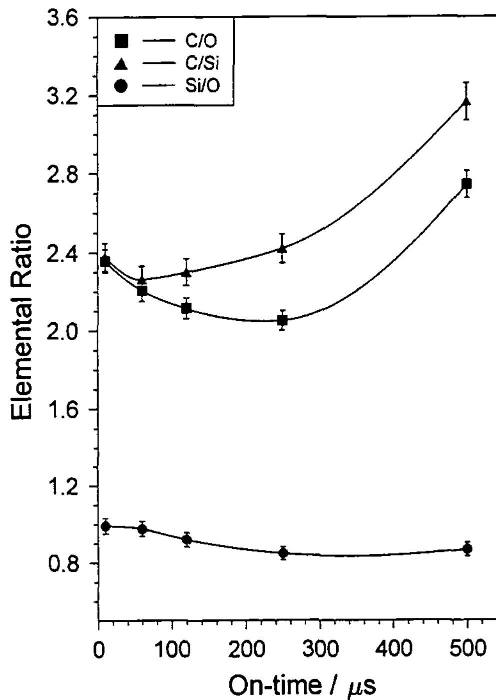

Fig. 5-9: Plot of elemental ratios versus on-time for plasma polymers deposited from pulsed plasmas of TVS onto nylon substrates; off-time = 6000 μs, peak power = 70 W.

5.3.3 Deposition Rate Studies

The results of the deposition rate studies carried out on the pulsed plasmas of TVS are shown in Fig. 5-10 to Fig. 5-13.

Fig. 5-10 is a plot of deposition rate measured in Angstroms per minute as a function of off-times for TVS plasmas with different on-times of 10, 20 and 50 μs. To compare the results from the different on-times as a function of average power a plot of deposition rate versus average power is shown in Fig. 5-11. As was seen in the case of the fluoromonomers, chapter four, for any particular on-time the deposition rate per minute decreases with increasing off-time. However unlike the earlier studies the decrease is not continuous. In the case of the experiments with 20 and 50 μs on-times the deposition rate per minute remains approximately constant for off-times between 200 and 1000 μs. At off-times shorter than 1000 μs the on-time is critical in determining the deposition rate. Interestingly the plasmas with the shortest on-times i.e. 10 μs give highest deposition rates for a given off-time in this region. As the average power will obviously be different when comparing results from experiments with the same off-time but different on-times, it is necessary to determine if this is the principle reason for the difference in deposition rates with on-times.

Fig. 5-11 is a plot of deposition rate/min versus average power for the same experiments as in Fig. 5-10. As can be seen the difference in deposition rates for different on-times remains, even when average power is taken into account. For an average power of 2 W (duty cycle of 2.8%) the deposition rate from a pulsed plasma with an on-time of 10 μs is approximately twice that of 20 μs on-time and three times that of a plasma with 50 μs on-time.

For pulsed plasmas with off-times greater than 2000 μs the deposition rate is recorded as between 30 and 50 Å/min regardless of the on-time. When the deposition rate is measured as Angstroms per Joule, Fig. 5-12, this means that at off-times greater than 2000 μs the deposition efficiency is greater for shorter on-times. This plot also

illustrates the efficiency of deposition from plasmas with 10 μs on-time initially starts to rise with increasing off-time to a maximum of 4.5 Å/J for off-times up to ~1000 μs, then falls rapidly to its final value of approximately 2.5 Å/J. For on-times of 20 μs, the efficiency shows no such rise and fall, instead climbing gradually from 0.5 Å/J at 200 μs off-time to a steady value of approximately 2 Å/J at or above 1000 μs. Pulsed plasmas with on-times of 50 μs show the same gradual increase to a steady value of greater than 1000 μs but the final value of ~ 0.7 Å/J is lower than for the shorter on-time experiments.

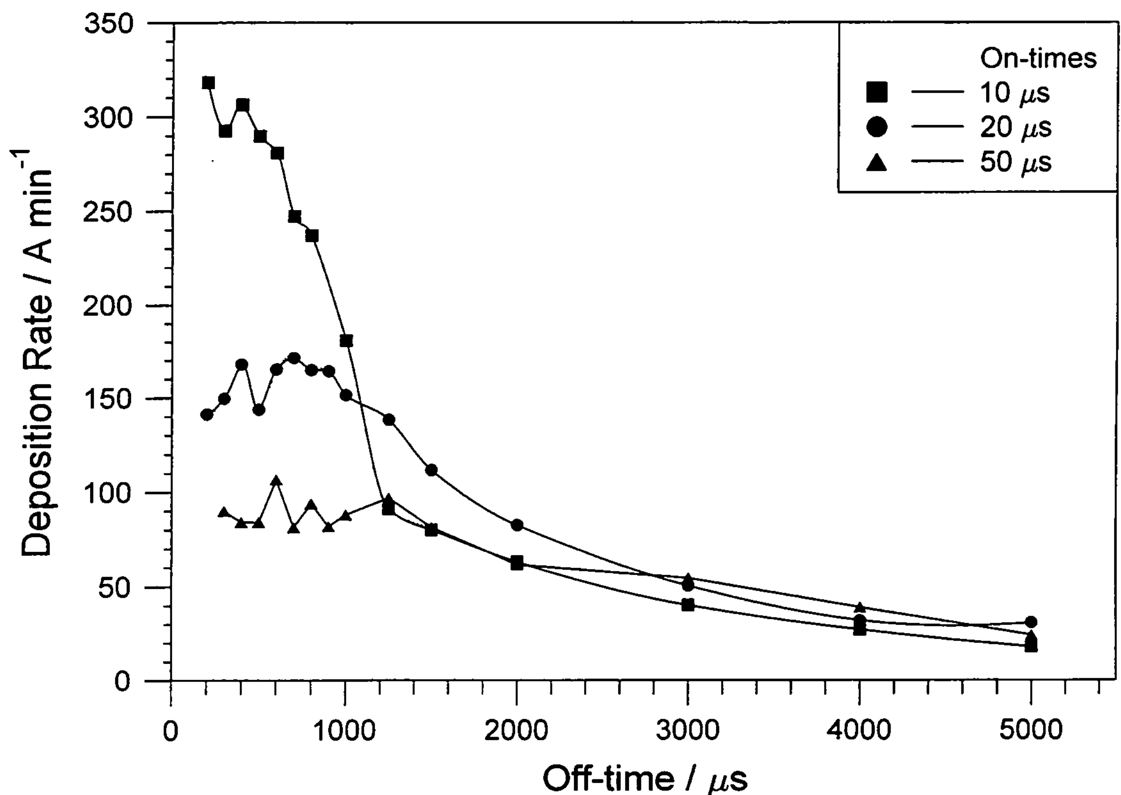

Fig. 5-10: Graph of deposition rate in A/min versus off-time for pulsed TVS discharges with different on-times.

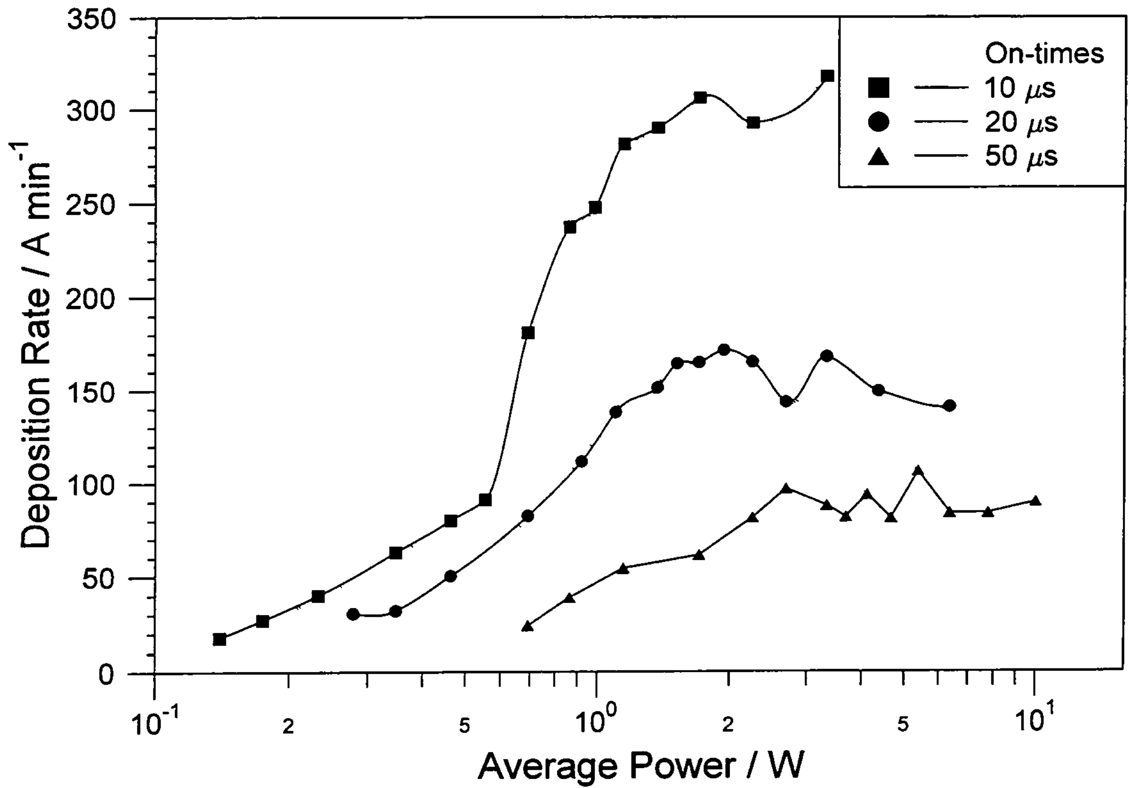

Fig. 5-11: Graph of deposition rate in A/min versus average power for pulsed TVS discharges with different on-times.

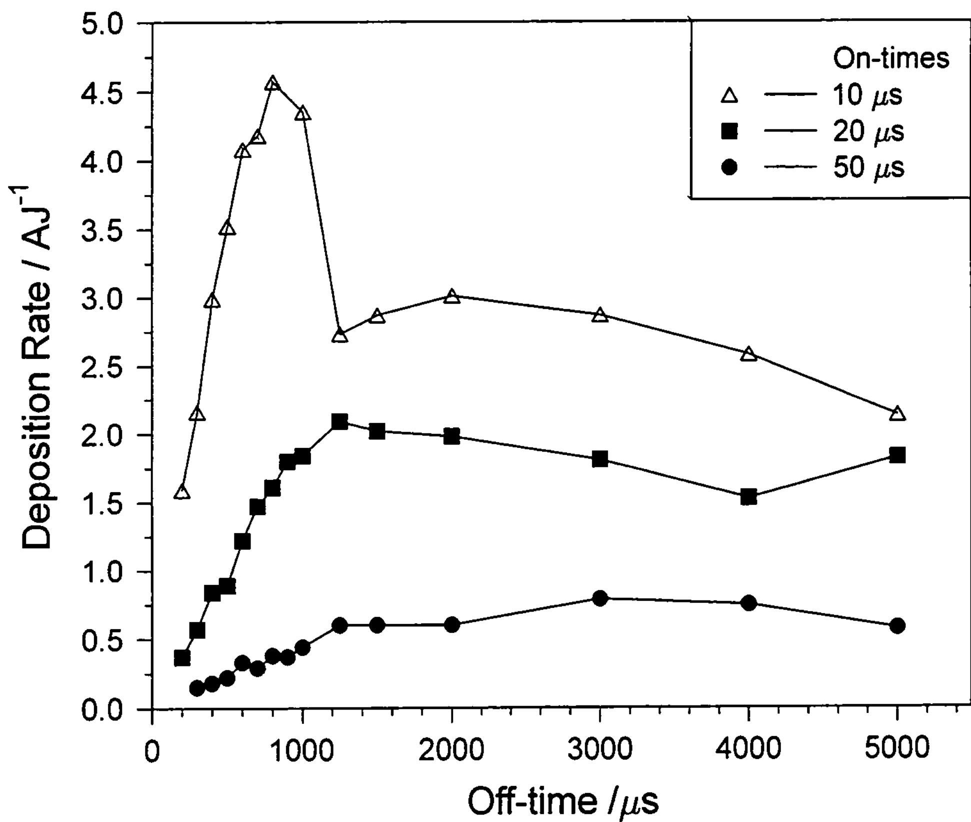

Fig. 5-12: Graph of deposition rate in A/J versus off-time for pulsed TVS discharges with different on-times.

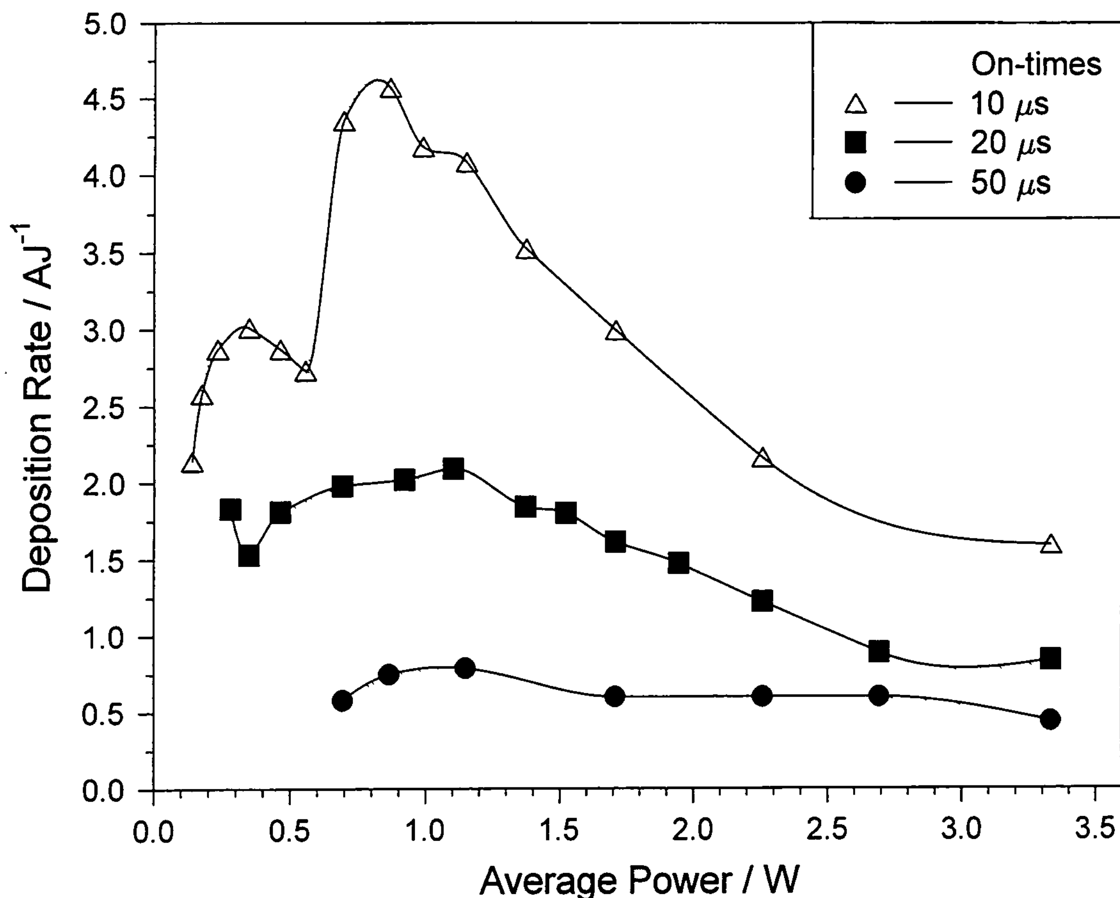

Fig. 5-13: Graph of deposition rate in A/J versus average power for pulsed TVS discharges with different on-times

5.4 DISCUSSION

5.4.1 Continuous Wave Plasma Polymerisation

Continuous wave plasma polymerisation of TVS results in the generation of an organo-silicon surface the composition of which depends on the discharge power. At the lowest discharge power possible, 1.5 Watts, the plasma polymer has a infrared spectrum dominated by absorptions associated with silicon containing species. This is the case regardless of discharge power, the three dominant peaks in the spectrum being at 1250 cm^{-1}, 1050 cm^{-1} and 800 cm^{-1} corresponding to Si-CH_3 bending, Si-O stretch and Si-CH_3 rocking respectfully. The strength of the Si-C absorptions reflects the fact that the Si-C bond has some ionic character (~12%).[52] While the plasma polymer deposited from a 1.5 W continuous wave plasma does show some fine structure on the peak around 800

cm^{-1}, in general the infrared spectra of the plasma polymers from continuous wave discharges are typical of plasma polymers i.e. the absorption peaks are broad and poorly resolved. The presence of high energy electrons, near and vacuum ultraviolet radiation, ions, and excited metastables leads to a highly energetic environment both in the gas phase and at the surface of the growing organo-silicon film.[55] This results in extensive fragmentation of the precursor molecules in the gas phase to yield a wide variety of species for incorporation into the plasma polymer.[56] In addition to the range of different contributing species the plasma polymer itself is exposed to intensive and continuous ion and electron bombardment along with irradiation from ultraviolet, visible and infrared radiation. The result is a polymer with a wide variety of bond lengths and angles leading to broad and featureless infrared absorption bands relative to the precursor. As the discharge power is increased the peaks become even less resolved and absorption is noted at wavenumbers not at all associated with the starting material TVS e.g. 800-900 cm^{-1} and 2800-2900 cm^{-1}.

The absence of the peaks associated with the vinyl group from the infrared spectra of the continuous wave polymers indicate either that the group is cleaved from the siloxane backbone or else remains attached to the silicon but takes an active part in the plasma polymerisation process.

The XPS results show that all polymers have carbon contents lower that the starting material. This implies that C_xH_y species are being lost during the plasma polymerisation process. In the case of siloxane precursors it has previously been suggested that the Si-C bonds attaching the organic sidegroups to the siloxane backbone are likely to be the first bonds to be cleaved under plasma conditions, resulting in the abstraction of alkyl groups, Fig. 5-14.[57] The drop in carbon content and slight decrease in Si:O ratio found in this study also support the assertion that cleavage of the Si-C bonds are significant reactions in the plasma polymerisation process.

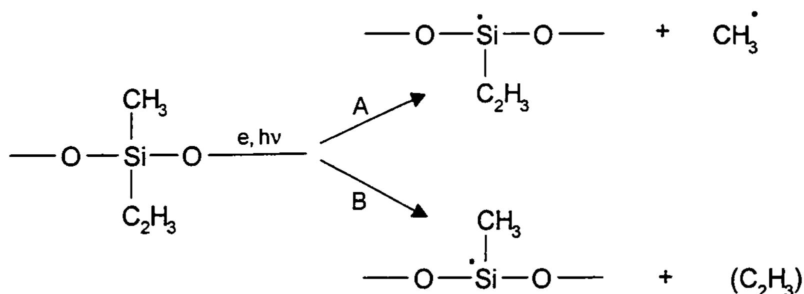

Fig. 5-14: Possible free radical generation reactions with accompanying loss of C_xH_y species from TVS following electron and/or UV bombardment of precursor.

5.4.2 Pulsed Plasma Polymerisation

In the case of polymers deposited from pulsed plasmas with high duty cycles the results are similar to those obtained from CW discharges. The absorption bands associated with vinyl groups have completely disappeared. The asymmetric Si-O-Si peak has become wider and shifted to slightly lower wavenumber and there are continuous absorbances from this peak down to 800 cm^{-1}.

The polymers deposited from low duty cycle pulsed plasmas on the other hand, show significant differences to both the continuous wave and high duty cycle polymers. The infrared spectra of these polymers show a much sharper Si-O-Si peak at approximately the same position as in the TVS monomer. This would indicate the Si-O bond angles and lengths to be approximately the same in the low duty cycle pulsed plasma polymers as they are in the monomer, i.e. that the siloxane rings have remained intact in these polymers. Also of interest is the fact that the peak at ~ 800 cm^{-1} has retained its structure and the two components of the doublet are still visible. XPS data shows the Si/O ratio to be approximately equal to that of the starting material (Si:O = 1) for these low duty cycle polymers again suggesting retention of the siloxane rings at the surface of the substrate.

Even with low duty cycle pulsed plasmas the susceptibility of the vinyl group to plasma polymerisation is again evident as the associated peaks are extremely weak in these

spectra. There is however some evidence that at very low duty cycles not all of the vinyl groups have been lost. The two shoulders on the lower wavenumber side of the Si-O peak at 1008 and 961 cm^{-1} originate from the C=C twisting and $=CH_2$ wagging modes respectively of the vinyl group in the monomer. Hence it would appear that due to the high proportion of vinyl groups in the starting material at very low average powers a small proportion of these are retained in the plasma polymer.

5.4.3 Deposition Rate Studies

Deposition rate experiments were carried out to gain more information about the effect of pulsing on the plasma polymerisation of TVS. The results are different from those obtained from pulsed plasmas of the perfluoromonomers studied in earlier chapters. In Fig. 5-10 and Fig. 5-11 it can be seen that at off-times below 1000 μs the expected drop in deposition rate with increasing off-time is not present for on-times of 20 and 50 μs . Also the deposition rate depends on the length of the on-time and this dependence on the on-time is independent of average power. Surprisingly the plasmas with greater on-times give lower deposition rates.

These trends can be explained if we consider the pulsed plasma polymerisation process as a two-step process. The first stage (on-time) acts principally to initiate the polymerisation by generating radicals through electron and ion bombardment and UV irradiation of the gaseous precursor and any surfaces in contact with the plasma. The longer the on-time the greater will be the initiation and the number of potential sites for reaction and hence continued deposition in the off-time. However as the infrared and XPS results show a longer on-time also leads to greater fragmentation of the precursor. This will lead to a greater number of low molecular weight species which may not be incorporated into the plasma polymer and will simply be pumped away from the reaction zone. The second stage (off-time) is free from electron, ion and UV bombardment and reactions occurring here are principally a result of free-radical induced processes either in the gas phase or at the surface of the plasma polymer.

The vinyl groups in the TVS precursors are particularly susceptible to these free-radical propagation reactions and hence deposition continues in the off-time. In contrast to the low molecular weight deposition likely to be occurring in the on-time, off-time deposition will involve larger molecular weight fragments or entire precursor molecules being incorporated in the growing polymer network. Hence a shorter on-time producing a greater amount of deposition can be explained by an increase in the (off-time/on-time) deposition ratio leading to a greater number of higher molecular weight precursors depositing per unit time. This off-time deposition also leads to a retention of the siloxane rings in the final plasma polymer, Fig. 5-15.

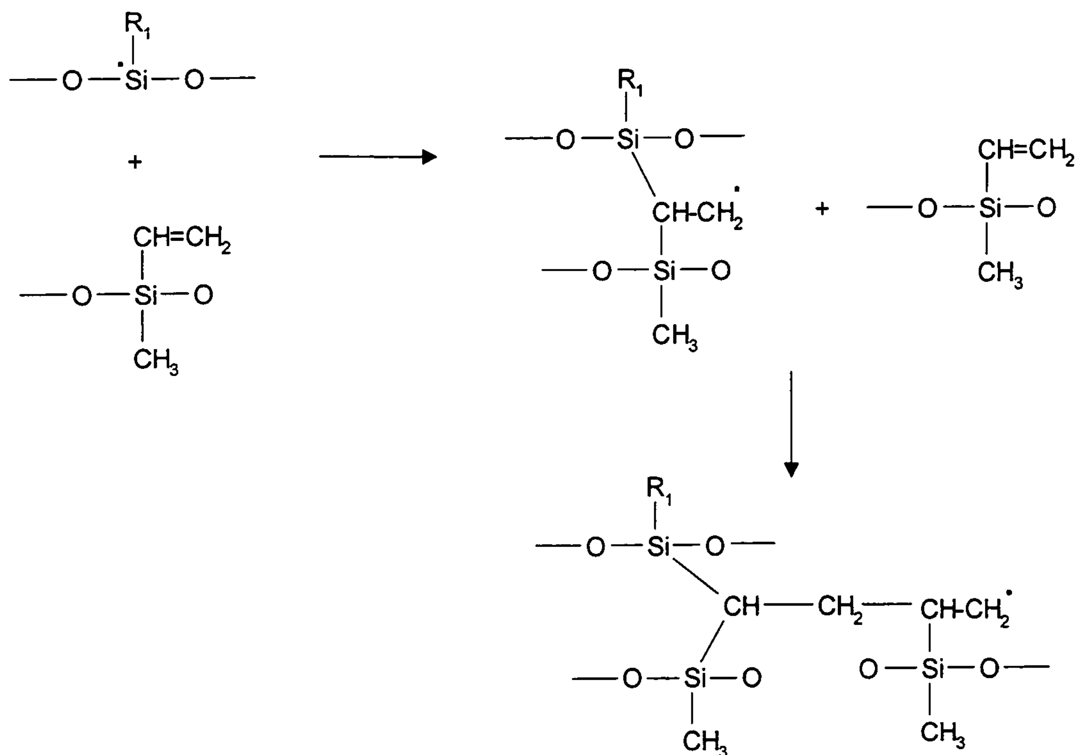

Fig. 5-15: Possible free radical reactions of vinyl groups leading to retention of siloxane structure in plasma polymer.

To explain the constant deposition rate with increasing off-time from plasmas with on-times of 20 and 50 μs and off-times less than 1000 μs it must be assumed that deposition in the off-time is occurring to such a significant extent that it is the same or greater than that occurring in the on-time. Hence at off-times less than 1000 μs the off-

stage deposition is occurring quickly enough to mean that no re-initiation is necessary to maintain the growth rate of the plasma polymer.

The plots of deposition efficiency i.e. deposition rate/Joule versus off-time and average power, Fig. 5-12 and Fig. 5-13 receptively, confirm that deposition in the first millisecond of the off-stage is critical in maintaining a deposition rate for plasma polymers from the pulsed TVS discharges. Fig. 5-11 shows the efficiency of deposition rise for all on-times up to an off-time of 1000 μs after which it levels off. Fig. 5-13 show a duty cycle of 1.5%, leading to an average power of approximately 1 W, results in the highest efficiency of deposition of the three on-times. At this duty cycle the pulsed plasmas with 10 μs on-time are over six times more efficient at depositing plasma polymer than plasmas with on-times of 50 μs.

5.5 CONCLUSIONS

The aim of this chapter was to exploit the advantages of pulsed plasmas to generate surfaces consisting of polysiloxane chains linked in an organic matrix. The starting material tetramethyl-tetravinyl-cyclotetrasiloxane was chosen as it consisted of the siloxane backbone with a vinyl substituent on each of the silicon atoms, while in addition to this having a high enough vapour pressure to sustain a discharge. This is the first reported work on the plasma polymerisation of this compound. It was hoped that suitable pulsing conditions would result in polymerisation via free-radical reaction of the vinyl groups in the off-time hence allowing generation of plasma polymers with the structure of the monomer i.e. the siloxane rings, intact.

The continuous wave plasma polymers from TVS discharges showed evidence that loss of carbon containing fragments from the precursor was a prominent reaction pathway in the plasma polymerisation process. In addition to this the spectra indicated cleavage of the Si-O-Si bonds was also occurring in the continuous wave discharges. Analysis of the spectra indicated a large variety of bond lengths, angles and types in these plasma

polymers, confirming significant scrambling of the structure of the precursor in the final product.

In contrast pulsed plasmas of TVS resulted in significantly better results than the continuous wave discharges. In the case of pulsed plasmas with high duty cycles the loss of monomer structure was again evident from the infrared and XPS spectra. In the case of plasmas with low duty cycles however the retention of monomer structure in the plasma polymer was significantly improved relative to both continuous wave and high duty cycle pulsed plasmas. The infrared spectra indicated Si absorption bands in almost the exact same position as in the monomer and these bands remained narrow and well resolved. In particular the shape and position of the absorption associated with the anti-symmetric Si-O-Si stretch, in combination with the Si:O ratio obtained from XPS analysis, suggests the siloxane rings remain intact in the plasma polymer.

The assertion that this retention of monomer structure is achieved via off-time polymerisation is confirmed by deposition rate studies. These indicate that shorter on-times lead to more efficient deposition probably due to greater incorporation of higher molecular weight fragments into the polymer. Significant off-time polymerisation is shown to occur for up to 1000 μs in the off-time after which time the polymer growth rate is reduced.

The results of these preliminary studies have shown how pulsed plasmas can be exploited to retain the monomer structure in the surfaces generated by plasma polymerisation. High selectivity to free-radical reactions of the substituent vinyl groups in the off-time of a pulsed plasma results in the production of colourless coatings consisting of siloxane rings in an organic matrix. Further work is necessary to obtain more information regarding the structure of these surfaces and their properties in relation to their application as transparent permselective membranes or barrier coatings.

5.6 REFERENCES

(1) Biswas, M.; Mukherjee, A. *Advances In Polymer Science* **1994**, *115*, 89.

(2) Allcock, H.R.; Lampe, F.W. *Contemporary Polymer Chemistry,* 2nd Ed., Academic Press, San Diego, CA, 1990, Ch. 9.

(3) Mark, J.E.; Allcock, H.R.; West, R. *Inorganic Polymers*, Prentice Hall: Englewood Cliffs, NJ, 1992.

(4) Allcock, H.R. *Adv. Mater.* **1994**, *6(2)*, 106.

(5) Ref # 3, Ch. 4.

(6) Taylor, C.E.; Boerio, F.J.; Zeik, D.B.; Conners, K.D.; Clarson, S.J. *Abs. Paps. Am. Chem. Soc.* **1993**, *206*, 177.

(7) Wrobel, A.M.; Klemberg, J.E., Wertheimer, M.R.; Schreiber, H.P. *J. Macromol. Sci. Chem.* ***1981***, A15, *197.*

(8) Shreiber, H.P.; Wertheimer, M.R.; Wrobel, A.M. *Thin Solid Films* **1980**, *72*, 487.

(9) Sadhir, R.K.; James,W.J.; Yasuda, H.K.; Sharma, A.K.; Nichols, M.F.; Hahn, A.W. *Biomaterials* **1981**, *2*, 239.

(10) Sharma, A.K.; Yasuda, H. *Thin Solid Films* **1983**, *110(2)*, 171.

(11) Wertheimer, M.R.; Schreiber, H.P. *J. Appl. Polym. Sci.* **1981**, *26*, 2087

(12) Klemberg-Sapieha, J.E.; Sapeiha, S.; Wertheimer, M.R.; Yelon, A. *Appl. Phys. Lett.* **1980**, *37*, 104.

(13) Charlson, E.J.; Charlson, E.M.; Sharma, A.K.; Yasuda, H.K. *J. Appl. Polym. Sci. Appl. Polym. Symp.* **1984**, *38*, 137.

(14) Sandved, J.S.; Kristiansen, K. *Vacuum* **1977**, *27*, 235.

(15) Radeva, E. *Vacuum* **1997**, *48(1)*, 41

(16) Tien, P.K.; Smolinsky, G.; Martin, R.J. *Appl. Opt.* **1972**, *11*, 637.

(17) Poll, H.U.; Meichsner, J.; Arzt, M.; Freidrich,M.; Rochotzki, R.; Kreyssig, E. *Surface & Coatings Tech.* **1993**, *59(1-3),* 365.

(18) Rochotzki, R.; Arzt, M.; Blaschta, F.; Kreyssig, E.; Poll, H.U. *Thin Solid Films* **1993**, *234,* 463.

(19) Thompson, L.F.; Smolinsky, G. *J. Appl. Polym. Sci.* **1972**, *16*, 1179.

(20) Theirlich, D.; Ningel, K.P.; Engemann, J. *Surface & Coatings Tech.* **1996**, *86-87,* 628.

(21) Chen, K.S.; Inagaki, N.; Katsuura, K. *Kobunshi Ronbunshu* **1981**, *38(10)*, 673.

(22) Morra, M.; Occhiello, E.; Garbassi, F. *J. Appl. Polym. Sci.* **1993**, *48*, 1331.

(23) Wertheimer, M.R.; Klemberg-Sapieha, J.E.; Schreiber, H.P. *Thin Solid Films* **1984**, *115*, 109.

(24) Sacher, E.; Klemberg-Sapieha, J.E., Schreiber, H.P.; Wertheimer, M.R. *J. Appl. Polym. Sci. Appl. Polym. Symp.* **1984**, *38*, 163.

(25) Sacher, E.; Schreiber, H.P.; Wertheimer, M.R. **1985**, U.S. Patent 4,557,946.

(26) Benz, G. *Bosch Techn. Ber.* **1987**, *8*, 219.

(27) Klemberg-Sapieha, J.E.; Martinu, L.; Kuttel, O.M. *Proc. Ann. Tech. Conf.-Soc. Vacuum Coaters* **1993**, P. 445.

(28) Gombotz, W.R.; Hoffman, A.S. In *Critical Reviews In Biocompatibility* Williams, D. Ed.; CRC Press, Boca Raton, 1987.

(29) Lin, J.C.; Cooper, S.L. *J. Appl. Polym. Sci. Appl. Polym. Symp.* **1994**, *54*, 157.

(30) Hasirci, N. *J. Appl. Polym. Sci.* **1987**, *34*, 1135.

(31) Hasirci, N. *J. Appl. Polym. Sci.* **1987**, *34*, 2457.

(32) Vargo, T.G; Gardella, J.A. *Polym. Prep.* **1988**, *2*, 303.

(33) Ishikawa, Y.; Sasakawa, S.; Takase, M.; Iriyama, Y.; Osada, Y. *Makromol. Chem. Rapid. Commun.* **1985**, *6*, 495.

(34) Ref. 57, p 163

(35) Chan,C.-M.; Ko, T.-M.; Hiraoka, H. *Surface Science Reports* **1996**, *24*, 1.

(36) Chawla, A.S. *Biomaterials* **1981**, *2*, 83.

(37) Chawla, A.S. *Artificial Organs* **1979**, *3*, 92.

(38) Nehlsen, S.; Hunte, T.; Muller, J. *J. Membrane Sci.* **1995**, *106(1-2),* 1.

(39) Matsuyama, H.; Shiraishi, T.; Teramoto, M. *J. Appl. Polym. Sci.* **1994**, *51*, 1665.

(40) Sakata, J.; Yamamoto, M.; Hirai, M. *J. Appl. Polym. Sci.* **1986**, *31*, 1999.

(41) Nomura, H.; Kramer, P.W.; Yasuda, H. *Thin Solid Films* **1984**, *118*, 187.

(42) Sakata, J.; Yamamoto, M.; *J. Appl. Polym. Sci. Appl. Polym. Symp.* **1988**, *42*, 339.

(43) Osada, Y.; Takase, M. *J. Polym. Chem. Polym. Chem. Ed.* **1985**, *23*, 2425.

(44) Matsuyama, H.; Kariya, A.; Teramoto, M. *J. Appl. Polym. Sci.* **1994**, *51*, 689.

(45) Janca, J.; Sodomka, L. *Thin Solid Films* **1992**, *216(2)*, 235.

(46) Nagaoka, K.; Naruse, H.; Shinohara, I. *J. Polym. Sci. Polym. Lett Ed.* **1984**, *22*, 659.

(47) Ogomi, Z.; Uchimoto, Y.; Takehara, Z. *J. Electrochem. Soc.* **1989**, 136(3), 625.

(48) Urban, M.W.; Stewart, M.T. *J. Appl. Polym. Sci.* **1990**, *39*, 265.

(49) Smith, A.L.; *Spectrochemica Acta* **1960**, *16*, 87

(50) Lord, R.C.; Robinson, D.W.; Schub, W.C. *J. Am. Chem. Soc.* **1956**, *78*, 1327.

(51) Bellamy, L.J., *Infrared Spectra of Complex Molecules, Vol. 1*, Chapman & Hall: New York, 1975.

(52) Wright, N.; Hunter, M.J. *J. Am. Chem. Soc.* **1947**, *69*, 603.

(53) Briggs, D.; Seah, M. P.; *Practical Surface Analysis* 2nd ed; Wiley & Sons: Chichester, 1990.

(54) Wells, R.K.; Ryan, M.E.; Badyal, J.P.S. *J. Phys. Chem.* **1993,** *97*, 12879.

(55) M^c^Taggart, F.K. *Plasma Chemistry in Electrical Discharges*; Elsevier Publishing Company: London, 1967.

(56) Yasuda, H. *Plasma Polymerization*; Academic Press: Orlando, 1985.

(57) Wrobel, A.M.; Wertheimer, M.R. In *Plasma Deposition, Treatment and Etching of Polymers*; d'Agostino, R. Ed.; Academic Press: London, 1990; p.178.

CHAPTER SIX

PULSED PLASMA POLYMERISATION OF STYRENE OXIDE

CHAPTER SIX

PULSED PLASMA POLYMERISATION OF STYRENE OXIDE.

6.1 INTRODUCTION

Pulsed plasma polymerisation has been shown to be effective in retaining the functional groups of precursors in the final plasma polymers, c.f. chapters three to five. The basic principle lies in exploiting a functional group in the precursor which reacts preferentially to other portions of the molecule. This is achieved via a combination of a reduction in the overall energy within the plasma, both in the gas phase and at the surface of the substrate and through controlled conventional polymerisation reactions in the off-phase of the duty cycle. The presence of unsaturation in the starting material assists in retention of the precursor structure by providing preferential sites for free-radical reactions in the off-time.

In this chapter pulsed plasmas will be used to control the stoichiometry of surfaces generated by the plasma polymerisation of styrene oxide **(1)**. Styrene oxide consists of a monosubstituted benzene ring with an epoxy group as a substituent, Fig. 6-1. The epoxide ring is the sacrificial functional group in this case, taking the place of the vinyl groups reported in previous chapters. It is likely to be far more susceptible to reaction both in the on and off-stages than the aromatic benzene ring. The use of pulsed plasmas should allow maximum retention of the benzene ring in the final plasma polymer. Styrene oxide also has the advantage of being inexpensive and volatile at room temperature. The plasma polymerisation of styrene has been extensively studied[1-7,30-33,39,40,35,53,54] and some work has also been carried out on the plasma polymers of oxiranes,[8,9] principally ethylene oxide or propylene oxide, however this is the first reported study of the plasma polymerisation of styrene oxide. Whilst plasma polymers

of styrene have been used as hydrophobic layers, those of ethylene oxide have hydrophilic surfaces.

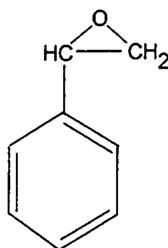

(1)

Fig. 6-1: Structure of styrene oxide

6.1.1 Applications of plasma polymers from aromatic precursors

The polyaromatics are an important group of industrial polymers due to their physical and chemical properties such as thermal stability and irradiation resistance.[10] This interest in polyaromatics has been transferred to the area of plasma chemistry. Aromatic compounds have been widely studied as precursors for plasma polymerisation.[11-35] The resultant plasma polymers have been used in a variety of applications ranging from electronic components such as thin film capacitors[21,22] and dielectric layers,[23] to their use as impermeable protective coatings.[24-27] Plasma polymers from aromatic precursors have also been used as reverse osmosis[28] and permselective membranes.[29]

Plasma polymers and copolymers of styrene have been studied for use as resist layers in lithographic applications.[30-33] Low atomic weight elements have low X-ray absorption coefficients so heavy metals need to be incorporated into the resist. An Au-C film was deposited for use as a mask layer in x-ray lithography by simultaneous evaporation of gold and plasma polymerisation of styrene.[34]

Plasma polymerised coatings have also been investigated for use in gas sensor devices.[6,7,35] A plasma polymer of styrene has been shown to adsorb moisture

depending on the circumstantial humidity and this property has been exploited in its use as a moisture sensor.[35]

The unique electronic structure of aromatic plasma polymers has led to their use as semiconductive[20,36,37] and electroluminescent thin films[38]. Plasma polymers of quinoline have been studied[37] with a view towards their use as conducting thin films and the results compared to the plasma polymers of benzene and pyridine. Retention of the aromatic nature of the precursor in the final plasma polymer is essential in order to yield a film composed of a highly conjugated π-electron system, the conductivity of which could be increased by doping with iodine. Styrene and other aromatic plasma polymers have also been used as switching elements in microelectronic components.[39-42]

6.2 EXPERIMENTAL

The experimental set-up for both continuous wave and pulsed plasma polymerisation experiments was as described as in chapter three, sec. 3.2. Styrene oxide liquid was purchased from Aldrich, b.p. 194°C and transferred to a pyrex monomer tube. Five freeze thaw cycles were used to further purify the liquid. The reactor was pumped to a base pressure $<4 \times 10^{-3}$ torr and then the monomer vapour allowed to flow through the reactor at a flow rate of $\sim 5.9 \times 10^{-8}$ kg s^{-1}. These conditions ensured a pressure of 0.2 torr with the monomer accounting for >99% of the contents of the reactor.

After two minutes purging the reactor with styrene oxide vapour the r.f was turned on and the plasma sustained for ten minutes. Continuous wave powers between 1.5 and 8 Watts were used with pulsing on and off-times in the range 10 - 6000 μs. The plasma polymers were deposited onto potassium bromide disks and glass slides for infrared and XPS analysis respectively. Following plasma polymerisation the r.f. was turned off and the reactor purged for a further 10 minutes with styrene oxide vapour. The reactor was then pumped to base pressure and underwent two nitrogen pump/purge cycles before the samples were removed and immediately characterised.

A BP300 XPS spectrometer was used to acquire high resolution XPS spectra from the C(1s), O(1s) and Si(2p) regions for each plasma polymer. Spectra were acquired at a 30 ° take-off angle from the substrate normal. Instrumentally determined sensitivity factors for unit stoichiometry were taken as C(1s) : O(1s) : Si(2p) equal to 1:00 : 0.62 : 1.08. The absence of a Si(2p) peak was indicative of complete coverage of the glass substrate.

Transmission infrared spectra were acquired on a Mattson Polaris spectrometer. The monomer spectrum was acquired as a thin film between two potassium bromide disks whilst the plasma polymers were deposited on the surface of a single disk. Typically 100 scans at a resolution of 4 cm^{-1} were collected.

6.3 RESULTS

6.3.1 Infrared Spectroscopy

The infrared spectrum of the starting material is shown in Fig. 6-2. The low frequency region of the spectrum is enlarged for clarity. As seen the spectrum is relatively complex with a large number of absorption bands below 2000 cm^{-1}. The complexity of the spectrum arises from the combination of the absorption bands associated with the substituted phenyl group and the cyclic ether or epoxide group.[43,44] Both of these functional groups have group stretching modes associated with ring stretching modes of vibration.[43] The presence of dipole-inducing oxygen in the molecule means the epoxide ring generates a complex series of strong absorptions even when unsubstituted e.g. ethylene oxide. Whilst no attempt will be made to assign vibrational modes to all peaks in the spectrum, the more characteristic absorptions are discussed below.

6.3.1.1 Infrared Absorption Bands of Styrene Oxide

6.3.1.1.1 Absorptions associated with phenyl stretching modes.

The strong absorption peaks in the region 3050-3100 cm^{-1} are due to aromatic C-H stretching vibrations.[43,44] The three weak bands in the region 1800-2000 cm^{-1} are known as summation bands and have been assigned to binary combinations and overtones of aryl C-H wag modes with fundamentals in the region 800-964 cm^{-1}.[45] The pattern of these bands is characteristic for a particular substitution. For a mono-substituted phenyl ring the pattern consists of 5 weak bands and one very weak band. In the case of styrene oxide only the first three members of the series are visible. The absorptions at 1607 cm^{-1}, 1497 cm^{-1} and 1452 cm^{-1} are due to 'ring breathing' vibrations involving skeletal stretching modes of the semi-unsaturated C-C bonds of the benzene ring. When combined with the presence of the C-H stretching bands above 3000 cm^{-1} the presence of these bands is usually sufficient for the positive identification

of the presence of a substituted benzene group.[44] The medium intensity bands at 1072 cm^{-1} and 1026 cm^{-1} are characteristic of mono-substituted benzenes, while the strong bands at 758 cm^{-1} and 698 cm^{-1} are due to out-of-plane C-H and out-of-plane ring deformation vibrations respectively. Their presence and position also indicate mono-substitution of the benzene ring.

6.3.1.1.2 Absorptions associated with the epoxy group.

The aliphatic C-H stretching vibrations of aliphatic groups generally result in absorptions in the region 2800-2950 cm^{-1}. In the case of epoxy CH_2 groups however the characteristic frequency is raised to closer to 3000 cm^{-1}.[43,46] This is the case for styrene oxide and it results in the overlap of the aliphatic and aromatic C-H stretching bands. The strong peak at 1476 cm^{-1} (between the pair of aryl deformation peaks) is due to O-CH_2 deformation. Skeletal ring breathing vibrations causes a strong absorption peak at 1254 cm^{-1} due to change in the C-O bond length. The strong absorption band at 876 cm^{-1} can be assigned to symmetric C-O-C stretching. Other peaks in the region 1400-900 cm^{-1} are due to ring-breathing deformation modes of the epoxide group.

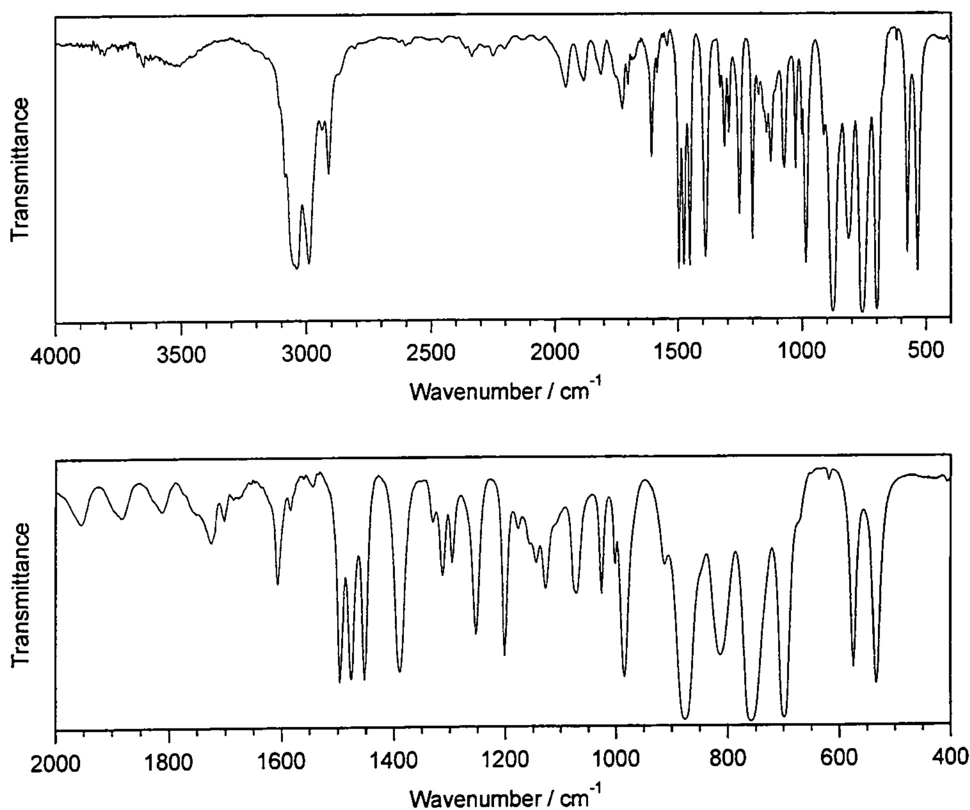

Fig. 6-2: Transmission infrared spectrum of styrene oxide liquid and an expanded view of the low frequency end of the spectrum.

6.3.1.2 Infrared spectra of plasma polymers of styrene oxide

The transmission infrared spectra of the polymers deposited from continuous wave and pulsed plasmas of styrene oxide are shown in Fig. 6-1, Fig. 6-4 and Fig. 6-5. The spectra of all plasma polymers are significantly different from that of the starting material. The absorption bands at approximately 3000 cm^{-1} have separated into two separate groups, one in the range 3000-3100 cm^{-1}, the other from 2800-2950 cm^{-1}.

All the plasma polymers have strong absorptions at ~700 cm^{-1} and a doublet of medium strength absorptions at 1497 cm^{-1} and 1452 cm^{-1}. There is also a medium intensity peak at ~760 cm^{-1}. The summation bands evident in the styrene oxide spectrum around 2000 cm^{-1} are still discernible in the spectra of the plasma polymers. The presence of these peaks in association with the C-H stretching bands above 3000 cm^{-1} confirm the retention of phenyl rings in the plasma polymers.

The peaks associated with C-O stretching at 1476 cm^{-1} and 876 cm^{-1} in the monomer are absent from the spectra of the plasma polymers. Similarly other strong absorption peaks in the 1400-900 cm^{-1} range of the spectrum of styrene oxide are missing from the infrared spectra of the plasma polymers regardless of discharge power or pulsing conditions employed. However all plasma polymers show absorptions of varying intensity in the region 1700-1800 cm^{-1} and 1000-1200 cm^{-1}.

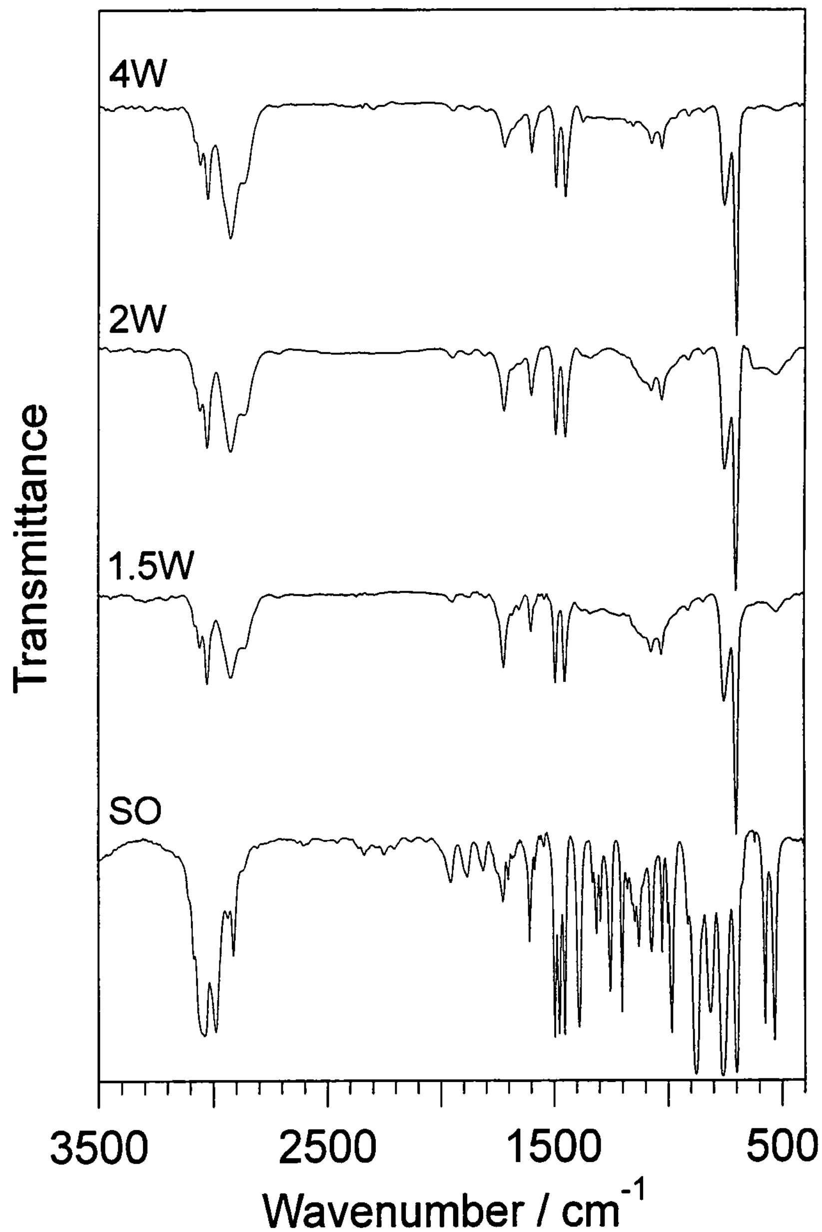

Fig. 6-3: Transmission FT-IR spectra of plasma polymers deposited from continuous wave styrene oxide plasmas as a function of discharge power.

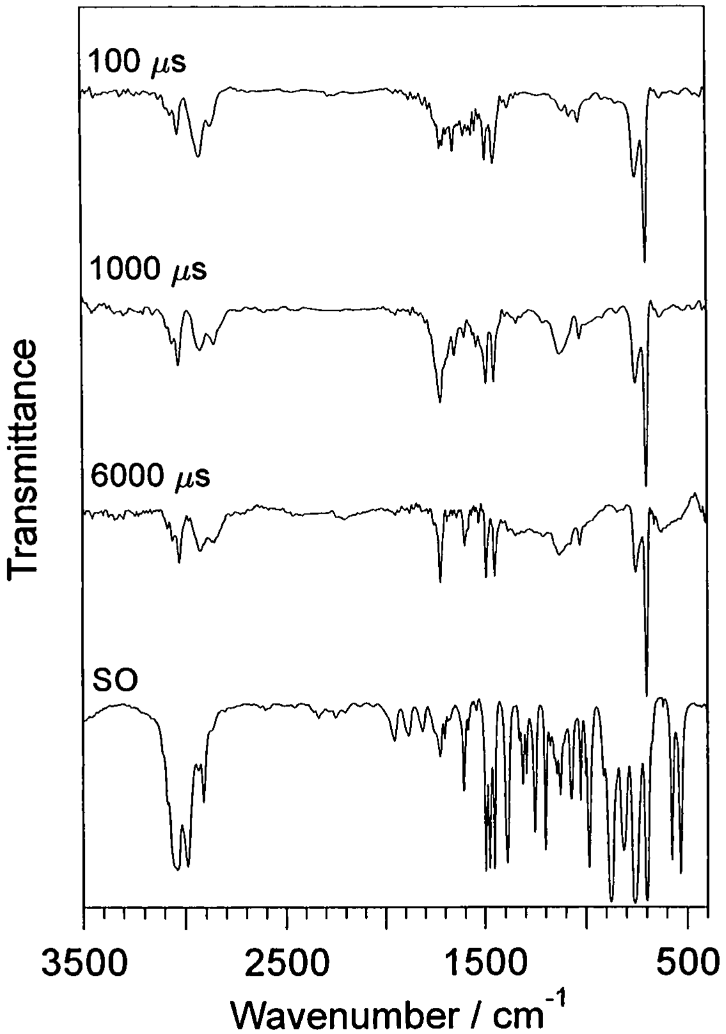

Fig. 6-4: Transmission FT-IR spectra of plasma polymers deposited from pulsed styrene oxide discharges as a function of off-time; on-time = 10 μs, peak power = 70 W.

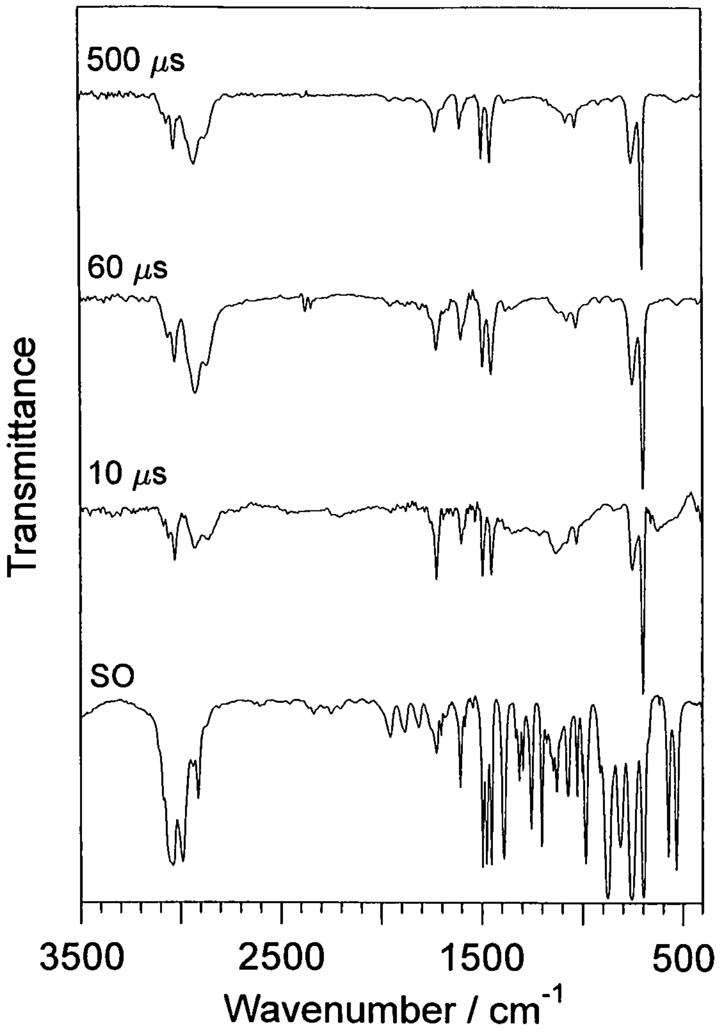

Fig. 6-5: Transmission FT-IR spectra of plasma polymers deposited from pulsed styrene oxide discharges as a function of on-time; off-time = 6 ms, peak power = 70 W.

6.3.2 X-ray photoelectron spectroscopy

C(1s) XPS spectra of styrene oxide continuous wave plasma polymers are shown in Fig. 6-7. XPS spectra of pulsed plasma polymers are shown in Fig. 6-8 and Fig. 6-9. The spectra consist of a major component centred at 285.0 eV which corresponds to carbon atoms in a crosslinked/hydrocarbon environment.[47] On the higher binding energy side of this peak a weak shoulder is discernible indicating the presence of electronegative oxygen atoms in the plasma polymer. The relative intensity of this shoulder varies with discharge power and duty cycle in the case of continuous wave plasmas and pulsed plasmas respectively. Also apparent in the C(1s) spectra is a small peak situated approximately 7 eV above the main $\underline{C}$-H peak. This peak is a result of low energy π–π^* shake-up transitions accompanying the core level ionisation of the hydrocarbon carbon atoms.[48,49] The presence of this peak confirms the aromatic nature of the carbon atoms associated with the main peak.[49,50] The C(1s) profile of the plasma polymer deposited from the lowest duty cycle pulsed plasma used in this study is shown in Fig. 6-6. Three Mg $K\alpha_{1,2}$ components of equal FWHM corresponding to $\underline{C}$-H (285.0 eV), $\underline{C}$-O (286.6 eV) and C=O (287.9 eV) were used to fit the main portion of the spectrum.[51,52] The π–π^* shake-up peak had a different FWHM to the other components.

The relative contributions of each type of carbon environment to the overall profile is calculated by dividing the component peak area by the total C(1s) area. The XPS spectrum shown in Fig. 6-6 shows the polymer to consist of 84 ± 1% $\underline{C}$-H, 10 ± 1% $\underline{C}$-O and 1 ± 0.5% $\underline{C}$=O with the π–π^* peak accounting for 5% of the total C(1s) area. This polymer had the highest percentage of oxygen of all samples analysed. Upon increasing duty cycle the amount of oxygen dropped to approximately 4% in the case of the highest duty cycles used. The loss was principally from the C-O peak with negligible variation in the C=O peak. The percentage oxygen was greater in low duty cycle pulsed plasmas than in low power continuous wave plasmas. The intensity of the π–π^* peak

showed no significant variation as it remained between 4 and 5% regardless of plasma parameters.

6.3.3 Physical properties of the plasma polymers

Apart from the chemical differences between plasma polymers deposited using varying plasma conditions there were also noticeable differences in some of the physical properties of the plasma polymers. Low duty cycle pulsed plasma polymers resulted in relatively high energy surfaces. The plasma polymers were colourless but had adhesive properties and were wettable, giving contact angles similar to those observed with water on untreated glass. In contrast the high power continuous wave polymers and high duty cycle pulsed plasma polymers yielded relatively low energy surfaces which were non-adhesive and hydrophobic.

In addition to the plasma polymers deposited as films on the reactor walls and substrate it was also noted that downstream from the plasma zone a fine white powder was deposited during the plasma polymerisation runs. The majority of the powder accumulated at the first obstruction to gas flow in the reactor i.e. a right-angle bend in the outlet pipe, approximately 40 cm from the centre of the coils. This dust was deposited to varying degrees in all experiments except under high power continuous wave conditions. The powder was white in colour and was apparently insoluble in water, isopropyl alcohol, acetonitrile, and acetone, although slight solubility was observed following 6 hours toluene reflux. Similar powder formation has previously been reported in studies of the plasma polymerisation of styrene.[53,54] and benzene.[55] Its formation has been attributed to oligomerisation/agglomeration reactions in the gas phase and in the case of plasma polymerisation of benzene electron microscopy studies showed it to consist of 0.12 μm diameter spheres agglomerated into chains or clumps.[55]

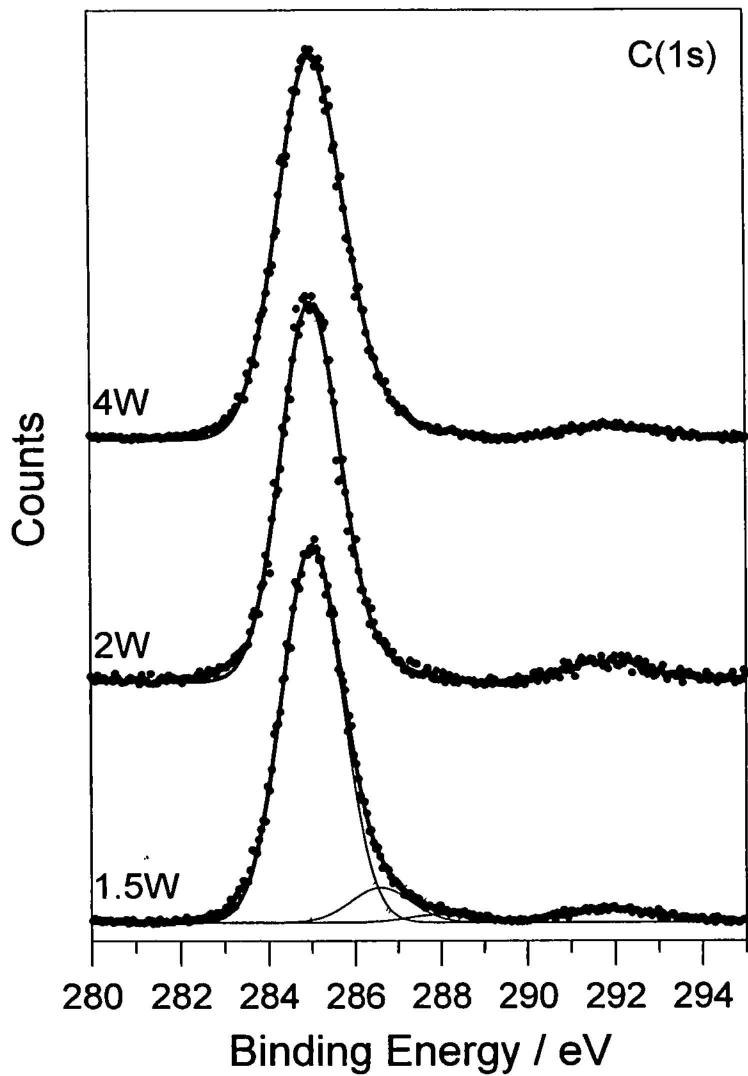

Fig. 6-6: C(1s) XPS spectrum of styrene oxide plasma polymer.2

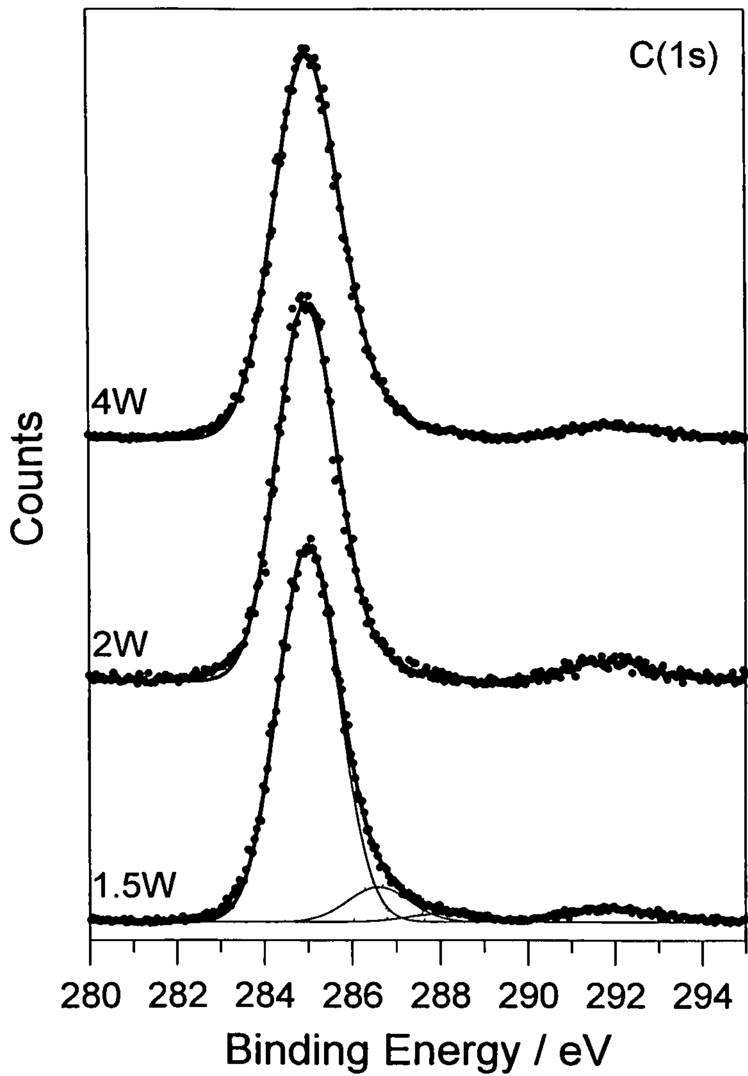

Fig. 6-7: C(1s) XPS spectra of plasma polymers deposited from continuous wave styrene oxide discharges as a function of discharge power.

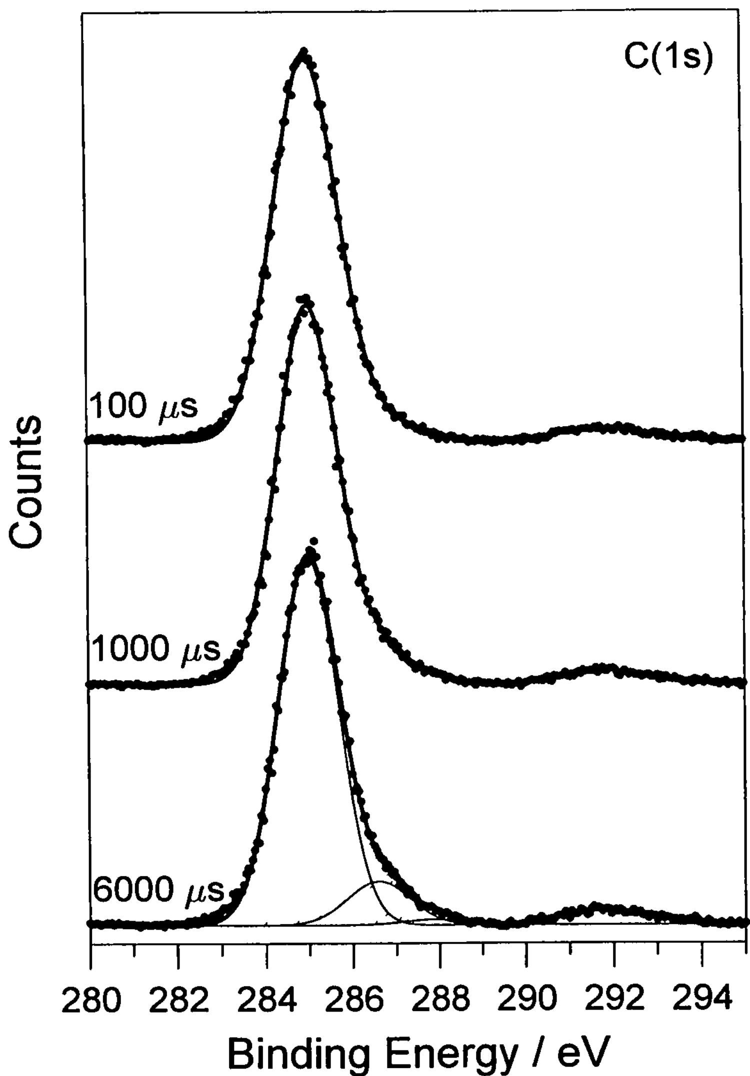

Fig. 6-8: C(1s) XPS spectra of plasma polymers deposited from pulsed styrene oxide discharges as a function of off-time; on-time = 10 μs, peak power = 70 W.

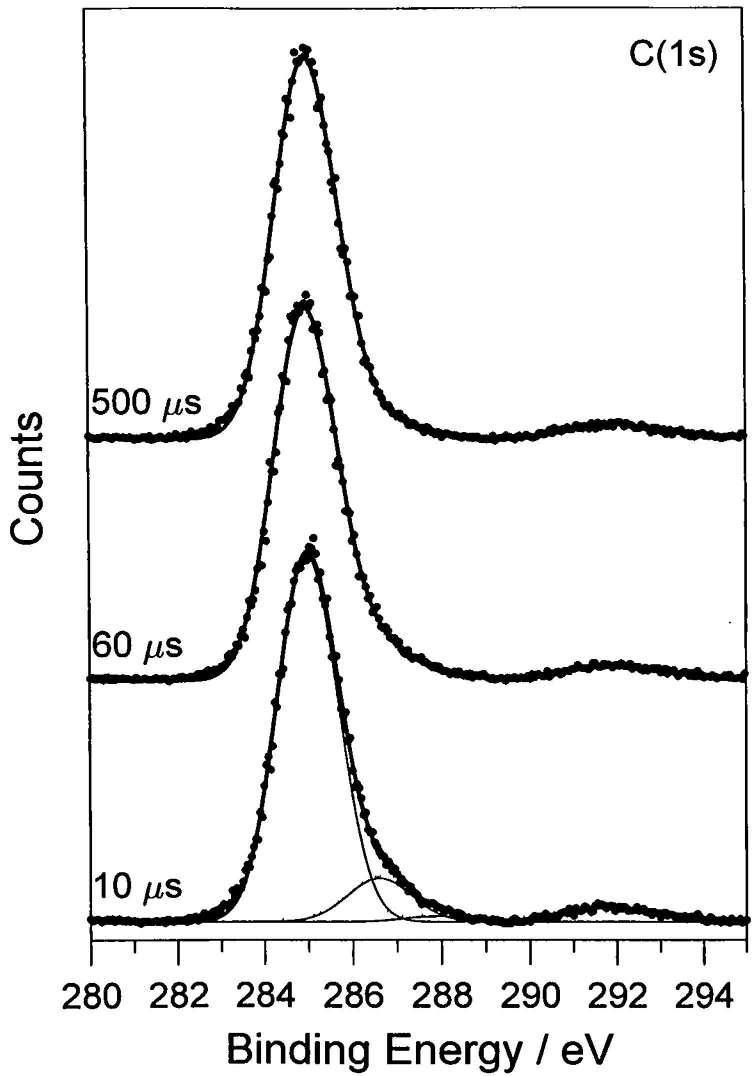

Fig. 6-9: C(1s) XPS spectra of plasma polymers deposited from pulsed styrene oxide discharges as a function of on-time; off-time = 6 ms, peak power = 70 W.

6.3.4 Deposition Rate Studies

Deposition rate studies were carried out to examine the effect of various pulsing regimes on the deposition rate of plasma polymers from styrene oxide plasmas. The deposition rate of plasma polymers from pulsed styrene oxide plasmas decreases with increasing off-time regardless of on-time, Fig. 6-10. Plasmas with longer on-times give greater deposition for a given off-time, however for an particular off-time plasmas with shorter on-times are slightly more efficient in terms of deposition rate per Joule, Fig. 6-11. The differences between different on-times are not very large compared to those seen in the case of TVS in chapter five for example. In fact when the results are analysed as a function of average power the three on-times yield practically the same deposition rate and efficiency, Fig. 6-12.

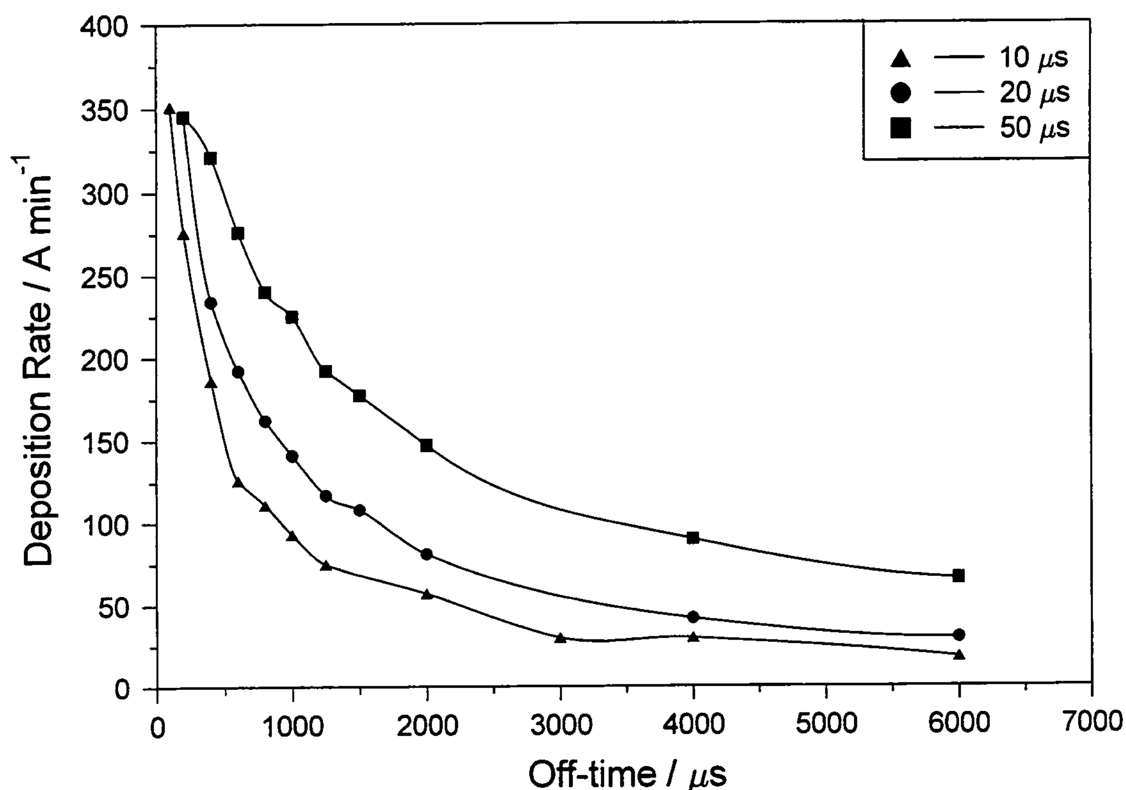

Fig. 6-10: Plot of deposition rate versus off-time for pulsed plasmas of styrene oxide with various on-times.

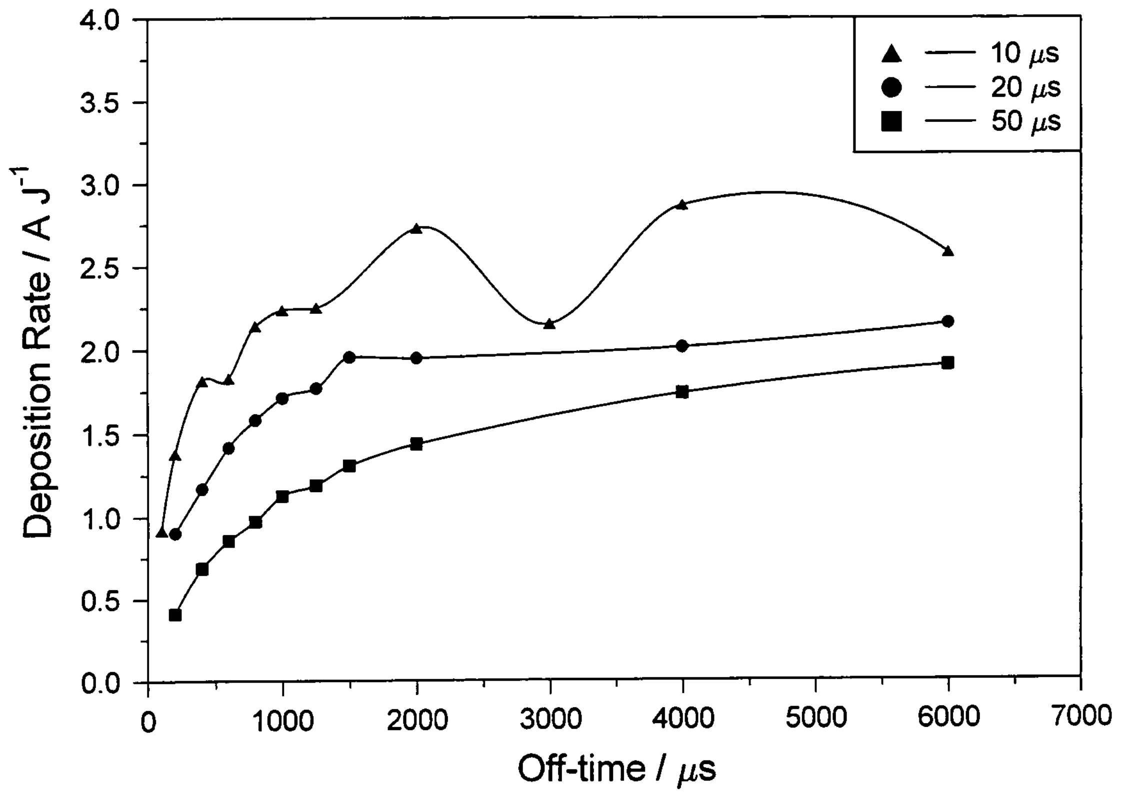

Fig. 6-11: Plot of deposition efficiency versus off-time for pulsed plasmas of styrene oxide with various on-times.

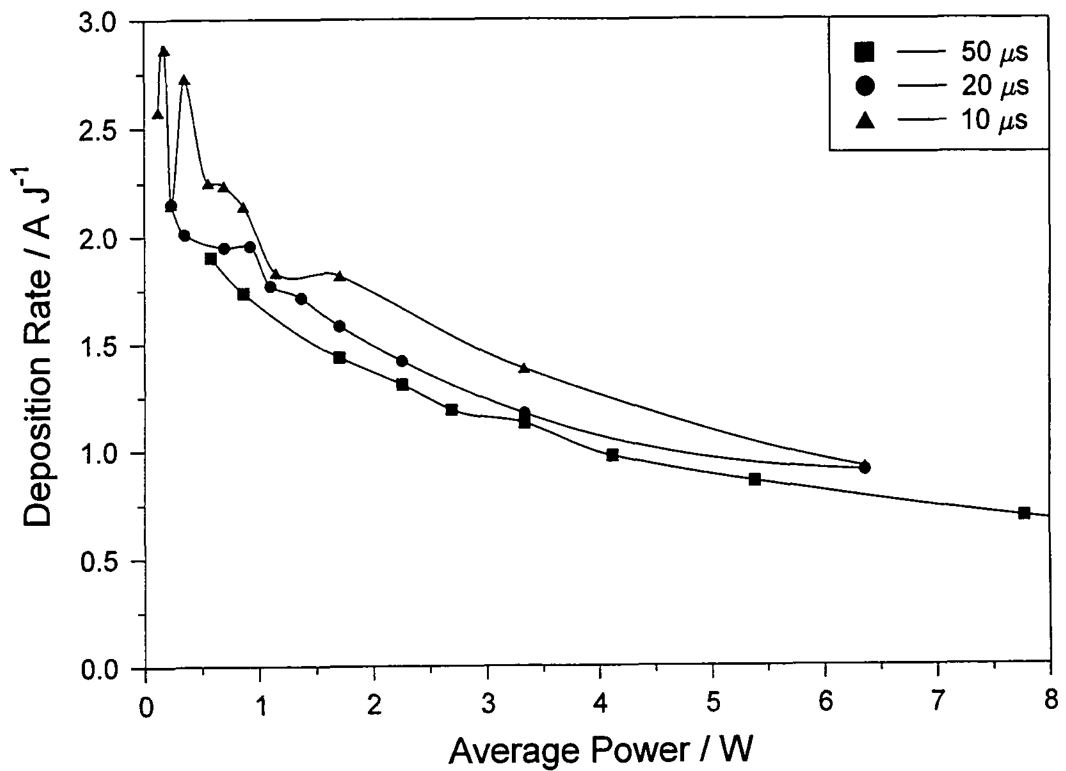

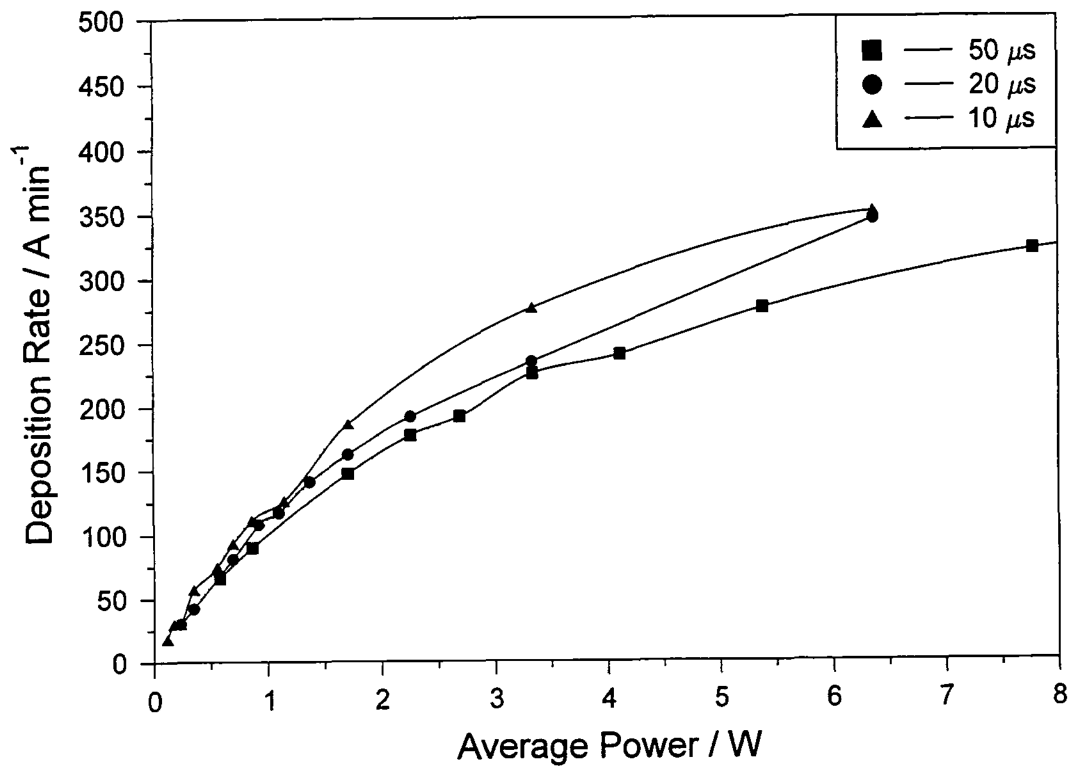

Fig. 6-12: Deposition rate plots from pulsed plasma polymerisation of styrene oxide showing variation in deposition rate and efficiency as a function of average power for various on-times.

6.4 DISCUSSION

Fig. 6-3 to Fig. 6-5 show the infrared transmission spectra of plasma polymers deposited from pulsed and continuous wave discharges differ significantly from the spectrum of the monomer. In the spectrum of the monomer the aryl and epoxy C-H stretching vibrations overlap as a result of the unusually high frequency for vibrations involving CH_x groups in an epoxy ring.[43,46] In the plasma polymers the aliphatic C-H stretch vibrations have moved to lower wavenumber indicating a change in the environment of the CH groups i.e. loss of the epoxy ring. This assertion is further supported by the loss of the strong absorptions at 1476 cm^{-1}, 1254 cm^{-1} and 876cm^{-1} all of which were assigned to the epoxy group in the parent compound. These differences indicate loss of the epoxy group readily occurs regardless of the pulsing conditions or the discharge power.

The infrared spectra also indicate that whilst loss of the epoxy group is universal, the plasma polymerisation process does not result in loss of the benzene ring from the plasma polymers. All plasma polymers show strong evidence of the presence of substituted phenyl groups in their infrared spectra. In fact the spectra of the plasma polymers show remarkable similarity to the infrared spectrum of polystyrene, Fig. 6-13. The peaks associated with a substituted benzene ring, in particular those at 3040 cm^{-1}, 1607 cm^{-1}, 1497 cm^{-1}, 1452 cm^{-1}, 758 cm^{-1} and 698 cm^{-1}, are all evident in the spectra of the plasma polymers. In addition the retention of aromaticity is better in the case of low duty cycle pulsed plasmas than for continuous wave plasmas. This is indicated by the relative intensities of the aromatic and aliphatic C-H stretch vibrations around 3000 cm^{-1}. Increasing the discharge power or duty cycle results in increased loss of aromaticity in the plasma polymers.

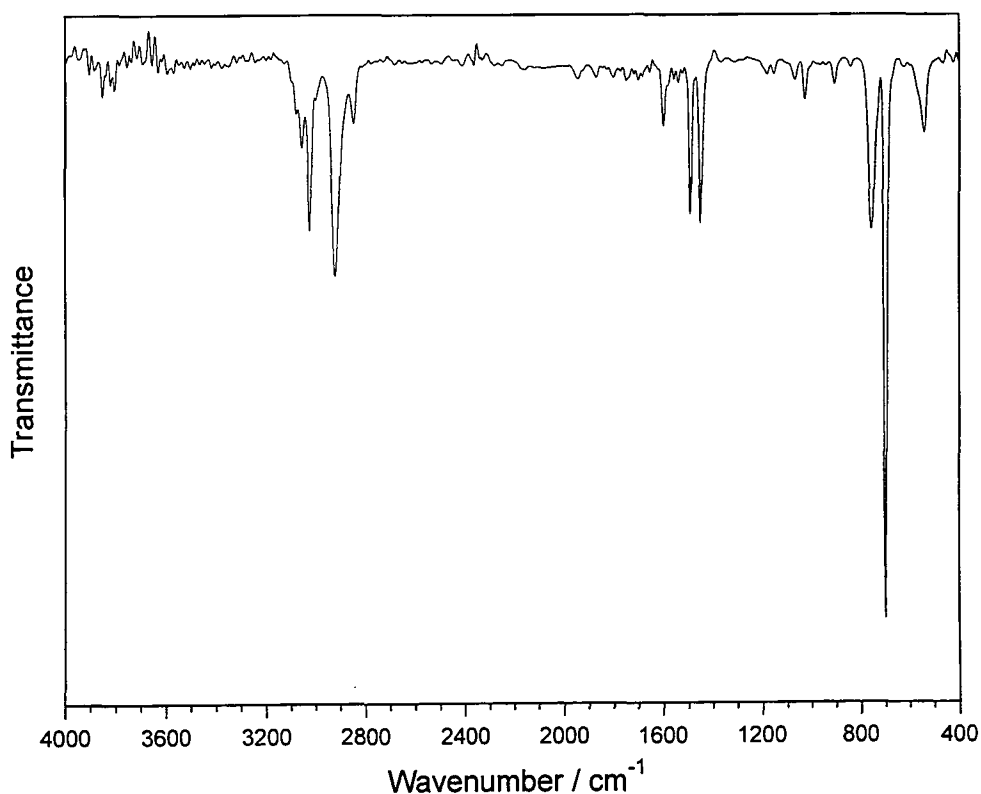

Fig. 6-13: Transmission infrared spectrum of polystyrene thin film spin-coated onto potassium bromide disk from 2% w/v toluene solution.

However there does exist some significant differences between the spectra of the plasma polymers and polystyrene, namely;

(i) The aliphatic C-H stretching band in the plasma polymer is broader and less resolved than in polystyrene and

(ii) The plasma polymers have vibrational modes resulting in peaks at 1700 cm-1 and a broad peak in the 1200-1000 cm-1 region, neither of which are present in polystyrene.

The difference in the C-H band is most likely due to the plasma polymers consisting of a greater variety of bond lengths and environments due to the inherently complex nature of the plasma polymerisation process.[56]

The peak at approximately 1700 cm^{-1} may be due to C-O stretching vibrations. These vibrations generate intense absorptions which will be obvious in the infrared spectra even if only a low percentage of oxygen is present in the sample. It is of interest to note

that the intensity of this band at 1700 cm^{-1} varies depending on the plasma parameters. The intensity of the broad band at 1200-1000 cm^{-1} mirrors the intensity of the peak at 1700 cm^{-1} so it reasonable to assume that this is due to the same oxygenated species. These bands are more intense at lower discharge powers in the continuous wave samples and at lower duty cycles in the pulsed plasma polymers. This peak may result from either retention or re-incorporation of the oxygen from the epoxide ring of the styrene oxide in the plasma polymers. This being the case it indicates that lower powers and reduction of duty cycle improves retention of the oxygen in the final plasma polymer and that pulsing the r.f power significantly improves retention of the oxygen over continuous wave plasma polymerisation. This is supported by the XPS results, sec. 6.3.2, which show plasma polymers from pulsed discharges have a greater oxygen content than continuous wave plasma polymers. Deposition rate measurements suggest that polymerisation in the off-stage, most likely at the reactive epoxy-ring, aids in the retention of oxygen in the plasma polymers. The higher oxygen content results in a surface which has adhesive properties and is hydrophilic.

An alternative origin for the oxygen-containing groups is reaction of residual radicals in the plasma polymer with oxygen in the atmosphere prior to analysis.[56,57] The variation in relative intensity of the peak would then be a result of the relative proportion of oxidised/unreacted plasma polymer. Since all experiments were carried out for the same length of time higher discharge powers and duty cycles result in thicker samples, sec. 6.3.4, hence if oxidation is occurring at or near the surface of the film then it will be proportionately smaller for these samples. However higher discharge powers/duty cycles would also produce a more energetic plasma environment resulting in a polymer with a greater number of residual radicals[56-58] which would be expected to result in greater oxidation, contrary to what is observed.

In order to clarify the origin of the oxygen in the plasma polymers an angle-resolved depth profile study was carried out in the XPS spectrometer. As explained in chapter one the angle between the electron energy analyser to the surface of the sample is

critical in determining the sampling depth in XPS analysis.[47] The results in Fig. 6-14 indicate that the percentage oxygen is lowest at the surface of the plasma polymer. Hence it would appear that the origin of the oxygen peaks in the infra-red spectra of the samples does not come from post-deposition contamination/reaction but is primarily due to retention/re-incorporation of oxygen from the precursor.

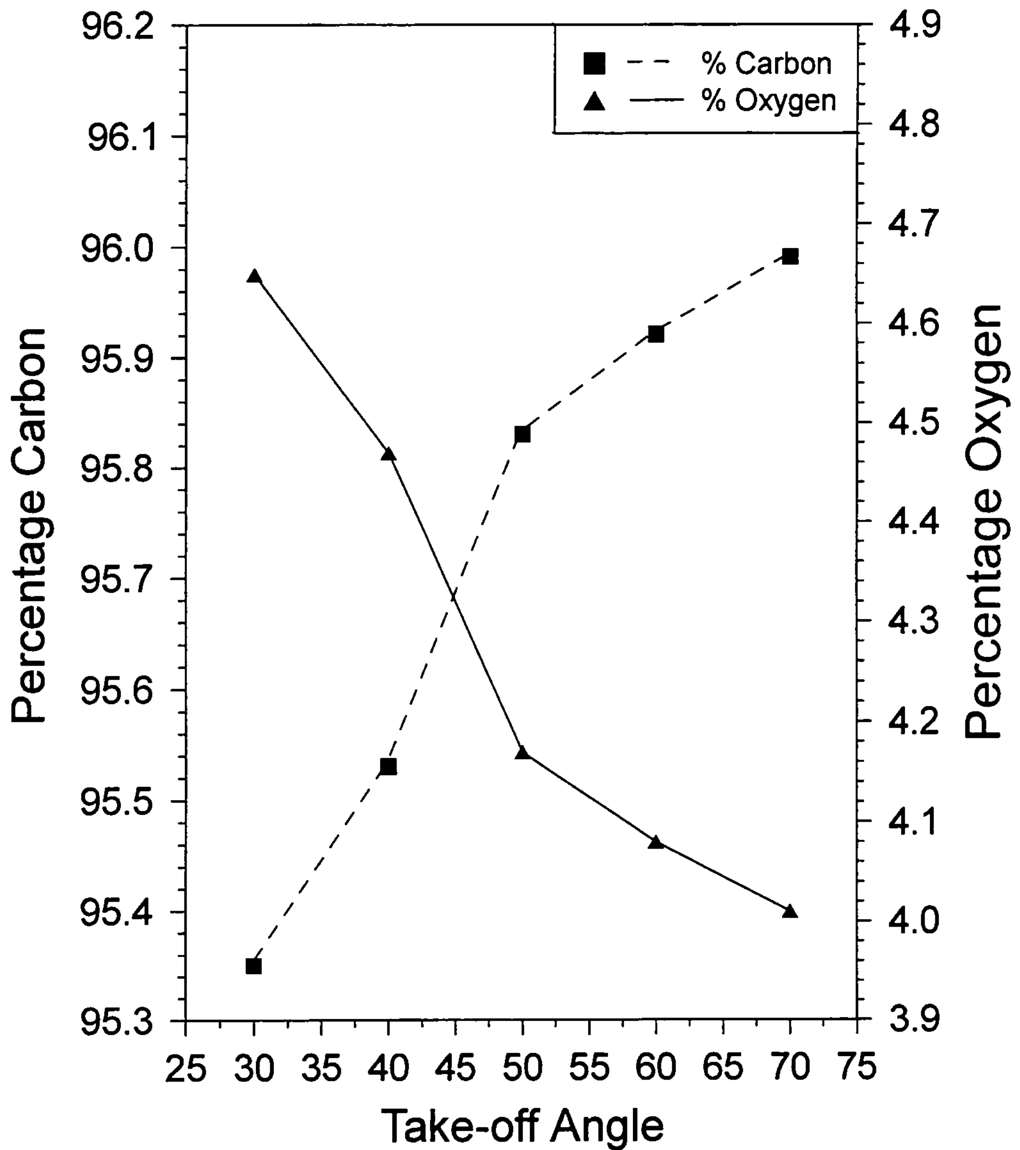

Fig. 6-14: Plot of percentage oxygen and carbon versus substrate angle from a 1.5 W plasma polymer; increasing angle indicates increasing surface sensitivity.

6.5 CONCLUSION

These preliminary investigations into the pulsed and continuous wave plasma polymerisation of styrene oxide indicate universal loss of the epoxy-group from the resultant plasma polymer regardless of discharge conditions. All plasma polymers show some level of retention of the aromatic benzene ring of the precursor, this being greatest for low duty cycle pulsed plasmas.

The oxygen content of the plasma polymers is also a function of the deposition conditions. Pulsed plasmas result in plasma polymers with a higher oxygen content than continuous wave polymers. Deposition rate measurements indicate some off-stage deposition is occurring most likely due to reaction of the epoxy-ring with residual radicals in the gas phase or at the surface of the growing polymer. Post-deposition oxidation of the plasma polymer surface is not responsible for the variation in oxygen content. The physical properties of the resultant surfaces change with the oxygen content. Plasma polymers with the highest oxygen content generate high energy hydrophilic surfaces.

6.6 REFERENCES

(1) Lee, J.H.; Kim, D.S.; Lee, Y.H. *Abs. Paps. Am. Chem. Soc.* **1994,** *208(2)*, 369.

(2) Schelz, S.; Schuler, N.; Richmond, T.; Oelhafen, P. *Thin Solid Films* **1995** *266(2)*, 133.

(3) Potter, W.; War, A.J.; Short, R.D. *Polymer Degradation And Stability* **1994**, *43(3)*, 321.

(4) Chen, M.; Yang,T.C.; Zhou, X. *J. Polym. Sci. B: Polym. Phys.* **1996**, *34(1)*, 113.

(5) Lee, J.H.; Kim, D.S.; Lee, Y.H.*ACS Symp. Ser.* **1996,** *620*, 167.

(6) Takeda, S. *Thin Solid Films* **1996,** *282(1-2)*, 539.

(7) Radloff, D.B.; Kurosawa, S.; Hiriyama, K.; Arimura, T.; Otake, K.; Sekiya, A.; Minoura, N.; Rapp, M.; Ache, H.J. *Mol. Crys.& Liq. Crys. Sci. & Tech* **1997,** *A294*, 439.

(8) Sugiyama, K.; Shirashi, K.; Ihara, T.; Kiboku, M. *Polymer Journal* **1991,** *23(10),* 1287.

(9) Chen, C.F.; Chen, S.H.; Hong, T.M.; Wu, S.H. *Diamond & Related Materials* **1993**, *2(5-7)*, 732.

(10) McGrail, P.T, *Polymer International* **1996,** *41(2)*, 103

(11) Bhat, N.V.; Joshi, N.V. *Plas. Chem. & Plas. Proc.* **1994**, *14(2)*, 151.

(12) Boluk, M.Y.; Akovali, G. *Polym. Eng. & Sci.* **1981**, *21(11)*, 664.

(13) Diaz, K.F.; Hernandez, R. *J. Polym. Sci. Polym. Chem. Ed.* **1984,** *22, 1123.*

(14) Clark, D.T.; Abrahman, M.Z. *J. Polym. Sci. Polym. Chem. Ed.* **1981,** *19,* 2129.

(15) Clark, D.T.; Abrahman, M.Z. *J. Polym. Sci. Polym. Chem. Ed.* **1981,** *19,* 2689.

(16) Clark, D.T.; Abrahman, M.Z. *J. Polym. Sci. Polym. Chem. Ed.* **1982,** *20*, 691.

(17) O'Connor, P.J.; Ellaboudy, A.S.; Tou, J.C. *J. Appl. Polym.Sci.* **1996**, *60(4)*, 637.

(18) Vanooij, W.J.; Eufinger, S.; Guo. S.Y. *Plasma Chem. & Plasma Process.* **1997**, *17(2),* 123.

(19) Bobnov, A.G.; Grinevich, V.I.; Aleksandrova, S.N.; Kostrov, V.V. *High Energy Chemistry* **1997**, *31(4)*, 264.

(20) Cruz, G.J.; Morales, J.; CastilloOrtega, M.M.; Olayo, R. *Synthetic Metals* **1997**, *88(3),* 213

(21) Connell, R.A.; Gregor, L.V. *J. Electrochem. Soc.* **1965**, *112*, 1198.

(22) Carbajal, B.G. *Trans. Met. Soc. AIME* **1966,** *236*, 365.

(23) Kanazono, T.; Takamura, M.; Kojima, K. *Mem. Inst. Sci. Ind. Res. (Osaka Univ.)* **1967,** *24*, 65.

(24) Brick, R.M.; Knox, J.R. *Modern Packaging* **1965,** *123.*

(25) Williams, T.; Hayes, M.W. *Nature* **1966,** *209*, 769.

(26) Williams, T.; Edwards, J.H. *Trans. Inst. Metal Finishing* **1966,** *44*, 119.

(27) Redmond, J.P.; Pitas, A.F. NASA Contract Rep. NASA-Cr-94310,1968.

(28) Yasuda, H. Final Report to Office of Saline Water, U.S. Dept. of the Interior, Contract No. 14-30-2658, Research Triangle Park, N.C. 1972.

(29) Stancell, A.F.; Spencer, A.T. *J. Appl. Polym. Sci.* **1972**, *16*, 1505.

(30) Miyamura, M.; Sakamoto,M.; Inomata, S. *Proc. of 2nd Symp. on Dry Process,* **1980**, Tokyo, P139.

(31) Morita, S.; Hattori, S.; Ieda, M.; Tamano, J.; Yamada, M. *Kobunshi Ronbunshu (Polymer Papers),* **1981**, *38(10)*, 657.

(32) Hattori,S.; Yamada, M.; Tamano, J.; Ieda, M.; Morita, S.; Yoneda, K.; Ikeda, S.; Ishibashi, S. *J. Appl. Polym. Sci. Appl. Polym. Symp.* **1984**, *38*, 127.

(33) Fong, F.O.; Kuo, H.C.; Wolfe, J.C. *J. Vac. Sci. Technol.* **1988**, *B6(1)*, 375.

(34) Hori, M.; Yoneda, T.; Yamada,H.; Morita, S.; Hattori, S. *Plasma Chem. & Plasma Process.* **1987**, *7(2)*, 155.

(35) Takeda, S. *Jpn. J. Appl. Phys.* **1981**, *20(7)*, 1219.

(36) Tanaka, K.; Nishio, S.; Matsuura, Y.; Yamabe, T. *Synthetic Metals*, **1993**, *55(2-3)*, 896

(37) Xie, X.; Oelhafen, P. *Thin Solid Films*, **1996**, *278*, 118.

(38) Sun, R.G.; Peng, J.B.; Kobayashi, T.; Ma, Y.G.; Zhang, H.F.; Liu, S.Y. *Jap. J. Appl. Phys. Part 2* **1996**, *35(11b)*, L1506-L1508.

(39) Gregor, L.V. *Physics Of Thin Films III;* Thun, R.E.; Hass, G. Eds.; Academic: New York, 1966.

(40) Gregor, L.V. *IBM J. Res. And Dev.* **1968**, *12(2)*, 140.

(41) Carchano, H.; Lacoste, R.; Segui, Y. *Appl. Phys. Lett.* **1971**, *19*, 414.

(42) Segui, Y.; Ai, Bui, Carchano, H. *J. Appl. Phys.* **1976**, *47*, 140.

(43) *The Handbook of Infrared and Raman Characteristic Frequencies of Organic Molecules;* Lin-Vien, D.; Colthup, N.B.; Fateley, W.G.; Grasselli, J.G. Ed.; Academic Press:New York, 1991, p. 277.

(44) Bellamy, L.J. *The Infrared Spectra of Complex Molecules, Vol. 1, 3rd ed.;* Chapman & Hall: London, 1975, p. 72.

(45) Whiffen, D.H. *Spectrochim. Acta* **1955**, *7*, 253.

(46) Field, Cole And Woodford, *J. Chem. Phys.* **1950**, *18*, 1298.

(47) Briggs, D.; Seah, M. P.; *Practical Surface Analysis 2nd Ed*; Wiley: Chichester,1990.

(48) Clark, D.T.; Adams, D.B.; Dilks, A.; Peeling, J.; Thomas, H.R. *J. Electron. Spec.* **1976**, *8*, 51.

(49) Yasuda, H.; Marsh, H.C.; Brandt, E.S.; Reilley, C.N. *Am. Chem. Soc. Polym. Pr.* **1975**, *16*, 142

(50) Abrahman, M.Z. Ph.D. Thesis, University of Durham, 1981.

(51) Greenwood, O.D.; Tasker, S.; Badyal, J.P.S. *J. Polym. Sci. Polym. Chem. Ed.* **1994**, *32*, 2479.

(52) Beamson, G.; Briggs, D. *High Resolution XPS of Organic Polymers: The Scienta ESCA300 Database;* Wiley: Chichester, 1992.

(53) Thompson, L.F.; Mayhan, K.G.; *J. Appl. Polym. Sci.* **1972**, *16*, 2317.

(54) Thompson, L.F.; Mayhan, K.G.; *J. Appl. Polym. Sci.* **1972**, *16*, 2291.

(55) Neiswender, D.D. *In Chemical Reactions In Electrical Discharges,* Advances In Chemistry 80; American Chemical Society: Washington, D.C., 1969, p. 338.

(56) Yasuda, H. *Plasma Polymerisation*; Academic Press: Orlando, 1985.

(57) Grill, A. *Cold Plasmas in Materials Technology*; IEEE Press: Piscataway, New Jersey, 1994.

(58) McTaggart, F.K. *Plasma Chemistry in Electrical Discharges*; Elsevier Publishing Company: London, 1967.

CHAPTER SEVEN

CONCLUSIONS

CHAPTER SEVEN

CONCLUSIONS

The work in this thesis was aimed at exploring the possibility of using pulsed power to a plasma to achieve greater control over the composition of the surfaces generated via plasma polymerisation. A variety of precursors were studied under a range of plasma conditions using both continuous wave and pulsed plasmas. Surface and bulk analytical techniques were used to characterise the deposited plasma polymers whilst deposition rate measurements aided in understanding the effects of altering the various plasma parameters. The results were interpreted in terms of the various potential reaction pathways available for each precursor during the plasma polymerisation process.

Continuous wave plasma polymerisation of saturated cyclic fluorocarbons yielded plasma polymers with high fluorine:carbon ratios. At low plasma power densities the chemistry of the precursor was reflected in the composition of the plasma polymers, however at higher powers the high energy plasma environment leads to a scrambling of the monomer structure in the final plasma polymer. A lower power density limit exists below which a continuous wave plasma is unstable. This limits the extent to which continuous wave power can be used to achieving good selectivity.

The plasma polymerisation of two cyclic perfluorocarbons, perfluorocyclohexane and perfluorocyclopentene was compared in chapter three. The presence of the double bond in PFCP altered the response of the monomer to changes in plasma parameters. Whereas for PFCH increasing the plasma energy, either continuous wave or pulsed, led to an increase in cross-linking and a reduction in the F/C ratio of the deposited film, PFCP plasma polymerisation resulted in a constant F/C ratio regardless of discharge power in the range investigated. Pulsed plasmas produced enhanced retention of precursor structure relative to CW plasmas resulting in a higher CF_2 content and F/C ratio at the

substrate surface.

In chapter four the pulsed plasma polymerisation of perfluoroallylbenzene was investigated in detail to examine the influence of the various pulsing parameters viz. on-time, off-time, duty cycle, frequency and pulsed power, on the pulsed plasma polymerisation process. The choice of monomer allowed the selectivity of the process to be followed by monitoring the retention of the aromatic ring in the plasma polymers. Deposition rate experiments indicated polymerisation was definitely taking place in the off-portion of the duty cycle for precursors with a reactive centre i.e. a double bond. Reducing the duty cycle of the pulsing increased the deposition rate per pulse i.e. deposition efficiency. Low duty cycle pulsed plasmas resulted in highly aromatic surfaces with extremely good retention of the perfluorobenzene ring from the precursor.

Pulsed plasma polymerisation of a cyclic siloxane precursor, tetravinyl-tetramethyl-cyclotetrasiloxane exploited the principles studied in chapter four to produce a surface consisting of siloxane rings in an organic matrix. The monomer structure was retained through the reaction of the vinyl groups in the off-portion of the duty cycle. For low duty cycle pulsed plasmas polymers the Si/O ratio of the plasma polymers was identical to that of the monomer, indicating successful retention of monomer structure using pulsed plasmas.

Preliminary investigations of the pulsed plasma polymerisation of styrene oxide were undertaken to examine the behaviour of another functional group, the epoxide ring, to pulsed plasma conditions. A range of polymer compositions with varying oxygen contents were observed. The properties of the resultant surfaces varied with oxygen content.

Suitable choice of precursor structure allows pulsed plasmas to give significant enhancements in control over surface composition and properties. Future work should focus on two broad areas. More information is required on the nature of the pulsed plasma polymerisation and how the processes occurring differ from continuous wave

process. Time-resolved gas phase diagnostics such as mass spectrometry, optical emission spectroscopy and laser induced fluorescence could be used to study on and off-time reactions in more detail. Pulsed voltage to a powered substrate would aid in understanding the effect of a pulsed plasma on the ion bombardment of the surface. Finally a broader range of chemistries of both the gas phase precursor and the substrate surface could be investigated to gain the maximum benefits from pulsed plasmas.

APPENDIX

SEMINARS AND CONFERENCES

University of Durham - Board of Studies in Chemistry

Colloquia, Lectures and Seminars from Invited Speakers

1993

October 4	Prof. F.J. Feher, University of California Bridging the Gap Between Surfaces and Solution with Sessilquioxanes
October 27	Dr. R.A.L. Jones, Cavendish Laboratory Perambulating Polymers
November 10	Prof. M.N.R. Ashfold, University of Bristol High Resolution Photofragment Translational Spectroscopy: A New Way to Watch Photodissociation
November 17	Dr. A. Parker, Rutherford Appleton Laboratory Applications of Time Resolved Resonance Raman Spectroscopy to Chemical and Biochemical Problems

1994

January 26	Prof. J. Evans, University of Southampton Shining Light on Catalysts
February 2	Dr. A. Masters, University of Manchester Modelling Water Without Using Pair Potentials
February 16	Prof. K.H. Theobald, University of Delaware Paramagnetic Chromium Alkyls: Synthesis and Reactivity
February 23	Prof. P.M. Maitlis, University of Sheffield Across the Border: From Homogeneous to Heterogeneous Catalysis

October 19 Prof. N. Bartlett, University of California

Some Aspects of Ag(II) and Ag(III) Chemistry

November 23 Dr. J.M. Williams, University of Loughborough

New Approaches to Asymmetric Catalysis

December 7 Prof. D. Briggs, ICI and University of Durham

Surface Mass Spectrometry

1995

January 18 Dr. G. Rumbles, Imperial College

Real or Imaginary Third Order Non-Linear Optical Materials

March 1 Dr. M. Rosseinsky, Oxford University

Fullerene Intercalation Chemistry

April 26 Dr. M. Schroder, University of Edinburgh

Redox-active Macrocyclic Complexes: Rings, Stacks and Liquid Crystals

May 3 Prof. E.W. Randall, Queen Mary and Westfield College

New Perspectives in NMR Imaging

October 11 Prof. P. Lugar, University of Berlin

Low Temperature Crystallography

November 17 Prof. D. Bergbreiter, Texas A&M

Design of Smart Catalysts, Substrates and Surfaces from Simple Polymers

November 22 Prof. I. Soutar, Lancaster University

A Water of Glass? Luminescence Studies of Water Soluble Polymers

1996

January 10	Dr. B. Henderson, Waikato University
	Electrospray Mass Spectrometry-A New Sporting Technique
January 17	Prof. J.W. Emsley, Southampton University
	Liquid Crystals: More Than Meets the Eye
January 31	Dr. G. Penfold, ?
	Soft Soap and Surfaces
March 6	Dr. R. Whitby, University of Southampton
	New Approaches to Chiral Catalysts: Induction of Planar and Metal Centred Asymmetry
March 12	Prof. V. Balzani, University of Bologna
	Supramolecular Photochemistry

Conference Attended

August 20 - 25, 1996	12th International Symposium on Plasma Chemistry, University of Minnesota, USA.